UNIVERSITÀ
DEGLI STUDI
DI PADOVA

Sede Amministrativa: Università degli Studi di Padova

Dipartimento di Scienze Biomediche

CORSO DI DOTTORATO DI RICERCA IN:

SCIENZE BIOMEDICHE SPERIMENTALI

CICLO: XXX

STUDY OF THE MECHANISM OF ACTION OF BOTULINUM NEUROTOXINS TO DEVELOP INHIBITORS AND TO IMPROVE THEIR PHARMACOLOGICAL APPLICATION

Coordinatore: Ch.mo Prof. Paolo Bernardi

Supervisore: Ch.mo Prof. Cesare Montecucco

Dottorando: Giulia Zanetti

Alla mia famiglia

Table of contents

Abbreviation index:

ACh = acetylcholine neurotransmitter

BoNTs = Botulinum neurotoxins

CDC = center for disease control and prevention

EGA = 4-bromobenzaldehyde N-(2,6-dimethylphenyl) semicarbazone

GSH = glutathione

HA = hemagglutination activity protein

H = heavy chain

HC = C-terminal part of H (can be divided in HC_C and HC_N)

HN = N-terminal part of H

L = light chain

LD_{50} = median lethal dose

MAT = motor axon terminal

NADPH = nicotinamide adenine dinucleotide phosphate

NMJ = neuromuscular junction

NT = neurotransmitter

NTNHA = nontoxic nonhemagglutinin protein

PSG = polysialoganglioside

SNAP-25 = synaptosomal-associated protein of 25 kDa

SNARE = soluble NSF attachment protein receptors

SV = synaptic vesicle

SV2 = synaptic vesicle protein 2

Stx = syntaxin

Syt = synaptotagmin

TeNT = Tetanus neurotoxin

Trx = thioredoxin

Trx-TrxR =thioredoxin-thioredoxin reductase system

TrxR = thioredoxin reductase

VAMP = vesicle-associated membrane proteins (or synaptobrevin)

Summary

Seven antigenically different botulinum neurotoxin types (BoNT/A through /G) and many subtypes (BoNT/A1, BoNT/A2, etc.) constitute a growing family of bacterial exotoxins that specifically paralyze the cholinergic peripheral nerve terminals of vertebrates. Most notably, BoNTs intoxicate the neuromuscular junction, thereby causing a severe neuro-muscular paralysis known as botulism.

Despite the heterogeneity of their primary sequence, BoNTs are structurally and functionally conserved and composed of a 50 kDa light chain (L) and a 100 kDa heavy chain (H), linked *via* a unique, and fundamental, disulphide bridge. The C-terminal (HC, 50 kDa) and the N-terminal halves (HN, 50 kDa) of H constitute a sophisticated nanomolecular machine that mediates both the neurospecific binding of the molecule to peripheral nerve endings and the delivery of L into the neuronal cytosol. L is a zinc-dependent protease that specifically cleaves SNARE proteins (SNAP-25 (synaptosomal-associated protein of 25 kDa), VAMP (vesicle-associated membrane protein) and Stx (syntaxin)), the three proteins that form the SNARE complex which is the core of the nanomachine that mediates the fusion of synaptic vesicles (SV) with the presynaptic membrane, thus allowing neurotransmitter release. Cleavage causes impairment of SNARE complex assembly/function and thus a blockade of neuroexocytosis, which results in the flaccid paralysis typical of botulism. Patients can die for respiratory failure but, if vital functions are maintained by intensive care, they fully recover as the botulism neuroparalysis is completely reversible.

The mechanism of action of BoNTs can be conveniently divided into five fundamental steps: 1) binding to nerve terminals, 2) internalization by SV recycling, 3) pH-dependent translocation of L into the cytoplasm, 4) reduction of the interchain disulphide bond and 5) hydrolysis of SNARE proteins. BoNT/A and /E cleave SNAP-25, BoNT/B, /D, /F and /G cleave VAMP. BoNT/C is unique because it cleaves two substrates, SNAP-25 and syntaxins.

BoNTs are the most poisonous substances known to vertebrates, and are classified as potential biological weapons. Currently, the only treatment available consists in passive immunisation with antisera raised against the seven main toxin types. Unfortunately, antisera are variably reactive against subtypes and, moreover, no licensed vaccine are available for human use. This situation has promoted an intense research to develop new antitoxins.

At the same time, neurospecificity and reversibility of action make BoNTs the therapeutic of choice for the treatment of a heterogeneous number of human diseases characterized by the hyperactivity of peripheral nerve terminals.

Given this dichotomy of BoNTs, the aim of my PhD has been double: i) to develop pan-inhibitors that would prevent/treat botulism and ii) to better understand the toxin functioning *in vivo* to improve its use in human therapy.

i) BoNT's intoxication strictly depends on the reduction of the interchain disulphide bond. Without it, L remains attached to H and cannot exert its catalytic activity. By using a pharmacological approach, I found that the Thioredoxin-Thioredoxin Reductase (Trx-TrxR) system is responsible for the reduction of all BoNT serotypes and that inhibitors of Trx-TrxR strongly reduce their neurotoxicity *in vitro* and *in vivo* in a model that recapitulates clinical botulism. These results are remarkable because they show for the first time that the different BoNTs can be inhibited by a single drug (a pan-inhibitor) by impacting on their common mechanism of action.

Following the same concept, the trafficking of BoNTs within the synaptic terminal represents another rational target to develop pan-inhibitors. Recently, it was reported that the chemical compound EGA inhibits pathogens or toxins that enter cells *via* acidic endosomes. Since also BoNTs have a similar requirement to trigger the translocation of L into the cytosol, I tested the activity of EGA and I found that it significantly inhibits the neurotoxic activity of BoNT/A, BoNT/B and BoNT/D *in vitro* and *in vivo*, tested because are serotypes frequently involved in human and animal botulism, respectively. Interestingly, none of the main steps underlying toxin's cellular mechanism is directly affected by the drug. Rather, I provided indirect evidence that EGA interferes with the sorting of BoNTs inside

nerve terminals, hampering their trafficking toward acidic compartments essential for L translocation.

Together, these studies show that BoNT's activity can be significantly mitigated independently from their intertypic differences by using drugs targeting common steps of their mechanism of action. These inhibitors represent lead compounds for the development of new drugs against botulism.

ii) BoNTs are successful human therapeutic agents. Despite their use is almost invariably restricted to BoNT/A and BoNT/B, recent data on human volunteers suggest that BoNT/C can be used to treat non-responder individuals with similarly effective pharmacological outcomes. However, little is known about the mechanism by which BoNT/C paralyzes peripheral nerve terminals *in vivo*. In fact, at variance from all the other BoNTs, BoNT/C cleaves two substrates, SNAP-25 and syntaxin-1A/1B. Therefore, I undertook a study to evaluate the individual contribution of SNAP-25 and syntaxin cleavage to BoNT/C activity *in vivo*. I took advantage from a recent publication where two triple-mutated BoNT/C L, L200W/M221W/I226W (BoNT/C α-3W) and S51T/R52N/N53P (BoNT/C α-51), were reported to cleave selectively syntaxins.

Thanks to a collaboration with Dr. T. Binz, I received the full-length BoNT/C mutants produced by recombinant methods and I tested their biochemical and toxicological properties. I found that both mutants cleave syntaxin with similar efficiency with respect to wild type BoNT/C (BoNT/C-wt), but unexpectedly, they maintain a residual activity on SNAP-25 which is higher for BoNT/C α-3W than for BoNT/C α-51. Interestingly, this different activity on SNAP-25 strictly correlates with the lethality of mutant toxins *in vivo*. At the same time, the proteolysis of syntaxin provides a substantial and prolonged neuromuscular impairment without the complete blockage of neurotransmission. These results suggest that SNAP-25 cleavage is the main determinant of BoNT/C neuroparalyzing activity and that BoNT/C derivatives with selective activity for syntaxins represent an appealing strategy to develop BoNTs endowed with long lasting activity and a wide safety margin.

Riassunto

Le neurotossine botuliniche (BoNTs) sono esotossine batteriche, agenti eziologici del botulismo. In base alla diversa antigenicità si possono dividere in sette sierotipi principali (BoNT/A-/G) che comprendono ulteriori sottotipi (BoNT/A1, BoNT/A2 ecc.). Presentano tutte tropismo specifico per la giunzione neuromuscolare dove esercitano un'azione neuroparalizzante.

Nonostante la sequenza amminoacidica eterogenea, dal punto di vista strutturale e funzionale le BoNTs appaiono altamente conservate: sono composte da due catene polipeptidiche, una pesante di 100 kDa (H) e una leggera di 50 kDa (L), unite da un unico, ma fondamentale, ponte disolfuro. Il C-terminale (HC, 50 kDa) e l'N-terminale (HN, 50 kDa) di H costituiscono una sofisticata macchina molecolare che media sia il legame neurospecifico della molecola ai terminali nervosi periferici che la traslocazione di L nel citoplasma dei motoneuroni. L è una proteasi zinco-dipendente che idrolizza in modo specifico le proteine SNARE (SNAP-25 (synaptosomal-associated protein of 25 kDa), VAMP (vesicle-associated membrane protein) and Stx (syntaxin)), tre proteine che costituiscono il nucleo della macchina molecolare, il cosiddetto "SNARE complex", che media la fusione delle vescicole sinaptiche (SV) con la membrana presinaptica permettendo il rilascio di neurotrasmettitore. Il taglio di una di queste importanti proteine provoca una riduzione nella funzionalità del complesso e quindi un blocco della neuroesocitosi: ciò determina la paralisi flaccida tipica del botulismo. I pazienti possono morire di insufficienza respiratoria ma, se le funzioni vitali vengono sostenute, essi recuperano completamente la mobilità in quanto la neuroparalisi è reversibile.

Il meccanismo d'azione delle BoNTs può essere riassunto in cinque fasi fondamentali: 1) riconoscimento specifico e legame al terminale sinaptico, 2) internalizzazione tramite il riciclo delle SV, 3) traslocazione pH-dipendente di L nel citoplasma 4) riduzione del ponte disolfuro intercatena e 5) idrolisi delle proteine SNARE.

In particolare, la BoNT/A e BoNT/E agiscono sulla SNAP-25, mentre BoNT/B, /D, /F e /G idrolizzano la VAMP. La BoNT/C è unica perché taglia sia SNAP-25 che la proteina sintaxina.

Le BoNTs sono le sostanze più velenose note, classificate dal Centro per il Controllo e la Prevenzione delle Malattie (CDC) come agenti in categoria A, cioè tossine potenzialmente utilizzabili come armi biologiche. Attualmente non esiste nessun vaccino approvato per l'uso umano e l'unico trattamento disponibile consiste nell'immunizzazione passiva con antisieri prodotti per contrastare i sette sierotipi principali e di conseguenza variabilmente reattivi nei confronti dei sottotipi. Questa situazione ha promosso un'intensa ricerca per sviluppare nuove antitossine.

Tuttavia, allo stesso tempo, la loro neurospecificità e la reversibilità della paralisi rendono le BoNTs degli agenti terapeutici di prima scelta per il trattamento di un'ampia varietà di malattie umane caratterizzate da iperattività dei terminali nervosi periferici.

Considerando questa dicotomia, il mio progetto di dottorato si può dividere in due parti principali aventi lo scopo di: i) sviluppare pan-inibitori in grado di prevenire/trattare il botulismo e ii) capire meglio il funzionamento delle BoNTs *in vivo* per migliorare e ampliare l'uso di queste molecole in terapia.

i) Considerando il meccanismo d'intossicazione delle BoNTs, uno step fondamentale è la riduzione del ponte disolfuro intercatena, senza la quale L rimane attaccata a H e non può esercitare la sua attività catalitica. Utilizzando un approccio farmacologico ho dimostrato che il sistema Tioredossina-Tioredossina Reduttasi (Trx-TrxR) è il principale responsabile della riduzione per tutti i sierotipi di tossina botulinica e che inibitori di questa coppia redox producono una sostanziale protezione dall'intossicazione sia *in vitro* che *in vivo* in un modello che ricapitola il botulismo. Questo risultato è importante perché è il primo che mostra che sierotipi diversi di BoNTs possono essere inibiti da un'unica molecola (pan-inibitore) che agisce sul meccanismo d'azione comune.

Un altro aspetto importante nella tossicità di queste neurotossine è il loro traffico all'interno del terminale nervoso. Questo potrebbe essere un altro target razionale.

Recentemente, è stato riportato che il composto chimico EGA inibisce agenti patogeni o tossine che necessitano del passaggio attraverso compartimenti acidi (endosomi) per poter penetrare nel citoplasma di cellule bersaglio. Dal momento che anche le BoNTs necessitano di condizioni simili perché avvenga la traslocazione di L nel citoplasma, ho saggiato l'effetto di questa molecola sull'azione delle BoNTs. Consistentemente, ho trovato che EGA inibisce significativamente l'attività neurotossica della BoNT/A, BoNT/B e BoNT/D *in vitro* e *in vivo.* Sono stati scelti questi tre sierotipi perché sono quelli più comunemente associati al botulismo umano (BoNT/A e /B) ed animale (BoNT/D). È interessante notare come nessuno degli steps del meccanismo d'azione sia direttamente inibito dalla molecola: ciò è compatibile con la possibilità che EGA interferisca con il traffico delle BoNTs all'interno del terminale nervoso ostacolando il raggiungimento del compartimento acido essenziale per la traslocazione di L.

Complessivamente, questi studi mostrano come l'attività delle BoNTs possa essere significativamente inibita, indipendentemente dalle loro differenze antigeniche, usando molecole che agiscano su steps comuni del meccanismo d'azione. Questi inibitori rappresentano *lead compounds* per lo sviluppo di farmaci capaci di prevenire il botulismo.

ii) Le BoNTs sono agenti terapeutici di successo. Nonostante il loro impiego sia quasi esclusivamente limitato alle BoNT/A e BoNT/B, dati recenti ottenuti su volontari umani suggeriscono che la BoNT/C possa essere utilizzata per trattare individui non rispondenti a BoNT/A e BoNT/B con risultati farmacologici altrettanto efficaci.

Tuttavia, al momento ci sono poche conoscenze riguardo al meccanismo con il quale la BoNT/C paralizza i terminali nervosi periferici *in vivo*: infatti, a differenza di tutti gli altri sierotipi, la BoNT/C è l'unica che idrolizza due substrati, SNAP-25 e sintaxina-1A/1B. Per questo motivo, ho intrapreso uno studio per valutare il

contributo individuale del taglio di SNAP-25 e di quello della sintaxina nell'attività della BoNT/C *in vivo*.

Per fare questo mi sono basata su una recente pubblicazione in cui è stato riportato che due BoNT/C triple-mutanti, L200W/M221W/I226W (BoNT/C α-3W) e S51T/R52N/N53P (BoNT/C α-51), sono risultate selettive per la sintaxina.

Grazie alla collaborazione col gruppo del Dr. T. Binz, ho ottenuto queste due BoNT/C mutanti, prodotte con metodi ricombinanti, e ne ho testato le loro proprietà biochimiche e tossicologiche. Quello che ho scoperto è che entrambe le triple-mutanti idrolizzano la sintaxina con un'efficienza simile alla tossina WT (BoNT/C-wt) ma, inaspettatamente, entrambe mantengono anche un'attività residua nei confronti della SNAP-25 (più elevata per la BoNT/C α-3W rispetto alla BoNT/C α-51). È interessante notare come questa attività sulla SNAP-25 sia strettamente correlata alla letalità delle tossine mutanti *in vivo*. D'altra parte, la proteolisi della sintaxina fornisce una sostanziale e prolungata compromissione neuromuscolare senza provocare il completo blocco della neurotrasmissione. Questi risultati suggeriscono che il taglio di SNAP-25 sia il principale determinante dell'attività neuroparalizzante e che derivati della BoNT/C, aventi attività selettiva per le sintaxina, potrebbero rappresentare una buona strategia per lo sviluppo di BoNTs dotate di attività prolungata e con un ampio margine di sicurezza.

Chapter 1

Introduction

1.1 Neuromuscular junction as a target of toxins

The nervous system plays an essential role in animal physiology and any perturbation can cause enormous variations in its activity, resulting in deep changes in the behavior and health of the individual. Synaptic transmission, the mechanism through which a nervous impulse propagates, is the key event of the functioning of the nervous tissue, as it provides the ability to receive and spread stimuli, thus governing all body functions. Synaptic transmission occurs both between neurons and between neurons and other cell types, such as muscle and secretory cells. The structure that allows this communication is the synapse. The best characterized synapse is the neuromuscular junction (NMJ), which is composed by the motor axon terminal (MAT, presynaptic) and the skeletal muscle fiber (postsynaptic effector)[1] (see Figure 1).

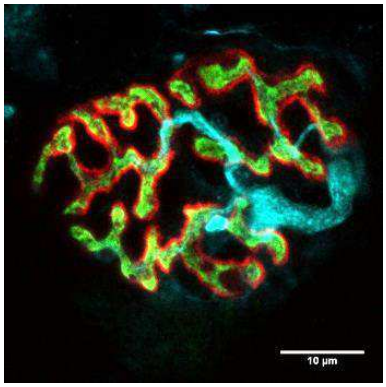

Figure 1. Anatomical structure of mammalian NMJ. Immunohistochemistry on soleus muscles. Nerve is labelled with anti-neurofilaments antibody (in cyan); nerve terminal with anti-SNAP-25 antibody (in green) and the muscle end-plate is stained with α-Bungarotoxin Alexa 555-conjugated (in red). From Duregotti *et al.*, 2015[2].

The NMJ is a chemical synapse where the electrical stimulus, running along the motor axon, is translated into mechanical movement of muscles following the fusion of synaptic vesicles (SV) with the presynaptic plasma membrane and the release into the intersynaptic space of the neurotransmitter acetylcholine (ACh)[1] (see the figure 2).

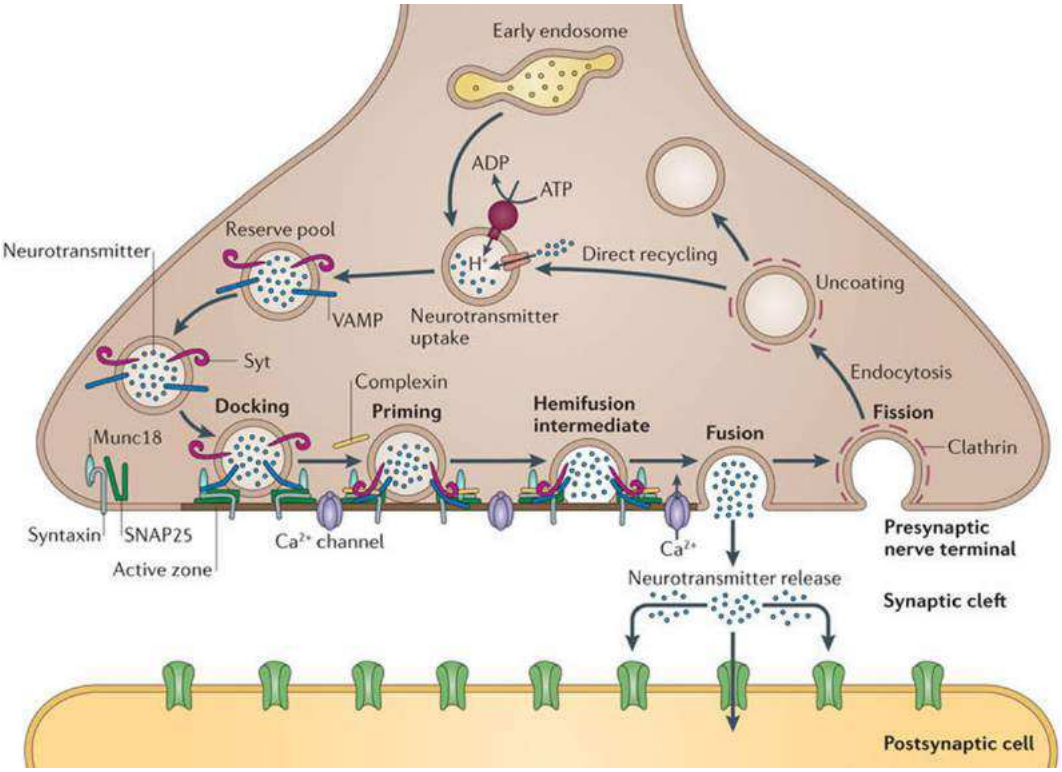

Figure 2. Neurotransmission at the synapse. From Rossetto *et al.*, 2014[3].

SV are present at the MAT in a reserve pool and docked to the active zone, a specialized site of presynaptic membrane where the neurotransmitter (NT) release occurs[4-9]. Upon motor neuron stimulus, an action potential propagates along the axon and enables the rapid fusion of the SV with the active zone in response to Ca^{2+} influx. Fusion is promoted by the interaction among vesicle-associated membrane protein (also known as synaptobrevin (VAMP)), synaptosomal-associated protein of 25 kDa (SNAP-25) and syntaxin (Stx). These three proteins form a coiled-coil complex, known as the SNARE (soluble *N*-ethylmaleimide-sensitive factor attachment protein receptor) complex. This is the core of the nanomachine that mediates NT release. Interestingly, it has been reported that multiple SNARE complexes can assemble in a radial supercomplex

which mediates SV fusion[10-12]. This latter phenomenon is calcium-dependent, since the Ca^{2+}-sensor synaptotagmin has been shown to regulate the fusion of the SV juxtaposed to the plasma membrane (primed SV), thus allowing NT release[13]. NT diffuses out of the nerve terminal and is captured by specialized receptors (nicotinic receptors) located on the postsynaptic membrane. The opening of these ionotropic receptors induces a depolarization of the end-plate giving rise to an end-plate potential; this in turn opens neighbouring voltage-gated sodium channels, eventually leading to the onset of an action potential, which propagates along the muscle fiber promoting muscle contraction[1].

During NT release, the lumen of SV is transiently opened to the outside, but it is later internalized into the nerve terminal by endocytosis[14,15]. Exocytosis and endocytosis of SV are strictly coupled, and the inhibition of one process leads to the inhibition of the other[15]. Upon membrane retrieval, SV need to be refilled with NT, a process driven by the electrochemical proton gradient generated by the vesicular ATPase proton pump, located in the SV membrane. At the end of this process, a new cycle of neurotransmission can start again (see figure 2).

Throughout evolution, many microorganisms and animals have developed different strategies to alter neurotransmission at the NMJ as this synapse is not protected by anatomical barriers like central synapses. This is often achieved through neurotoxins, which can act with different mechanisms of action according to their molecular properties.

Many are relatively small molecules that bind ion channels and block the propagation of the nervous impulse through the modification of ion permeability: this is the case of tetradotoxin and charybdotoxin. Others, such as α-latrotoxin or beta-bungarotoxin are proteins which perturb the integrity of the presynaptic plasma membrane causing a massive calcium intake. This, in turn, induces a massive fusion of SV and Ca^{2+} toxicity leading to the complete degeneration of the presynaptic terminal and ensuing neuroparalysis. Some other toxins have evolved a more sophisticated mechanism which allows their internalization into the nerve terminal and the modification of a cytosolic target to alter the normal physiology of the neurotransmission; this is the case of

neurotoxins produced by certain *Clostridium* strains such as tetanus and botulinum neurotoxins (TeNT and BoNTs).

1.2 Botulinum neurotoxins

Clostridium is a genus of sporulating and anaerobic Gram-positive bacteria, including more than 150 species. Several Clostridia, such as *Clostridium difficile*, *Clostridium perfringens* and *Clostridium sordelli*, are pathogenic, owing to the release of protein toxins, that are not neurotoxic. On the other hand, six phylogenetically distinct Clostridia (*Clostridium botulinum* groups I-IV and some strains of *Clostridium butyricum* and *Clostridium baratii*) produce seven distinct BoNTs (serotype A-G) distinguished on the basis of their immunological properties. Recently, the development of next generation sequencing has permitted the analysis of clinical cases of botulism accumulated over time[16]. As a result, the number of BoNT molecules known has dramatically grown (see Figure 3), reaching more than forty molecules in a few years, and this number is continuously increasing[17].

As a consequence, BoNTs have been categorized as subtypes, i.e. toxins immunogenically related to the parental serotypes but with an amino acidic composition difference higher than 2.6% (indicated as BoNT/A1, BoNT/A2, etc.)[3,17,18]. Moreover, it has been discovered that some other molecules are composed by the combination of different serotypes: accordingly, they have been classified as mosaic toxins and indicated as BoNT/CD and /DC[19,20] (see Figure 3).

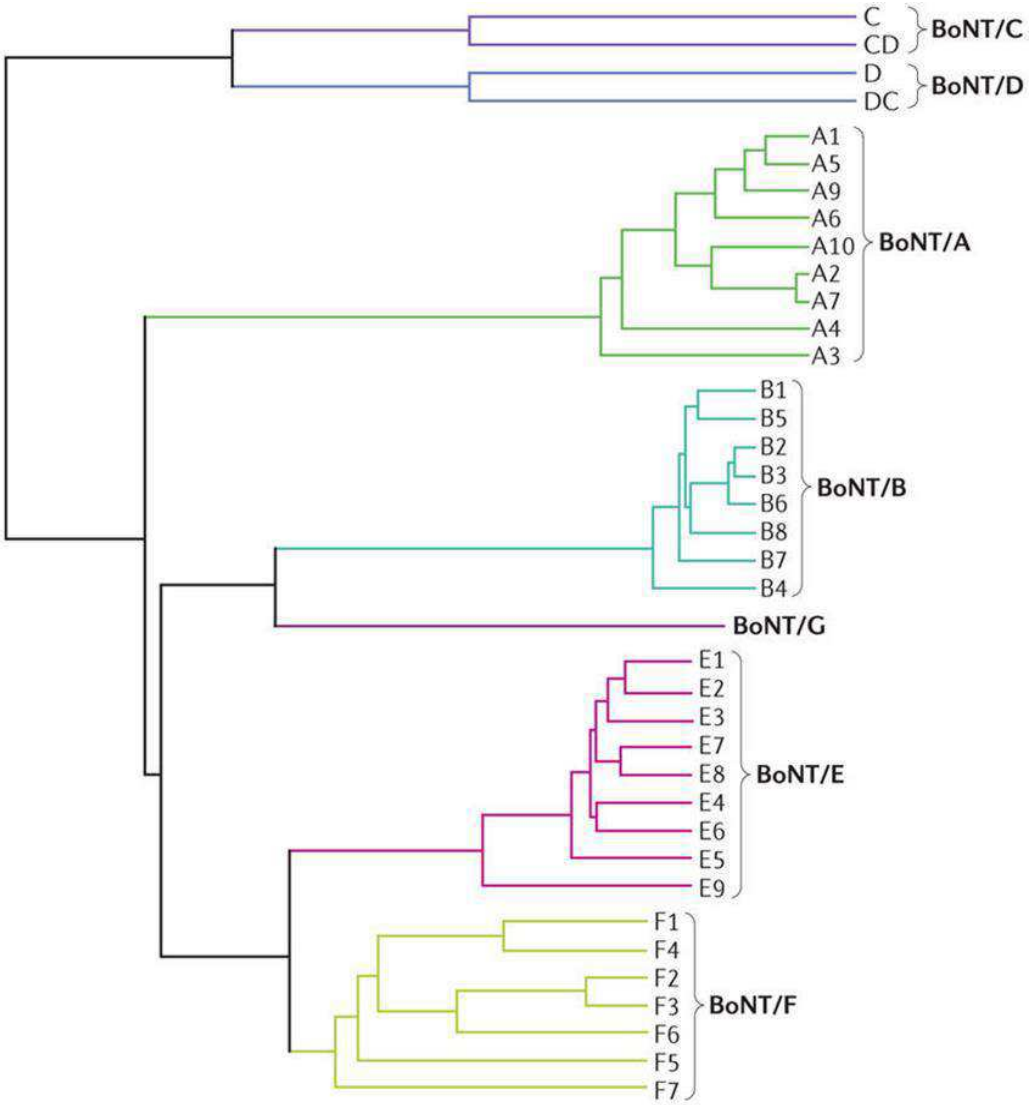

Figure 3. Different serotypes and subtypes are produced by several neurotoxigenic species of Clostridia. Six phylogenetically distinct Clostridia produce seven antigenically different botulinum neurotoxins (BoNTs serotypes A-G). From Rossetto *et al.*, 2014[3].

1.2.1 BoNTs: from bacteria to paralysis

Clostridia are obligate anaerobes and are present in the environment as spores, strongly resistant to both chemical and physical agents[21,22]. Germination can only occur in an anaerobic situation, low acidity (pH> 4.5), in the presence of nutrients and low saline concentrations[23,24]. In a proper environment, spores can undergo transition to a vegetative state, growth and, *via* autolysis, release the neurotoxins[3,25].

Poisoning is mainly caused by the ingestion of mature toxin rather than a real infection, indeed, competition with saprophytic flora blocks *Clostridium* proliferation in the intestine. The occurrence of a real infection takes place in infants and children where the poorly developed of resident microbiota is unable to stop colonization of the gastrointestinal tract; this case is referred as infantile botulism[26]. However, there are other uncommon forms of intoxication, such as iatrogenic botulism caused by inappropriate administration or toxin abuse during pharmaceutical and cosmetic treatments[27]. Skin lesion infection (as for tetanus) is much rarer although some cases have been reported. Last, the casual poisoning by inhalation, due to BoNT-containing aerosols, is unlikely but could be used for the exploitation of botulinum toxin as a biological weapon[3,24,28] (see Figure 4).

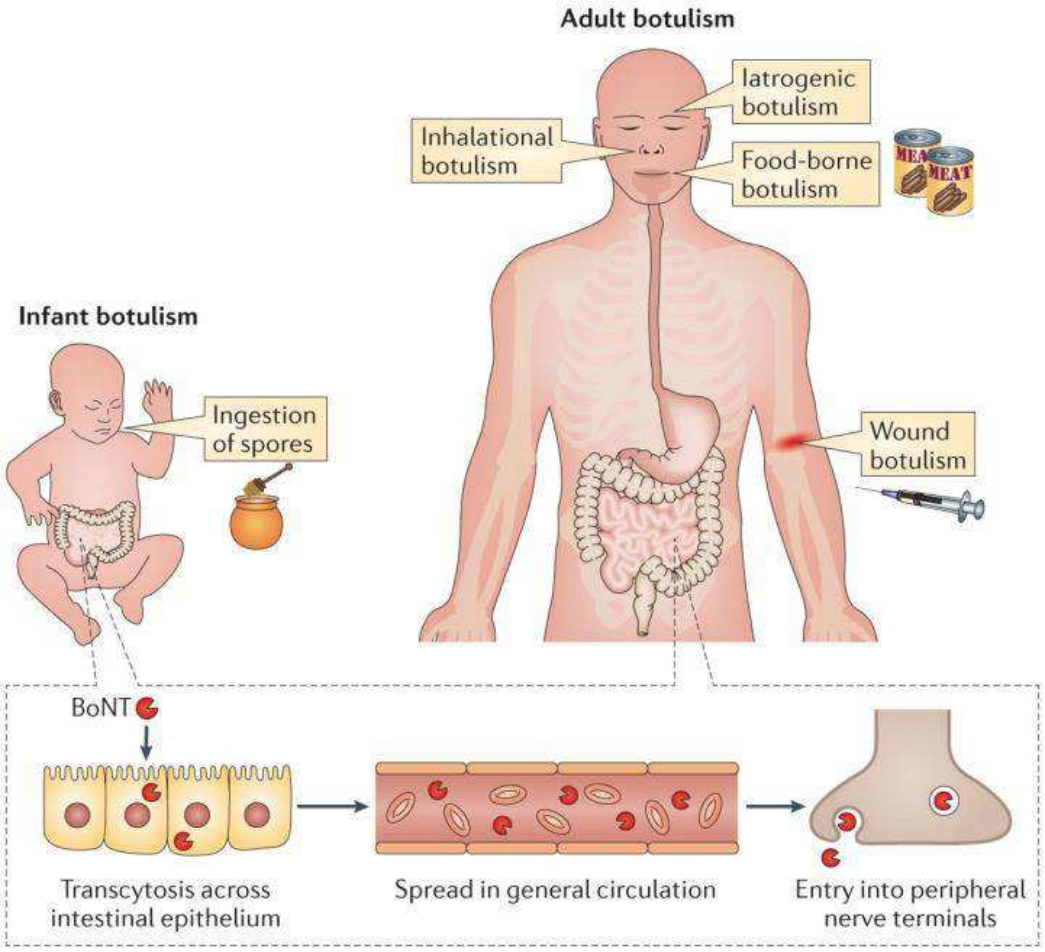

Figure 4. Five forms of human botulism. From Rossetto *et al.*, 2014[3].

Among the five forms of human botulism the most common forms is food-borne botulism, which occurs following the intake of BoNT-containing foods, typically canned foods. Importantly, after the ingestion, the toxin must survive the proteolytic environment of the gastrointestinal tract to reach the intestines, where it is absorbed[3,25]. To this purpose the toxin is produced together with other proteins, NTNHA (nontoxic nonhemagglutinin) and neurotoxin-associated protein (hemagglutination activity (HA) protein or OrfX, depending to the strains). NTNHA is significantly similar to BoNTs structure but lacks the ability to bind the catalytic zinc[29,30]. This protein forms a handin-hand-shaped heterodimer with the toxic molecule[31,32], suggesting that it shields and protects BoNT from chemical attacks[25,31,33]. On the other hand, accessory protein (HA or OrfX) seem to mediate the binding of the complex to the intestinal mucus and to the polarized epithelial monolayer[25,34-42]. All together, these proteins constitute the progenitor toxin complexes that, once reached the slightly basic pH found in the intestine, dissociates and releases the toxic molecule.

Free BoNT actuates transcytosis through intestinal epithelium, thus dispersing in extracellular fluids, entering the lymphatic system and then in the blood circulation[43]. Eventually, BoNT reaches peripheral cholinergic nerve terminals where exerts its toxic activity blocking the neurotransmission and causing muscle flaccid paralysis.

Human botulism is much rarer than animal botulism and is generally associated with serotypes A, B, E and F[24], whereas for serotypes C and D there are no known cases of human intoxication. The latter two serotypes are in fact mostly associated with animal and avian botulism[44,45].

1.2.2 BoNTs structure and mechanism of action

BoNT molecules share a very similar molecular architecture and mechanism of intoxication. All of them are produced by bacteria as a single polypeptide chain of 150 kDa which is subsequently nicked by specific bacterial or host proteases, resulting in the active toxin[46]. As shown in Figure 5, mature BoNT are composed of two chains linked *via* a single disulphide bridge[40] (see Figure 5, in orange).

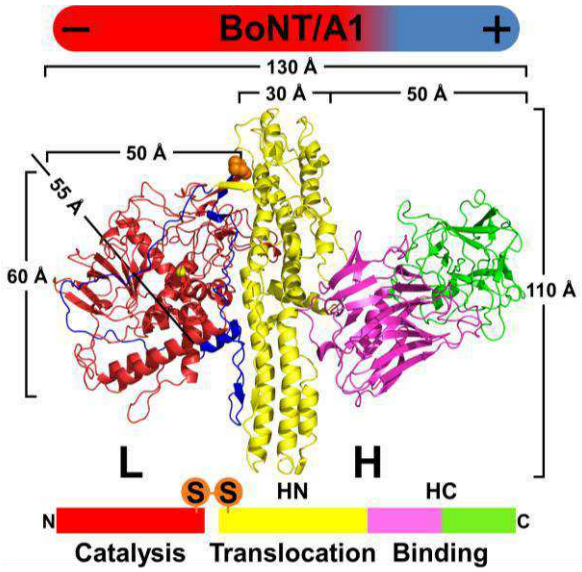

Figure 5. Structure of isolated BoNT/A1 molecule. Crystal structure of BoNT/A1[47] showing its associated electrical dipole and the organization of individual toxin domains.

The largest chain, 100 kDa, is called heavy chain (H) and can be functionally divided into two domains. The first one is the carboxy-terminal part (HC, 50 kDa), again subdivided in HC_c (25 kDa, see Figure 5, in green) and HC_N (25 kDa, see Figure 5, in purple). This domain is responsible for the specific binding to the neuronal surface and for the internalization of the toxin in the compartments exploited for their neuronal endocytosis. The second one is the amino-terminal part (HN, 50 kDa, see Figure 5, in yellow), also known as translocation domain. This domain is responsible for the toxin movement from the SV lumen to the cytosol[46,48] and is composed of two long amphipathic α-helices and four shorter ones running parallel to each other. In addition to them, HN also comprises a long unstructured amino acids string, called belt region, which encircles and partially shields the active site of the L (see Figure 5, in blue). This spatial arrangement suggests that belt structure could work as a false substrate to inhibit protease activity until the L is released into the cytosol[49].

The smallest chain, 50 kDa, is called light chain (L, see Figure 5, in red); its structure is globular with a mixture of both α-helix and β-strand. It is a Zn^{2+}-dependent protease that displays a very specific activity against SNARE proteins, the cleavage of which results in the flaccid paralysis typical of botulism[46].

This particular molecular structure is functional to BoNTs action, in fact, each part plays an essential role in the sophisticated intoxication mechanism that takes advantage from the normal physiology of the NMJ.

The intoxication process consists of five major steps[50-52]: (A) neurospecific binding of the HC to the MAT, (B) endocytosis into the neuronal cell, (C) pH-dependent translocation through the membrane of the endocytic vesicle, (D) reduction of the disulphide bond that links H to L and (E) proteolysis of SNAREs with consequent blockage of neuroesocytosis (see Figure 6). Peripheral neuroparalysis is the most evident symptom of botulism, however, indirect evidence showed that BoNTs can be retroaxonal transported within spinal cord and brain neuronal circuits[53-55].

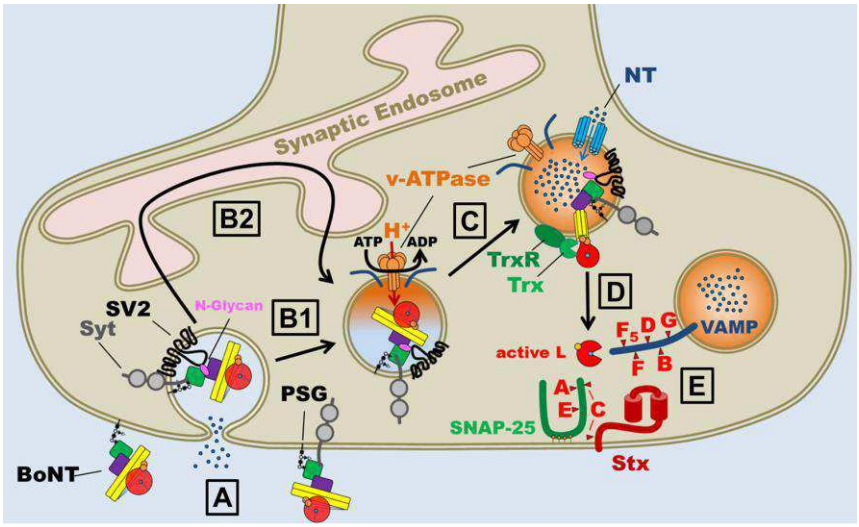

Figure 6. BoNTs mechanism of action. The nerve terminal intoxication by BoNTs is a multi-step process: (A) Binding of the HC domain (in green) to the nerve terminal. (B) Internalization inside SVs, which are directly recycled (B1) or inside SVs that fuse with the synaptic endosome and re-enter SV cycle by budding from this intermediate compartment (B2). (C) Membrane translocation of the L into the cytosol thank to the acidification of the compartment. (D) Reduction of disulphide bridge. (E) Cleavage of SNARE proteins. Modified from Pirazzini *et al.*, 2017[25].

A) Neurospecific binding

The first step in the toxic mechanism is the cell-specific binding of BoNT molecules. Importantly, BoNTs only bind to peripheral nerve terminals, particularly to those of skeletal and autonomic cholinergic nerves[56], whose

surface constitutes only a little percentage of the total cell area exposed to extracellular fluids.

To explain the higher neurotropism of BoNTs, a "double receptor model" has been proposed[48,57]. The idea is that BoNTs bind neurons *via* two receptors: one with low affinity, that increases toxin density on the target membrane[46,48,57], and a secondary one, with high affinity, located in the luminal part of SV. The second receptor triggers the internalization of the toxin into the endocytic pathway[58] (see Figure 7). This binding mode appears functional to BoNTs which, despite their low concentrations in circulating fluids and their high velocity of movement around peripheral nerve terminals[3], can be efficiently captured by the receptorial system.

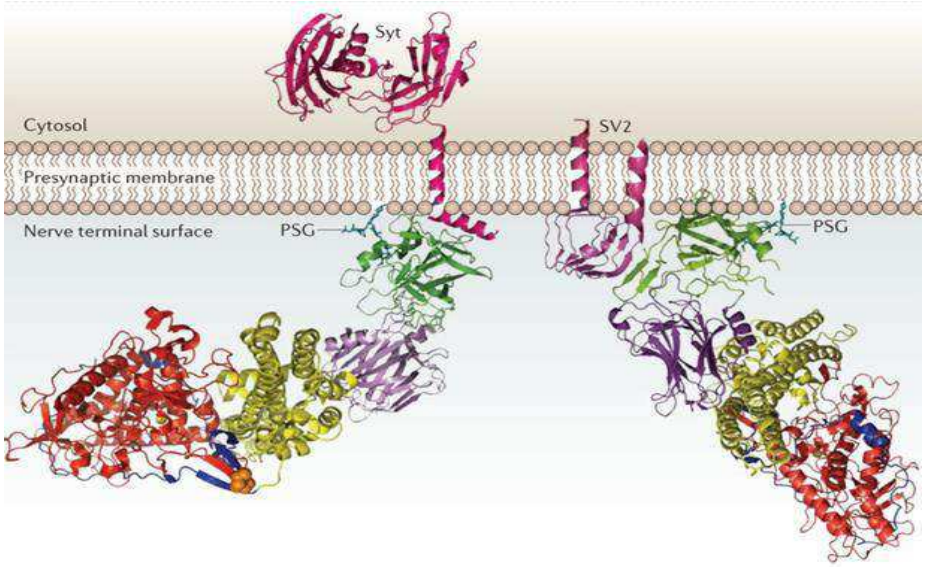

Figure 7. Binding of BoNTs to the nerve terminals. The crystal structure of BoNT/B bound to PSG and Syt is shown on the left-hand side, while the crystal structure of BoNT/A bound to PSG and to SV2 is shown on the right-hand side. Modified from Rossetto *et al.*, 2014[3].

More in detail, the first receptor is represented by polysialoganglioside (PSG): this "evolutionary choice"[59,60] appears to be perfect because PSG molecules are present at a high density on the presynaptic membrane, where they are involved in many pathways like cell signalling, protein sorting and in membrane domain formation and organization[61,62].

Importantly, the most distal part of the PSG is a negatively charged sugar head: this makes possible the interaction with BoNTs, that are dipoles, with the

positively charged end located in the HC domain, in particular in the HC_C, where the PSG-binding site is localized. For BoNT/A, /B, /E, /F and /G this site is characterized by the conserved motif E (or D or Q)...H (or K or G)...SXWY...G (where X is any amino acid and points denote a variable number of residues)[63-65]; while, for BoNT/C, BoNT/DC and BoNT/D the PSG-binding side is found in a similar position, but the motif is different[66-68].

This recognition is probably very rapid and seems to promote BoNTs reorientation, thus allowing the interaction with the second receptor[3]. Accordingly, following the attachment to PSG, HC_C binds to the luminal part of an integral membrane protein of SV. Unlike PSG, these receptors are not exposed on the nerve terminal surface, therefore, are not accessible to BoNT. However, they become available following the fusion of the SV with the presynaptic membrane: in fact, this process exposes the SV lumen to the extracellular environment[3].

Such recognition in mediated by another binding site, always located in the HC_C, close to the PSG-binding site. The currently knowledge identifies Syt I-II as a receptor for BoNT/B, /DC, and /G[65,68-75] and glycosylated synaptic vesicle protein 2 (SV2) for BoNT/A and /E, in particular SV2C appears to be the main receptor involved in BoNT/A binding, while SV2A e SV2B mediate BoNT/E entry[66,76-78]. The second receptors of other BoNTs have not been fully characterized yet, albeit SV2A-C seems to play an important role in the uptake mechanism of BoNT/D and BoNT/F[78].

It is worth to note that BoNTs “choose” as receptors SV proteins that are highly conserved and fundamental for nerve physiology: SV2 renders primed SV competent for Ca^{2+}-induced exocytosis[79], while synaptotagmin is a presynaptic calcium receptor that may be involved in transducing a presynaptic calcium rise into the signal necessary for SV membrane fusion[80].

Also the HC_N participates in the process but its specific function is still unknown, although there is evidence indicating that it may improve BoNTs adhesion to the presynaptic membrane by interacting with anionic lipids [3,81-84].

B) Internalization into nerve terminal

The second step in the intoxication mechanism concerns BoNT internalization into motor neuron. Regarding the peripheral trafficking, BoNT/A take advantage from the SV recycling mechanism, indeed, after membrane fusion and NT release[85], SV are directly recycled or re-enter in the cycle by fusion and subsequent budding from endosome compartiment[25].

In both cultured neurons and *in vivo*, BoNT/A1 enters into SV, and the number of toxins per SV (one or two molecules) seems to be strictly related with the number of SV2 molecules in the lumen (see Figure 8)[86-88].

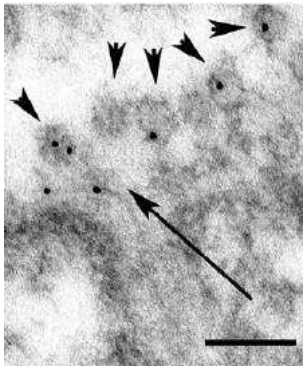

Figure 8. BoNT/A1 is internalized within SV. The immunogold electron micrograph of the NMJ of BoNT injected muscle shows that toxins exploit SV for the internalization in the nerve terminal and that the number of toxins per vesicle is related to protein receptor abundance. Modified from Colasante *et al.,* 2013[86]

Moreover, the rate of BoNT/A entry correlates with endocytosis velocity[15] and it is consistent with toxin potency[89].

The mechanism of internalization of other BoNTs remains to be fully established but the various similarities among different serotypes suggest that the trafficking of BoNTs may occur *via* SV or different endocytic pathways depending on their protein receptors.

C) Translocation into the cytosol

The third step in the intoxication is represented by the translocation of the L within the cytosol. After the internalization, BoNT molecule is found inside SV, used as Trojan horse to penetrate into the neuronal cell. Nevertheless, to promote its toxic action, the molecule has to be in the cytosol where it can reach its protein targets.

Also in this case BoNT takes advantage from the physiology of the NMJ and in particular from the refilling of SV. When endocytosis is completed, the SV lumen is acidified by the proton pumping action of the v-ATPase present on the SV membrane[90,91]. This produces an electrochemical gradient able to drive the accumulation of NT from the cytosol to the SV lumen *via* a specific vesicle NT transporter[85,92].

To date, the molecular aspects of the translocation have been only partially elucidated and are still matter of debate[84,93]. However, it is well known that this step comprises a concerted structural rearrangement involving three players at the same time: the L, the HN and lipids. This conformational change results in the formation of ion conducting channel, which mediates the translocation of the L into the cytosol[84,94-97].

Montal and colleagues gave the major contribution in the comprehension of this process with patch-clamping experiments on the cell membranes and with single-molecule resolution technique, conditions that mimic those found *in vivo*[84,96,98]. They propose a sequential mechanism (see Figure 9) in which the first event is the pH-dependent structural reconfiguration of the HN with the subsequent production of the translocation ion channel.

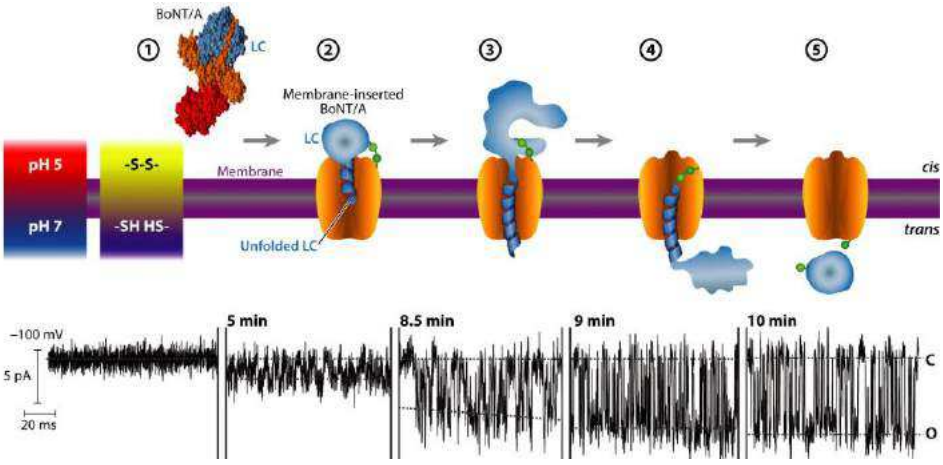

Figure 9. Sequence of events underlying membrane translocation of BoNT L. 1) Crystal structure of BoNT/A before the binding to the lipid bilayers; 2) Ion channel formation; 3) L unfolding with consequent increase in the conductance among the membrane; 4) L translocation through the channel; 5) L refolding in the SV cytosolic side and increase of current flux that reaches its maximum (C and O denote closed and open states of the channel). From Montal, 2010[84,94].

This corresponds to a limited increase of transmembrane currents across the plasma membrane (~ 10 pS) because the channel is partially blocked by the L (see Figure 9, step 2). This first event is a prerequisite and only after that, L unfolds and passes to the SV cytosolic versant. This allows for further increase in the conductance through the lipid membranes (~ 65 pS; see Figure 9, step 3 and 4). Finally, the current flux will reach its maximum when L is refolded and released within the cytosol (~ 110 pS; see Figure 9, step 5)[84].

However, this model does not take into account of other significant data present in literature: i) the conformational change occurs only in the presence of lipids or PSG, in fact, BoNT/B or the L and HN domain of BoNT/A do not change their structure in solution even if a low pH [97,99-103]; ii) membrane studies showed that both the L and H of BoNT/A1, /B1 and /E1 get in touch with phospholipids in a membranes model at low pH[102,104]; iii) the anthrax toxin complex consists of three different molecules, the protective antigen and two active enzymes. Protective antigen inserts at low pH in biological membranes forming ion channels, this is necessary to translocate the enzymes in the cell cytosol. Notably, the ion conductance along this transmembrane channel is blocked even by fragments of transported protein[105-107]. All these evidences do not fit perfectly with the model presented in figure 9, in fact, it is shown that L is protected from the contact with lipids by the H channel and that the channel conductance increase corresponds to the L unfolding.

Recently, our group have provided a revised mechanism of BoNT translocation that takes in account of all these data[93] (see figure 10).

In this new model, we considered that the translocation occurs in a range of pH between 4.5 and 6, consistent with the pH found in the SV lumen. In this condition, amino acids histidine, glutamate and aspartate become protonated. BoNTs lack conserved histidine residues outside the active site but, importantly, in the structure there are nineteen completely conserved carboxylate residues (pKa~5): three in the L, five in the belt region, ten in HN and one in the HC_N portion[93].

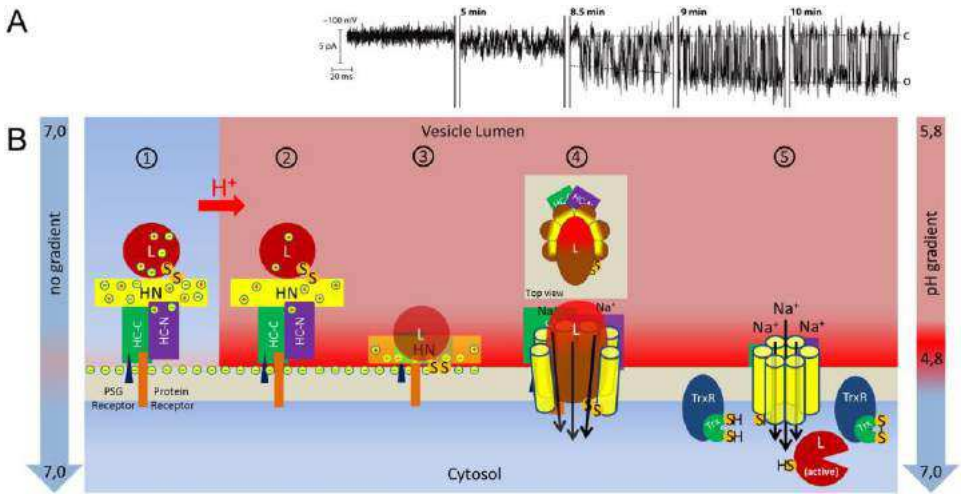

Figure 10. A revised model of SV membrane translocation of BoNT. A) The upper panel shows the increase of plasma membrane conductance of Neuro2A cell induced by BoNT/A action at low pH, taking from Montal, 2010[84]. B) The bottom panel present BoNT structure and the molecular mechanism of translocation. The four domains of the toxin are depicted with different colours and with some conserved charged residues: L (red), HN (yellow), HC_N (purple) and HC_C (green). The HC_c is bound to its two receptors (PSG, blue triangle, and protein, orange rectangle). (1) BoNT molecule has been internalized in the SV; (2) SV lumen acidifies (in pink) thank to the v-ATPase proton pump; (3) electrostatic attraction between HN domain, positively charged, and the lipid membrane, negatively charged; (4) Structural changes involving at the same time L, HN and lipids. At this point there is an increase in the membrane conductance shown in the corresponding upper panel. (5) L arrives in the cytosolic side, refolds and, after disulphide bond reduction, is released. Modified from Pirazzini *et al.*, 2016[93,95].

Notably, these carboxylate residues are located within the BoNT face containing the disulphide bond[93] and the segment 637–688 (numbering related to BoNT/B1), the region that interacts with the membrane[100].

The position of these residues suggests a precise function, probably as pH sensors protonable in a sequential way, according to their pKa, with the lowering of the vesicular pH (Figure 10B, step 2). Partially protonated BoNT has a net positive charge that determine an electrostatic attraction with the negatively charged membrane, thus resulting in the transfer of BoNT towards the membrane surface (Figure 10B, step 3). The approach of BoNTs to the membrane promotes hydrogen bond formation, van der Waals interactions with lipids and an additional protonation of other carboxylate residues (with lower pKa). Owing to Guy-Chapman effect, in fact, the layer of solvent above the

membrane surface is more acidic (Figure 10B, the red layer) than the lumen (Figure 10B, in pink). All these interaction promote the reorganization of the molecule through a series of events: i) disulphide bond inserts into bilayer drawing L towards the membrane; ii) L becomes molten globule, thus increasing its hydrophobicity and making possible the insertion in the lipids; and iii) the α-helices of the HN break and generate amphipathic segments. These, together with other shorter α-helices, open a transmembrane channel surrounding L, inducing lipids destabilization and promoting an increase in the membrane conductance (see Figure 10A and B, step 4).

After L has passed through the SV membrane, the neutral pH of the cytosol promotes L refolding and, as a consequence of disulphide bond reduction, the catalytic activity of the toxin is released within the cell; on the other hand HN channel is empty and reaches its full conductance (see Figure 10A and B, step 5).

This model is different from the previous one: translocation was seen as a concerted process in which the channel formation is a consequence and not a prerequisite for L passage and in which HN domain, together with lipids, act as a molecular chaperons for the translocation of L[93].

However, whether this actually occurs is unknown and additional studies are needed to clarify this step in the BoNT intoxication process. Anyway, is known that the acidification is necessary for BoNTs translocation, since, the inhibition of this process completely abrogate BoNT toxicity[108-110].

D) Reduction of disulphide bond

The fourth step of BoNTs mechanism of action is the reduction of the disulphide bond that links L with the ion channel formed by H.

The reduction of the S-S interchain bridge is a *conditio sine qua non* to free the metalloprotease activity of the molecule in the cytosol of motor neurons, where BoNT can reach its substrate. Consistently, more experimental evidences showed that BoNTs can exert the toxicity toward recombinant substrates exclusively if the disulphide has previously been reduced.

At the same time, is important to note that the integrity of the interchain bond is a requirement for the toxigenicity of the molecule[111], indeed, for a productive

translocation the disulphide must remain intact until L arrives into the cytosol[112,113]. For this reason, the reduction at any preliminary stage aborts channel formation and L translocation[96,114,115]. For example, single chain toxins cannot intoxicate cultured neurons and are not effective *in vivo*[116].

In general, cytosol is considered as a cellular compartment in which the reduced state is largely favoured for maintaining ROS and cysteine oxidation at very low levels[117]. For this reason, there are several redox systems aimed to maintain this situation [118-121]. The major are the glutathione-glutaredoxin and the NADPH-Thioredoxin (Trx)-Thioredoxin reductase (TrxR) systems.

Previous work has shown that the interchain disulphide bridge (but not the other intracatene disulphide present in the structure) of different clostridial neurotoxins can be selectively reduced *in vitro* in the presence of NADPH and Trx-TrxR system (expressed and purified from E. coli)[111] or the same system present in a rat brain lysate[122].

Recently, it has been reported by Pirazzini and colleagues[52] that the glutathione (GSH) system is not involved in the intake of TeNT and BoNT/D toxins, since specific inhibitors that almost totally deplete the GSH's reduced capacity, have been shown to be inefficient in protect cultured neurons from SNAREs proteolysis. This is confirmed also *in vitro,* where GSH has no effect on L release[111]. Conversely, Auranofin, an inhibitor reported to be specific for TrxR and therefore able to effectively decrease the Trx-TrxR system[52,123], proved to be effective. Together, these data suggest that the couple Trx-TrxR is the system involved in the release of BoNTs catalytic domain in the cytosol.

E) SNAREs cleavage

The fifth and last step in BoNTs toxicity is the manifestation of its catalytic activity. Indeed, once released into the cytosol, L works by hydrolysing specific peptide bonds of neuronal SNAREs.

L is an endopeptidase consisting in a compact globule of both α-helix and β-strand presenting the characteristic zinc-binding motif, HExxH (where x is any amino acids). This sequence is conserved for all BoNTs and coordinates the catalytic metal, essential for the catalysis.[49,124]. Considering the tertiary

structure, the active site is located inside a large open cavity that shares a similar architecture among different serotypes, suggesting a common catalytic mechanism[49].

In the intact molecule this groove is occupied by the belt peptide, however, when the L is released, the catalytic site is depleted and the substrate can then inserts itself and be hydrolyzed[47].

Unlike other zinc endopeptidases, BoNTs hydrolyse large polypeptides (SNARE proteins), therefore there are many points of contact between the substrate and the enzyme (so-called exosites). These sites are unique for each serotype with different sizes and distances from the scissile peptide bonds. They are very important in the positioning of the target bond of the substrate and make it accessible to the active site residues of L[49,125-128]. Consistently, mutation in the exosites disrupted substrate binding to the active site decreasing BoNTs catalytic efficiency[127,129].

Although BoNTs active site is conserved and all serotypes are very similar in the structural organization, these different interactions away from the active site result in high selectivity for the substrate and hydrolysable bond selection[125-127,129,130].

As shown in Figure 11, L has a unique SNARE specificity[84,131,132], in particular, BoNT/B, /D, /F, /G cleave VAMP (blue); BoNT/A and BoNT/E cleave SNAP-25 (green); and BoNT/C cleaves both SNAP-25 and Stx (red)[25,133].

With the exception of BoNT/A and BoNT/C, all BoNTs cleave a large portion of SNARE proteins and this prevents the formation of the SNARE complex. On the other hand, BoNT/A and BoNT/C cleave very close to the C-terminal of SNAP-25 and remove only a few residues. This truncated form of SNAP-25 is still able to form a stable SNARE complex but decreases exocytosis efficiency[134]. This suggest that the C-terminal segment is necessary for protein-protein interactions underpinning the formation of a radial SNARE super-complex[11,135].

Nevertheless, each of these proteolysis is sufficient to abrogate SV fusion with a consequent inhibition of the neurotransmission, thus leading to the neuroparalysis typical of botulism[11,135-138].

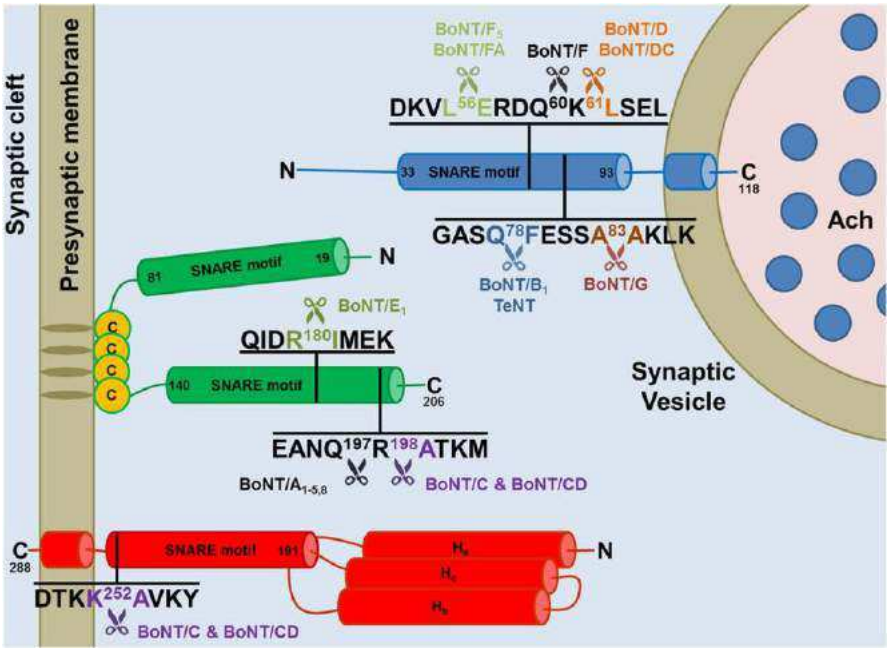

Figure 11. Cleavage sites of the neuronal SNARE proteins by the different BoNT types and subtypes. The BoNT proteolytic activity is highly specific and directed toward unique peptide bonds within the sequence of their respective SNARE protein targets. VAMP of the synaptic vesicle (in blue, isoform 1) or SNAP-25 (in green) or syntaxin (in red, isoform 1B) mainly localized on the cytosolic side of the presynaptic membrane. From Pirazzini *et al.*, 2017[25].

To summarize, BoNTs have evolved to exploit two major physiological events occurring at nerve terminals: SV endocytosis (to selectively enter nerve terminals) and NT refilling of the SV (to deliver the L metalloprotease into the cytosol). Moreover, the efficacy of BoNTs is the result of targeting a physiological function that is essential for life in all vertebrates, the neuroexocytosis. This seems to be an obligatory survival strategy for an anaerobic organism that can multiply only within a non-oxygenated medium, such as a cadaver[3].

1.2.3 The double face of BoNTs

BoNT can be defined “Janus toxins”, from the Greek mythological creature with two faces[25]. In fact, these toxins are the most potent yet known, with an estimated median lethal dose (LD_{50}) for humans around 1 ng/Kg of body weight[25,139] and, at the same time, one of the safest drugs used in several human pathologies[3].

Toxicity of BoNTs:

Although many BoNTs exist, all of them hydrolyze SNARE proteins thus causing SV accumulation in the active zone of the MAT[140], with consequent blockage of the neurotransmission. For this reason, the clinical manifestation of botulism are the same among the different serotypes.

Following intoxication, symptoms start in the muscles supplied by the cranial nerves, the face and throat muscles becoming progressively weaker until complete paralysis is achieved. Diplopia, ptosis, loss of facial expression, swallowing problems and dysphagia may therefore occur (see Figure 12A)[141].

Figure 12. Examples of botulism patients. A) Adult botulism and B) infant botulism. Pictures collected on internet.

Then, the paralysis progressively descends to affect muscles of the trunk, including the autonomic nervous system, resulting in dry mouth, nausea and vomiting. The weakness then spreads to upper and lower limbs[142]. Severe botulism affects also the visceral and respiratory muscles leading to dyspnea and respiratory failure, in this case death comes from suffocation[141].

Infant botulism was caused by the intestinal colonization of infants, it is characterized by lethargy, listlessness, feeble crying, poor feeding, weakness, hypotonia, ptosis and apnea[141] (see Figure 12B). However, the disease does not affect the consciousness and the senses and mental state do not appear altered[142].

Importantly, from a morphological and anatomical point of view, the intoxicated neurons do not appear damaged and axonal neurodegeneration does not occur *in vivo*[143-148]: in fact, the contact between the muscle and the nerve are

completely maintained. For this reason, if properly treated, muscle paralysis is followed by a complete functional recovery and botulism-affected patient survives[24,25,141].

There is currently no approved pharmacological therapy for BoNTs intoxication and no licensed vaccine available for human use. The only treatment consists in mechanical ventilation (to bypass respiratory muscles block), antibiotics (to block the production of toxins) and antisera (to neutralize any circulating toxins)[3,24]. However, the recovery is slow and the time needed to reverse the functional block may vary from a few months to more than a year, depending on the type of nervous terminal involved, the vertebrate species, the dosage, the serotype of BoNT and its half-life in the nerve terminal[3,11,149-153]. In particular, the order of duration in humans is: BoNT/A ~ BoNT/C > BoNT/B[141] ~ BoNT/F, and /G > BoNT/E[24,154-158] with the exception of BoNT/D that is poorly active in humans but very potent in mice[25,152].

Beyond the extreme potency, BoNTs are also relative easy to produce, reason why these toxins have been categorized by the Center for Disease Control and Prevention (CDC) as category A agents, hence substances that can be potentially used as biological weapons[28,159-161].

Pharmacology use of BoNTs:

At the same time, their absolute neurotropism and reversibility of action have enabled BoNTs to be used as effective therapeutic agents. Scott and colleagues were the first to understand the potential of BoNTs in their studies in which, back in 1970s, they treated monkey and human strabismus by injecting BoNT/A1 into the orbicularis muscles[162-164]. It was immediately clear that these toxins could be used for a growing and heterogeneous number of human diseases characterized by hyperfunctioning nerve terminals[3,24,165-169]. The first serotype used to treat human disease was BoNT/A1, approved by the FDA in 1989 for the treatment of blepharospasm, followed by BoNT/B1, which received FDA license in 2000 for cervical dystonia. Since 2002 BoNTs are also used in the cosmetic field[170]. Today BoNTs are approved also for the treatment of strabismus, hemifacial spasm, focal spasticity, cerebral palsy, hyperhidrosis, overactive

bladder and so on (see Table 1) and the number of possible therapeutic applications is growing[171].

Table 1
Therapeutic uses for botulinum neurotoxin

Ophtalmology		
	Strabismus[a,b,c]	
	Nistagmus	
Neurology		
	Focal Dystonias	
		Blepharospasm[a,b,c]
		Cervical dystonia[a,b,c] (Torticollis, anterocollis, laterocollis)
		Occupational dystonias (writer's cramp[b], musician's cramps)
		Laryngeal Dysphonia[c]
		Oromandibular dystonia
		Lingual dystonia
	Nondystonic disorders	
		Hemifacial spasm[a,b,c]
		Tremor (essential, parkinsonism)
		Tics
		Bruxism
	Spasticity (poststroke, multiple sclerosis, brain or spinal cord injury)	
		Focal spasticity[a,b,c]: Upper and lower limb spasticity
		Nonfocal: hemispasticity, paraspasticity, tetraspasticity
		Cerebral palsy[a,b]
	Hyperhidrosis[a,b,c]	
		Focal: axillary, palmar, plantar
		Diffuse
	Hypersalivation	
		Sialorrhea[b] (motoneuron diseases/amyotrophic lateral sclerosis)
		Drooling[b] (Parkinsonian syndromes)
		Frey's syndrome/gustatory sweating
	Aesthetic (muscle)	
		Glabellar rythides[a,b,c]
Pain		
	Muscular	
		Dystonia
		Spasticity
		Chronic myofascial pain
		Temporomandibular disorders
		Low back pain
	Nonmuscular	
		Migraine (chronic[a] and tension type migraine)
		Neuropathic pain
		Trigeminal pain
		Pelvic pain
Urology		
	Detrusor sphincter dyssynergia	
	Overactive bladder[a,b,c] (Idiopathic or neurogenic detrusor overactivity)	
	Urinary retention	
	Bladder pain syndrome	
	Pelvic floor spasms	
	Benign prostate hyperplasia	
Gastroenterology		
	Achalasia	
	Chronic anal fissures	
Psychiatry		
	Depression[d]	

Modified from Pirazzini *et al.*, 2017[25]. [a]USA approved indication; [b]EU approved indication; [c]evidence-based therapeutic indication and [d]to be evaluated.

To date, unfortunately, little is known about the use of other BoNT serotypes or mosaic toxins, therefore, expanding knowledge could represent a great therapeutic potential. This could be also helpful for subjects who did not respond to BoNT/A1 treatment as well as for those who have developed resistance producing anti-BoNTs antibodies[172,173].

This, together with the numerous applications shown in the Table 1, highlight the importance to continue studying BoNTs both from a functional and a therapeutic point of view in order to make the most of their potential.

Chapter 2

Aim of the thesis

Botulinum neurotoxins (BoNTs) are the most poisonous poisons known[3,24,25,139] but, at the same time, their specificity and reversibility of action[141] is at the basis of their therapeutic use for the treatment of human diseases characterized by hyperactive peripheral nerve terminals[3,25,165-169].
During my PhD I focused on both these aspects.

Aim i) To study BoNTs mechanism of action to find new strategies to block their toxicity. Currently, available therapy is designed to neutralize circulating toxin by using anti-botulinum sera[3,24,25]. However, the discovery of many BoNT subtypes and new serotypes[3,16,17] challenges the possibility of controlling BoNT toxicity exclusively *via* immunological methods[24]. In fact, antisera are raised against progenitor serotypes (i.e. subtype 1 BoNTs) and the real neutralization capacity toward BoNT subtypes is not known[25]. However, it may change significantly considering that intratypic variability may reach 30%[174]. At the same time such a variability strongly limit the possibility of developing an effective pan-vaccine[175-178]. Moreover, the action of antibodies is restricted to circulating BoNTs and not to the molecules already internalized in nerve terminals. This situation has stimulated an intense research of alternative strategies all around the world. So far, many research group have focused on molecules aimed at blocking the catalytic activity of BoNTs inside nerve terminal[179-181] or to prevent their binding to peripheral nerve terminals[182]. However, these approaches have been poorly

successful mainly because the molecular steps they target are still strongly dependent on the toxin type.

As a consequence, no adequate countermeasures have been made available[183]. During my PhD, I explored an alternative strategy to block the intoxication process by targeting steps of their mechanism of action which are common to all BoNTs, regardless of their antigenic difference[3,18]. The results of this part of my work are reported in section 3.1.

Aim ii) To better understand how BoNT/C displays its neuroparalytic action *in vivo* as this toxin was shown to be a valid alternative to BoNT serotypes licensed for human therapy[147,148,184].

The use of BoNTs as therapeutics is indeed currently restricted to BoNT/A1 and BoNT/B1. However, in the last years, other serotypes have been investigated for clinical use in humans[148,155,184,185] to overcome primary or secondary resistance (development of anti-toxin antibodies).

During my PhD, I investigated the mechanism by which BoNT/C paralyses the neuromuscular junction *in vivo* as this toxin, at variance from all other serotypes, cleaves more than one SNARE protein. The results of this research are shown in section 3.2.

Chapter 3

Results

3.1 Study of pan-inhibitors to prevent BoNTs toxicity

Each BoNT serotype includes a growing number of subtypes (BoNT/A1, /A2, etc.) forming a large family of more than 40 different variants which are poorly cross-reactive with existing serotype-specific antisera[3]. This calls for the research of novel antidotes, effective regardless of BoNT's immunological properties. This can be achieved by interfering with conserved steps of their mechanism of action.

- The reduction of the interchain disulphide bond offers a good target, as it represents a *conditio sine qua non* to enable the metalloprotease activity of all BoNT variants. During my PhD, I contributed to the finding that the Trx-TrxR system is primarily involved in this step and that it is highly expressed at the NMJ, the major site of action of BoNTs. Notably, Trx-TrxR is associated with SVs, the organelles that BoNTs use as Trojan horse to penetrate in the neurons and where the reduction is expected to occur. I tested a series of well characterized inhibitors of TrxR (Auranofin, Juglone, Myricetin and Curcumin) and Trx (PX12 and Ebselen) for their capacity of inhibiting the action of all BoNT serotypes. Performing *in vivo* and *in vitro* experiments, I found that these drugs prevent the toxicity of all BoNT regardless of the serotype. Interestingly the effective concentration range of inhibitors is similar for the different BoNTs,

indicating that these neurotoxins are comparably dependent on disulphide reduction and that the Trx-TrxR system is part of the basic uptake mechanism of all BoNTs and can be considered a rational target for the development of mechanism-based pan-inhibitors.

- BoNT's toxicity is strictly dependent on the passage through an acidic environment, which is required to trigger the translocation of L within the cytosol. Accordingly, the trafficking of BoNTs toward acidifying endosomes represents another rational target to develop pan-inhibitors. In 2013, EGA (4-bromobenzaldehyde N-(2,6-dimethylphenyl) semicarbazone) was shown to inhibit the action of bacterial toxins and viruses with a similar requirement, by interfering with their entry route[186]. I decided to test the activity of EGA on BoNTs action.

  I focused my attention on BoNT/A, BoNT/B and BoNT/D because they are associated with human and animal botulism, respectively.

  I found that EGA hinders BoNT's activity in neuronal cultures in a concentration dependent manner. Interestingly, any specific step of the intoxication process (binding, internalization, acidification/translocation and catalytic activity) is not directly affected by the drug, suggesting that EGA may alter the trafficking of BoNTs after their internalization, possibly preventing them to reach their translocation-competent compartment.

  EGA is effective also *in vivo* against BoNT toxicity, suggesting that this compound might be a promising candidate for the development of pan-inhibitors.

3.1.1 Thioredoxin and its reductase are present on synaptic vesicle, and their inhibition prevents the paralysis induced by botulinum neurotoxin

Marco Pirazzini[1,5], Domenico Azarnia Tehran[1,5], Giulia Zanetti[1], Aram Megighian[1], Michele Scorzeto[1], Silvia Fillo[2], Clifford C. Shone[3], Thomas Binz[4], Ornella Rossetto[1], Florigio Lista[2] and Cesare Montecucco[1]

[1]Department of Biomedical Sciences and National Research Council Institute of Neuroscience, University of Padova, Via Ugo Bassi 58/B, 35151 Padova, Italy

[2]Histology and Molecular Biology Section, Army Medical and Veterinary Research Center, Via Santo Stefano Rotondo 4, 00184 Rome, Italy

[3]Public Health England, Porton Down, Salisbury, Wiltshire SP4 OJG, UK

[4]Institut für Biochemie, Medizinische Hochschule, Hannover, 30623, Hannover, Germany

[5]Co-first author

Pirazzini M, Azarnia Tehran D. *et al.* Thioredoxin and Its Reductase Are Present on Synaptic Vesicles, and Their Inhibition Prevents the Paralysis Induced by Botulinum Neurotoxins. *Cell Rep* 8, 1870-1878.
doi: 10.1016/j.celrep.2014.08.017 (2014).

Article

Cell Reports

Thioredoxin and Its Reductase Are Present on Synaptic Vesicles, and Their Inhibition Prevents the Paralysis Induced by Botulinum Neurotoxins

Graphical Abstract

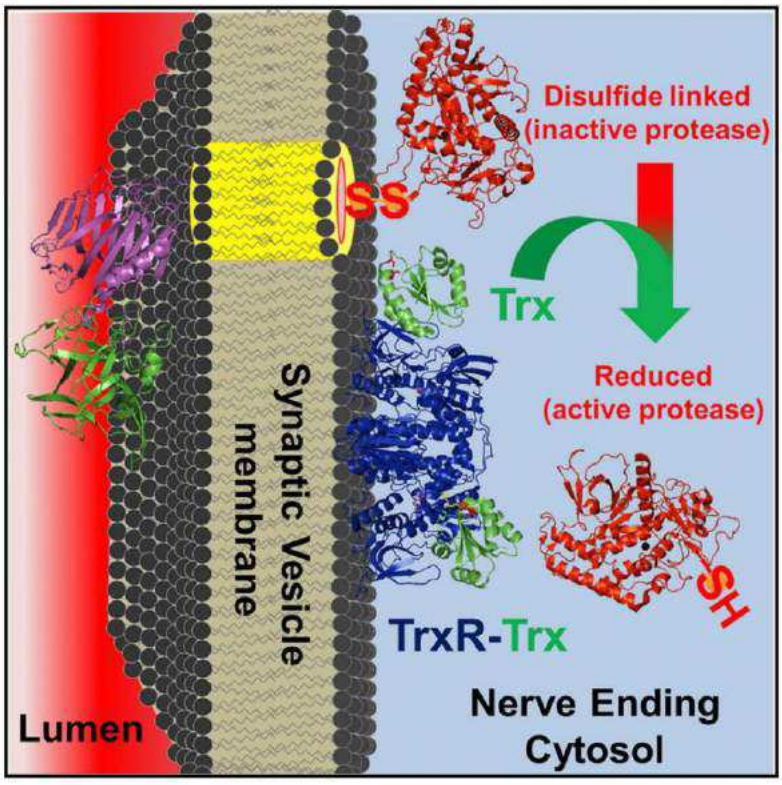

Authors

Marco Pirazzini, Domenico Azarnia Tehran, ..., Florigio Lista, Cesare Montecucco

Correspondence

cesare.montecucco@gmail.com

In Brief

About 40 botulinum neurotoxins have been recently discovered, highlighting the need for chemical inhibitors that target these potent toxins. Pirazzini et al. now find that synaptic vesicles possess the thioredoxin reductase-thioredoxin system and show that it is responsible for the selective cleavage of a key toxin disulfide bond, a step required for the entry of all such neurotoxins into neurons. The authors thus uncover a class of inhibitors capable of acting in vivo.

Highlights

Synaptic vesicles possess an active thioredoxin reductase-thioredoxin system

The two proteins are on the cytosolic side of the synaptic vesicle membrane

This system reduces the interchain disulfide bond of botulinum neurotoxins

Specific inhibitors prevent the neuroparalysis induced by botulinum neurotoxins

Pirazzini et al., 2014, Cell Reports 8, 1–9
September 25, 2014 ©2014 The Authors
http://dx.doi.org/10.1016/j.celrep.2014.08.017

CellPress

Please cite this article in press as: Pirazzini et al., Thioredoxin and Its Reductase Are Present on Synaptic Vesicles, and Their Inhibition Prevents the Paralysis Induced by Botulinum Neurotoxins, Cell Reports (2014), http://dx.doi.org/10.1016/j.celrep.2014.08.017

Cell Reports
Article

Thioredoxin and Its Reductase Are Present on Synaptic Vesicles, and Their Inhibition Prevents the Paralysis Induced by Botulinum Neurotoxins

Marco Pirazzini,[1,5] Domenico Azarnia Tehran,[1,5] Giulia Zanetti,[1] Aram Megighian,[1] Michele Scorzeto,[1] Silvia Fillo,[2] Clifford C. Shone,[3] Thomas Binz,[4] Ornella Rossetto,[1] Florigio Lista,[2] and Cesare Montecucco[1,*]
[1]Department of Biomedical Sciences and National Research Council Institute of Neuroscience, University of Padova, Via Ugo Bassi 58/B, 35121 Padova, Italy
[2]Histology and Molecular Biology Section, Army Medical and Veterinary Research Center, Via Santo Stefano Rotondo 4, 00184 Rome, Italy
[3]Public Health England, Porton Down, Salisbury, Wiltshire SP4 OJG, UK
[4]Institut für Biochemie, Medizinische Hochschule Hannover, 30623 Hannover, Germany
[5]Co-first author
*Correspondence: cesare.montecucco@gmail.com
http://dx.doi.org/10.1016/j.celrep.2014.08.017

SUMMARY

Botulinum neurotoxins consist of a metalloprotease linked via a conserved interchain disulfide bond to a heavy chain responsible for neurospecific binding and translocation of the enzymatic domain in the nerve terminal cytosol. The metalloprotease activity is enabled upon disulfide reduction and causes neuroparalysis by cleaving the SNARE proteins. Here, we show that the thioredoxin reductase-thioredoxin protein disulfide-reducing system is present on synaptic vesicles and that it is functional and responsible for the reduction of the interchain disulfide of botulinum neurotoxin serotypes A, C, and E. Specific inhibitors of thioredoxin reductase or thioredoxin prevent intoxication of cultured neurons in a dose-dependent manner and are also very effective inhibitors of the paralysis of the neuromuscular junction. We found that this group of inhibitors of botulinum neurotoxins is very effective in vivo. Most of them are nontoxic and are good candidates as preventive and therapeutic drugs for human botulism.

INTRODUCTION

The botulinum neurotoxins (BoNTs) are released by different species of Clostridia in dozens of different isoforms that are grouped into seven different serotypes (BoNT/A–BoNT/G) (Hill and Smith, 2013; Rossetto et al., 2014). They inhibit peripheral cholinergic nerve terminals and cause the flaccid paralysis and autonomic dysfunctions of botulism (Johnson and Montecucco, 2008). BoNTs are so toxic to humans as to be considered for potential use in bioterrorism (CDC, 2012). At the same time, their neurospecificity and reversibility of action makes them excellent therapeutics for a growing and heterogeneous number of human diseases that are characterized by a hyperactivity of peripheral nerve terminals (Davletov et al., 2005; Dressler, 2012; Masuyer et al., 2014; Montecucco and Molgó, 2005).

BoNTs consist of a metalloprotease light chain (L; 50 kDa) and a heavy chain (H; 100 kDa) linked by a strictly conserved interchain disulfide bond. BoNTs bind specifically to the presynaptic membrane of peripheral nerve terminals (Dolly et al., 1984) and enter into the cytosol, where they block neurotransmitter release by the L-mediated cleavage of the essential SNARE proteins (Binz and Rummel, 2009; Pantano and Montecucco, 2014). The seven BoNT serotypes exhibit exclusive specificities with respect to the different SNARE proteins and therefore can be used as simple tools to determine the effect of knocking out specific SNAREs in cell physiology (Pantano and Montecucco, 2014). To penetrate into neurons, BoNTs exploit the endocytosis of synaptic vesicles (SVs) (Colasante et al., 2013), and the acidification of the SV lumen induces the H-mediated membrane translocation of L (Fischer and Montal, 2013; Montal, 2010). It has been demonstrated that, once on the cytosolic side, the L metalloprotease remains attached to H via the interchain SS bridge and the reduction of this bond releases the L metalloprotease activity, unblocking at the same time the ion channel formed by H in the membrane (Fischer and Montal, 2007). Here, we show that the thioredoxin reductase (TrxR)-thioredoxin (Trx) redox system is highly expressed in the motor neurons nerve terminals and that it is present on the SV cytosolic surface. This redox system is shown here to be functional, as inhibitors of TrxR or Trx effectively prevent the cleavage of SNAP25 by the L chains of BoNT/A, BoNT/C, and BoNT/E within neurons in culture and largely reduce the neuroparalysis of these neurotoxins in mice. Such a high inhibition of BoNTs by small-molecule drugs in vivo strongly suggests that these drugs may be useful to prevent and treat botulism.

RESULTS

Thioredoxin Reductase and Thioredoxin Are Present on the Cytosolic Surface of SVs

The recent finding that auranofin, a TrxR inhibitor, prevented the action of tetanus neurotoxin in cultured neurons (Pirazzini

OPEN ACCESS
CellPress

Please cite this article in press as: Pirazzini et al., Thioredoxin and Its Reductase Are Present on Synaptic Vesicles, and Their Inhibition Prevents the Paralysis Induced by Botulinum Neurotoxins, Cell Reports (2014), http://dx.doi.org/10.1016/j.celrep.2014.08.017

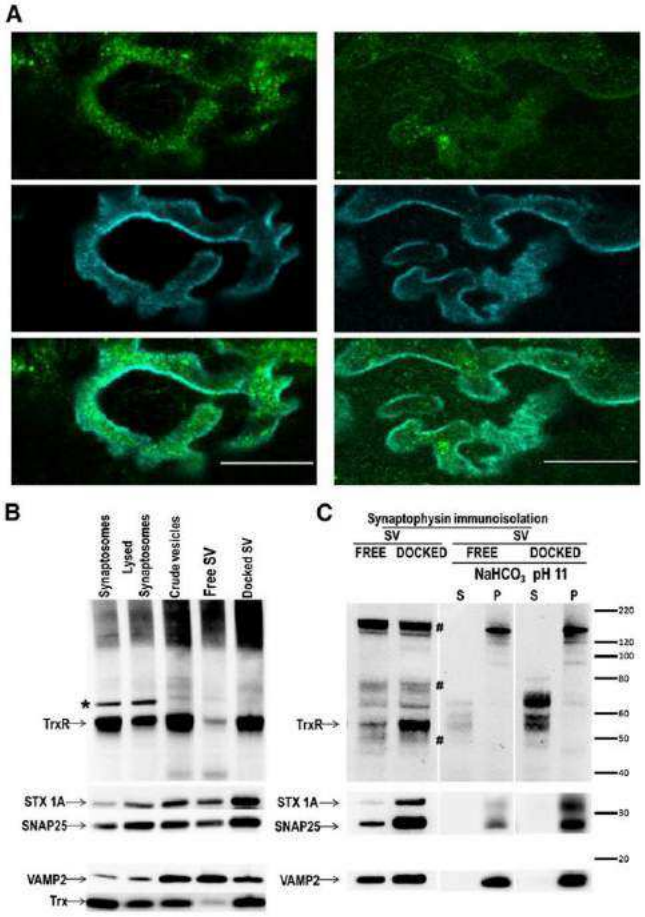

Figure 1. Thioredoxin Reductase and Thioredoxin Are Present in Nerve Terminals and Are Loosely Bound to the Surface of Synaptic Vesicles

(A) The left panels show representative confocal images of the *levator aureus longus* mouse neuromuscular junction stained with primary antibodies specific for thioredoxin reductase (TrxR, green) and α-bungarotoxin (cyan); similarly, the right panels refer to thioredoxin (Trx, green) and α-bungarotoxin (cyan). As expected, both proteins appear to be present also in muscle fibers; scale bar, 10 μm. See also Figure S1A.

(B) The immunoblot staining of different preparations from the rat brain (indicated on the top of the lanes; 10 μg of total lysate proteins per lane) after SDS-PAGE are shown. TrxR, anti-thioredoxin reductase; Trx, anti-thioredoxin; STX 1A, anti-syntaxin; SNAP25, anti-SNAP25; VAMP2, anti-VAMP2. The electrophoretic mobility corresponding to the different molecular weight markers is indicated. The asterisk indicates an immunoreactive band relative to an alternative splicing form of TrxR of 66 kDa (UniProt database).

(C) This panel shows immunoblottings with different specific antibodies of free and active zone-docked synaptic vesicles immunoisolated with an antibody specific for synaptophysin and probed for TrxR presence. The four lanes on the right part of the panel show that TrxR is detached from SVs upon treatment with bicarbonate/carbonate pH 11 buffer (S, supernatant; P, pellet). In both panels, membranes were stripped and restained for SNARE proteins. Hashtags indicate antibody bands.

et al., 2013) prompted us to investigate the presence of the TrxR-Trx system within nerve terminals and on synaptic vesicles, which are the Trojan horses used by BoNT/A to deliver its L chain in the cytosol (Colasante et al., 2013; Harper et al., 2011). Figure 1A shows that the neuromuscular junction, which is the major site of action of BoNTs, highly expresses both TrxR and Trx, as do primary cultures of neurons (Figure S1A). This is in agreement with previous work, where it was shown that both TrxR and Trx are transported from the cell body to axon terminals (Rozell et al., 1985; Stemme et al., 1985). Figure 1B demonstrates that both TrxR and Trx are present in synaptosomes purified from rat brain as well as in a crude preparation of SVs extracted from the same synaptosomes (Figure 1B). Further purification of SV indicates that this enzymatic redox system is indeed associated with SVs and that it is highly enriched in docked SVs (Figure 1B); i.e., SVs that are bound to the active zones in the presynaptic nerve terminal (Boyken et al., 2013; Morciano et al., 2005, 2009), and includes portions of the presynaptic plasma membrane, as disclosed by the presence of plasma membrane markers (Figure S1B, Ca-ATPase and Na/K-ATPase pumps); at the same time, all the fractions display the typical relative abundance of presynaptic proteins (Figure S1B). Notably, the staining of PSD95, a postsynaptic protein, is present only in synaptosomes but essentially absent in free and docked synaptic vesicles, suggesting that the TrxR-Trx belongs to the presynaptic compartment (Figure S1B). Moreover, Figure 1C shows that SVs immunoisolated with an antibody specific for synaptophysin, a protein marker of SVs (Fykse et al., 1993), do contain TrxR. The TrxR-Trx redox system is bound extrinsically to the SV surface, as it is removed upon incubation with bicarbonate/carbonate buffer at pH 11 (Figure 1C). Such a location explains why these proteins were not detected before in thorough proteomics studies of SVs, because bicarbonate-washed SVs were employed (Boyken et al., 2013; Morciano et al., 2005; Takamori et al., 2006). At the same time, it indicates that the TrxR-Trx redox system may play an important role in neuroexocytosis.

Inhibitors of Thioredoxin Reductase Prevent the Intoxication of Neurons by Botulinum Neurotoxin Serotypes A, C, and E

Even if the role(s) of the TrxR-Trx system in SV function remains to be discovered, we used BoNT intoxication as readout of its functionality, following the demonstration that the cytosolic reduction of the single interchain disulfide bond is essential to enable their metalloprotease activity (Fischer and Montal, 2007; Schiavo et al., 1993). Here, and in the next sections, we show the effects of a large series of TrxR-Trx inhibitors on its capability to reduce the interchain disulfide bridge of BoNT/A, BoNT/C, and BoNT/E. These three botulinum neurotoxins were chosen because they have different structures (Kumaran et al., 2009; Lacy et al., 1998) and are implicated in human and animal botulism, and because BoNT/A is used in human therapy (Dressler, 2012; Hallett et al., 2013; Naumann et al., 2013).

Figure 2A shows that an antibody specific for the BoNT/A-truncated SNAP25 stains well a BoNT/A-treated primary culture of neurons consisting of more than 95% cerebellar granular neurons (CGNs), while no labeling was detectable when neurons were pretreated with the TrxR-specific inhibitors juglone

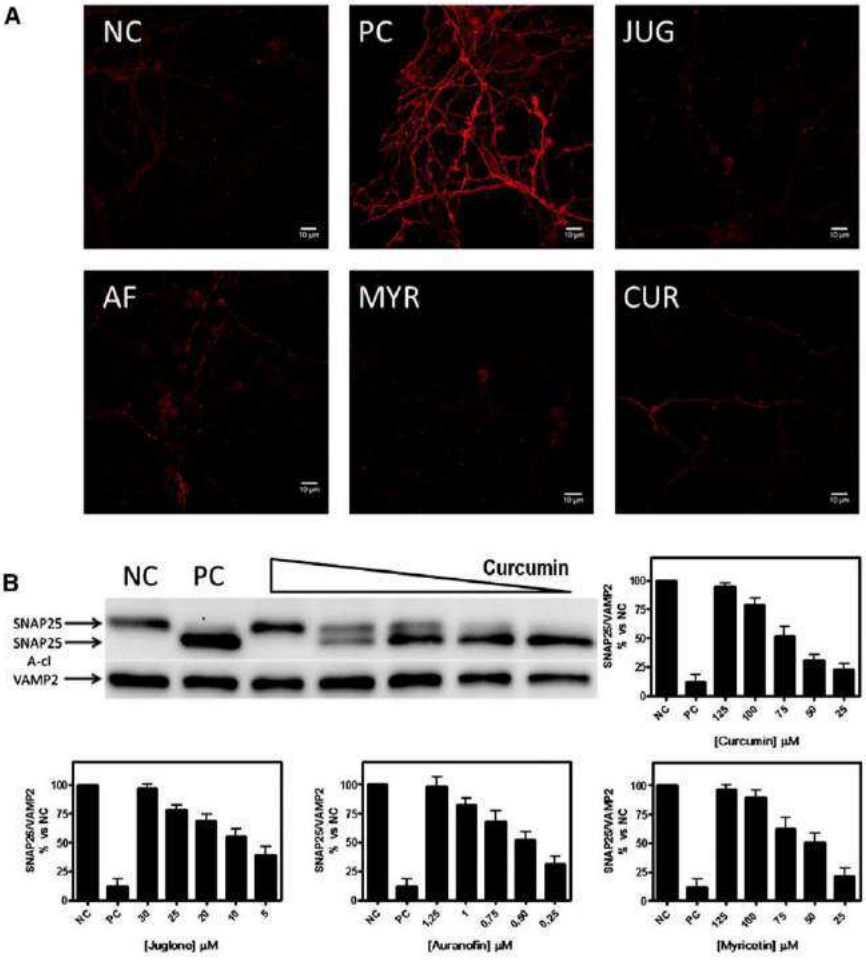

Figure 2. The BoNT/A-Induced Cleavage of SNAP25 Is Prevented in Cerebellar Granular Neurons by Thioredoxin Reductase Inhibitors

(A) CGNs were treated with TrxR inhibitors (JUG, 20 µM; AUR, 1 µM; MYR, 75 µM; CUR, 100 µM) or vehicle (NC, no toxin; PC, toxin treated) at 37°C. After 30 min, BoNT/A 1 nM was added for an additional 30 min to all samples except NC, and then neurons were washed and incubated in the presence of the same concentration of inhibitors for an additional 2 hr. Samples were fixed and stained with an antibody specific for the C terminus of the BoNT/A-cleaved SNAP25 ($SNAP25_{1-197}$). Anti-BoNT/A-cleaved SNAP25 was detected with an Alexa Fluor 555-conjugated secondary antibody. Images shown are representative of three independent sets of experiments. Scale bar, 10 µm. See also Figure S2A.

(B) Quantification of SNAP25 by immunoblotting. CGNs were preincubated for 30 min with the indicated concentration of inhibitor at 37°C, BoNT/A 1 nM was added for 15 min, cells were washed, and culture medium with the same concentration of inhibitor was restored and incubation prolonged for 12 hr at 37°C. Cells were lysed and the SNAP25 content was estimated with an antibody that recognizes both the cleaved and the intact form of SNAP25 and another one specific for VAMP2, as an internal control. The top left panel reports a typical immunoblot resulting from an experiment in which curcumin was present (NC, no toxin no inhibitor added; PC, no inhibitor plus BoNT/A 1 nM final concentration; the five right lanes refer to sample treated with the increasing curcumin concentrations indicated in the right panel). The other panels report the amount of SNAP25 determined as a ratio to VAMP2 staining, which serves as internal control, taking the value in nontreated cells (NC) as 100% in CGNs samples treated with the indicated amounts of the different inhibitors and with BoNT/A. SD values derive from three independent experiments performed in triplicate. See also Figures S2B and S2C. Similar results were obtained when 10 pM BoNT/A was left, together with inhibitors, for 12 hr at 37°C before cell lysis and evaluation of SNAP25 cleavage (not shown).

(JUG), auranofin (AUR), myricetin (MYR), and curcumin (CUR) (Cai et al., 2012; Fang et al., 2005; Lu and Holmgren, 2012; Lu et al., 2006; Omata et al., 2006; Rackham et al., 2011). Figure 2B shows that the inhibition of the BoNT/A-mediated cleavage of SNAP25 by these inhibitors is dose dependent. In control experiments, we found that these TrxR inhibitors do not significantly affect the viability of CGNs at the maximal doses used and that they do not affect the metalloproteolytic activity of BoNT/A tested in vitro with recombinant SNAP25 (not shown). Similar experiments were performed with CGNs treated with BoNT/E (Figure S2A and S2B) and BoNT/C (Figure S2C); in this latter case, the readout of inhibitor activity was also performed with an antibody specific for syntaxin, as BoNT/C cleaves both SNAP25 and syntaxin (Pantano and Montecucco, 2014). It should be noted that the TrxR inhibitors used here show similar dose-dependence patterns versus the three different neurotoxins, indicating that the step they inhibit has similar relevance for the display of the SNARE cleavage activity of the three different BoNTs.

Inhibitors of Thioredoxin Prevent the Intoxication of Neurons by Botulinum Neurotoxin Serotypes A, C, and E

The reduction of the protein disulfides in the cytosol by the TrxR-Trx system is the end result of the transfer of reducing equivalents from NADPH to TrxR and then to Trx (Arnér and Holmgren, 2000; Hanschmann et al., 2013; Lu and Holmgren, 2009). The majority of available inhibitors of this redox system are directed toward TrxR, but recently, specific inhibitors of Trx have been tested in humans: PX-12 is under clinical trial as and anticancer agent (Baker et al., 2013; Kirkpatrick et al., 1998; Ramanathan et al., 2011), and ebselen is under investigation as a postischemia and poststroke therapeutic (Aras et al., 2014; Yamaguchi et al., 1998; Zhao et al., 2002). PX-12 and ebselen (EBS) inhibit the BoNT/A-induced cleavage of SNAP25 in CGNs as detected by immunofluorescence (Figure 3A) and by quantitative immunoblotting (Figure 3B). At the same time, neither PX-12 nor ebselen affects the viability of CGNs at the maximal doses used here, nor do they show any effect on the metalloproteolytic activity of BoNT/A (not shown). A similar efficacy of these inhibitors was

Please cite this article in press as: Pirazzini et al., Thioredoxin and Its Reductase Are Present on Synaptic Vesicles, and Their Inhibition Prevents the Paralysis Induced by Botulinum Neurotoxins, Cell Reports (2014), http://dx.doi.org/10.1016/j.celrep.2014.08.017

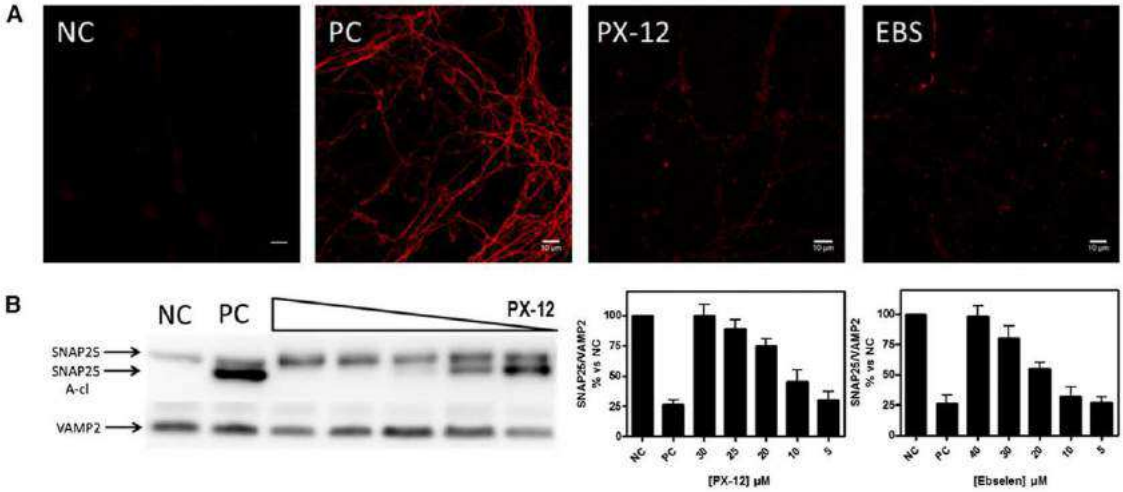

Figure 3. Inhibitors of Thioredoxin Prevent the SNAP25 Cleavage by BoNT/A in Cerebellar Granular Neurons

(A) CGNs were treated with Trx inhibitors (PX-12 25 μM or EBS 30 μM) or vehicle (NC, no toxin; PC, toxin treated) at 37°C. After 30 min, BoNT/A 1 nM was added for an additional 30 min, neurons were washed, and the incubation with the same concentration of inhibitors was prolonged for 2 hr. Treated neurons were fixed and stained with an antibody specific for the BoNT/A-cleaved form of SNAP25 ($SNAP25_{1-197}$). BoNT/A-cleaved SNAP25 was detected with an Alexa Fluor 555-conjugated secondary antibody. These images are representative of three independent sets of experiments. Scale bar, 10 μm. See also Figure S3A.

(B) Quantification of SNAP25 by immunoblotting. CGNs were preincubated for 30 min with the indicated concentration of inhibitor at 37°C, BoNT/A 1 nM (final concentration) was added for 15 min, cells were washed, and culture medium with the same concentration of inhibitor was restored and incubation prolonged for 12 hr at 37°C. Cells were lysed and the SNAP25 content was estimated with an antibody that recognizes both the cleaved and the intact form of SNAP25 and another one specific for VAMP2, as an internal control. The left panel reports the result of a typical experiment aimed at determining the effect of thioredoxin inhibitor PX-12. The right five lanes derive from samples exposed to increasing concentrations of PX-12 indicated in the middle panel. NC, no toxin added; PC, toxin added in absence of PX-12. The middle and right panels report the amount of SNAP25 determined as a ratio to VAMP2 staining, which serves as internal control in samples treated with the indicated amounts of the two inhibitors, taking the value of nontreated cells (NC) as 100%. SD values derive from three independent experiments performed in triplicates. See also Figures S3B and S3C. Similar results were obtained when 10 pM BoNT/A was left, together with inhibitors, for 12 hr at 37°C before cell lysis and evaluation of SNAP25 cleavage (not shown).

found in the prevention of the intoxication of CGNs by BoNT/E (Figures S3A and S3B) or by BoNT/C (Figure S3C).

Thioredoxin and Thioredoxin Reductase Inhibitors Inhibit the Peripheral Neuroparalysis Induced by Botulinum Neurotoxin Serotypes A and C

The panel of inhibitors of TrxR and of Trx used here have been extensively tested in animals and in humans as possible therapeutics in different diseases (Hanschmann et al., 2013; Holmgren and Lu, 2010; Mahmood et al., 2013) and are nontoxic at the doses used here. This encouraged us to test their activity in preventing BoNT toxicity in mice by using as a readout the digit abduction score (DAS) assay, which provides a reliable estimation of the paralysis induced by a local injection of toxin (Broide et al., 2013). Notably, such an experiment avoids the death of the animal and allows one to follow the rate of muscular activity recovery with time. In fact, this assay exploits a remarkable property of BoNTs; i.e., the complete reversibility of their peripheral neuroparalytic action (Rossetto et al., 2014). Figures 4 and S4 report these profiles for BoNT/A and BoNT/C, respectively, which are the two BoNT serotypes characterized by a long duration of action (Eleopra et al., 1997; Morbiato et al., 2007). It is clearly shown that the intramuscular injection of auranofin, myricetin, and curcumin (Figures 4A and S4A), and of PX-12 and ebselen (Figures 4B and S4B), are effective in lowering the neuroparalytic effect of these neurotoxins, permitting a more rapid recovery of the muscle activity. Notably, the latter two inhibitors, which act on Trx, are particularly effective. The DAS assay with BoNT/E does not provide significant results due to the very short duration of action of this BoNT serotype in mice (Rossetto et al., 2006). The inhibitory effect was also demonstrated by classical electrophysiological recordings (Molgo et al., 1990) of the treated hindlimbs. Figure 4C shows that the soleus muscle excided 1 week after BoNT/A local injection presents the complete blockade of the evoked end-plate potential (EEPP). On the other hand, muscles that were pretreated before the local injection of BoNT/A with myricetin, which acts upon TrxR, or with PX-12, which acts upon Trx, show an almost complete recovery of the EEPP, while the injection of the sole drugs does not alter the EEPP (Figure S4C). Finally, the possible inhibitory activity of these drugs in the prevention of death from botulism was evaluated. We used ebselen to perform this proof of principle, since this drug is representative of the other ones used here as it interacts with both TrxR and Trx (Zhao et al., 2002). More extensive trials of this kind were not allowed by the local animal ethical committee because of the large number of animals required. Figure 4D shows that a systemic pretreatment of mice with a well-tolerated dose of ebselen (7.5 mg/kg) (Meotti et al., 2003) significantly reduces the number of deaths induced by a 2-fold lethal dose of BoNT/A. Remarkably, this pretreatment also largely extends the life of the remaining animals, a figure of great significance for human botulism.

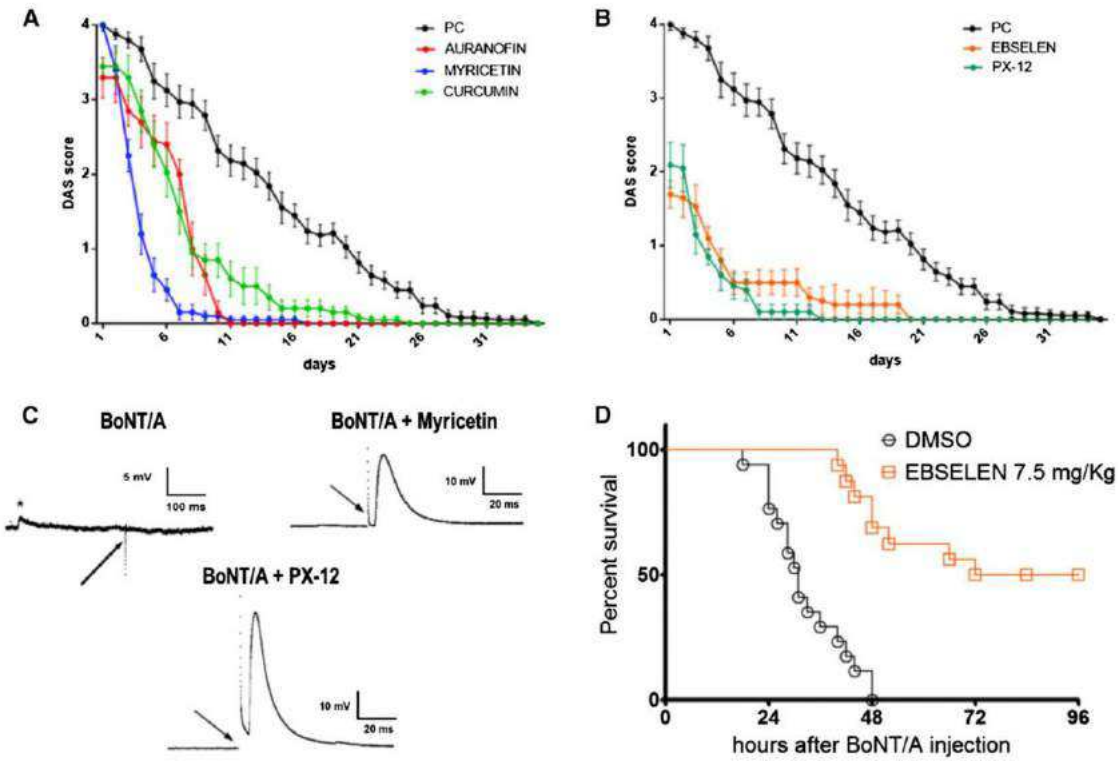

Figure 4. Thioredoxin and Thioredoxin Reductase Inhibitors Largely Prevent the Local Paralysis and Death Induced by BoNT/A

(A and B) Digit abduction score (DAS) changes with time after injection of 15 pg of BoNT/A in the mouse hindlimb after a previous injection with the indicated TrxR (A) or Trx (B) inhibitors or vehicle only (PC); DAS scores for animals treated with inhibitors only are not shown for clarity. All values are means ± SEM from four individual experiments using at least three animals per condition. See also Figures S4A and S4B.

(C) Representative traces of evoked postsynaptic potential by nerve stimulation in *soleus* muscles dissected at day 6 from mice treated as PC (left) or as in (A) (middle) or (B) (right). Traces represent intracellular recordings of evoked postsynaptic potentials following nerve stimulation (arrow), with resting membrane potential clamped at −70 mV. In BoNT/A-treated muscle fibers, no postsynaptic potentials could be evoked, indicating complete nerve block. Star indicates a spontaneous miniature end-plate potential. See also Figure S4C.

(D) Ebselen reduces BoNT/A lethality. Adult male CD1 mice preconditioned with ebselen 7.5 mg/kg (n = 15) or vehicle (n = 15) (see Experimental Procedures) were i.p. injected with 2 × MLD_{50} of BoNT/A. The animals were monitored every 4 hr for 96 hr. The survival curves were compared and found to be significantly different ($p < 0.0001$).

DISCUSSION

The control of the redox potentials of the cell cytosol and organelles is essential for cell life, and this is exerted via connected redox systems consisting of several redox couples. A cell redox event of particularly high relevance is the control of the formation and breakdown of protein disulfide bonds, which are implicated in controlling a variety of cell functions and are altered in a number of human diseases. In addition to glutathione and cysteine-dependent reducing systems, protein disulfide reduction is performed by the NADPH-thioredoxin reductase-thioredoxin system (Holmgren, 1989). The paramount importance of the TrxR-Trx system is indicated by its high conservation along biological evolution and by its localization in the nucleus and inside mitochondria, in addition to the cytosol (Hanschmann et al., 2013; Holmgren, 1985; Lu and Holmgren, 2012; Rigobello and Bindoli, 2010). This redox system is also expressed in neurons and Schwann cells, and it is axonally transported in both directions (Rozell et al., 1985; Stemme et al., 1985). All TrxR-Trx isoforms are essential for cell life as deduced by the fact that their suppression leads to cell death and are associated to various human diseases, including cancer (Arnér and Holmgren, 2000; Holmgren and Lu, 2010; Mukherjee and Martin, 2008). Accordingly, a large number of drugs were developed to be evaluated as candidates for clinical use. Using the TrxR-specific drug auranofin, which is currently used in the treatment of rheumatoid arthritis and seems to have a great potential for the treatment of other pathological conditions (Madeira et al., 2012), we have provided indirect evidence that the TrxR-Trx system reduces the disulfide bond linking the L and H chains of tetanus neurotoxin (Pirazzini et al., 2013). Building on this observation and on the fact that synaptic vesicles mediate the entry of tetanus neurotoxin inside neurons (Matteoli et al., 1996), we have investigated the association of the TrxR-Trx system with SVs and found that it is indeed present on the cytosolic surface of SVs as extrinsic proteins that can be removed with a high pH bicarbonate/carbonated buffer incubation. Intriguingly, TrxR-Trx is enriched in those synaptic vesicles that are docked to active zones and are ready to release their neurotransmitter content upon depolarization of the presynaptic membrane. This finding

Please cite this article in press as: Pirazzini et al., Thioredoxin and Its Reductase Are Present on Synaptic Vesicles, and Their Inhibition Prevents the Paralysis Induced by Botulinum Neurotoxins, Cell Reports (2014), http://dx.doi.org/10.1016/j.celrep.2014.08.017

suggests that the TrxR-Trx system may play a role in maintaining SV protein function by reducing protein disulfides. For example, the cysteine string protein forms disulfide-mediated dimers that may be noncompatible with its essential chaperone function (Braun and Scheller, 1995). Moreover, the cytosolic domains of several other SV proteins include cysteines (Morciano et al., 2009; Takamori et al., 2006). In addition, it should be recalled that Trx has the folding of primitive chaperones (Arnér and Holmgren, 2000; Berndt et al., 2008; Dekker et al., 2011; Ingles-Prieto et al., 2013), and a chaperone role on the cytosolic surface is a possibility to be considered. Previous careful studies of SV proteomics have not found TrxR and Trx (Boyken et al., 2013; Morciano et al., 2005, 2009), but this is explained by the present finding of the extrinsic nature of the binding of TrxR and Trx to SVs and by the fact that bicarbonate-stripped SVs were used in the mass spectrometry studies. Here, experimental evidence that TrxR and Trx have to be added to the complex composition and structure of the synaptic vesicles is provided. It also adds to the list of the several SV membrane components whose physiological role is still unknown. The identification of the SV protein substrates of Trx requires a study in itself. Nevertheless, here we have shown that this redox system is functional on the cytosolic surface of SVs by using botulinum neurotoxins, for which it was previously established that the reduction of the single interchain disulfide bridge is an essential prerequisite to free the metalloprotease activity of BoNT/A and BoNT/E (Fischer and Montal, 2007; Schiavo et al., 1993). Accordingly, a series of well-characterized inhibitors of TrxR and Trx prevent, in a concentration-dependent manner, the display of metalloproteolytic activity of the three different BoNTs tested in neuronal cultures. It is noteworthy that the scale of potency of the various inhibitors is closely similar for the three BoNT serotypes, indicating that the BoNTs are similarly dependent on disulfide reduction. Such data strongly support the rather general conclusion that the interchain disulfide reduction is a very essential molecular step of the intoxication process performed by all clostridial neurotoxins into neurons. Of even greater importance it is the finding that such inhibitors are very effective in lowering the paralysis induced by a local injection of BoNT/A and BoNT/C. Perhaps more importantly, ebselen elicits a remarkable protection of mice from a 2-fold lethal dose of BoNT/A, a serotype often associated with human botulism. As a consequence, the present experiments identify a class of inhibitors of BoNTs that should be active on all BoNTs independently of their different primary sequence and immunoreactivity, as the single interchain disulfide bond is strictly conserved. This class of inhibitors includes several compounds that have long been tested or are currently under validation for human therapy and that have a substantial record of safety. Our data therefore provide a proof of principle for using these BoNT inhibitors in the prevention and therapy of human botulism. Clearly, these inhibitors are not effective once the L chain is already in the cytosol, but it is known that in clinical botulism the neurotoxin remains in circulation for weeks after the initial symptoms (Fagan et al., 2009; Sheth et al., 2008), and these drugs may prevent further entry of BoNT L chains. This is more important in infant botulism, where there is a continuous supply of BoNT from the vegetative bacteria implanted into the intestine (Johnson and Montecucco, 2008). Remarkably, as these inhibitors act on a common step for all BoNTs, such a strategy may be used immediately after diagnosis, without the need for serotype identification. With the growing number of BoNTs (>40 types already reported) (Rossetto et al., 2014), this is a matter of concern with respect to the current use of BoNT antisera, and such a pharmacological approach could parallel and synergize with the antisera treatment. In addition, these drugs could be used as preventive therapy for individuals who have to enter environments where BoNTs have been released.

EXPERIMENTAL PROCEDURES

Purification of Synaptic Vesicles from Rat Cerebral Cortex

SV isolation was performed with established methods (Boyken et al., 2013; De Camilli et al., 1983; Morciano et al., 2005). Briefly, 15 rats were used. Cerebral cortices were pulled from the cerebellum, brainstem, and most of the midbrain and were mechanically homogenized in 320 mM sucrose, 4 mM HEPES (pH 7.3) supplemented with protease inhibitors (complete EDTA-free, Roche). After differential centrifugations, crude synaptic vesicles were separated through a continuous sucrose gradient (0.25–1.5 M sucrose, 4 mM HEPES [pH 7.3]) in a Beckmann XL-80 ultracentrifuge for 5 hr with a SW28 rotor. Vesicles sedimenting at about 300–400 mM sucrose (free SVs) and those sedimenting at 800–1,000 mM (docked SVs) were collected and pelleted by centrifugation in a 70Ti rotor (Morciano et al., 2005). These vesicle fractions were resuspended in SV buffer (4 mM HEPES, 300 mM glycine [pH 7.4] supplemented with protease inhibitors). In some experiments, free and docked SVs (1 mg of total protein) were incubated with 100 µl of G protein-coupled Dynabeads (Life Technology), previously coupled with anti-synaptophysin, and were immunoisolated by overnight incubation. The immunoisolated SVs were directly lysed in nonreducing loading sample buffer, subjected to SDS-PAGE, and transferred onto a nitrocellulose membrane. Proteins were then labeled with specific antibodies, as indicated in the legends of Figures 1B and S1B legends. In some cases, SV bound to the Dynabeads were removed, washed, and stripped of extrinsic proteins upon incubation with 100 mM Na-bicarbonate buffer adjusted to pH 11.0. After centrifugation, the supernatant and the pellets were subjected to SDS-PAGE and then western blotted with the antibodies indicated in the Figure 1C legend.

Botulinum Neurotoxin Inhibition Assay on CGNs

CGNs at 6–8 days in vitro (DIV) were preincubated for 30 min with increasing concentrations of the indicated inhibitors in basal medium Eagle (BME) 10% fetal bovine serum (FBS), 25 mM KCl at 37°C and 5% CO_2. The indicated toxin was then added and left for 15 min at 37°C (BoNT/A and BoNT/C, 1 nM; BoNT/E, 2 nM). Thereafter, the toxin was washed away and the normal culture medium was restored with the same indicated concentration of inhibitor for 12 hr at 37°C and 5% CO_2.

Alternatively, CGNs at 6–8 DIV were preincubated for 30 min with different concentrations of the indicated inhibitors in BME 10% FBS, 25 mM KCl at 37°C and 5% CO_2. The BoNT was then added (BoNT/A, 10 pM; BoNT/E and BoNT/C, 50 pM), in the same medium, and left for 12 hr at 37°C in the presence of inhibitors. In both cases, the translocation of the L chains of the various neurotoxins was evaluated following their specific proteolytic activity by immunoblotting with specific antibodies against their SNARE protein targets.

Immunocytochemistry and Immunohistochemistry

Neurons were seeded onto 24-well plates at a cell density of 2.5×10^5 cells per well. CGNs at 6–8 DIV were preincubated for 30 min with the indicated concentration of inhibitor in BME 10% FBS, 25 mM KCl at 37°C and 5% CO_2. BoNT/A 1 nM was added and the incubation carried out for 30 min, the neurons were washed, and the incubation with the proper inhibitor was prolonged for 2 hr. In the case of serotype E, the toxin was added (2 nM) and left for 2 hr. The translocation of the L chains of the two neurotoxins was evaluated following the generation of the cleaved form of SNAP25 with specific primary antibodies.

This was determined by fixing neurons for 15 min at room temperature with 4% paraformaldehyde in PBS, quenched (50 mM NH_4Cl in PBS) for 20 min, and permeabilized with 5% acetic acid in ethanol for 20 min at −20°C. Neurons were then incubated with primary antibodies specific for the BoNT/A- or BoNT/E-truncated forms of SNAP25 (Antonucci et al., 2008), using VAMP2 staining as internal control. For the identification of Trx and TrxR, CGNs were fixed at 6–8 DIV and immunostained with specific antibodies, which were detected with Alexa-conjugated secondary antibodies. Coverslips were mounted in 90% glycerol in PBS containing 3% N-propylgallate and examined by either confocal (Leica TCS SP5) or epifluorescence (Leica DMIRE2) microscopy.

Digit Abduction Score Assay

Swiss-Webster adult male CD1 mice weighing 26–28 g were housed under controlled light/dark conditions, and food and water were provided ad libitum. All experiments were performed in accordance with Italian guidelines (law n. 116/1992) and approved by the animal ethical committee of Padova University. Inhibitors were dissolved in an ethanol stock solution. Gastrocnemii muscles were injected (injection volume 50 μl) with 0.05 mg of auranofin, curcumin, PX-12, or ebselen (10% ethanol) or with 0.01 mg of myricetin (20% ethanol) or vehicle alone (20% ethanol in 0.9% NaCl). After 30 min, the muscles were further injected with 15 pg of BoNT/A or 20 pg of BoNT/C (injection volume 25 μl). Hindlimb paralysis was evaluated at least once per day and DAS score provided (Aoki, 2001; Broide et al., 2013).

Mouse Death Assay

Swiss-Webster adult male CD1 mice weighing 24–26 g were housed under controlled light/dark conditions, and food and water were provided ad libitum. All experiments were performed in accordance with Italian guidelines (law n. 116/1992) and were by the animal ethical committee of our university. Ebselen was dissolved in a stock solution (10 mg/ml) with DMSO. Mice were conditioned for 3 days with an intraperitoneal (i.p.) injection of ebselen 7.5 mg/kg or with vehicle every 12 hr. The fourth day, BoNT/A was prepared as a stock solution (1.75 pg/μl), and 30 min after the last inhibitor dose, mice were weighted and i.p. injected with 1 μl/g body weight, corresponding to 1.75 ng/kg BoNT/A (2 × MLD_{50}). Mice were monitored every 4 hr for 96 hr, after which the experiment was considered ended.

Electrophysiological Recordings

One week after inhibitor and toxin injections, the treated (left hind leg) and control nontreated (right hind leg) soleus muscles were quickly excised with particular care to leave a length of 1–1.5 mm of nerve stump. Excised muscles were immediately placed in a Tyrode physiological solution and bubbled with a 5% CO_2 95% O_2 gas mixture at room temperature (20–22°C). The composition of Tyrode solution was 139 mM NaCl, 12 mM $NaHCO_3$, 4 mM KCl, 2 mM $CaCl_2$, 1 mM $MgCl_2$, 1 mM KH_2PO_4, and 11 mM glucose (pH 7.4). After 10 min incubation, muscles were transferred to a Sylgard-coated 35 mm Petri dish, placed with the region of nerve insertion up, and then pinned to the bottom using insect pins (Fine Science Tools). The dish was filled with Tyrode physiological solution bubbled with a 5% CO_2 95% O_2 gas mixture. A 3 μM final concentration of μ-Conotoxin GIIIB (Alomone Labs) was added from a stock solution to block muscle action potentials (Sons et al., 2006). Excitatory postsynaptic potentials were intracellularly recorded from single muscle fibers using borosilicate glass microelectrodes (inner diameter 0.86, outer diameter 1.5; 15 MOhm resistance) (Science Products). Intracellularly recorded signals were amplified using a SEVC amplifier (NPI electronic) in the current-clamp condition. Amplified signals were then sent to an A/D converter (National Instruments) and fed to a personal computer. Digitized recordings were analyzed offline using the WinEDR software for electrophysiology (Strathclyde and Pclamp6, Axon).

SUPPLEMENTAL INFORMATION

Supplemental Information includes Supplemental Experimental Procedures and four figures and can be found with this article online at http://dx.doi.org/10.1016/j.celrep.2014.08.017.

AUTHOR CONTRIBUTIONS

M.P., O.R., F.L., and C.M. conceived the project; D.A.T., G.Z., A.M., M.S., and M.P. performed and evaluated the experiments together with O.R., F.L., and C.M.; C.C.S., T.B., S.F., and O.R. produced, purified, and tested botulinum neurotoxins and other essential reagents and provided advice; and M.P. and C.M. wrote the paper with contributions of all other coauthors.

ACKNOWLEDGMENTS

We thank Valentina Pittiglio and Francesco Giordani for valuable technical assistance. This work was supported by the Italian Ministry of Defence (Progetto PNRM - NIB, Segretariato Generale della Difesa V Reparto), Fondazione CARIPARO "Synaptic Functions and Role of Glial Cells in Brain and Muscle Diseases" (to C.M.), and a grant from the Ministero dell'Università e della Ricerca (Progetto PRIN) to O.R.

Received: June 3, 2014
Revised: July 29, 2014
Accepted: August 7, 2014
Published: September 11, 2014

REFERENCES

Antonucci, F., Rossi, C., Gianfranceschi, L., Rossetto, O., and Caleo, M. (2008). Long-distance retrograde effects of botulinum neurotoxin A. J. Neurosci. *28*, 3689–3696.

Aoki, K.R. (2001). A comparison of the safety margins of botulinum neurotoxin serotypes A, B, and F in mice. Toxicon *39*, 1815–1820.

Aras, M., Altaş, M., Meydan, S., Nacar, E., Karcıoğlu, M., Ulutaş, K.T., and Serarslan, Y. (2014). Effects of Ebselen on ischemia/reperfusion injury in rat brain. Int. J. Neurosci., Published online January 10, 2014 http://dx.doi.org/10.3109/00207454.2013.879581.

Arnér, E.S., and Holmgren, A. (2000). Physiological functions of thioredoxin and thioredoxin reductase. Eur. J. Biochem. *267*, 6102–6109.

Baker, A.F., Adab, K.N., Raghunand, N., Chow, H.H.S., Stratton, S.P., Squire, S.W., Boice, M., Pestano, L.A., Kirkpatrick, D.L., and Dragovich, T. (2013). A phase IB trial of 24-hour intravenous PX-12, a thioredoxin-1 inhibitor, in patients with advanced gastrointestinal cancers. Invest. New Drugs *31*, 631–641.

Berndt, C., Lillig, C.H., and Holmgren, A. (2008). Thioredoxins and glutaredoxins as facilitators of protein folding. Biochim. Biophys. Acta *1783*, 641–650.

Binz, T., and Rummel, A. (2009). Cell entry strategy of clostridial neurotoxins. J. Neurochem. *109*, 1584–1595.

Boyken, J., Grønborg, M., Riedel, D., Urlaub, H., Jahn, R., and Chua, J.J. (2013). Molecular profiling of synaptic vesicle docking sites reveals novel proteins but few differences between glutamatergic and GABAergic synapses. Neuron *78*, 285–297.

Braun, J.E., and Scheller, R.H. (1995). Cysteine string protein, a DnaJ family member, is present on diverse secretory vesicles. Neuropharmacology *34*, 1361–1369.

Broide, R.S., Rubino, J., Nicholson, G.S., Ardila, M.C., Brown, M.S., Aoki, K.R., and Francis, J. (2013). The rat Digit Abduction Score (DAS) assay: a physiological model for assessing botulinum neurotoxin-induced skeletal muscle paralysis. Toxicon *71*, 18–24.

Cai, W., Zhang, L., Song, Y., Wang, B., Zhang, B., Cui, X., Hu, G., Liu, Y., Wu, J., and Fang, J. (2012). Small molecule inhibitors of mammalian thioredoxin reductase. Free Radic. Biol. Med. *52*, 257–265.

CDC (Centers for Disease Control and Prevention), Department of Health and Human Services (HHS) (2012). Possession, use, and transfer of select agents and toxins; biennial review. Final rule. Fed. Regist. *77*, 61083–61115.

Colasante, C., Rossetto, O., Morbiato, L., Pirazzini, M., Molgó, J., and Montecucco, C. (2013). Botulinum neurotoxin type A is internalized and translocated from small synaptic vesicles at the neuromuscular junction. Mol. Neurobiol. *48*, 120–127.

Please cite this article in press as: Pirazzini et al., Thioredoxin and Its Reductase Are Present on Synaptic Vesicles, and Their Inhibition Prevents the Paralysis Induced by Botulinum Neurotoxins, Cell Reports (2014), http://dx.doi.org/10.1016/j.celrep.2014.08.017

Davletov, B., Bajohrs, M., and Binz, T. (2005). Beyond BOTOX: advantages and limitations of individual botulinum neurotoxins. Trends Neurosci. *28*, 446–452.

De Camilli, P., Harris, S.M., Jr., Huttner, W.B., and Greengard, P. (1983). Synapsin I (Protein I), a nerve terminal-specific phosphoprotein. II. Its specific association with synaptic vesicles demonstrated by immunocytochemistry in agarose-embedded synaptosomes. J. Cell Biol. *96*, 1355–1373.

Dekker, C., Willison, K.R., and Taylor, W.R. (2011). On the evolutionary origin of the chaperonins. Proteins *79*, 1172–1192.

Dolly, J.O., Black, J., Williams, R.S., and Melling, J. (1984). Acceptors for botulinum neurotoxin reside on motor nerve terminals and mediate its internalization. Nature *307*, 457–460.

Dressler, D. (2012). Clinical applications of botulinum toxin. Curr. Opin. Microbiol. *15*, 325–336.

Eleopra, R., Tugnoli, V., Rossetto, O., Montecucco, C., and De Grandis, D. (1997). Botulinum neurotoxin serotype C: a novel effective botulinum toxin therapy in human. Neurosci. Lett. *224*, 91–94.

Fagan, R.P., McLaughlin, J.B., and Middaugh, J.P. (2009). Persistence of botulinum toxin in patients' serum: Alaska, 1959-2007. J. Infect. Dis. *199*, 1029–1031.

Fang, J., Lu, J., and Holmgren, A. (2005). Thioredoxin reductase is irreversibly modified by curcumin: a novel molecular mechanism for its anticancer activity. J. Biol. Chem. *280*, 25284–25290.

Fischer, A., and Montal, M. (2007). Crucial role of the disulfide bridge between botulinum neurotoxin light and heavy chains in protease translocation across membranes. J. Biol. Chem. *282*, 29604–29611.

Fischer, A., and Montal, M. (2013). Molecular dissection of botulinum neurotoxin reveals interdomain chaperone function. Toxicon *75*, 101–107.

Fykse, E.M., Takei, K., Walch-Solimena, C., Geppert, M., Jahn, R., De Camilli, P., and Südhof, T.C. (1993). Relative properties and localizations of synaptic vesicle protein isoforms: the case of the synaptophysins. J. Neurosci. *13*, 4997–5007.

Hallett, M., Albanese, A., Dressler, D., Segal, K.R., Simpson, D.M., Truong, D., and Jankovic, J. (2013). Evidence-based review and assessment of botulinum neurotoxin for the treatment of movement disorders. Toxicon *67*, 94–114.

Hanschmann, E.M., Godoy, J.R., Berndt, C., Hudemann, C., and Lillig, C.H. (2013). Thioredoxins, glutaredoxins, and peroxiredoxins—molecular mechanisms and health significance: from cofactors to antioxidants to redox signaling. Antioxid. Redox Signal. *19*, 1539–1605.

Harper, C.B., Martin, S., Nguyen, T.H., Daniels, S.J., Lavidis, N.A., Popoff, M.R., Hadzic, G., Mariana, A., Chau, N., McCluskey, A., et al. (2011). Dynamin inhibition blocks botulinum neurotoxin type A endocytosis in neurons and delays botulism. J. Biol. Chem. *286*, 35966–35976.

Hill, K.K., and Smith, T.J. (2013). Genetic diversity within Clostridium botulinum serotypes, botulinum neurotoxin gene clusters and toxin subtypes. Curr. Top. Microbiol. Immunol. *364*, 1–20.

Holmgren, A. (1985). Thioredoxin. Annu. Rev. Biochem. *54*, 237–271.

Holmgren, A. (1989). Thioredoxin and glutaredoxin systems. J. Biol. Chem. *264*, 13963–13966.

Holmgren, A., and Lu, J. (2010). Thioredoxin and thioredoxin reductase: current research with special reference to human disease. Biochem. Biophys. Res. Commun. *396*, 120–124.

Ingles-Prieto, A., Ibarra-Molero, B., Delgado-Delgado, A., Perez-Jimenez, R., Fernandez, J.M., Gaucher, E.A., Sanchez-Ruiz, J.M., and Gavira, J.A. (2013). Conservation of protein structure over four billion years. Structure *21*, 1690–1697.

Johnson, E.A., and Montecucco, C. (2008). Botulism. Handb. Clin. Neurol. *91*, 333–368.

Kirkpatrick, D.L., Kuperus, M., Dowdeswell, M., Potier, N., Donald, L.J., Kunkel, M., Berggren, M., Angulo, M., and Powis, G. (1998). Mechanisms of inhibition of the thioredoxin growth factor system by antitumor 2-imidazolyl disulfides. Biochem. Pharmacol. *55*, 987–994.

Kumaran, D., Eswaramoorthy, S., Furey, W., Navaza, J., Sax, M., and Swaminathan, S. (2009). Domain organization in Clostridium botulinum neurotoxin type E is unique: its implication in faster translocation. J. Mol. Biol. *386*, 233–245.

Lacy, D.B., Tepp, W., Cohen, A.C., DasGupta, B.R., and Stevens, R.C. (1998). Crystal structure of botulinum neurotoxin type A and implications for toxicity. Nat. Struct. Biol. *5*, 898–902.

Lu, J., and Holmgren, A. (2009). Selenoproteins. J. Biol. Chem. *284*, 723–727.

Lu, J., and Holmgren, A. (2012). Thioredoxin system in cell death progression. Antioxid. Redox Signal. *17*, 1738–1747.

Lu, J., Papp, L.V., Fang, J., Rodriguez-Nieto, S., Zhivotovsky, B., and Holmgren, A. (2006). Inhibition of Mammalian thioredoxin reductase by some flavonoids: implications for myricetin and quercetin anticancer activity. Cancer Res. *66*, 4410–4418.

Madeira, J.M., Gibson, D.L., Kean, W.F., and Klegeris, A. (2012). The biological activity of auranofin: implications for novel treatment of diseases. Inflammopharmacology *20*, 297–306.

Mahmood, D.F., Abderrazak, A., El Hadri, K., Simmet, T., and Rouis, M. (2013). The thioredoxin system as a therapeutic target in human health and disease. Antioxid. Redox Signal. *19*, 1266–1303.

Masuyer, G., Chaddock, J.A., Foster, K.A., and Acharya, K.R. (2014). Engineered botulinum neurotoxins as new therapeutics. Annu. Rev. Pharmacol. Toxicol. *54*, 27–51.

Matteoli, M., Verderio, C., Rossetto, O., Iezzi, N., Coco, S., Schiavo, G., and Montecucco, C. (1996). Synaptic vesicle endocytosis mediates the entry of tetanus neurotoxin into hippocampal neurons. Proc. Natl. Acad. Sci. USA *93*, 13310–13315.

Meotti, F.C., Borges, V.C., Zeni, G., Rocha, J.B.T., and Nogueira, C.W. (2003). Potential renal and hepatic toxicity of diphenyl diselenide, diphenyl ditelluride and Ebselen for rats and mice. Toxicol. Lett. *143*, 9–16.

Molgo, J., Comella, J.X., Angaut-Petit, D., Pecot-Dechavassine, M., Tabti, N., Faille, L., Mallart, A., and Thesleff, S. (1990). Presynaptic actions of botulinal neurotoxins at vertebrate neuromuscular junctions. J. Physiol. (Paris) *84*, 152–166.

Montal, M. (2010). Botulinum neurotoxin: a marvel of protein design. Annu. Rev. Biochem. *79*, 591–617.

Montecucco, C., and Molgó, J. (2005). Botulinal neurotoxins: revival of an old killer. Curr. Opin. Pharmacol. *5*, 274–279.

Morbiato, L., Carli, L., Johnson, E.A., Montecucco, C., Molgó, J., and Rossetto, O. (2007). Neuromuscular paralysis and recovery in mice injected with botulinum neurotoxins A and C. Eur. J. Neurosci. *25*, 2697–2704.

Morciano, M., Burré, J., Corvey, C., Karas, M., Zimmermann, H., and Volknandt, W. (2005). Immunoisolation of two synaptic vesicle pools from synaptosomes: a proteomics analysis. J. Neurochem. *95*, 1732–1745.

Morciano, M., Beckhaus, T., Karas, M., Zimmermann, H., and Volknandt, W. (2009). The proteome of the presynaptic active zone: from docked synaptic vesicles to adhesion molecules and maxi-channels. J. Neurochem. *108*, 662–675.

Mukherjee, A., and Martin, S.G. (2008). The thioredoxin system: a key target in tumour and endothelial cells. Br. J. Radiol. *81*, S57–S68.

Naumann, M., Dressler, D., Hallett, M., Jankovic, J., Schiavo, G., Segal, K.R., and Truong, D. (2013). Evidence-based review and assessment of botulinum neurotoxin for the treatment of secretory disorders. Toxicon *67*, 141–152.

Omata, Y., Folan, M., Shaw, M., Messer, R.L., Lockwood, P.E., Hobbs, D., Bouillaguet, S., Sano, H., Lewis, J.B., and Wataha, J.C. (2006). Sublethal concentrations of diverse gold compounds inhibit mammalian cytosolic thioredoxin reductase (TrxR1). Toxicol. In Vitro *20*, 882–890.

Pantano, S., and Montecucco, C. (2014). The blockade of the neurotransmitter release apparatus by botulinum neurotoxins. Cell. Mol. Life Sci. *71*, 793–811.

Pirazzini, M., Bordin, F., Rossetto, O., Shone, C.C., Binz, T., and Montecucco, C. (2013). The thioredoxin reductase-thioredoxin system is involved in the

entry of tetanus and botulinum neurotoxins in the cytosol of nerve terminals. FEBS Lett. *587*, 150–155.

Rackham, O., Shearwood, A.-M.J., Thyer, R., McNamara, E., Davies, S.M.K., Callus, B.A., Miranda-Vizuete, A., Berners-Price, S.J., Cheng, Q., Arnér, E.S.J., and Filipovska, A. (2011). Substrate and inhibitor specificities differ between human cytosolic and mitochondrial thioredoxin reductases: Implications for development of specific inhibitors. Free Radic. Biol. Med. *50*, 689–699.

Ramanathan, R.K., Abbruzzese, J., Dragovich, T., Kirkpatrick, L., Guillen, J.M., Baker, A.F., Pestano, L.A., Green, S., and Von Hoff, D.D. (2011). A randomized phase II study of PX-12, an inhibitor of thioredoxin in patients with advanced cancer of the pancreas following progression after a gemcitabine-containing combination. Cancer Chemother. Pharmacol. *67*, 503–509.

Rigobello, M.P., and Bindoli, A. (2010). Mitochondrial thioredoxin reductase purification, inhibitor studies, and role in cell signaling. Methods Enzymol. *474*, 109–122.

Rossetto, O., Morbiato, L., Caccin, P., Rigoni, M., and Montecucco, C. (2006). Presynaptic enzymatic neurotoxins. J. Neurochem. *97*, 1534–1545.

Rossetto, O., Pirazzini, M., and Montecucco, C. (2014). Botulinum neurotoxins: genetic, structural and mechanistic insights. Nat. Rev. Microbiol. *12*, 535–549. http://dx.doi.org/10.1038/nrmicro3295.

Rozell, B., Hansson, H.A., Luthman, M., and Holmgren, A. (1985). Immunohistochemical localization of thioredoxin and thioredoxin reductase in adult rats. Eur. J. Cell Biol. *38*, 79–86.

Schiavo, G., Santucci, A., Dasgupta, B.R., Mehta, P.P., Jontes, J., Benfenati, F., Wilson, M.C., and Montecucco, C. (1993). Botulinum neurotoxins serotypes A and E cleave SNAP-25 at distinct COOH-terminal peptide bonds. FEBS Lett. *335*, 99–103.

Sheth, A.N., Wiersma, P., Atrubin, D., Dubey, V., Zink, D., Skinner, G., Doerr, F., Juliao, P., Gonzalez, G., Burnett, C., et al. (2008). International outbreak of severe botulism with prolonged toxemia caused by commercial carrot juice. Clin. Infect. Dis. *47*, 1245–1251.

Sons, M.S., Busche, N., Strenzke, N., Moser, T., Ernsberger, U., Mooren, F.C., Zhang, W., Ahmad, M., Steffens, H., Schomburg, E.D., et al. (2006). alpha-Neurexins are required for efficient transmitter release and synaptic homeostasis at the mouse neuromuscular junction. Neuroscience *138*, 433–446.

Stemme, S., Hansson, H.A., Holmgren, A., and Rozell, B. (1985). Axoplasmic transport of thioredoxin and thioredoxin reductase in rat sciatic nerve. Brain Res. *359*, 140–146.

Takamori, S., Holt, M., Stenius, K., Lemke, E.A., Grønborg, M., Riedel, D., Urlaub, H., Schenck, S., Brügger, B., Ringler, P., et al. (2006). Molecular anatomy of a trafficking organelle. Cell *127*, 831–846.

Yamaguchi, T., Sano, K., Takakura, K., Saito, I., Shinohara, Y., Asano, T., and Yasuhara, H.; Ebselen Study Group (1998). Ebselen in acute ischemic stroke: a placebo-controlled, double-blind clinical trial. Stroke *29*, 12–17.

Zhao, R., Masayasu, H., and Holmgren, A. (2002). Ebselen: a substrate for human thioredoxin reductase strongly stimulating its hydroperoxide reductase activity and a superfast thioredoxin oxidant. Proc. Natl. Acad. Sci. USA *99*, 8579–8584.

Cell Reports, Volume *8*

Supplemental Information

Thioredoxin and Its Reductase Are Present on Synaptic Vesicles, and Their Inhibition Prevents the Paralysis Induced by Botulinum Neurotoxins

Marco Pirazzini, Domenico Azarnia Tehran, Giulia Zanetti, Aram Megighian, Michele Scorzeto, Silvia Fillo, Clifford C. Shone, Thomas Binz, Ornella Rossetto, Florigio Lista, and Cesare Montecucco

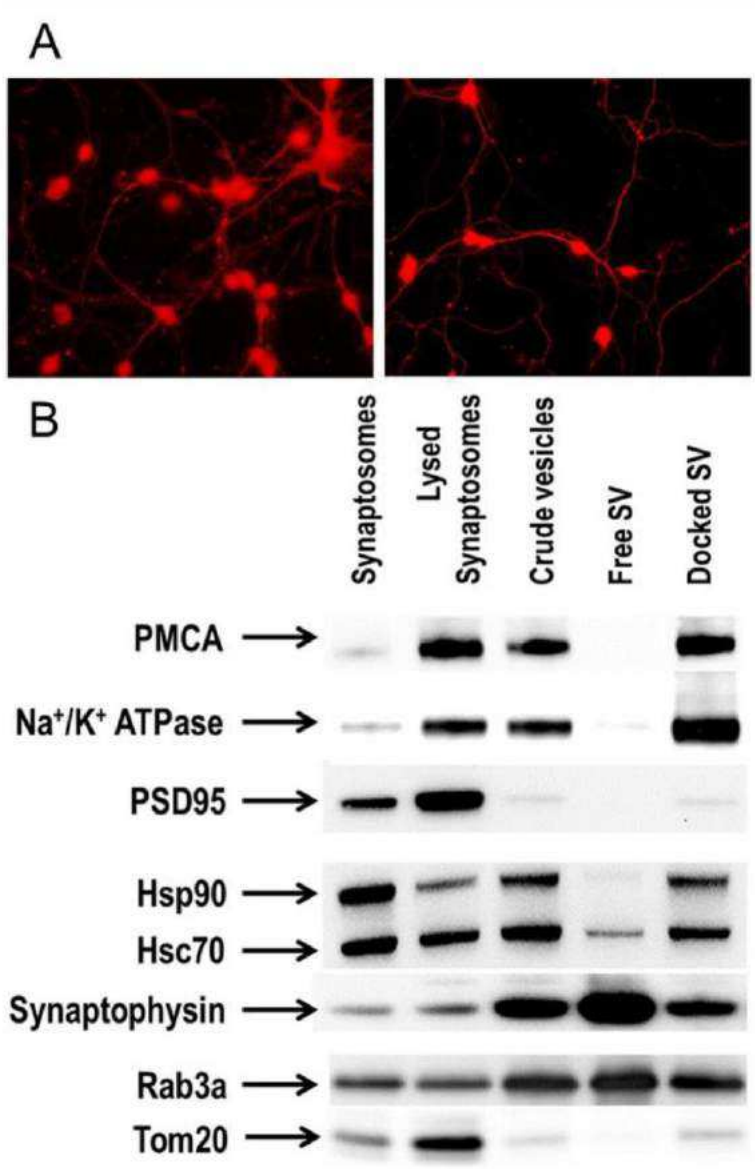

Figure S1. Thioredoxin Reductase and Thioredoxin are present in nerve terminals. (A) Confocal images showing thioredoxin reductase (left) and thioredoxin (right) highly expressed in primary cultures of Cerebellar Granular Neurons. The staining is present in cell bodies as well as inside nerve projections and terminals. (B) Post synaptic (PSD95), mitochondrial (Tom20) or presynaptic markers (all the others) protein content into rat brain synaptosomes and their sub-fractions (indicated on the top of the lanes, 10µg of total lysate proteins per lane). PMCA, Plasma Membrane Calcium ATPase; NA^+/K^+ ATPase, Sodium-Potassium pump; PSD95, Post Synaptic Density protein 95; Hsp90, Heat shock protein 90; Hsc70, Heat shock cognate 70; Rab3a, Ras-related protein 3a; Tom20, translocase of outer mitochondrial membranes 20 kDa. Related to Figure 1.

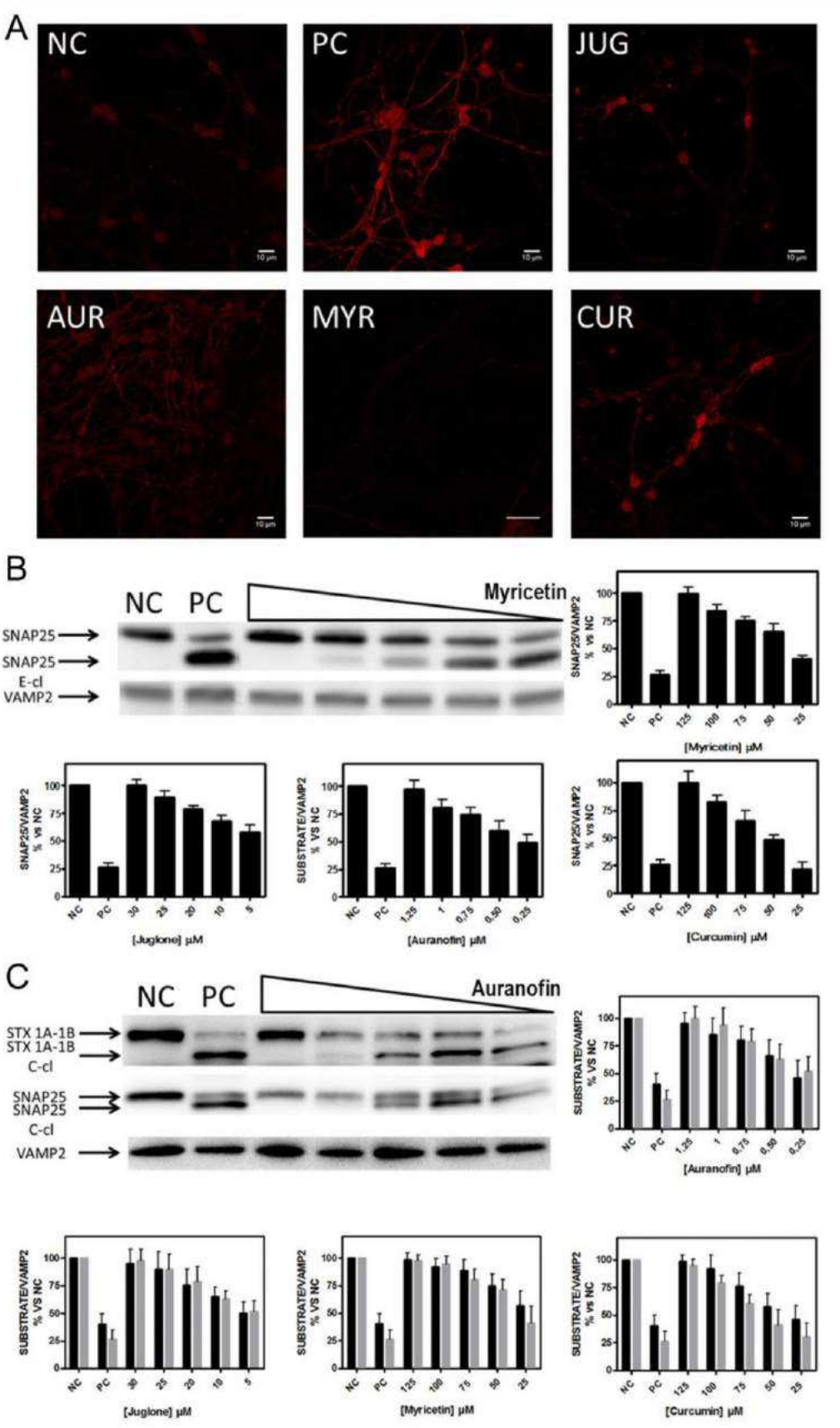

Figure S2. The BoNT/E and BoNT/C induced cleavage of SNARE proteins is prevented in cerebellar granular neurons by Thioredoxin Reductase inhibitors. (A)

CGNs were treated with TrxR inhibitors (JUG 20 μM; AUR 1 μM; MYR 75 μM; CUR 100 μM) or vehicle (NC, no toxin and PC, toxin treated) at 37 °C. After 30 minutes, BoNT/E 2 nM was added for further 120 min to all samples except NC. Samples were washed, fixed and stained with an antibody specific for the C terminus of the BoNT/E-cleaved SNAP25 ($SNAP25_{1-180}$). Anti BoNT/E-cleaved SNAP25 was detected with an Alexa555-conjugated secondary antibody. Images shown are representative of three independent sets of experiments. Bar =10 μm. (B) Quantification of SNAP25 cleavage induced by BoNT/E: CGNs were pre-incubated for 30 min with the indicated concentration of inhibitor at 37 °C, BoNT/E 2 nM was added for 15 min, cells were washed and culture medium with the same concentration of inhibitor was restored and incubation prolonged for 12 h at 37 °C. Cells were lysed and the SNAP25 content was estimated with an antibody which recognizes both the cleaved and the intact form of SNAP25 and another one specific for VAMP2, as internal control. The top left panel reports a typical immunoblot resulting from an experiments in which myricetin was present (NC, no toxin no inhibitor added, PC no inhibitor plus BoNT/E 2 nM final concentration, the five right lanes refer to sample treated with increasing myricetin concentrations, indicated in the side panel). The other panels report the amount of SNAP25 determined as a ratio to VAMP2 staining which serves as internal control, taking the value in non-treated cells (NC) as 100%, in CGNs samples treated with the indicated amounts of the different inhibitors and with BoNT/E. S.D. values derive from at least three independent experiments performed in triplicates. Closely similar results were obtained when 50 picoMolar BoNT/E was left, together with inhibitors, for 12 h at 37 °C before cell lysis and evaluation of SNAP25 cleavage (not shown). (C) Quantification of SNAP25 and syntaxin 1A-1B cleavage induced by BoNT/C (1nM): samples were treated as in B, with the only exception that immunoblotting was performed also against syntaxin 1A-1B. S.D. values derive from at least three independent experiments performed in triplicates. Closely similar results were obtained when 50 picoMolar BoNT/C was left, together with inhibitors, for 12 h at 37 °C before cell lysis and evaluation of SNAREs cleavage (not shown). Related to Figure 2.

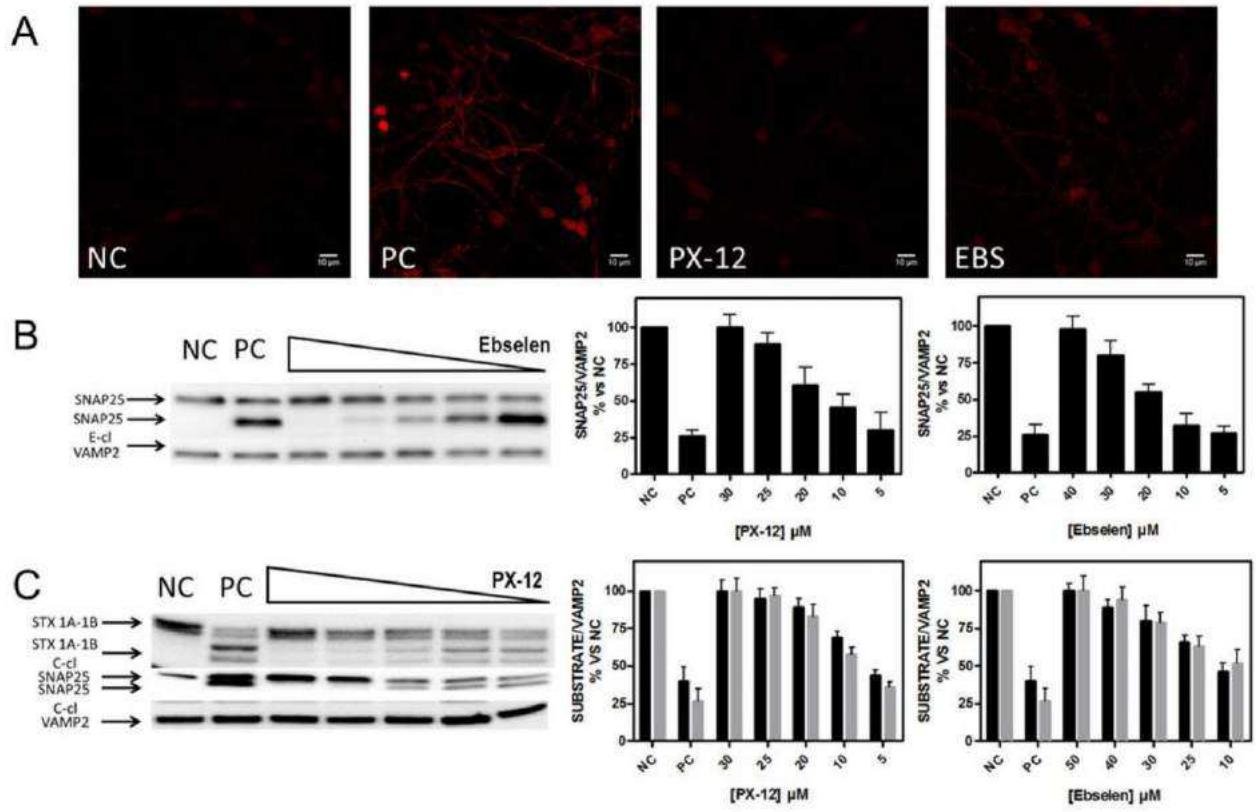

Figure S3. The BoNT/E and BoNT/C induced cleavage of SNARE proteins is prevented by Thioredoxin inhibitors in cerebellar granular neurons. (A) CGNs were treated with the thioredoxin inhibitors (PX-12 25 µM or EBS 30 µM) or the vehicle (NC, no toxin and PC, toxin treated) at 37 °C. After 30 minutes, BoNT/E 2 nM was added and the incubation prolonged for 2 h. Treated neurons were fixed and stained with an antibody against $SNAP25_{1-180}$ and VAMP2. BoNT/E cleaved SNAP25 was detected with an Alexa555 conjugated secondary antibody while VAMP2 with an Alexa488 secondary antibody (not shown for clarity). Images shown are representative from three independent experiments. Bar =10 µm. (B) Quantification of SNAP25 cleavage induced by BoNT/E: CGNs were pre-incubated for 30 min with the indicated concentration of inhibitor at 37 °C, BoNT/E 2 nM was added for 15 min, cells were washed and culture medium with the same concentration of inhibitor was restored and incubation prolonged for 12 h at 37 °C. Cells were lysed and the SNAP25 content was estimated with an antibody which recognizes both the cleaved and the intact form of SNAP25 and another one specific for VAMP2, as loading control. The left panel shows a typical immunoblot obtained with increasing concentrations of ebselen (reported on the side panel). The other panels report the quantification of residual SNAP25 with the indicated concentrations of inhibitors, plotted as a ratio with respect to VAMP2 staining, used as an internal standard, taking the value in non-treated cells (NC) as 100%. S.D. values derive from three independent experiments

performed in triplicates. Closely similar results were obtained when 50 picoMolar BoNT/E was left, together with inhibitors, for 12 h at 37 °C (not shown). (C) Quantification of SNAP25 and syntaxin 1A-1B cleavage induced by BoNT/C (1nM): samples were treated as in B, with the only exception that immunoblotting was performed also against syntaxin 1A-1B. S.D. values derive from at least three independent experiments performed in triplicates. Closely similar results were obtained when 50 picoMolar BoNT/C was left, together with inhibitors, for 12 h at 37 °C before cell lysis and evaluation of SNAREs cleavage (not shown). Related to Figure 3.

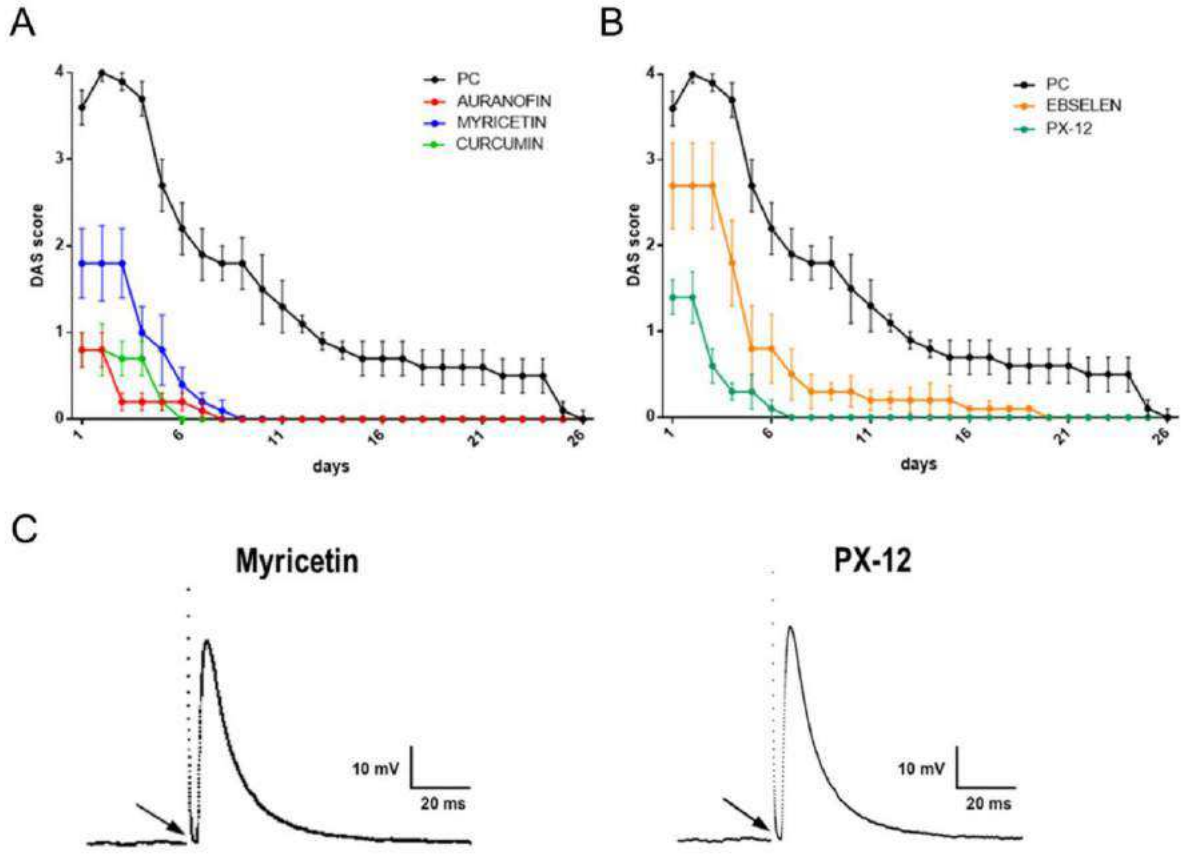

Figure S4. Thioredoxin or Thioredoxin Reductase inhibitors largely prevent and shorten the muscle paralysis induced by BoNT/C in mice. DAS changes with time induced by 20pg of BoNT/C injected in the mouse hind limb after pre-injection in the leg of different TrxR (A) or Trx (B) inhibitors or vehicle (PC). Values are the means ±SEM derived from four experiments using at least three animals per condition. (C) Representative traces of post-synaptic potential evoked by nerve stimulation in mouse soleus muscles dissected 6 days after injection with the indicated inhibitors. Traces represent intracellular recordings of EPPP following nerve stimulation (arrow). Resting membrane potential was clamped at -70 mV. Related to Figure 4.

Supplementary Experimental procedures

Reagents

Auranofin [1-Thio-β-D-glucopyranosatotriethylphosphine gold-2,3,4,6-tetraacetate], Myricetin [3,3',4',5,5',7-Hexahydroxyflavone], Curcumin [(E,E)-1,7-bis(4-Hydroxy-3-methoxyphenyl)-1,6-heptadiene-3,5-dione], Juglone [5-Hydroxy-1,4-naphtoquinone], cytosine β-D-arabinoside, DNAse I, poly-L-lysine were purchased from Sigma Aldrich. PX-12 [2-[(1-Methylpropyl)dithio]-1H-imidazole] and Ebselen [2-Phenyl-1,2-benzisoselenazol-3(2H)-one] were purchased from Santa Cruz Biotechnology. Anti-VAMP2 (104 211) and anti SNAP25 (SMI81, ab24737) monoclonal antibodies were from Synaptic System and Abcam, respectively. Anti-BoNT/A cleaved SNAP25, anti-BoNT/E cleaved SNAP25 and anti-syntaxin 1A-1B polyclonal antibodies have been previously characterized (Antonucci et al., 2008; Schiavo et al., 1995), anti PMCA (plasma membrane calcium pump ATPase) was from Thermo Scientific, $Na^{+/}K^{+}$ ATPase was from Abcam, anti-synaptophysin mAb (clone SY38) was from Dako, anti-thioredoxin reductase 1 (07-613) was from Merck Millipore, anti-thioredoxin 1 Mab (clone EPR6111) was from GeneTex, anti-PSD95 Mab was from Sigma Aldrich, anti-Hsc70 Mab was from Synaptic Sytem, anti-Hsp90 Mab was from BD transduction Laboratories™, anti-tom20 (FL-145) was from SantaCruz Biotechnology. BoNT/A and /C were prepared and purified as described (Schiavo and Montecucco, 1995; Shone and Tranter, 1995) whilst BoNT/E was produced in *Escherichia coli* via recombinant methods (Binz et al., 1994).

Cell cultures

Primary cultures of rat cerebellar granule neurons (CGNs) were prepared from 6- to 8-days-old rats as previously described (Rigoni et al., 2004). Cerebella of 6 days post-natal rats were mechanically disrupted and then trypsinized in the presence of DNase I. Cells were collected and plated into 24 well plates, coated with poly-L-lysine (50 µg/mL), at a cell density of 4 x 10^5 cells per well. Cultures were maintained at 37 °C, 5% CO_2, 95% humidity in BME supplemented with 10% fetal bovine serum, 25 mM KCl, 2 mM glutamine and 50 µg/mL gentamicin. To arrest growth of non-neuronal cells, cytosine arabinoside (10 µM) was added to the medium 18–24 h after plating.

Immunoblotting

Cells were lysed with 100 mM Tris-HCl, 1% SDS, pH 6.8, containing protease inhibitors (complete Mini EDTA-free, Roche). Protein concentration was determined with the BCA test (Pierce BCA protein assay, Thermo Scientific), and equal amounts were loaded onto a 4-12% or 10-20% NuPage gel (Invitrogen) and separated by electrophoresis in 1X MES buffer (Invitrogen) or 1X Tris-Glycine buffer. Proteins were then transferred onto Protran nitrocellulose membranes (Whatman) and saturated for 1 h in PBST (PBS containing 0.1% Tween20) supplemented with 5% non-fatty milk. Incubation with primary antibodies was performed overnight at 4°C. The membranes were washed three times with PBST and incubated with secondary HRP-conjugated antibodies. Finally, membranes were washed several times with PBST and visualization was carried out using Luminata Crescendo (Merck Millipore).

In vitro proteolytic activity

BoNT/A or BoNT/E (2 µg) was reduced with reducing buffer (150 mM NaCl, 10 mM NaH_2PO_4, 15 mM DTT pH 7.4) in the presence of indicated Trx-TrxR inhibitor for 30 minutes at 37° C. 5 µg of recombinant GST-SNAP25 was added to the reduced toxins and the reaction was carried out for 12 hours at 37° C. SNAP25 cleavage was assessed by SDS-PAGE and immunoblotting with an anti SNAP25 antibody.

Viability test

CGNs were seeded in a 96 wells plates at a cell density 10^5 cells per well. After 6 div, different concentration of Trx or TrxR inhibitors, ranging from 0 to the maximum concentration used in the experiments, were added and left for 12 hours. Neurons were the washed and MTS assay (Promega) performed according to manufacturer indication.

Supplemental references

Antonucci, F., Rossi, C., Gianfranceschi, L., Rossetto, O., and Caleo, M. (2008). Long-distance retrograde effects of botulinum neurotoxin A. J Neurosci. *28*, 3689-3696.

Binz, T., Blasi, J., Yamasaki, S., Baumeister, A., Link, E., Südhof, T.C., Jahn, R., and Niemann, H. (1994). Proteolysis of SNAP-25 by types E and A botulinal neurotoxins. J Biol Chem *269*, 1617-1620.

Rigoni, M., Schiavo, G., Weston, A.E., Caccin, P., Allegrini, F., Pennuto, M., Valtorta, F., Montecucco, C., and Rossetto, O. (2004). Snake presynaptic neurotoxins with

phospholipase A2 activity induce punctate swellings of neurites and exocytosis of synaptic vesicles. J Cell Sci. *117*, 3561-3570.

Schiavo, G., and Montecucco, C. (1995). Tetanus and botulism neurotoxins: isolation and assay. Methods Enzymol *248*, 643-652.

Schiavo, G., Shone, C.C., Bennett, M.K., Scheller, R.H., and Montecucco, C. (1995). Botulinum neurotoxin type C cleaves a single Lys-Ala bond within the carboxyl-terminal region of syntaxins. J Biol Chem. *270*, 10566-10570.

Shone, C.C., and Tranter, H.S. (1995). Growth of clostridia and preparation of their neurotoxins. Curr Top Microbiol Immunol *195*, 143-160.

3.1.2 Inhibition of botulinum neurotoxins interchain disulfide bond reduction prevents the peripheral neuroparalysis of botulism

Giulia Zanetti[a,1], Domenico Azarnia Tehran[a,1], Marco Pirazzini[a], Thomas Binz[c], Clifford C. Shone[d], Silvia Fillo[e], Florigio Lista[e], Ornella Rossetto[a], Cesare Montecucco[a,b]

[a]Department of Biomedical Sciences and [b]National Research Council Institute of Neuroscience, University of Padova, Via Ugo Bassi 58/B, 35151 Padova, Italy

[c]Institut für Biochemie, Medizinische Hochschule, Hannover, 30623, Hannover, Germany

[d]Public Health England, Porton Down, Salisbury, Wiltshire SP4 OJG, UK

[e]Histology and Molecular Biology Section, Army Medical and Veterinary Research Center, Via Santo Stefano Rotondo 4, 00184 Rome, Italy

[1]These authors contributed equally to this work

Zanetti G., Azarnia Tehran D. *et al.* Inhibition of Botulinum Neurotoxins Interchain Disulfide Bond Reduction Prevents the Peripheral Neuroparalysis of Botulism. *Biochem Pharmacol*, 98, 522-530.

doi: 10.1016/j.bpc.2015.09.023 (2015).

Biochemical Pharmacology 98 (2015) 522–530

Contents lists available at ScienceDirect

Biochemical Pharmacology

journal homepage: www.elsevier.com/locate/biochempharm

Inhibition of botulinum neurotoxins interchain disulfide bond reduction prevents the peripheral neuroparalysis of botulism

Giulia Zanetti[a,1], Domenico Azarnia Tehran[a,1], Marcon Pirazzini[a], Thomas Binz[c], Clifford C. Shone[d], Silvia Fillo[e], Florigio Lista[e], Ornella Rossetto[a], Cesare Montecucco[a,b,*]

[a] Dipartimento di Scienze Biomediche, Università di Padova, Via U. Bassi 58/B, 35121 Padova, Italy
[b] Istituto CNR di Neuroscienze, Università di Padova, Via U. Bassi 58/B, 35121 Padova, Italy
[c] Institut für Biochemie, OE 4310, Medizinische Hochschule Hannover, 30623 Hannover, Germany
[d] Public Health England, Porton Down, Salisbury, Wiltshire SP4 0JG, UK
[e] Histology and Molecular Biology Section, Army Medical and Veterinary Research Center, Via Santo Stefano Rotondo 4, 00184 Rome, Italy

ARTICLE INFO

Article history:
Received 5 August 2015
Accepted 29 September 2015
Available online 9 October 2015

Chemical compounds studied in this article:
Myricetin (PubChem CID: 5281672)
Curcumin (PubChem CID: 969516)
Ebselen (PubChem CID: 3194)
PX12 (PubChem CID: 219104)

Keywords:
Botulism
Botulinum neurotoxins
Thioredoxin system
Ebselen
Inhibitors
Peripheral neuroparalysis

ABSTRACT

Botulinum neurotoxins (BoNTs) form a growing family of metalloproteases with a unique specificity either for VAMP, SNAP25 or syntaxin. The BoNTs are grouped in seven different serotypes indicated by letters from A to G. These neurotoxins enter the cytosol of nerve terminals *via* a 100 kDa chain which binds to the presynaptic membrane and assists the translocation of a 50 kDa metalloprotease chain. These two chains are linked by a single disulfide bridge which plays an essential role during the entry of the metalloprotease chain in the cytosol, but thereafter it has to be reduced to free the proteolytic activity. Its reduction is mediated by thioredoxin which is continuously regenerated by its reductase. Here we show that inhibitors of thioredoxin reductase or of thioredoxin prevent the specific proteolysis of VAMP by the four VAMP-specific BoNTs: type B, D, F and G. These compounds are effective not only in primary cultures of neurons, but also in preventing the *in vivo* mouse limb neuroparalysis. In addition, one of these inhibitors, Ebselen, largely protects mice from the death caused by a systemic injection. Together with recent results obtained with BoNTs specific for SNAP25 and syntaxin, the present data demonstrate the essential role of the thioredoxin–thioredoxin reductase system in reducing the interchain disulfide during the nerve intoxication mechanism of all serotypes. Therefore its inhibitors should be considered for a possible use to prevent botulism and for treating infant botulism.

1. Introduction

Several species of anaerobic bacteria of the genus *Clostridium* produce botulinum neurotoxins which belong to seven different serotypes (BoNT/A-/G) [1,2]. Their number is rapidly growing and many different sub-serotypes are presently known. The biological and toxicological properties of these novel BoNTs are poorly understood, but the limited amount of experimental data indicate that they act predominantly at peripheral cholinergic nerve terminals, causing a long lasting blockade of acetylcholine release with ensuing paralysis of skeletal and autonomic nerve terminals, characteristic of botulism [3]. Apart from BoNT/D [4–6], BoNTs are the most toxic poisons for humans and are classified as potential bioterrorist weapons [7,8]. This extremely high toxicity results from their neurospecificity and from their catalytic activity, which leads to knock-out of proteins essential to the neurotransmitter release apparatus [2,9]. All BoNTs consist of a metalloprotease light chain (L, 50 kDa) and a heavy chain (H, 100 kDa) linked by a strictly conserved interchain disulfide bond. This molecular structure has been shaped during evolution in order to exploit essential physiological features of the vertebrate nervous system. Indeed BoNTs bind specifically to peripheral nerve terminals presynaptic membrane [10] *via* the C-terminus of the H chain which interacts with polysialogangliosides leading to toxin accumulation. The subsequent binding to a protein receptor, transiently exposed on the membrane, is harnessed for their endocytosis [11,12]. In the case of BoNT/A the endocytic organelles were identified as synaptic vesicles [13,14]. Similar data are not available for the other BoNTs, but several experiments performed with vacuolar ATPase proton pump inhibitors clearly indicate that all these neurotoxins enter the lumen of an acidic compartment [15,16]. Indeed it is established that all serotypes have to undergo a low-pH driven

* Corresponding author at: Istituto CNR di Neuroscienze, Università di Padova, Via U. Bassi 58/B, 35121 Padova, Italy.
E-mail address: cesare.montecucco@gmail.com (C. Montecucco).
[1] These authors contributed equally to this work.

http://dx.doi.org/10.1016/j.bcp.2015.09.023
0006-2952/

membrane translocation of the L chain, mediated by the N-terminal part of H chain [9,17,18]. Once on the cytosolic side, the L metalloprotease remains attached to the H chain *via* the interchain disulfide bridge. This bond is strictly conserved among serotypes, sub-serotypes and also tetanus neurotoxin, which is structurally and functionally related to BoNTs. Remarkably, the premature reduction of this disulfide completely abrogates the toxicity of all clostridial neurotoxins, underscoring its fundamental role in the intoxication process [19–23]. The reduction of this bond is essential to release the catalytic activity of the L metalloprotease within the cytosol versus the three SNARE proteins [20]. Indeed, also in the test-tube BoNTs cannot cleave their recombinant substrates unless this linkage is reduced [24,25]. Once enabled through reduction, the L chain of BoNT/B, /D, /F and /G cleave VAMP at different peptide bonds, BoNT/A and /E cleave SNAP25, while BoNT/C is particular because it is the only one capable to cleave two substrates, SNAP25 and syntaxin [26,27].

We recently reported that the thioredoxin reductase (TrxR)–thioredoxin (Trx) redox system is present on the cytosolic surface of synaptic vesicles and that its inhibition with specific drugs very effectively prevented the neuroparalysis induced by the three SNAP25 specific BoNTs (A, C and E) [28,29]. Here, we extended the study to the four VAMP-specific BoNTs (B, D, F and G) [16,30] using the four chemicals whose structures are shown in Fig. 1 and which are well characterized inhibitors of TrxR–Trx system. Myricetin is a flavonoid which reacts with the selenium atom present in the active site of the reduced TrxR, providing its irreversible inhibition [31]. Curcumin is a polyphenol of vegetal origin that irreversibly inhibits TrxR forming a 1:2 adduct [32]. In both cases, the direct consequence of inhibition is the loss of Trx reducing potential. PX12 acts mainly on thioredoxin by alkylating a non-catalytic cysteine residue, generating a steric hindrance that prevents the interaction with its reductase. As a result, Trx remains permanently in the oxidized, inactive, form [33,34]. Ebselen acts on both members of the redox couple, as it is an excellent substrate for the mammalian TrxR and a highly efficient oxidant of reduced Trx. Thus, Ebselen prevents the normal function of both enzymes [35].

Together with our previous reports [28,36], the present results provide a strong indication that the reduction of the single interchain disulfide bond is a newly identified key event in nerve intoxication of all BoNTs. We therefore propose that TrxR–Trx inhibitors can be considered as a novel and general class of anti-BoNTs drugs and discuss their possible use in humans.

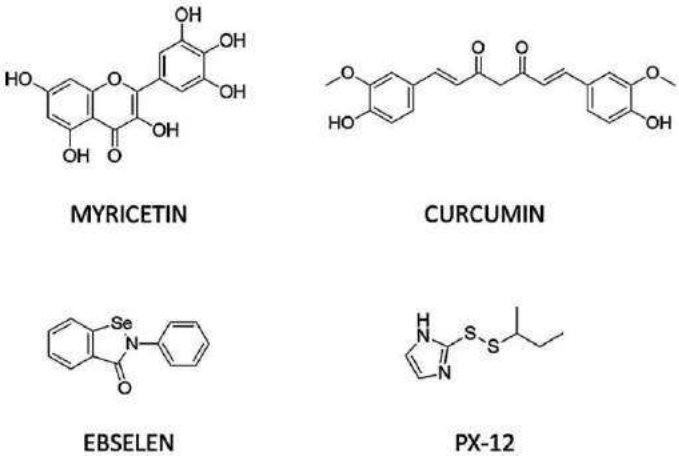

Fig. 1. Thioredoxin–thioredoxin reductase inhibitors used in this study. 3,3′,4′,5,5′,7-Hexahydroxyflavone (Myricetin) and (E,E)-1,7-bis(4-hydroxy-3 methoxyphenyl)-1,6 heptadiene-3,5-dione (Curcumin) preferentially inhibit thioredoxin reductase, 2-phenyl-1,2-benzisoselenazol-3(2H)-one (Ebselen) both thioredoxin and thioredoxin reductase and 2-[(1-methylpropyl) dithio]-1H-imidazole (PX12) inhibits thioredoxin.

2. Materials and methods

2.1. Reagents

3,3′,4′,5,5′,7-Hexahydroxyflavone (Myricetin), (E,E)-1,7-bis(4-hydroxy-3 methoxyphenyl)-1,6 heptadiene-3,5-dione (Curcumin), cytosine β-D-arabinoside, DNAse I and poly-L-lysine were purchased from Sigma– Aldrich. 2-[(1-Methylpropyl) dithio]-1H-imidazole (PX12) was purchased from Santa Cruz Biotechnology and 2-phenyl-1,2-benzisoselenazol-3(2H)-one (Ebselen) was purchased from Cayman Chemical. Antibodies: VAMP2 (104 211) and Syntaxin-1A (110 111) were from Synaptic System, SNAP25 (SMI81, ab24737) was from Abcam. Botulinum neurotoxins B, D and G were produced in *Escherichia coli via* recombinant methods [37–39] whilst BoNT/F was purified as previously described [40].

2.2. Neuronal cultures

Primary cultures of rat cerebellar granule neurons (CGNs) were prepared from 6- to 8-days-old rats as previously described [41]. Briefly, cerebella were isolated, mechanically disrupted and then trypsinized in the presence of DNase I. Cells were then collected and plated into 24 well plates, pre-coated with poly-L-lysine (50 μg/ml), at a cell density of 4×10^5 cells per well. Cultures were maintained at 37 °C, 5% CO_2, 95% humidity in BME supplemented with 10% fetal bovine serum, 25 mM KCl, 2 mM glutamine and 50 μg/ml gentamicin (hereafter indicated as complete culture medium). To arrest growth of non-neuronal cells, cytosine arabinoside (10 μM) was added to the medium 18–24 h after plating.

2.3. Botulinum neurotoxins inhibition assay on CGNs

CGNs at 6–8 days *in vitro* (DIV) were incubated with increasing concentrations of the indicated inhibitor in complete culture medium for 30 min at 37 °C. Thereafter, the indicated toxin was diluted in complete culture medium and added to CGNs in order to obtain the following final concentrations: BoNT/B (2 nM) or BoNT/F (4 nM) or BoNT/G (4 nM). Incubation was prolonged for 12 h at 37 °C. In the case of BoNT/D, owing to its potency, the toxin was added at a final concentration of 0.025 nM and incubated for 15 min at 37 °C. The neuronal culture was then washed and the culture medium with the same concentration of inhibitor was restored for 12 h. Toxicity was evaluated following the specific proteolytic activity of BoNTs *via* immunoblotting with antibodies specific for VAMP2, SNAP25 and syntaxin. All inhibitors were dissolved in DMSO and stored at −80 °C.

2.4. Immunoblotting

Cells were directly lysed with Laemmli sample buffer containing protease inhibitors (complete Mini EDTA-free, Roche). Cell lysates were loaded onto a 4–12% NuPage gel (Life technologies) and separated by electrophoresis in 1X MES buffer (Life technologies). Proteins were transferred onto Protran nitrocellulose membranes (Whatman) and saturated for 1 h in PBST (PBS, 0.1% Tween 20) supplemented with 5% non-fatty milk. Incubation with primary antibodies was performed overnight at 4 °C. The membranes were then washed three times with PBST and incubated with secondary HRP-conjugated antibodies for 1 h. Finally, membranes were washed twice with PBST and once with PBS; visualization was carried out using Luminata Crescendo (Merck Millipore).

2.5. Immunocytochemistry

Neurons were seeded onto 13 mm round glasses in 24-well plates at a cell density of 4×10^5 cells per well. CGNs at 6–8 DIV were pre-incubated for 30 min with the indicated concentration of inhibitor in complete culture medium at 37 °C and 5% CO_2. BoNT/D was added to reach a final concentration of 0.2 nM and the incubation carried out for 10 min at 4 °C. Neurons were washed and the incubation with the indicated inhibitor in the same medium was prolonged for 90 min at 37 °C and 5% CO_2. After treatments, isolated CGNs were fixed for 10 min with 4% paraformaldehyde in PBS and processed for immunocytochemistry. Coverslips were mounted using Fluorescent Mounting Medium (Dako) and examined by epifluorescence (Leica DMIRE2) microscopy. BoNT/D activity was evaluated following the decrease of VAMP2 staining, detected with an antibody specific for the intact form of the protein.

2.6. Digit abduction score assay

Swiss-Webster adult male CD1 mice weighing 26–28 g were housed under controlled light/dark conditions, and food and water were provided *ad libitum*. All experiments were performed in accordance with the European Communities Council Directive n° 2010/63/UE and approved by the Italian Ministry of Health. Curcumin and PX12 were dissolved in ethanol to make stock solutions (10 mg/ml and 5 mg/ml, respectively and stored at −20 °C), whilst Ebselen was dissolved in DMSO (10 mg/ml and stored at −20 °C). A freshly opened aliquot of Ebselen must be used. Hind limb skeletal muscles were injected (total injection volume 25 μl) with 0.02 mg of Curcumin or PX12 or Ebselen or vehicle alone (8% ethanol or DMSO in 0.9% NaCl with 0.2% gelatin). After 30 min, muscles were further injected with BoNT/B (0.5 pg/g) or BoNT/D (0.02 pg/g) or BoNT/F (2 pg/g) or BoNT/G (5 pg/g) or vehicle alone (0.9% NaCl with 0.2% gelatin). Hind limbs paralysis was evaluated at least once per day using the Digit Abduction Score (DAS) assay, performed as previously reported [42,43].

2.7. Lethality assay

Swiss-Webster adult male CD1 mice weighing 24–26 g were housed under controlled light/dark conditions, and food and water were provided *ad libitum*. All experiments were performed in accordance with the European Communities Council Directive n° 2010/63/UE and approved by the Italian Ministry of Health. A stock solution of Ebselen in DMSO was prepared (7.5 mg/ml). Mice were conditioned for 3 days with intraperitoneal (i.p.) injections of Ebselen at a dose of 7.5 mg/kg or with vehicle (DMSO) every 12 h. Each experiment was conducted with a freshly opened aliquot of Ebselen. The third day, BoNT/B or BoNT/D or BoNT/F was prepared as a stock solution (BoNT/B 0.9 pg/μl, BoNT/D 0.04 pg/μl and BoNT/F 2.5 pg/μl in 0.9% NaCl with 0.2% gelatin), and 30 min after the injection of the last inhibitor dose, mice were weighted and i.p. injected with 1 μl/g body weight, roughly corresponding to a 2 fold MLD_{50} for each toxin. The respective MLD_{50} have been determined through preliminary experiments: BoNT/B 0.45 ng/kg, BoNT/D 0.02 ng/kg and BoNT/F 1.25 ng/kg). Mice were monitored every 4 h for 96 h, at which the experiment was considered ended.

3. Results

3.1. Inhibitors of thioredoxin reductase and thioredoxin prevent cleavage of VAMP by botulinum neurotoxins type B, D, F and G in cultured neurons

The most convenient and rapid way to screen the ability of TrxR–Trx inhibitors in blocking the VAMP-specific BoNTs toxicity is the use of sensitive neuronal cultures. Fig. 2 shows that, upon overnight incubation of primary cultures of cerebellar granular neurons, 2 nM BoNT/B cleaves its substrate, as evaluated by

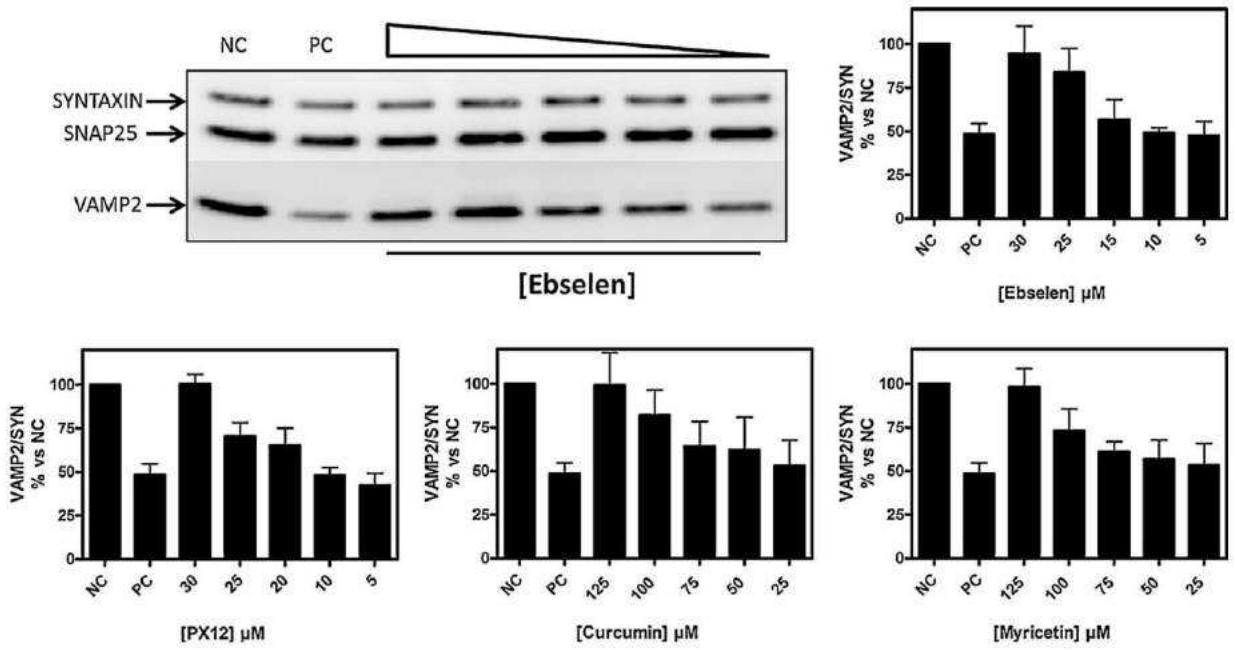

Fig. 2. Thioredoxin–thioredoxin reductase inhibitors prevent the BoNT/B-induced cleavage of VAMP2 in neuronal culture. CGNs were incubated with the indicated concentrations of inhibitors at 37 °C for 30 min. 2 nM BoNT/B was then added and incubation prolonged for 12 h at 37 °C; cells were then lysed and the VAMP2 content was estimated with an antibody recognizing the intact form of VAMP2. Syntaxin and SNAP25 staining was used as loading control. Upper left panel shows a representative immunoblot, obtained in experiments with Ebselen (NC, no toxin added; PC, only toxin added). Graphs show the quantification, of the experiments performed with the reported inhibitors, for VAMP2 determined as a ratio to Syntaxin staining, taking the value of non-treated cells as 100%. SD values derive from at least three independent experiments.

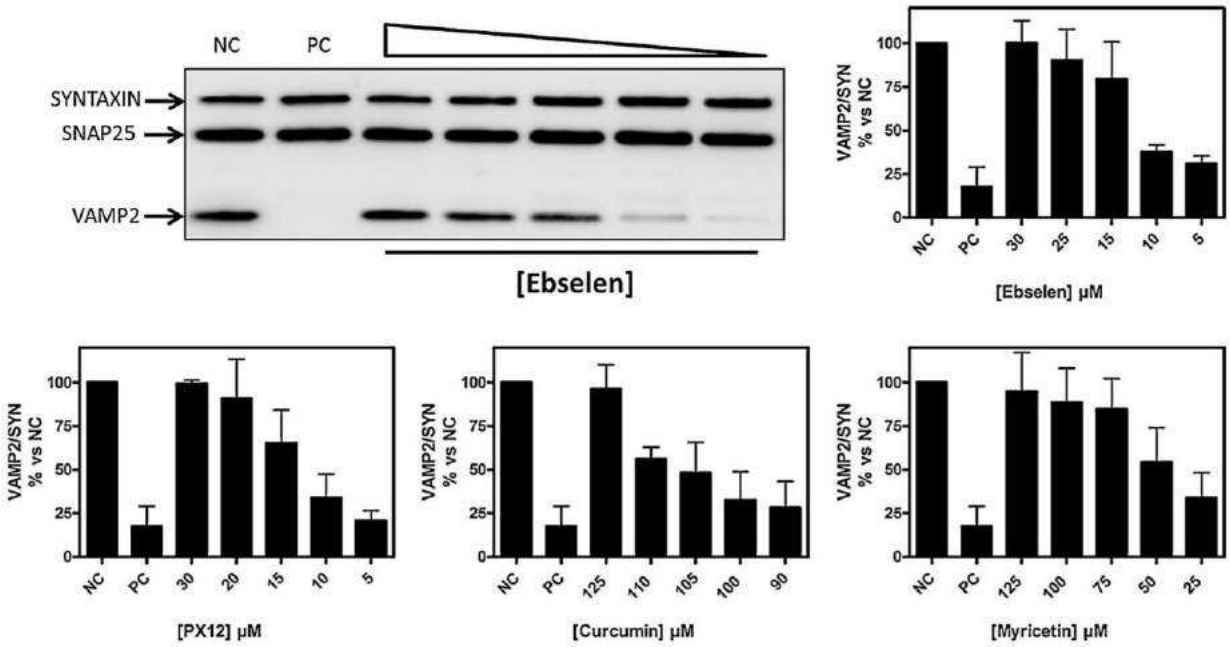

Fig. 3. Thioredoxin–thioredoxin reductase inhibitors prevent the BoNT/D-induced cleavage of VAMP2 in neuronal culture. CGNs were incubated with the indicated concentrations of inhibitor at 37 °C for 30 min. BoNT/D 0.025 nM was added for 15 min, cells were washed, and culture medium with the same concentration of inhibitor was restored and incubation prolonged for 12 h at 37 °C. Cells were then lysed and the VAMP2 content was estimated with an antibody recognizing the intact form of VAMP2. Syntaxin and SNAP25 staining was used as loading control. Upper left panel shows a representative immunoblot, obtained in experiments with Ebselen (NC, no toxin added; PC, only toxin added). Graphs show the quantification, of the experiments performed with the reported inhibitors, for VAMP2 determined as a ratio to Syntaxin staining, taking the value of non-treated cells as 100%. SD values derive from at least three independent experiments.

western blotting with an antibody specific for the intact form of the protein; a residual portion of VAMP2 not accessible to the metalloprotease L chain of BoNT/B is a common finding [19,44,45]. At the same time, Ebselen, PX12, Curcumin and Myricetin prevent the cleavage of VAMP2 in a dose dependent mode. Importantly, at the doses used here, these drugs do not affect cell viability, nor do they inhibit the cleavage of a recombinant VAMP2 (not shown).

Fig. 3 shows that BoNT/D is particularly active in CGNs and a concentration as low as 0.025 nM cleaves nearly all VAMP2. Nevertheless, the four compounds are effective in blocking such an activity with a profile of concentration dependence similar to that found with BoNT/B (Fig. 2), as determined by immunoblotting. This is even more evident in Fig. 4, which documents their effect using an immunofluorescence analysis. Importantly, the two assays provide fully consistent results even though different toxin concentrations, binding and incubation times were used. This reinforces the conclusion about the preventing activity of the four drugs used here.

We have no a direct explanation for the much higher potency of BoNT/D in VAMP2 cleavage with respect to BoNT/B, but it could be ascribed to a faster entry into the cytosol of BoNT/D than BoNT/B, which was reported to be particularly slow in cell cultures [44]. This may also explain why, when TrxR is not completely inhibited as in the case of lower concentrations of Curcumin, BoNT/D activity appears to be less blocked as compared to BoNT/B. Nevertheless, the comparable inhibition profile of these two BoNTs strongly indicates that the reduction of the interchain bond, catalyzed by the TrxR–Trx system, is of similar and essential importance to enable their intraneuronal catalytic activity. This conclusion is reinforced by the similar data obtained using BoNT/F and BoNT/G, whose inhibition profiles are reported in Fig. 5 and Fig. 6, respectively. Importantly, we achieved this result by using four different compounds, which belong to different chemical classes, have different molecular structures as well as different mechanisms to inhibit TrxR–Trx system.

3.2. Inhibitors of thioredoxin reductase and thioredoxin effectively lower the reversible flaccid paralysis induced by botulinum neurotoxins type B, D, F and G in mice

One remarkable aspect of BoNTs action *in vivo* is that they induce a reversible peripheral neuroparalysis. This property is clearly documented by the black traces in the panels of Fig. 7 which shows the recovery time course of mouse limb muscles function after the paralysis induced by a single local injection of BoNT/B, /D, /F and /G in sub-lethal doses. The neuromuscular paralytic effect was evaluated over time with the well-established DAS assay [42,43], which assigns a score to the severity of muscles paralysis according to the capability of the mouse to move the hind limb fingers, upon injection of BoNTs close to the EDL (*Extensor Digitoris Longus*) muscle. This score ranges from 0 (no paralysis) up to 4 (all fingers are paralyzed). Even though the paralytic effect exerted by the four BoNTs has different durations, it is worth noting that the local injection of the TrxR–Trx inhibitors effectively reduced both the severity and the duration of the paralysis. Owing to the very large number of sampling required by this type of analysis, we used three different inhibitors to dissect the entire TrxR–Trx system: Curcumin (inhibitor of TrxR), PX12 (inhibitor of Trx), and Ebselen (inhibitor of TrxR and Trx). All of them very effectively prevented the peripheral neuroparalysis induced by the four different BoNTs, with Ebselen being slightly more potent (Fig. 7).

3.3. Ebselen effectively prevents mice death caused by botulinum neurotoxins type B, D and F

On the basis of the results reported above, it became very relevant to test the capacity of the TrxR–Trx inhibitors in preventing the development of botulism upon systemic delivery of the four neurotoxins. Since such tests would have required a very large number of animals, we confined the experiments to one of the drugs. Ebselen was chosen because it best protected against paralysis in the DAS assay and because it has been used in clinical

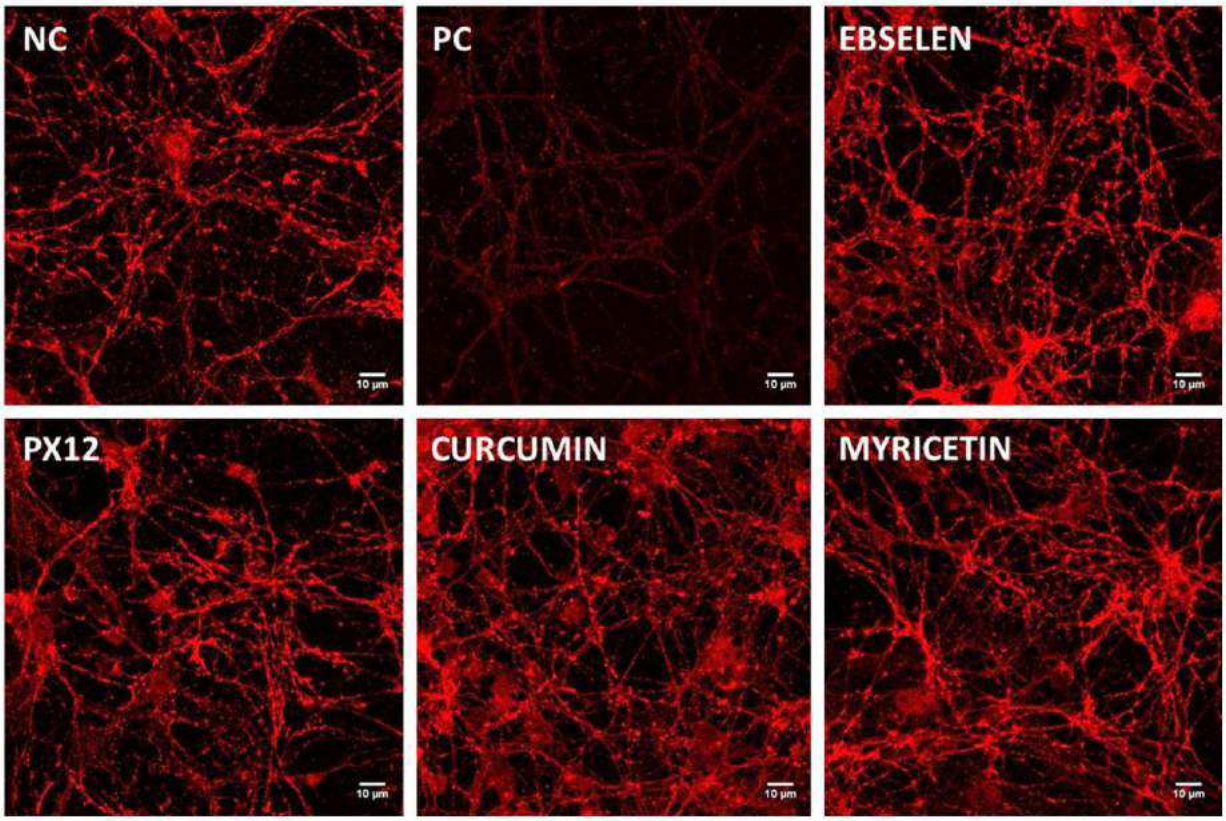

Fig. 4. Immunocytochemical evaluation of BoNT/D activity blockage by Inhibitors of thioredoxin–thioredoxin reductase system. CGNs were treated with Trx–TrxR inhibitors (Curcumin 100 µM, Ebselen 30 µM, Myricetin 100 µM or PX12 25 µM) or vehicle (NC, no toxin added; PC, only toxin added) at 37 °C. After 30 min, BoNT/D 0.2 nM was added for 10 min at 4 °C after which neurons were washed and incubated with the same concentration of inhibitors for further 90 min at 37 °C. Thereafter neurons were fixed and VAMP2 cleavage was assessed using a specific antibody. The images are representative of three independent sets of experiments (scale bar 10 µm).

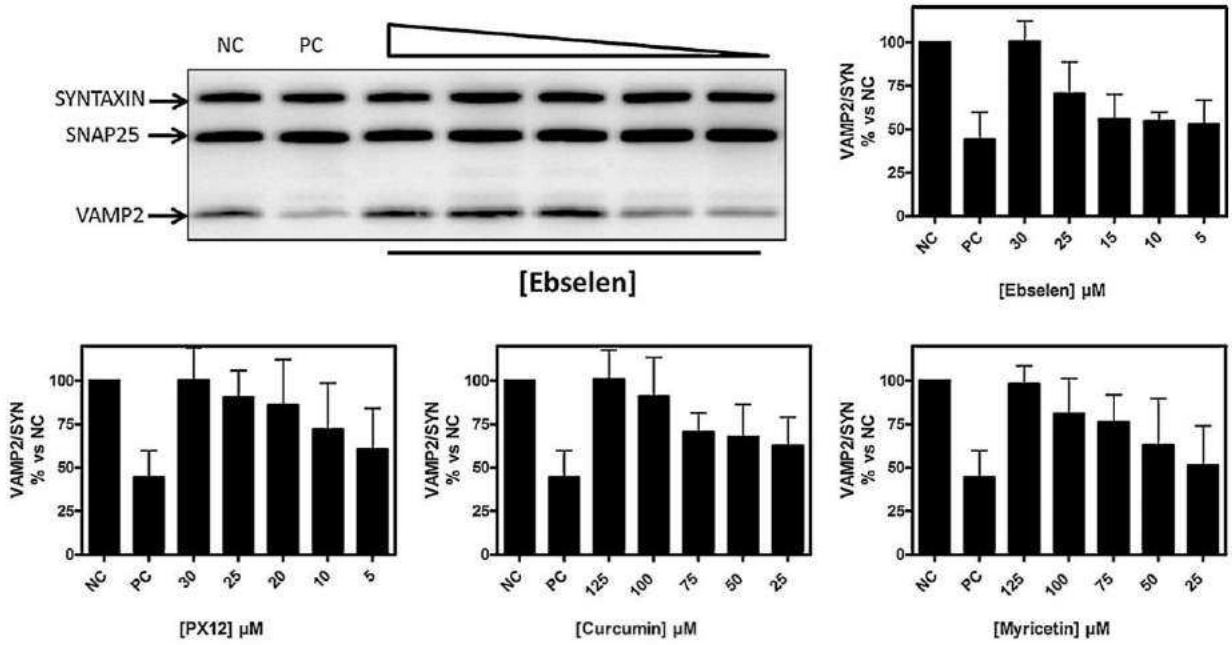

Fig. 5. Thioredoxin–thioredoxin reductase inhibitors prevent the BoNT/F-induced cleavage of VAMP2 in in neuronal culture. CGNs were incubated with the indicated concentrations of inhibitor at 37 °C for 30 min. 4 nM BoNT/F was then added and incubation prolonged for 12 h at 37 °C, cells were then lysed and the VAMP2 content was estimated with an antibody recognizing the intact form of VAMP2. Syntaxin and SNAP25 staining was used as loading control. Upper left panel shows a representative immunoblot, obtained in experiments with Ebselen (NC, no toxin added; PC, only toxin added). Graphs show the quantification, of the experiments performed with the reported inhibitors, for VAMP2 determined as a ratio to Syntaxin staining, taking the value of non-treated cells as 100%. SD values derive from at least three independent experiments.

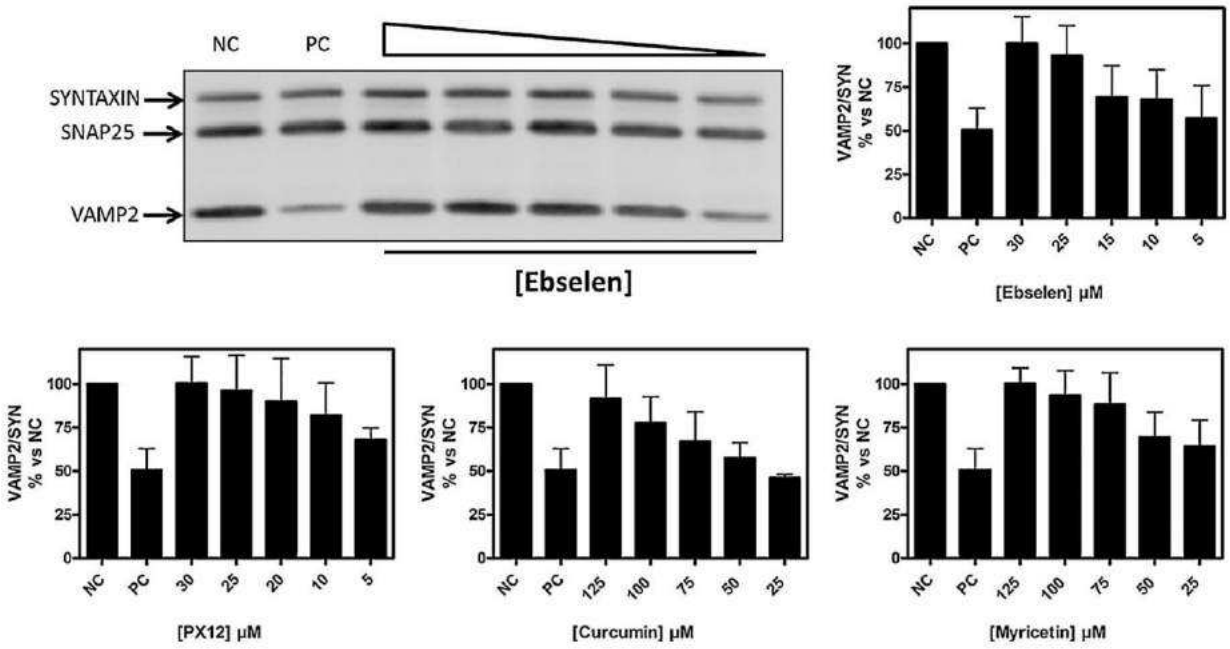

Fig. 6. Thioredoxin–thioredoxin reductase inhibitors prevent the BoNT/G-induced cleavage of VAMP2 in neuronal culture. CGNs were incubated with the indicated concentrations of inhibitor at 37 °C for 30 min. 4 nM BoNT/G was then added and incubation prolonged for 12 h at 37 °C, cells were then lysed and the VAMP2 content was estimated with an antibody recognizing the intact form of VAMP2. Syntaxin and SNAP25 staining was used as loading control. Upper left panel shows a representative immunoblot, obtained in experiments with Ebselen (NC, no toxin added; PC, only toxin added). Graphs show the quantification, of the experiments performed with the reported inhibitors, for VAMP2 determined as a ratio to Syntaxin staining, taking the value of non-treated cells as 100%. SD values derive from at least three independent experiments.

trials in humans for other diseases [46,47]. In addition, we focused our attention on BoNT/B and BoNT/F, because these serotypes are involved in human botulism and BoNT/D because it is often associated to animal botulism [2,3]. Type G was not tested because

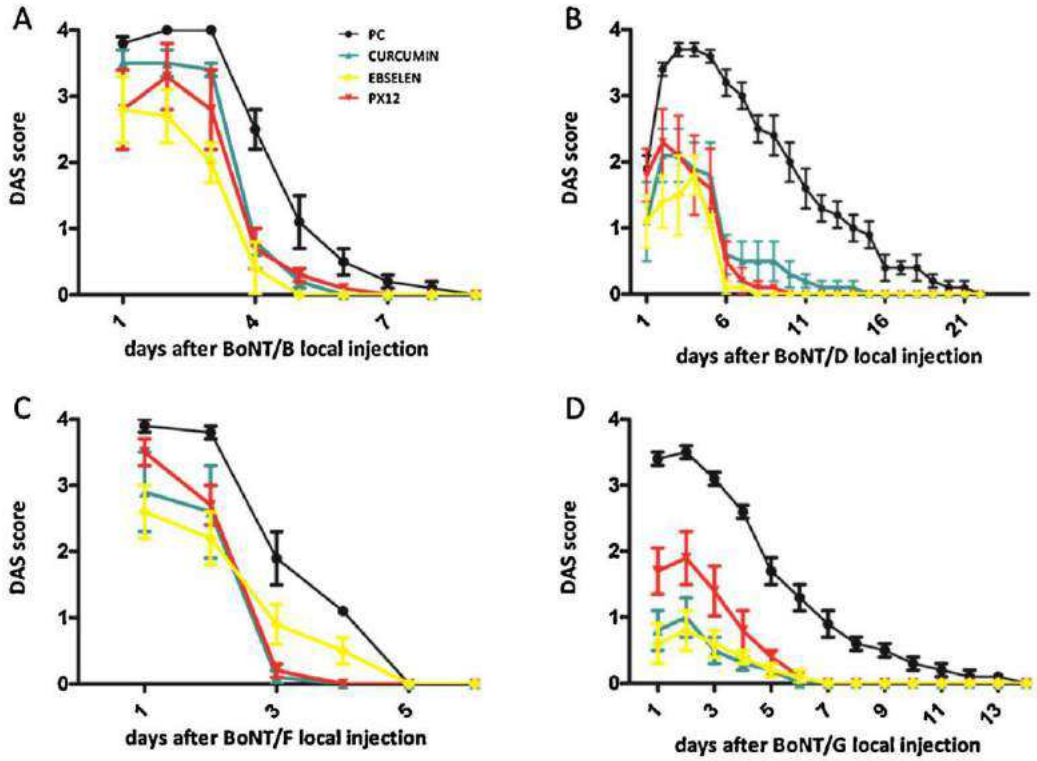

Fig. 7. Thioredoxin–thioredoxin reductase inhibitors decrease the local paralysis induced by BoNT/B, /D, /F and G. 0.02 mg of Curcumin (green traces) or PX12 (red traces) or Ebselen (yellow traces) or vehicle (PC, black traces) were injected in the hind limb of adult male CD1 mice. After 30 min the same hind limbs were injected with 0.5 pg/g of BoNT/B (A) or 0.2 pg/g of BoNT/D (B) or 2 pg/g of BoNT/F (C) or 5 pg/g of BoNT/G (D) and the severity of local paralysis was evaluated and reported as DAS score (see Section 2). DAS score of animals treated with only inhibitors are not shown for clarity. DAS values are means ± SEM from three individual experiments of at least eight animals per condition.

it has not been reported to cause botulism in humans or animals. Fig. 8 shows that Ebselen substantially protects mice from intraperitoneally injected BoNT/B, or BoNT/D or BoNT/F. Noteworthy, all mice treated displayed the symptoms typical of botulism, such as a generalized flaccid paralysis of muscles, but Ebselen-treated animals displayed milder symptoms and in several cases they were not severe enough to cause the respiratory failure or to prevent drinking and feeding that generally contribute to death of injected mice in the animal cage. Importantly, survivors fully recovered from developed symptoms in few days, suggesting that large amounts of the injected toxin did not reached VAMP.

4. Discussion

The results presented here are very relevant in several respects. The first one is that they provide experimental evidence that thioredoxin reductase-thioredoxin disulfide reducing system cleaves the single interchain disulfide bond of the four BoNT serotypes whose L chain proteolyses VAMP: BoNT/B, /D, /F and /G. Together with our previous reports on the SNAP25 and syntaxin cleaving BoNTs [28,36], it can now be concluded that this molecular event, which takes place on the cytosolic face of an intracellular acidic compartment [20], is an essential step of the cellular mechanism of intoxication of all BoNT serotypes. So essential, that it is sufficient to inhibit the TrxR–Trx redox system to completely prevent the toxicity of these very powerful neurotoxins in cultured neurons. This conclusion is even more important if one considers the large number of novel BoNTs that are being discovered [48,49]. They can be classified as subtypes of the main seven serotypes, which have now all been analyzed with respect to disulfide reduction (the present paper and [28,36]). Therefore, it can be concluded that the release in the cytosol of the L chain metalloprotease activity of all clostridial neurotoxins requires reduction of the interchain disulfide bridge by the TrxR–Trx system.

An important feature of BoNTs is their reversibility of action. This remarkable property has been exploited to evaluate the respective potency and duration of the different serotypes *in vivo* [50,51] through the DAS assay. This test is based on the intramuscular injection of a limited amount of BoNTs which can induce the local paralysis of mice hind legs without causing their death [42,43]. This is facilitated by a very limited diffusion from the site of injection, a feature which becomes very relevant in the therapeutic use of BoNTs, particularly when small muscles are injected [52,53]. Given that the intracellular degradation of the L chain seems to be the main reason of BoNTs reversibility of action, the duration of paralysis primarily depends on the amount L chains which have entered the nerve terminals, beside the intrinsic properties of the different L chains may also play a significant role [27,54,55]. Therefore, the second valuable result described here is that inhibitors of the TrxR–Trx system are general inhibitors of all BoNTs and are capable of preventing to a large extent their local neuroparalytic action in mice by reducing the number of L chains which have entered the nerve terminals. Accordingly, this result indicates the possible employment of these inhibitors in accidental events of over dosage of a BoNT during its therapeutic use.

We also assayed the efficacy of TrxR–Trx inhibitors in protecting mice from a systemic injection of BoNTs. This assay better recapitulates botulism, i.e., a generalized peripheral neuroparalysis which generally develops following the toxin absorption from a large organ such as the intestine (alimentary botulism) [2]. Botulism is reversible, provided that the intoxicated patient is mechanically ventilated to prevent death by respiratory muscles paralysis. Because of local regulations on experimentation involving animals, we could not assay the efficacy of all the inhibitors tested in neuronal cultures and capable of preventing local neuroparalysis (DAS assay), in mice lethality tests. However, using Ebselen we have provided a proof of principle that inhibitors of the TrxR–Trx system can effectively prevent the development of the flaccid paralysis caused by BoNT and protect a sizeable fraction of animals from deadly effects. Notably, the survivors recovered completely. This result is very relevant as it suggests that Ebselen, and probably the other TrxR–Trx inhibitors, can be used to prevent botulism in humans and in animals. This is also valid in the case of BoNT/D which, in our hands, is the most toxic of all BoNTs in mice with a MLD_{50} of 0.02 ng/kg to be compared with the literature data of 0.4 ng/kg [56].

On the basis of the present knowledge about the BoNTs mechanism of neuron intoxication, it is clear that once the reduction of the interchain disulfide bond has released the L chain metalloprotease activity, the inhibitors tested here are no longer effective. In other words, these inhibitors cannot be considered for the use after the symptoms of botulism have developed. Therefore the drugs tested here are to be considered as prophylactic and the limitation of a prophylaxis has been discussed before [57]. Notwithstanding, if given soon after diagnosis, these inhibitors may lessen symptoms severity by preventing the entry of circulating BoNT, and therefore shorten the period of hospitalization which is associated with the high costs of intensive care. It is indeed known that in adult botulism caused by the ingestion of BoNT poisoned food, there is a long persistence of the toxin in the general circulation [58,59]. Moreover, having a good record of safety in humans, as deduced from previous trials [60–65], these drugs may have a great potential in the treatment of human botulism where a continuous release of freshly produced BoNT takes place, which is the case of infant botulism [66]. In this form of the disease, the BoNT producing Clostridia colonize the intestine,

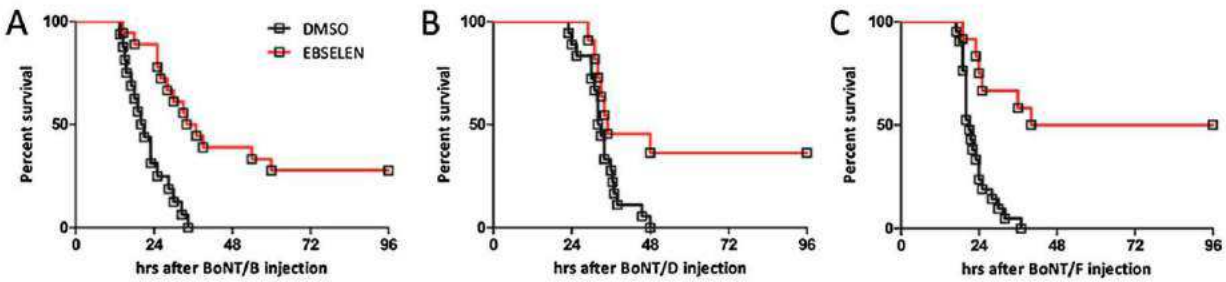

Fig. 8. Ebselen prevents the lethality of BoNT/B, /D and /F. Adult male CD1 mice were preconditioned with Ebselen 7.5 mg/kg ($n = 15$) or vehicle ($n = 15$) as described in Section 2. Thereafter, 2xMLD_{50} of BoNT/B (A) or BoNT/D (B) or BoNT/F (C) were injected i.p. Animals were monitored every 4 h for 96 h, after which the experiment was considered concluded. Graphs report the survival curves analyzed with the Log-rank (Mantel–Cox) test, and found to be significantly different (BoNT/B: $p < 0.0001$; BoNT/D: $p < 0.0058$; BoNT/F: $p < 0.0022$) from inhibitor free controls.

owing to the lack of competitive bacterial flora, and release the toxin in the general circulation for long periods of time [2,67].

There is growing interest in finding new mechanism-based antidotes against BoNTs, and some molecules were found to have beneficial potential (Fischer, Nakai et al., 2009). The main advantage of such molecules is that they act regardless of the serotypes causing envenomation. This is the more important in light of the large number of different BoNTs that are being discovered. These drugs can be administered without knowing the BoNT serotype and sub-type, thus saving the time required for toxin characterization. This is also relevant to those cases of botulism caused by Clostridia producing more than one BoNT (Barash and Arnon 2004, Barash and Arnon 2013, Dover, Barash et al., 2013, Maslanka, Lúquez et al., 2015).

Authors contributions

(1) Study conception and design: M.P. and C.M.
(2) Acquisition, analysis and/or interpretation of data: G.Z., D.A.T., M.P. and C.M.
(3) Drafting/revision of the work for intellectual content and context: M.P., G.Z., D.A.T., O.R., T.B. and C.M.
(4) Final approval and overall responsibility for the published work: G.Z., D.A.T., M.P., T.B., C.C.S., S.F., F.L., O.R. and C.M.

Conflict of interests

The authors declare that they have no conflict of interests.

Acknowledgements

This work has been mainly supported by a grant from the Italian Ministry of Defence (Progetto PNRM—NIB, Segretariato Generale della Difesa V Reparto) and from Fondazione CARIPARO "Synaptic Functions and Role of Glial Cells in Brain and Muscle Diseases" to C. M., and additionally by a grant from the Ministero dell'Università e della Ricerca (Progetto PRIN) to O.R. We thank Editor and Reviewers for their comments and criticisms that led to an improved paper.

References

[1] K.K. Hill, T.J. Smith, Genetic diversity within *Clostridium botulinum* serotypes, botulinum neurotoxin gene clusters and toxin subtypes, Curr. Top. Microbiol. Immunol. 364 (2013) 1–20.
[2] O. Rossetto, M. Pirazzini, C. Montecucco, Botulinum neurotoxins: genetic, structural and mechanistic insights, Nat. Rev. Microbiol. 12 (2014) 535–549.
[3] E.A. Johnson, C. Montecucco, Botulism, Handb. Clin. Neurol. 91 (2008) 333–368.
[4] J.A. Coffield, N. Bakry, R.D. Zhang, J. Carlson, L.G. Gomella, L.L. Simpson, In vitro characterization of botulinum toxin types A, C and D action on human tissues: combined electrophysiologic, pharmacologic and molecular biologic approaches, J. Pharmacol. Exp. Ther. 280 (1997) 1489–1498.
[5] R. Eleopra, C. Montecucco, G. Devigili, C. Lettieri, S. Rinaldo, L. Verriello, et al., Botulinum neurotoxin serotype D is poorly effective in humans: an in vivo electrophysiological study, Clin. Neurophysiol. 124 (2013) 999–1004.
[6] S. Pellett, W.H. Tepp, J.M. Scherf, C.L. Pier, E.A. Johnson, Activity of botulinum neurotoxin type D (strain 1873) in human neurons, Toxicon 101 (2015) 63–69.
[7] S.S. Arnon, R. Schechter, T.V. Inglesby, D.A. Henderson, J.G. Bartlett, M.S. Ascher, et al., Botulinum toxin as a biological weapon: medical and public health management, JAMA 285 (2001) 1059–1070.
[8] Centers for Disease Control and Prevention DoHaHS, Possession, use, and transfer of select agents and toxins; biennial review. Final rule, Fed. Regist. 77 (2012) 61083–61115.
[9] M. Montal, Botulinum neurotoxin: a marvel of protein design, Annu. Rev. Biochem. 79 (2010) 591–617.
[10] J.O. Dolly, J. Black, R.S. Williams, J. Melling, Acceptors for botulinum neurotoxin reside on motor nerve terminals and mediate its internalization, Nature 307 (1984) 457–460.
[11] A. Rummel, Double receptor anchorage of botulinum neurotoxins accounts for their exquisite neurospecificity, Curr. Top. Microbiol. Immunol. 364 (2013) 61–90.
[12] R.A. Kammerer, R.M. Benoit, Botulinum neurotoxins: new questions arising from structural biology, Trends Biochem. Sci. 39 (2014) 517–526.
[13] C. Colasante, O. Rossetto, L. Morbiato, M. Pirazzini, J. Molgo, C. Montecucco, Botulinum neurotoxin type A is internalized and translocated from small synaptic vesicles at the neuromuscular junction, Mol. Neurobiol. 48 (2013) 120–127.
[14] C.B. Harper, S. Martin, T.H. Nguyen, S.J. Daniels, N.A. Lavidis, M.R. Popoff, et al., Dynamin inhibition blocks botulinum neurotoxin type A endocytosis in neurons and delays botulism, J. Biol. Chem. 286 (2011) 35966–35976.
[15] L.L. Simpson, Ammonium chloride and methylamine hydrochloride antagonize clostridial neurotoxins, J. Pharmacol. Exp. Ther. 225 (1983) 546–552.
[16] G. Schiavo, M. Matteoli, C. Montecucco, Neurotoxins affecting neuroexocytosis, Physiol. Rev. 80 (2000) 717–766.
[17] A. Fischer, M. Montal, Molecular dissection of botulinum neurotoxin reveals interdomain chaperone function, Toxicon 75 (2013) 101–107.
[18] M. Pirazzini, D.A. Tehran, O. Leka, G. Zanetti, O. Rossetto, C. Montecucco, On the translocation of botulinum and tetanus neurotoxins across the membrane of acidic intracellular compartments, Biochim. Biophys. Acta (BBA) (2015) , doi: http://dx.doi.org/10.1016/j.bbamem.2015.08.014.
[19] M. Pirazzini, O. Rossetto, P. Bolognese, C.C. Shone, C. Montecucco, Double anchorage to the membrane and intact inter-chain disulfide bond are required for the low pH induced entry of tetanus and botulinum neurotoxins into neurons, Cell Microbiol. 13 (2011) 1731–1743.
[20] A. Fischer, M. Montal, Crucial role of the disulfide bridge between botulinum neurotoxin light and heavy chains in protease translocation across membranes, J. Biol. Chem. 282 (2007) 29604–29611 Epub 2007 July 31.
[21] A. de Paiva, B. Poulain, G.W. Lawrence, C.C. Shone, L. Tauc, J.O. Dolly, A role for the interchain disulfide or its participating thiols in the internalization of botulinum neurotoxin A revealed by a toxin derivative that binds to ecto-acceptors and inhibits transmitter release intracellularly, J. Biol. Chem. 268 (1993) 20838–20844.
[22] G. Schiavo, E. Papini, G. Genna, C. Montecucco, An intact interchain disulfide bond is required for the neurotoxicity of tetanus toxin, Infect. Immun. 58 (1990) 4136–4141.
[23] A. Kistner, D. Sanders, E. Habermann, Disulfide formation in reduced tetanus toxin by thioredoxin: the pharmacological role of interchain covalent and noncovalent bonds, Toxicon 31 (1993) 1423–1434.
[24] G. Schiavo, F. Benfenati, B. Poulain, O. Rossetto, P. Polverino de Laureto, B.R. DasGupta, et al., Tetanus and botulinum-B neurotoxins block neurotransmitter release by proteolytic cleavage of synaptobrevin, Nature 359 (1992) 832–835.
[25] G. Schiavo, O. Rossetto, S. Catsicas, P. Polverino de Laureto, B.R. DasGupta, F. Benfenati, et al., Identification of the nerve terminal targets of botulinum neurotoxin serotypes A, D, and E, J. Biol. Chem. 268 (1993) 23784–23787.
[26] T. Binz, Clostridial neurotoxin light chains: devices for SNARE cleavage mediated blockade of neurotransmission, Curr. Top. Microbiol. Immunol. 364 (2013) 139–157.
[27] S. Pantano, C. Montecucco, The blockade of the neurotransmitter release apparatus by botulinum neurotoxins, Cell. Mol. Life Sci. 71 (2014) 793–811.
[28] M. Pirazzini, T. Azarnia, D. ehran, G. Zanetti, A. Megighian, M. Scorzeto, S. Fillo, et al., Thioredoxin and its reductase are present on synaptic vesicles, and their inhibition prevents the paralysis induced by botulinum neurotoxins, Cell Rep. 8 (2014) 1870–1878.
[29] M. Montal, Redox regulation of botulinum neurotoxin toxicity: therapeutic implications, Trends Mol. Med. 20 (2014) 602–603.
[30] T. Binz, S. Sikorra, S. Mahrhold, Clostridial neurotoxins: mechanism of SNARE cleavage and outlook on potential substrate specificity reengineering, Toxins 2 (2010) 665–682.
[31] J. Lu, L.V. Papp, J. Fang, S. Rodriguez-Nieto, B. Zhivotovsky, A. Holmgren, Inhibition of mammalian thioredoxin reductase by some flavonoids: implications for myricetin and quercetin anticancer activity, Cancer Res. 66 (2006) 4410–4418.
[32] J. Fang, J. Lu, A. Holmgren, Thioredoxin reductase is irreversibly modified by curcumin: a novel molecular mechanism for its anticancer activity, J. Biol. Chem. 280 (2005) 25284–25290.
[33] D.L. Kirkpatrick, M. Kuperus, M. Dowdeswell, N. Potier, L.J. Donald, M. Kunkel, et al., Mechanisms of inhibition of the thioredoxin growth factor system by antitumor 2-imidazolyl disulfides, Biochem. Pharmacol. 55 (1998) 987–994.
[34] A. Mukherjee, S.G. Martin, The thioredoxin system: a key target in tumour and endothelial cells, Br. J. Radiol. 81 (2008) Spec No 1:S57–68.
[35] R. Zhao, H. Masayasu, A. Holmgren, Ebselen a substrate for human thioredoxin reductase strongly stimulating its hydroperoxide reductase activity and a superfast thioredoxin oxidant, Proc. Natl. Acad. Sci. U. S. A. 99 (2002) 8579–8584.
[36] M. Pirazzini, F. Bordin, O. Rossetto, C.C. Shone, T. Binz, C. Montecucco, The thioredoxin reductase-thioredoxin system is involved in the entry of tetanus and botulinum neurotoxins in the cytosol of nerve terminals, FEBS Lett. 587 (2013) 150–155.
[37] A. Rummel, S. Mahrhold, H. Bigalke, T. Binz, The HCC-domain of botulinum neurotoxins A and B exhibits a singular ganglioside binding site displaying serotype specific carbohydrate interaction, Mol. Microbiol. 51 (2004) 631–643.
[38] A. Rummel, T. Karnath, T. Henke, H. Bigalke, T. Binz, Synaptotagmins I and II act as nerve cell receptors for botulinum neurotoxin G, J. Biol. Chem. 279 (2004) 30865–30870 Epub 2004 April 30.
[39] S. Bade, A. Rummel, C. Reisinger, T. Karnath, G. Ahnert-Hilger, H. Bigalke, et al., Botulinum neurotoxin type D enables cytosolic delivery of enzymatically active cargo proteins to neurones via unfolded translocation intermediates, J. Neurochem. 91 (2004) 1461–1472.

[40] C.C. Shone, H.S. Tranter, Growth of clostridia and preparation of their neurotoxins, Curr. Top. Microbiol. Immunol. 195 (1995) 143–160.
[41] M. Rigoni, G. Schiavo, A.E. Weston, P. Caccin, F. Allegrini, M. Pennuto, et al., Snake presynaptic neurotoxins with phospholipase A2 activity induce punctate swellings of neurites and exocytosis of synaptic vesicles, J. Cell Sci. 117 (2004) 3561–3570.
[42] K.R. Aoki, A comparison of the safety margins of botulinum neurotoxin serotypes A, B, and F in mice, Toxicon 39 (2001) 1815–1820.
[43] R.S. Broide, J. Rubino, G.S. Nicholson, M.C. Ardila, M.S. Brown, K.R. Aoki, et al., The rat digit abduction score (DAS) assay: a physiological model for assessing botulinum neurotoxin-induced skeletal muscle paralysis, Toxicon 71 (2013) 18–24.
[44] S. Sun, W.H. Tepp, E.A. Johnson, E.R. Chapman, Botulinum neurotoxins B and E translocate at different rates and exhibit divergent responses to GT1b and low pH, Biochemistry 51 (2012) 5655–5662.
[45] S. Sun, S. Suresh, H. Liu, W.H. Tepp, E.A. Johnson, J.M. Edwardson, et al., Receptor binding enables botulinum neurotoxin B to sense low pH for translocation channel assembly, Cell Host Microbe 10 (2011) 237–247.
[46] T. Yamaguchi, K. Sano, K. Takakura, I. Saito, Y. Shinohara, T. Asano, et al., Ebselen in acute ischemic stroke: a placebo-controlled, double-blind clinical trial: Ebselen study group, Stroke 29 (1998) 12–17.
[47] I. Saito, T. Asano, K. Sano, K. Takakura, H. Abe, T. Yoshimoto, et al., Neuroprotective effect of an antioxidant, ebselen, in patients with delayed neurological deficits after aneurysmal subarachnoid hemorrhage, Neurosurgery 42 (1998) 269–277.
[48] C. Montecucco, M.B. Rasotto, On botulinum neurotoxin variability, MBio (2015) 2015.
[49] T.J. Smith, K.K. Hill, B.H. Raphael, Historical and current perspectives on *Clostridium botulinum* diversity, Res. Microbiol. 166 (2015) 290–302.
[50] Y. Torii, Y. Goto, M. Takahashi, S. Ishida, T. Harakawa, T. Sakamoto, et al., Quantitative determination of biological activity of botulinum toxins utilizing compound muscle action potentials (CMAP), and comparison of neuromuscular transmission blockage and muscle flaccidity among toxins, Toxicon 55 (2010) 407–414.
[51] F.r.A. Meunier, G. Lisk, D. Sesardic, J.O. Dolly, Dynamics of motor nerve terminal remodeling unveiled using SNARE-cleaving botulinum toxins: the extent and duration are dictated by the sites of SNAP-25 truncation, Mol. Cell. Neurosci. 22 (2003) 454–466.
[52] L. Carli, C. Montecucco, O. Rossetto, Assay of diffusion of different botulinum neurotoxin type a formulations injected in the mouse leg, Muscle Nerve 40 (2009) 374–380.
[53] R. Eleopra, V. Tugnoli, R. Quatrale, O. Rossetto, C. Montecucco, Different types of botulinum toxin in humans, Mov. Disord. 19 (Suppl. 8) (2004) S53–S59.
[54] S. Pellett, W.H. Tepp, R.C.M. Whitemarsh, M. Bradshaw, E.A. Johnson, In vivo onset and duration of action varies for botulinum neurotoxin A subtypes 1–5, Toxicon (2015) , doi:http://dx.doi.org/10.1016/j.toxicon.2015.06.021.
[55] C.B. Shoemaker, G.A. Oyler, Persistence of Botulinum neurotoxin inactivation of nerve function, Curr. Top. Microbiol. Immunol. 364 (2013) 179–196.
[56] D.M. Gill, Bacterial toxins: a table of lethal amounts, Microbiol. Rev. 46 (1982) 86–94.
[57] B. Thyagarajan, N. Krivitskaya, J.G. Potian, K. Hognason, C.C. Garcia, J.J. McArdle, Capsaicin protects mouse neuromuscular junctions from the neuroparalytic effects of botulinum neurotoxin a, J. Pharmacol. Exp. Ther. 331 (2009) 361–371.
[58] R.P. Fagan, J.B. McLaughlin, J.P. Middaugh, Persistence of botulinum toxin in patients' serum: Alaska, 1959–2007, J. Infect. Dis. 199 (2009) 1029–1031.
[59] A.N. Sheth, P. Wiersma, D. Atrubin, V. Dubey, D. Zink, G. Skinner, et al., International outbreak of severe botulism with prolonged toxemia caused by commercial carrot juice, Clin. Infect. Dis. 47 (2008) 1245–1251.
[60] A.F. Baker, K.N. Adab, N. Raghunand, H.H.S. Chow, S.P. Stratton, S.W. Squire, et al., A phase IB trial of 24-hour intravenous PX-12, a thioredoxin-1 inhibitor, in patients with advanced gastrointestinal cancers, Invest. New Drugs 31 (2013) 631–641.
[61] R.K. Ramanathan, J. Abbruzzese, T. Dragovich, L. Kirkpatrick, J.M. Guillen, A.F. Baker, et al., A randomized phase II study of PX-12, an inhibitor of thioredoxin in patients with advanced cancer of the pancreas following progression after a gemcitabine-containing combination, Cancer Chemother. Pharmacol. 67 (2011) 503–509.
[62] M.J. Parnham, H. Sies, The early research and development of ebselen, Biochem. Pharmacol. 86 (2013) 1248–1253.
[63] M. Parnham, H. Sies, Ebselen prospective therapy for cerebral ischaemia, Expert Opin. Investig. Drugs 9 (2000) 607–619.
[64] A. Goel, A.B. Kunnumakkara, B.B. Aggarwal, Curcumin as Curecumin: from kitchen to clinic, Biochem. Pharmacol. 75 (2008) 787–809.
[65] E. Middleton, C. Kandaswami, T.C. Theoharides, The effects of plant flavonoids on mammalian cells:implications for inflammation, heart disease, and cancer, Pharmacol. Rev. 52 (2000) 673–751.
[66] R. Koepke, J. Sobel, S.S. Arnon, Global occurrence of infant botulism, 1976–2006, Pediatrics 122 (2008) e73–e82.
[67] S.S. Arnon, Infant botulism, Annu. Rev. Med. 31 (1980) 541–560.

3.1.3 A novel inhibitor prevents the peripheral neuroparalysis of botulinum neurotoxin

Domenico Azarnia Tehran[1],*,Giulia Zanetti[1],*, Oneda Leka[1], Florigio Lista[3], Silvia Fillo[3], Thomas Binz[4], Clifford C. Shone[5], Ornella Rossetto[1], Cesare Montecucco[1,2], Cristina Paradisi[6], Andrea Mattarei[6], and Marco Pirazzini[1]

[1]Department of Biomedical Sciences and [2]National Research Council Institute of Neuroscience, University of Padova, Via Ugo Bassi 58/B, 35151 Padova, Italy

[3]Histology and Molecular Biology Section, Army Medical and Veterinary Research Center, Via Santo Stefano Rotondo 4, 00184 Rome, Italy

[4]Institut für Biochemie, Medizinische Hochschule, Hannover, 30623, Hannover, Germany

[5]Public Health England, Porton Down, Salisbury, Wiltshire SP4 OJG, UK

[6]Department of Chemical Sciences, University of Padova, Via F. Marzolo 1, 35131 Padova, Italy

*These authors contributed equally to this work

Azarnia Tehran D., Zanetti G. *et al.* A Novel Inhibitor Prevents the Peripheral Neuroparalysis of Botulinum Neurotoxins. *Sci Rep*, 5, 17513.
doi: 10.1038/srep17513 (2015).

SCIENTIFIC REPORTS

OPEN

A Novel Inhibitor Prevents the Peripheral Neuroparalysis of Botulinum Neurotoxins

Received: 18 September 2015
Accepted: 30 October 2015
Published: 16 December 2015

Domenico Azarnia Tehran[1,*], Giulia Zanetti[1,*], Oneda Leka[1], Florigio Lista[3], Silvia Fillo[3], Thomas Binz[4], Clifford C. Shone[5], Ornella Rossetto[1], Cesare Montecucco[1,2], Cristina Paradisi[6], Andrea Mattarei[6] & Marco Pirazzini[1]

Botulinum neurotoxins (BoNTs) form a large class of potent and deadly neurotoxins. Given their growing number, it is of paramount importance to discover novel inhibitors targeting common steps of their intoxication process. Recently, EGA was shown to inhibit the action of bacterial toxins and viruses exhibiting a pH-dependent translocation step in mammalian cells, by interfering with their entry route. As BoNTs act in the cytosol of nerve terminals, the entry into an appropriate compartment wherefrom they translocate the catalytic moiety is essential for toxicity. Herein we propose an optimized procedure to synthesize EGA and we show that, *in vitro*, it prevents the neurotoxicity of different BoNT serotypes by interfering with their trafficking. Furthermore, in mice, EGA mitigates botulism symptoms induced by BoNT/A and significantly decreases the lethality of BoNT/B and BoNT/D. This opens the possibility of using EGA as a lead compound to develop novel inhibitors of botulinum neurotoxins.

The most potent human poisons are the botulinum neurotoxins (BoNTs), which are neurospecific metalloproteases acting inside peripheral nerve terminals. They are synthesized by different species of Clostridia and have been grouped in seven serotypes (BoNT/A to/G) based on their immunological properties. All known BoNTs act by interrupting the release of neurotransmitter acetylcholine at peripheral cholinergic terminals causing a long lasting paralysis that may lead to death by respiratory failure[1]. Nonetheless, mechanically ventilated patients can fully recover in a time period which strongly depends on the toxin serotypes and on the amount of toxin molecules entered in the nerve terminals[2]. According to their extreme potency, and with the fact that they can be easily produced in large amounts, BoNTs are considered potential bioweapons[3,4]. On the other hand, due to their neurospecificity, reversibility and lack of diffusion from the site of injection, BoNT/A has worldwide become one of the safest therapeutics used for the treatment of a growing list of human syndromes, characterized by the hyperactivity of peripheral nerve terminals[5,6]. BoNTs consist of two polypeptide chains (L and H), kept together by a single disulphide bond. The overall structure can be subdivided in three 50 kDa domains which accomplish different tasks along the mechanism of neuron intoxication[2]. The L chain is the N-terminal domain endowed with metalloprotease activity. The C-terminal domain (HC) is responsible for the neurospecific binding to the presynaptic membrane of nerve endings, whilst the intermediate domain (HN) is involved in membrane translocation of L. The current view of BoNT mechanism of

[1]Department of Biomedical Sciences, Via U. Bassi 58/B, 35121, Padova, Italy. [2]Italian National Research Council Institute of Neuroscience, University of Padova, Via U. Bassi 58/B, 35121, Padova, Italy. [3]Histology and Molecular Biology Section, Army Medical and Veterinary Research Center, Via Santo Stefano Rotondo 4, 00184 Roma, Italy. [4]Institut für Biochemie, OE 4310, Medizinische Hochschule Hannover, 30623 Hannover, Germany. [5]Public Health England, Porton Down, Salisbury, Wiltshire, SP4 OJG, UK. [6]Department of Chemical Sciences, University of Padova, Via F. Marzolo 1, 35131 Padova, Italy. *These authors contributed equally to this work. Correspondence and requests for materials should be addressed to A.M. (email: andrea.mattarei@unipd.it) or M.P. (email: marcopiraz@gmail.com)

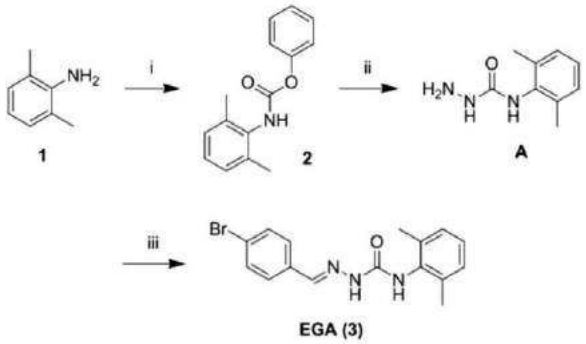

Figure 1. Synthesis of EGA. Synthesis of 2-(4-bromobenzylidene)-N-(2,6-dimethylphenyl) hydrazinecarboxamide (EGA); Reagents and conditions (i) $ClCO_2Ph$, Py, DCM (96% isolated yield); (ii) $NH_2NH_2{\cdot}H_2O$, DME (iii) 4-bromobenzaldehyde, $CHCl_3$ (88% isolated yield, passages ii and iii).

action envisages a first interaction with polysialogangliosides, which mediate the toxin binding to the plasma membrane. This is followed by lateral movements that make possible the encounter with a protein receptor which is the lumenal part of a synaptic vesicle (SV) protein[2,7,8]. The protein receptor has been identified as synaptotagmin I and II for BoNT/B,/DC and/G[8,9], and SV2 for BoNT/A,/E and F[8,10]; the protein receptor for the remaining serotypes remains to be established. This latter binding is preliminary to the internalization of the toxin-receptors complex inside an acidic intracellular compartment whose nature has been identified as SV only for tetanus neurotoxin and for BoNT/A[11–13]. Little is known on the nature of the endocytic vesicles/compartment used by the other serotypes, but considerable evidence indicate that the acidification of its lumen generally triggers a structural change of L and HN together with membrane lipids which ultimately leads to the translocation of the L chain into the cytosol[14–16]. This process is completed by the reduction of the interchain disulphide bond, on the cytosolic side of the acidic compartment performed by the thioredoxin reductase–thioredoxin system[17–20] . The released L metalloprotease specifically cleaves one of the three SNARE proteins thereby preventing the Ca^{2+} induced release of the neurotransmitter contained inside SVs[21,22]. Many novel BoNTs have been recently discovered and their sequences are present in databases, but many more have not yet been deposited. All known novel BoNTs are classified as subtypes, and indicated with an Arabic number added to the parental serotype (e.g. A2, A3 etc., when their amino acid sequences differ by more than 2.4% from the parental serotype A1)[2], or as mosaic BoNTs, and indicated with a double capital letter, e.g. BoNT/DC,/CD,/FA, when they are chimeras of the different serotypes. Due to their different origin, BoNT variants exhibit different antigenicity and are neutralized to a different degree by existing serotype specific antisera[23,24]. Accordingly, it is possible that the therapy with humanized monoclonal antibodies raised versus a BoNT subtype may not neutralize variants of the same serotype[25,26]. This situation calls for increased efforts in the identification of inhibitors effective in preventing the neuroparalytic action of BoNTs irrespectively of their serotype and subtype which could be used without knowing the particular type of BoNT involved. Recently, Gillespie *et al.* (2013), performing a high-throughput screening, identified 4-bromobenzaldehyde N-(2,6-dimethylphenyl)semicarbazone (abbreviated as EGA) as an inhibitor of pathogens that enter cells via intracellular acid compartments[27]. Since BoNTs toxicity is also strictly dependent on the passage through an acidic environment[2], we decided to test the activity of EGA on BoNT action in the light of the urgency and importance to find inhibitors capable of interfering with the large and still growing number of BoNTs with undefined immunological properties. Here, we focused our attention on BoNT/A and BoNT/B because most frequently associated with human botulism and used in human therapy[1,2]. We also considered BoNT/D, which scarcely affects humans[28], but it is very frequently involved in animal botulism. Here we show that EGA drastically hinders BoNTs activity on neuronal cultures, without interfering with specific steps of their cellular mechanism of intoxication. More importantly, this compound is also very effective in reducing neurotoxicity *in vivo*. Together, our results suggest that EGA represents a new tool for studying BoNTs trafficking and a good candidate for the development of new inhibitors. Notably, we also report an optimized procedure for the synthesis of EGA, which involves milder reaction conditions and provides much higher overall yield than previously reported[29].

Results

High yield synthesis of 4-bromobenzaldehyde N-(2,6-dimethylphenyl) semicarbazone (EGA). The reported approach by Jung in 2014 for the preparation of EGA has been adapted and improved to obtain higher yields. The synthesis involves the three steps reported in Fig. 1. In the first one (i), 2,6-dimethylaniline (1) is allowed to react with phenyl chloroformate to give the corresponding phenylcarbamate (2), which is next subjected to hydrazinolysis to give semicarbazide (indicated as A) (ii). The final step (iii) is the reaction of A with 4-bromobenzaldehyde to form the desired semicarbazone (3,

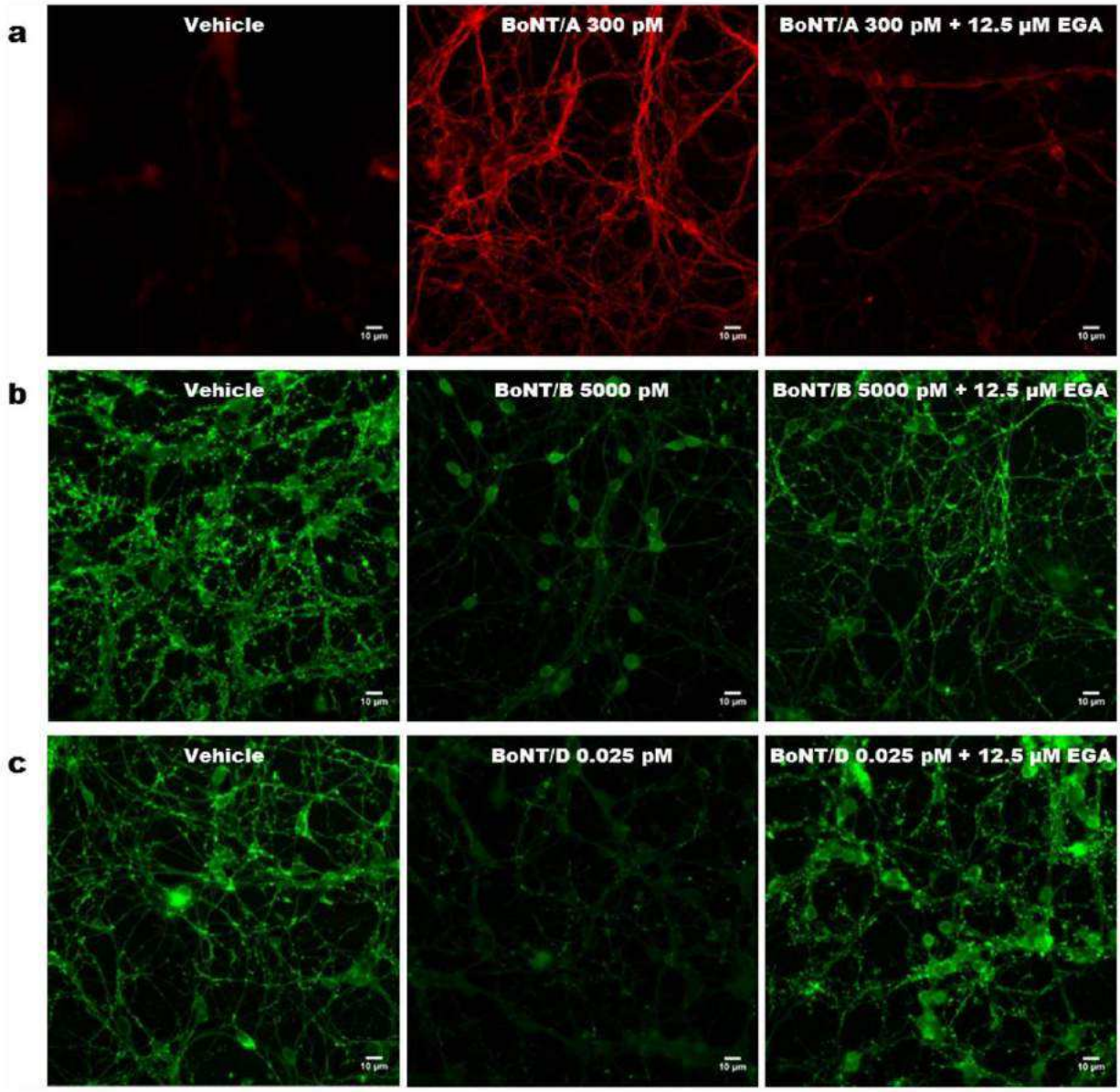

Figure 2. Immunocytochemical evaluation of EGA inhibition against different serotypes of BoNT in CGNs. (**a–c**) CGNs were treated with EGA 12.5 μM or vehicle (DMSO) at 37 °C for 30 min. Thereafter, the indicated amount of BoNT was added for 12 hrs. Samples were fixed and stained with an antibody specific for BoNT/A-cleaved SNAP25 (**a**) or intact VAMP2, (**b,c**). BoNT/A-cleaved SNAP25 was detected with an Alexa Fluor 555 goat anti-rabbit, while VAMP2 with an Alexa Fluor 488 goat anti-mouse. Images shown are representative of three independent experiments. Scale bar, 10 μm.

EGA). The procedure described by Jung *et al.* (2014) involves the isolation of A and rather drastic conditions (acidic solution and high temperature) in the last step, leading to an overall yield of 27%. A much higher overall yield (84%) is obtained by the new procedure that we have devised: 2 is isolated, whereas steps (ii) and (iii) are performed in one-pot without the isolation of A. Furthermore, much milder conditions are used in the last synthetic step. Details are found in the Supplementary information section.

EGA prevents the botulinum neurotoxins cleavage of SNARE proteins in cultured neurons. The use of cultured cerebellar granular neurons (CGNs) offers a simple and rapid way to screen the efficacy of candidate molecules in inhibiting BoNTs activity. The overnight incubation with 0.3 nM BoNT/A induces the cleavage of SNAP25, as assessed by the appearance in immunofluorescence (Fig. 2a, middle panel) and western blot (Fig. 3a, bottom panel) of its truncated form, revealed with a specific antibody. This toxin concentration is sufficient to induce a complete cleavage of its substrate, as evaluated using

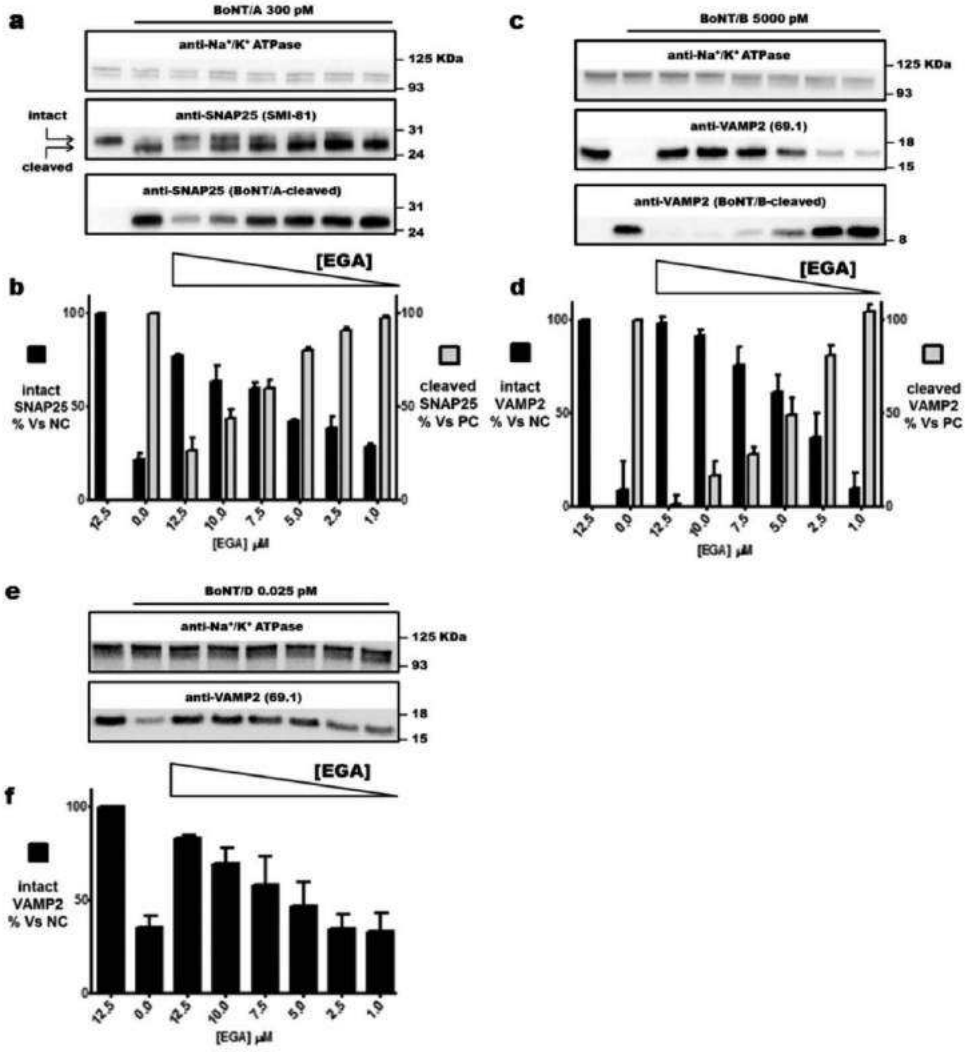

Figure 3. EGA interferes with the BoNT/A,/B and/D toxicity in CGNs. (**a,c,e**) CGNs were preincubated for 30 min with the indicated concentrations of EGA at 37 °C. Where indicated, BoNTs were added at the reported concentrations for 12 hrs. Then cells were lysed and the SNARE content was estimated with the indicated antibodies: (**a**) SMI81 recognizes both the full length and the cleaved form of SNAP25; BoNT/A-cleaved recognizes only BoNT/A-truncated SNAP25; (**c,e**) VAMP2 (69.1) recognizes the intact form of VAMP2 and, BoNT/B-cleaved recognizes only BoNT/B-cleaved VAMP2. In all experiments an antibody against the Na^+/K^+ ATPase antibody was used as loading control. Blots are representative of a typical experiment. (**b,d,f**) Densitometry analysis of western blots obtained in (**a,c**) and (**e**) respectively. All data are presented as mean values and error bars indicated the standard deviation obtained from at least three independent experiments.

an antibody recognizing both forms (intact and truncated) of SNAP25 (Fig. 3a, middle panel, SMI-81). Figure 3b shows that such activity is however inhibited by EGA in a concentration dependent manner, with a maximal effect at 12.5 μM. The inhibitory effect, though substantial, is not complete as a small amount of cleaved SNAP25 is still generated (Fig. 2a, right panel and Fig. 3b).

Figures 2b and 3c,d show that similar results are obtained with BoNT/B. Notably, to achieve the substantial cleavage of VAMP2, which is normally concentrated at synaptic contacts (Fig. 2b, left panel), BoNT/B had to be used at a concentration of 5 nM (Fig. 2b, middle panel). Nevertheless, the pre-treatment with 12.5 μM EGA is sufficient to abrogate its cleavage (Fig. 2b, right panel). EGA prevents this toxicity in a concentration dependent manner, as shown by the inhibition of VAMP2 cleavage, determined with two different antibodies (Fig. 3c middle and bottom panels). Interestingly, despite the high amount of toxin used, in this case the effect of EGA, at higher concentration, is complete (Fig. 3d).

The same set of experiments was replicated using BoNT/D. This serotype is the most potent in rodents[28] and, in CGNs, a minimal concentration (0.025 pM) induces the almost complete cleavage of VAMP2 (Fig. 2c, middle panel). Similar to what found for BoNT/A, we found that EGA substantially prevents the action of this potent neurotoxin (Fig. 2c, right panel), and this inhibition is dependent on

the amount of the chemical, as estimated in western blot with an antibody specific for the intact form of VAMP2 (Fig. 3e, bottom panel and Fig. 3f).

Importantly, Figure S1 shows that neurons viability is not significantly affected, even at the highest concentration of EGA used.

EGA does not interfere with the four basic steps of BoNTs' mechanism of action. The cellular target of EGA is not known and we investigated whether any of the four main steps of the BoNTs' cellular mechanism of action is directly impacted by the action of the drug.

The first step of intoxication is the specific binding of BoNTs to peripheral nerve endings followed by their internalization via endocytosis[2]. Given its chemical nature, EGA could in principle intercalate among lipids and alter the properties of the presynaptic membrane, making it less receptive for BoNTs binding. To investigate this possibility, we took advantage of two constructs consisting of the HC domain of BoNT/A and of BoNT/B fused to a fluorescent protein (cpV-HC/A) or tagged by a c-Myc epitope (c-Myc-HC/B), respectively. These chimeras fully maintain the capability of parental BoNTs to bind to the presynaptic membrane of neurons[8,30] and to become endocytosed[12,13]. We found that EGA, used at the concentration which displayed the maximum efficacy in protecting CGNs, does not interfere with the binding and the endocytosis of both BoNT/A and BoNT/B, as assessed by the internalization of their respective derivatives which show the same pattern regardless of drug presence (Fig. 4a and Figure S2a). Intriguingly, the two HCs displayed clearly different patterns of staining, suggesting that they may be internalized inside different compartments. Figure 4b and Figure S2b show via western blot analyses the quantitation of the results. We performed this experiment with higher concentrations of HCs to meet the sensitivity requirements of the antibodies used in Western Blot. Consistently, Fig. 4b show that the previous treatment of CGNs with BoNT/D, which cleaves VAMP1/2 thus impairing SVs recycling, significantly decreases the uptake of HC/A, as reported elsewhere[31,32]. At variance, the uptake of HC/B was only partially affected by VAMP1/2 cleavage (Figure S2b), leaving open the possibility of a different trafficking of BoNT/B with respect to BoNT/A.

Nevertheless, the fact that BoNT/A and BoNT/B use synaptic vesicle proteins as receptors (SV2A/B/C and Synaptotagmin I-II, respectively) strongly suggests that they exploit SVs for their initial step of endocytosis. Accordingly, we decided to test the possible interference of EGA with SVs dynamics using a well-established assay[33]. As shown in Figure S2c, EGA does not affect SVs endocytosis as an antibody specific for the lumenal domain of the synaptic vesicle marker Synaptotagmin I, is internalized at the same extent as controls. On the contrary, if neurons are previously treated with BoNT/D, the uptake of the same antibody is prevented. The quantitation of the result is shown in Figure S2d. Taken together, these results demonstrate that BoNTs binding and internalization through SV cycling are not perturbed by EGA.

The BoNT exposure to an intracellular acidic compartment is the next essential step for the neuron intoxication by all BoNTs[2]. Using Lysotracker Red DND-99, a highly sensitive probe of acidic organelles in live cells, we found that EGA does not significantly interfere with the maturation of acidic compartments, both within CGNs cell body and along neurites, where BoNTs act (Fig. 4c). At the same time, bafilomycin A1, which prevents BoNTs toxicity by inhibiting the vacuolar-type H^+-ATPase proton pump[12,34,35], completely blocks the acidification of intracellular organelles. This suggests that the essential conditions needed for BoNTs translocation, i.e. an acidic environment, are maintained in the presence of EGA.

The final step of the nerve intoxication, the one responsible for neuroparalysis, is the cleavage of SNARE proteins by the L chain. BoNT/A chops off the last 9 amino acids of SNAP25, whereas BoNT/B and BoNT/D cleave at two different sites VAMP1/2. This proteolytic activity can be easily assayed *in vitro* by using recombinant substrates. As shown in Fig. 4d (left panel), upon reduction of the interchain disulphide bond, BoNT/A cleaves SNAP25, as shown by the shift of its molecular weight in SDS-PAGE (compare lane 1 and 2, upper panels). This activity is however not affected by 12.5 μM EGA (Fig. 4d, compare lane 2 and 3). The same result was obtained using an antibody specific for the cleaved form of SNAP25 and western blotting as a read out (Fig. 4d). Figure S3a and Figure S3b show that similar results were obtained with BoNT/B and BoNT/D, respectively, suggesting that the enzymatic activity of BoNT L chains is not affected by the drug.

EGA interferes with BoNTs trafficking within neurons. Gillespie *et al.* (2013) reported that EGA prevents the toxicity of bacterial toxins and viruses by blocking their trafficking from early to late endosomes. Here, we have shown that EGA inhibits BoNTs without interfering with the main events along their mechanism of action. As a consequence, we reasoned that EGA could alter the trafficking of BoNTs after their internalization, possibly preventing them to reach their translocation-competent compartment. If it is the case, EGA should not be capable of inhibiting BoNTs toxicity when their trafficking is bypassed by inducing the entry of the L chain across the plasma membrane of neurons[36]. As this experimental approach strongly depends on the binding to both receptors at the plasma membrane[36], we could perform this experiment only with BoNT/B, using an established PC12 cell line expressing on the plasma membrane the lumenal domain of Synaptotagmin I, the BoNT/B protein receptor[9], and with BoNT/D, whose binding domain harbors two ganglioside binding sites[37], using CGNs[36]. Figure 5a,b show that a low pH jump in the extracellular medium induces the translocation of BoNT/B and BoNT/D L chains

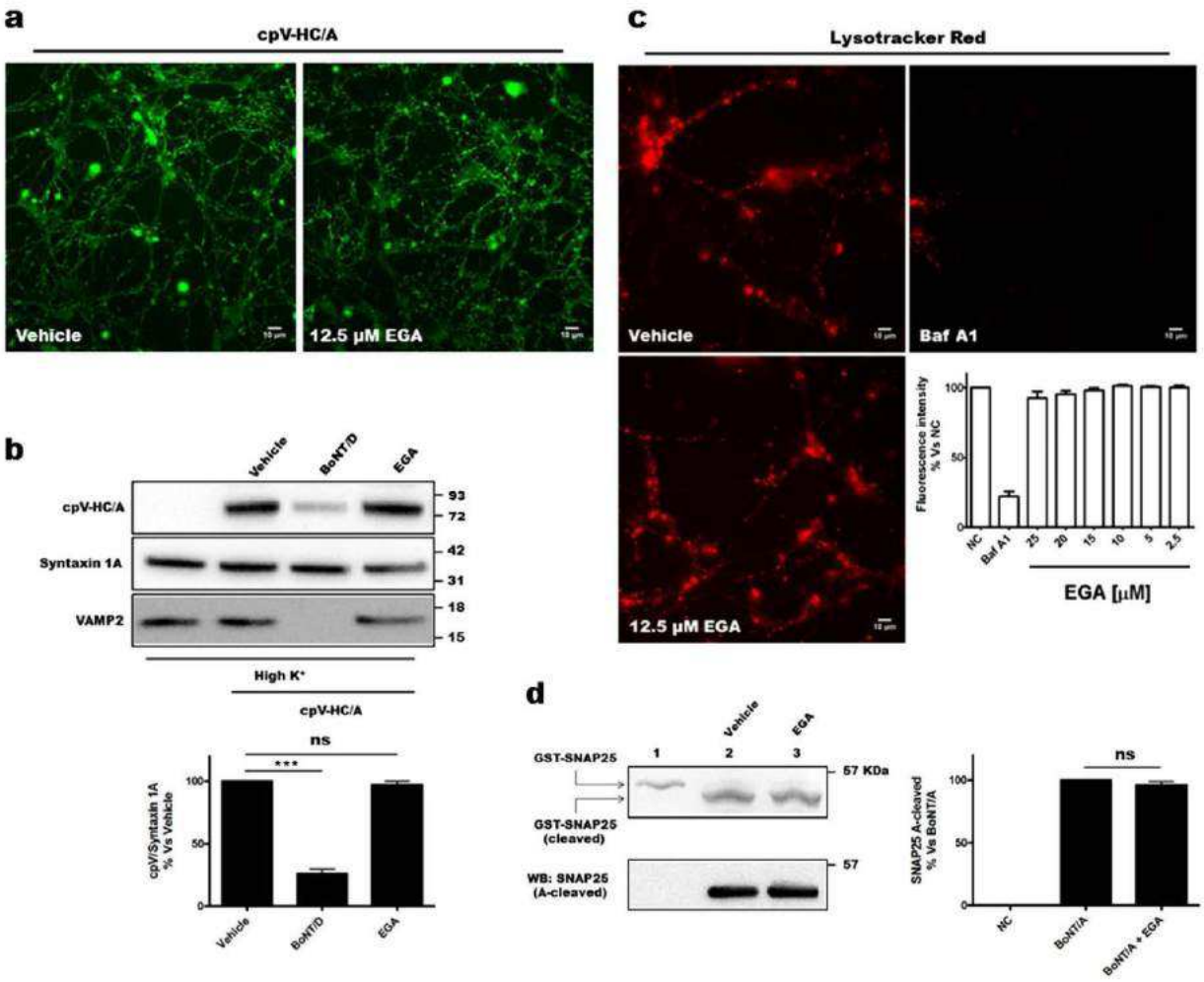

Figure 4. EGA does not inhibit the known steps of BoNT intoxication. (**a**) CGNs were treated with EGA (12.5 μM) or vehicle in culture medium at 37 °C. After 30 min, 100 nM cpV-HC/A was added in high K^+ buffer for 1 h. Neurons were then washed, fixed, and directly imaged. These images are representative of at least three independent sets of experiments. Scale bar, 10 μm. (**b**) CGNs were treated as in (**a**) with 250 nM cpV-HC/A and then lysed. The cpV-HC/A content was estimated with a GFP specific antibody. Syntaxin 1A serving as internal control was detected with a specific antibody and an anti-VAMP2 was used to assess BoNT/D cleavage. The amount of cpV-HC/A was determined as a ratio to Syntaxin 1A staining taking the value in non-treated cells (vehicle) as 100%. All data are presented as mean values and error bars indicated the standard deviation obtained from three independent experiments (***$p < 0.0001$; ns – non significant). (**c**) CGNs were treated with vehicle or 12.5 μM EGA or 10 nM Bafilomycin A1 for 30 min at 37 °C. Lysotracker Red was then added and the incubation prolonged for further 90 min. Cells were imaged by fluorescence microscopy. The graph shows the quantification of fluorescence intensity of acid compartments (% versus non-treated neurons) arising from CGNs treated with the indicated amount of EGA. Mean and standard deviation values refer to four different experiments. Scale bar, 10 μm. (**d**) 0.25 μg BoNT/A was reduced in the presence of 12.5 μM EGA for 30 min at 37 °C. 1 μg of GST-SNAP25 was added, the concentration of inhibitor was restored, and the reaction was carried out for 12 hrs at 37 °C. SNAP25 cleavage was assessed by SDS-PAGE and Coomassie staining (top-left panel) or immunoblotting (bottom-left panel) with an antibody specific for the BoNT/A-cleaved form of SNAP25. Lane 1 shows untreated GST-SNAP25. Right panel shows the densitometry analysis of western blots, tacking the value of BoNT/A without EGA (vehicle) as 100%. All data are presented as mean values and error bars indicated the standard deviation obtained from three independent experiments.

across the plasma membrane as evaluated by the cleavage of VAMP2. In agreement with our hypothesis, the same experiment performed in the presence of EGA showed the identical activity of both BoNTs on VAMP2. This suggests that, when these neurotoxins bypass their canonical entry routes, EGA cannot

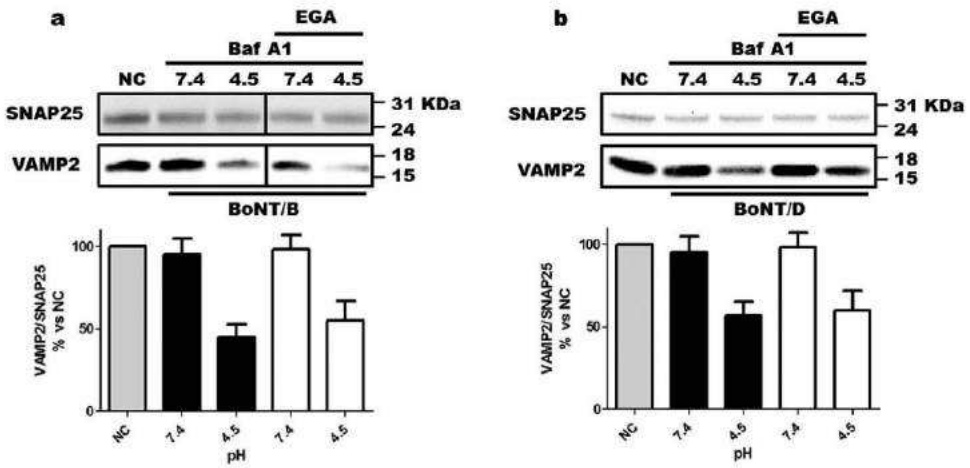

Figure 5. EGA does not inhibit the translocation and the reduction step. (**a**) PC12 cells expressing the lumenal domain of synaptotagmin I on their surface were pre-incubated with a mixture of gangliosides for 24 hrs. Cells were washed and, where indicated, treated with 12.5 μM EGA or vehicle for 30 min at 37 °C. Thereafter, BoNT/B (10 nM) was added in the cold for 15 min. Cells were then washed and incubated with medium A buffered at indicated pH at 37 °C for 10 min, in the presence or absence of EGA. Then, cells were washed and the incubation in culture medium containing 50 nM Bafilomycin A1 and the same concentration of EGA prolonged for 24 hrs at 37° C. The translocation of BoNT/B was assessed by monitoring the cleavage of VAMP2, determined via western blotting (top panel), and quantified (bottom panel) through the densitometry of VAMP2 as a ratio to SNAP25 staining which served as internal control, taking the value in non-treated cells (NC) as 100%. All data are presented as mean values and error bars indicated the standard deviation obtained from three independent experiments (ns – non significant).
(**b**) CGNs were treated with 12.5 μM EGA or vehicle for 30 min at 37 °C. Then, neurons were incubated with BoNT/D (2.5 pM) at 4 °C for 15 min, washed and incubated at 37 °C with buffers at different pH value (7.4 or 4.5) for 10 min; after washing, the neurons were incubated for 24 h with standard medium in the presence of 50 nM bafilomycin A1 and where indicated EGA. Then the SNARE protein content was estimated by immunoblotting with specific antibodies. Values are reported as the ratio between the staining with the antibody specific for VAMP2 and the staining with an antibody specific for SNAP25, and normalized vs. non-treated neurons (NC). All data are presented as mean values and error bars indicated the standard deviation obtained from three independent experiments (ns – non significant).

impact on their activity anymore. Taken together the results presented here indicate that EGA prevents the activity of BoNTs by inhibiting their intraneuronal trafficking.

EGA interferes with the neuroparalytic activity of BoNT/A, BoNT/B and BoNT/D at the mouse hemidiaphragm assay and *in vivo*. The main aim of the present work was to test the inhibitory capacity of EGA against BoNTs toxicity *in vivo*. Therefore, after the *in vitro* approach, we used the mouse hemidiaphragm muscle paralysis model, an *ex vivo* preparation which represents the standard method to assay the neuroparalytic activity of BoNTs at the neuromuscular junction. In this experimental set up, BoNTs induce a decrease in the twitch capability of the diaphragmatic muscle by exerting its metalloprotease activity within the attached phrenic nerve. This decay is followed over time, and is used to evaluate BoNT potency, but can also be adapted to determine the inhibitory capacity of antitoxins[38]. As shown in Fig. 6(a–c, black traces), BoNT/A, BoNT/B and BoNT/D induce a rapid drop in the twitch capability of the diaphragm muscle. On the other hand, the pre-treatment with 12.5 μM EGA, strongly delays the neuroparalytic activity of the three BoNTs (red traces). This inhibitory effect can be appreciated also by comparing the different parameters reported in Table S1, and the $t_{50\%}$ values in particular (Fig. 6d–f), namely the time needed to halve the muscle twitch capacity, which results greatly increased by the treatment with the drug, and found to be significantly different (Table S1).

We then tested the inhibitory effect of EGA *in vivo*. A wide range of doses from 7.5 mg/kg to 40 mg/kg per day was administered via b.i.d. intraperitoneal injections in mice: even after one week of treatment with this regimen, the drug was well tolerated by mice which did not show any sign of decreased vitality in terms of breathing, eating and drinking nor in terms of motility as compared with vehicle injected controls. The lethality of our preparations of BoNT/A,/B and/D was evaluated in preliminary experiments, and a dose of 0.5 ng/kg (BoNT/A), 0.9 ng/kg (BoNT/B) and 0.045 ng/kg (BoNT/D) was sufficient to progressively induce the classical symptoms of botulism (fur ruffling, sides musculature collapse, generalized weakness, labored breathing) and cause the deadly respiratory failure within 48 hours post injection (black traces of Fig. 6 panels g–i). The red traces of the same figure (panels h and i) show

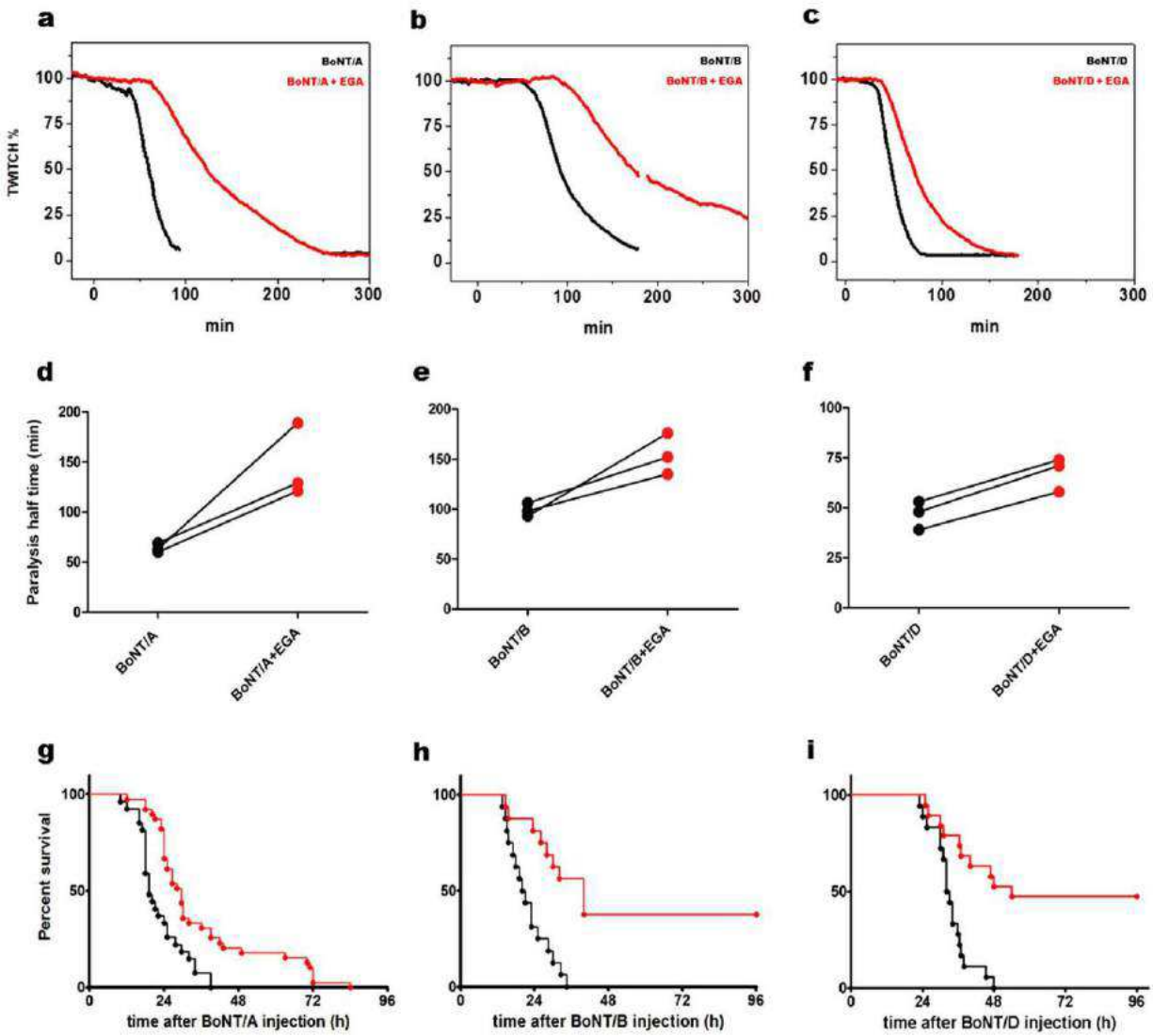

Figure 6. EGA provides protection against different serotypes of BoNTs in the phrenic nerve-hemidiaphragm twitch model, delays death induced by BoNT/A and strongly protect against death induced by BoNT/B and BoNT/D. (**a–c**) For each experiment, 12.5 μM EGA or vehicle (DMSO) was added to the nerve-muscle preparations in the bath at 37 °C; after 30 min, 10 pM BoNT/A (**a**) or 10 pM BoNT/B (**b**) or 100 pM BoNT/D (**c**) was added (time = 0). Muscle twitch was induced by nerve stimulation and monitored until paralysis. A representative experiment is reported for each toxin, showing the progressive twitch decrease in the presence of vehicle (black trace) or EGA (red trace). (**d–f**) Each experiment performed for (**a–c**) was expressed as the time required to decrease the twitch to 50% of the initial value (paralysis half time) in vehicle (black points) or EGA treated muscles (red points). (**g–i**) Adult CD1 mice preconditioned with EGA 12.5 mg/Kg (n = 20) or vehicle alone (n = 20) were i.p. injected with $2 \times MLD_{50}$ of BoNT/A (**g**) or BoNT/B (**h**) or BoNT/D (**i**). The animals were monitored every 4 hrs for 96 hrs. The survival curves were compared and found to be significantly different ($p < 0.0001$).

that EGA is particularly efficacious in preventing death from botulism induced by BoNT/B and BoNT/D. Importantly, in those mice that eventually died, the symptoms occurred with delay and were less pronounced. This was the case also for BoNT/A injected mice, where symptoms developed later and were milder, but without a reduced toxin lethality (Fig. 6g, red trace).

Discussion

The main result reported here is simple and very relevant at the same time. EGA is a potent inhibitor of the neuroparalytic activity of botulinum neurotoxins *in vitro* and *in vivo*, at doses that cause no apparent toxicity. This result indicates that EGA is the lead of a novel class of inhibitors potentially capable of preventing the activity of BoNTs in humans. This is the more relevant considering that the recent years have

witnessed the discovery of a large number of novel BoNTs, with different immunoreactivity[2,39,40], suggesting the possibility of the identification of BoNT variants that may be poorly neutralized by currently available antisera. This situation calls for the discovery of inhibitors capable of preventing the activity of all BoNTs. Necessarily, these novel inhibitors must be non-toxic to humans and must be effective *in vivo*. Notwithstanding long efforts of many laboratories, this goal has only partially been achieved[41]. We recently reported on inhibitors of the Thioredoxin reductase–Thioredoxin redox couple that effectively prevent the neuroparalytic activity of all BoNT serotypes without causing toxic effects in mice[19,20,42]

Here we add another lead compound with a different mechanism of inhibition. Despite our efforts using primary cultures of neurons and neuromuscular junction preparation, we have not identified the target of EGA, but we did not note toxic effects in mice treated with a dose that largely prevents the action of the three BoNTs used here. We have found that the main steps of BoNTs mechanism of action, i.e. binding, internalization, acidification of intracellular compartment, L chain translocation, disulphide reduction and substrate proteolysis, are not affected by this compound (Figs 4 and 5, Figure S2 and Figure S3). Notably, the range of concentration that block BoNTs in cultured neurons is the same previously found to inhibit the toxicity of different toxins and viruses in primary and immortalized macrophages. This suggests that, rather than having a direct effect on BoNTs (or on the other pathogens), EGA interferes with an intracellular host target responsible for their trafficking. This conclusion is reinforced by the result showing that EGA had no effect on the translocation of the L chain from the plasma membrane, when the canonical internalization route was bypassed (Fig. 5).

All known protein receptors of BoNTs are the lumenal domains of integral proteins of synaptic vesicles which suggests the general conclusion that all BoNTs are endocytosed inside these organelles at nerve terminals. However, the following trafficking of synaptic vesicles is not fully understood, though there is evidence that they may fuse with synaptic endosomes where they are quality controlled and then released to re-enter the synaptic vesicle cycle[43–48]. As a consequence, the fact that the three different serotypes considered here are differently protected by EGA, which inhibits the maturation of early endosomes[27], is an interesting aspect of the current study, because it revives the possibility that different BoNT may be trafficked through different routes inside the nerve terminals. Indeed, the diverse protein receptors of BoNTs may account for distinct fates of each toxin-receptor complexes, which have not yet been determined case by case. An alternative explanation is suggested by the finding that part of BoNT/A may enter terminals independently from SVs endocytosis[31,32], which is supported by studies showing that BoNTs display toxicity independently of the stimulation of SVs recycling[34,49–53]. The fact that EGA completely inhibits the activity of BoNT/B, although used at a concentration much higher than that of BoNT/A, opens the possibility that the activity of this toxin is dependent on a trafficking through endosomes and does not translocate its catalytic part into the cytosol across the SV membrane. This is a surprising finding which was unexpected on the basis of the knowledge that the SV protein synaptotagmin mediates the entry of BoNT/B[8,9]. However, considering that synaptotagmin can be trafficked through early endosome[54], the possibility that also BoNT/B may need the passage through this organelle to reach a membrane translocation-competent compartment becomes plausible. It is also in keeping with its slow time course of entry into cultured neurons as compared with other serotypes[34,55]. Moreover, a considerable amount of synaptotagmin molecules remains exposed on the plasma membrane surface, in a steady-state with those recycled through sorting endosomes[56], which makes possible that BoNT/B forms a toxin-receptor complex on the plasma membrane, rather than within SVs. This fits well with the present findings that: i) the internalization of c-Myc-HC/B was much less affected compared to that of cpV-HC/A, by the pre-treatment with BoNT/D (Fig. 4b and Figure S2b) and ii) the different staining pattern of the BoNT/A and BoNT/B binding domains (Fig. 4a and Figure S2a). This possibility is also supported by the *in vivo* finding that EGA has a remarkable effect against the lethality of BoNT/B and a lower one on BoNT/A (Fig. 6g,h).

The behavior of BoNT/D in response to inhibition of the endosomal pathway by EGA, in cultured neurons is more similar to that of BoNT/A rather than BoNT/B, as VAMP2 cleavage was not completely prevented (Figs 2c and 3e,f). On the other hand, BoNT/D was efficaciously inhibited by EGA *in vivo*, with an inhibitory profile similar to that of BoNT/B (Fig. 6i). The mechanism of BoNT/D binding to neurons is poorly understood and therefore its internalization and trafficking properties are not entirely clear[37,57], and as a consequence it is even more difficult to envisage how this toxin could be internalized and trafficked. The obtained results clearly show that the observations of cell culture experiments cannot be transferred *tout court* to *in vivo* conditions.

The present lack of knowledge on the biochemical target of EGA does not prevent research aimed at finding more potent inhibitors of the BoNT neuroparalytic action. Clearly, EGA action is a preventive one, as it cannot affect those L chains that have already translocated in the cytosol. Nevertheless, it can alleviate the symptoms of botulism after diagnosis because a considerable amount of BoNT remains in the general circulation of botulism patient for weeks after the first diagnosis[58–60]. Perhaps, more importantly, the present findings are relevant for infant botulism where a continuous entry of BoNT into the general circulation occurs via adsorption of the toxin produced by Clostridia that have colonized the gastrointestinal tract of infants owing to the reduced intestinal flora competing with Clostridia[2,61].

We would like to conclude by pointing out that the search for novel EGA-derived analogues is made simpler by the design of the novel method of synthesis of this compound described here, which provides a much higher yield with respect to the recently described method[29]. This procedure allowed us to rapidly

and efficiently synthesize large quantities of EGA, an essential pre-requisite to produce the considerable amount necessary for a possible employment of this or related compounds in humans.

Methods

Chemical Synthesis. Detailed protocol for EGA chemical synthesis is available in Supplementary Information.

Botulinum neurotoxin inhibition assay. EGA was dissolved in DMSO to prepare a stock solution (12.5 mM). CGNs at 6–8 days *in vitro* (DIV) were treated for 30 min with the indicated concentrations of EGA in complete culture medium at 37 °C and 5% CO_2. 0.3 nM BoNT/A, 5 nM BoNT/B or 0.025 pM BoNT/D was added, in the presence of the same concentration of inhibitor, and left for 12 hr at 37 °C and 5% CO_2. Further details can be found in the Supplementary Information.

cpV-HC/A and c-Myc-HC/B binding assay. CGNs were treated with EGA 12.5 μM or vehicle (DMSO) in culture medium at 37 °C. After 30 min, for immunocytochemistry experiments, 100 nM cpV-HC/A or c-Myc-HC/B was added in stimulating culture medium (complete culture medium, 57 mM KCl), for 1 hr. The same protocol was used with 250 nM of cpV-HC/A or c-Myc-HC/B but neurons were then lysed and immunoblotted to obtain a quantitative result. Details are in the Supplementary Information.

Low pH induced translocation of BoNT/B and BoNT/D across the plasma membrane. Experiment was conducted as previously described[36]. Detailed protocol is available in Supplementary Information.

Mouse diaphragm and lethality assay. All experiments were performed in accordance with the European Communities Council Directive n° 2010/63/UE and approved by the Italian Ministry of Health. Mouse diaphragms were isolated from CD-1 mice weighing about 20–25 g and halved into two contralateral hemi-diaphragms still innervated with the own phrenic nerve, and were treated as described in the Supplemental Experimental Procedures. Lethality assays were performed using Swiss-Webster adult male CD1 mice weighing 26–28 g as described in Supplementary Information.

Statistical analysis. For all the experiments, data are presented as mean values. Bars indicated the standard deviation. Significance was calculated by Student's t test (unpaired, two-side). $^{*}p < 0.05$, $^{**}p < 0.01$, $^{***}p < 0.0001$. Only values below 0.05 were considered significant (ns – non significant).

References

1. Johnson, E. A. & Montecucco, C. Botulism. *Handb Clin Neurol* **91,** 333–368 (2008).
2. Rossetto, O., Pirazzini, M. & Montecucco, C. Botulinum neurotoxins: genetic, structural and mechanistic insights. *Nat Rev Microbiol* **12,** 535–549 (2014).
3. Arnon, S. S. *et al.* Botulinum toxin as a biological weapon: medical and public health management. *JAMA.* **285,** 1059–1070 (2001).
4. Centers for Disease Control and Prevention. D. o. H. a. H. S. Possession, use, and transfer of select agents and toxins; biennial review. Final rule. *Fed Regist* **77,** 61083–61115 (2012).
5. Davletov, B., Bajohrs, M. & Binz, T. Beyond BOTOX: advantages and limitations of individual botulinum neurotoxins. *Trends Neurosci.* **28,** 446–452 (2005).
6. Dressler, D. Clinical applications of botulinum toxin. *Curr Opin Microbiol.* **15,** 325–336 (2012).
7. Rummel, A. Double receptor anchorage of botulinum neurotoxins accounts for their exquisite neurospecificity. *Curr Top Microbiol Immunol* **364,** 61–90 (2013).
8. Binz, T. & Rummel, A. Cell entry strategy of clostridial neurotoxins. *J Neurochem.* **109,** 1584–1595 (2009).
9. Nishiki, T. *et al.* Identification of protein receptor for Clostridium botulinum type B neurotoxin in rat brain synaptosomes. *J Biol Chem.* **269,** 10498–10503 (1994).
10. Dong, M. *et al.* SV2 is the protein receptor for botulinum neurotoxin A. *Science.* **312,** 592–596 (2006).
11. Matteoli, M. *et al.* Synaptic vesicle endocytosis mediates the entry of tetanus neurotoxin into hippocampal neurons. *Proc Natl Acad Sci USA* **93,** 13310–13315 (1996).
12. Colasante, C. *et al.* Botulinum neurotoxin type A is internalized and translocated from small synaptic vesicles at the neuromuscular junction. *Mol Neurobiol* **48,** 120–127 (2013).
13. Harper, C. B. *et al.* Dynamin inhibition blocks botulinum neurotoxin type A endocytosis in neurons and delays botulism. *J Biol Chem.* **286,** 35966–35976 (2011).
14. Montal, M. Botulinum neurotoxin: a marvel of protein design. *Annu Rev Biochem* **79,** 591–617 (2010).
15. Pirazzini, M. *et al.* On the translocation of botulinum and tetanus neurotoxins across the membrane of acidic intracellular compartments. *Biochimica et Biophysica Acta (BBA) - Biomembranes,* doi: http://dx.doi.org/10.1016/j.bbamem.2015.08.014.
16. Montecucco, C., Schiavo, G. & Dasgupta, B. R. Effect of pH on the interaction of botulinum neurotoxins A, B and E with liposomes. *Biochem J.* **259,** 47–53 (1989).
17. Fischer, A. & Montal, M. Crucial role of the disulfide bridge between botulinum neurotoxin light and heavy chains in protease translocation across membranes. *J Biol Chem.* **282,** 29604–29611 (2007).
18. Pirazzini, M. *et al.* The thioredoxin reductase-thioredoxin system is involved in the entry of tetanus and botulinum neurotoxins in the cytosol of nerve terminals. *FEBS Lett* **587,** 150–155 (2013).
19. Pirazzini, M. *et al.* Thioredoxin and its reductase are present on synaptic vesicles, and their inhibition prevents the paralysis induced by botulinum neurotoxins. *Cell Rep* **8,** 1870–1878 (2014).
20. Zanetti, G. *et al.* Inhibition of botulinum neurotoxins interchain disulfide bond reduction prevents the peripheral neuroparalysis of botulism. *Biochem Pharmacol,* doi: 10.1016/j.bcp.2015.09.023 (2015).

21. Binz, T. Clostridial neurotoxin light chains: devices for SNARE cleavage mediated blockade of neurotransmission. *Curr Top Microbiol Immunol* **364,** 139–157 (2013).
22. Pantano, S. & Montecucco, C. The blockade of the neurotransmitter release apparatus by botulinum neurotoxins. *Cell Mol Life Sci*, **71,** 793–811 (2013).
23. Kozaki, S., Miyazaki, S. & Sakaguchi, G. Development of antitoxin with each of two complementary fragments of Clostridium botulinum type B derivative toxin. *Infect Immun* **18,** 761–766 (1977).
24. Barash, J. R. & Arnon, S. S. A Novel Strain of Clostridium botulinum That Produces Type B and Type H Botulinum Toxins. *J Infect Dis*, **209,** 183–191 (2013).
25. Smith, T. J. *et al.* Sequence Variation within Botulinum Neurotoxin Serotypes Impacts Antibody Binding and Neutralization. *Infection and Immunity* **73,** 5450–5457.(2005).
26. Webb, R. P., Smith, T. J., Wright, P., Brown, J. & Smith, L. A. Production of catalytically inactive BoNT/A1 holoprotein and comparison with BoNT/A1 subunit vaccines against toxin subtypes A1, A2, and A3. *Vaccine* **27,** 4490–4497 (2009).
27. Gillespie, E. J. *et al.* Selective inhibitor of endosomal trafficking pathways exploited by multiple toxins and viruses. *Proc Natl Acad Sci USA* **110,** E4904–4912 (2013).
28. Eleopra, R. *et al.* Botulinum neurotoxin serotype D is poorly effective in humans: An *in vivo* electrophysiological study. *Clinical Neurophysiology* **124,** 999–1004 (2013).
29. Jung, M. E., Chamberlain, B. T., Ho, C.-L. C., Gillespie, E. J. & Bradley, K. A. Structure–Activity Relationship of Semicarbazone EGA Furnishes Photoaffinity Inhibitors of Anthrax Toxin Cellular Entry. *ACS Medicinal Chemistry Letters* **5,** 363–367 (2014).
30. Lalli, G. *et al.* Functional characterisation of tetanus and botulinum neurotoxins binding domains. *Journal of Cell Science* **112,** 2715–2724 (1999).
31. Restani, L. *et al.* Botulinum neurotoxins A and E undergo retrograde axonal transport in primary motor neurons. *PLoS pathogens* **8,** e1003087 (2012).
32. Blum, F. C., Chen, C., Kroken, A. R. & Barbieri, J. T. Tetanus Toxin and Botulinum Toxin A Utilize Unique Mechanisms To Enter Neurons of the Central Nervous System. *Infection and Immunity* **80,** 1662–1669 (2012).
33. Kraszewski, K. *et al.* Synaptic vesicle dynamics in living cultured hippocampal neurons visualized with CY3-conjugated antibodies directed against the lumenal domain of synaptotagmin. *The Journal of Neuroscience* **15,** 4328–4342 (1995).
34. Keller, J. E., Cai, F. & Neale, E. A. Uptake of botulinum neurotoxin into cultured neurons. *Biochemistry.* **43,** 526–532 (2004).
35. Simpson, L. L. Ammonium chloride and methylamine hydrochloride antagonize clostridial neurotoxins. *J Pharmacol Exp Ther.* **225,** 546–552 (1983).
36. Pirazzini, M., Rossetto, O., Bolognese, P., Shone, C. C. & Montecucco, C. Double anchorage to the membrane and intact inter-chain disulfide bond are required for the low pH induced entry of tetanus and botulinum neurotoxins into neurons. *Cell Microbiol.* **13,** 1731–1743 (2011).
37. Strotmeier, J. *et al.* Botulinum neurotoxin serotype D attacks neurons via two carbohydrate-binding sites in a ganglioside-dependent manner. *Biochem J.* **431,** 207–216 (2010).
38. Rasetti-Escargueil, C., Liu, Y., Rigsby, P., Jones, R. G. & Sesardic, D. Phrenic nerve-hemidiaphragm as a highly sensitive replacement assay for determination of functional botulinum toxin antibodies. *Toxicon* **57,** 1008–1016 (2011).
39. Smith, T. J., Hill, K. K. & Raphael, B. H. Historical and current perspectives on Clostridium botulinum diversity. *Research in Microbiology* **166,** 290–302 (2015).
40. Montecucco, C. & Rasotto, M. B. On botulinum neurotoxin variability. *MBio* **6** (2015).
41. Fischer, A. *et al.* Bimodal modulation of the botulinum neurotoxin protein-conducting channel. *Proc Natl Acad Sci USA* **106,** 1330–1335 (2009).
42. Montal, M. Redox regulation of botulinum neurotoxin toxicity: therapeutic implications. *Trends Mol Med* **20,** 602–603 (2014).
43. Jähne, S., Rizzoli, S. O. & Helm, M. S. The structure and function of presynaptic endosomes. *Experimental Cell Research* **335,** 172–179 (2015).
44. Cousin, M. A. Synaptic Vesicle Endocytosis and Endosomal Recycling in Central Nerve Terminals: Discrete Trafficking Routes? *Neuroscientist* **21,** 413–423 (2015).
45. Saheki, Y. & De Camilli, P. Synaptic vesicle endocytosis. *Cold Spring Harb Perspect Biol* **4** (2012).
46. Wucherpfennig, T., Wilsch-Bräuninger, M. & González-Gaitán, M. Role of Drosophila Rab5 during endosomal trafficking at the synapse and evoked neurotransmitter release. *The Journal of Cell Biology* **161,** 609–624 (2003).
47. Morgan, J. R., Comstra, H. S., Cohen, M. & Faundez, V. Presynaptic membrane retrieval and endosome biology: defining molecularly heterogeneous synaptic vesicles. *Cold Spring Harb Perspect Biol* **5,** a016915 (2013).
48. de Hoop, M. J. *et al.* The involvement of the small GTP-binding protein Rab5a in neuronal endocytosis. *Neuron* **13,** 11–22 (1994)
49. Pellett, S., Tepp, W. H., Scherf, J. M. & Johnson, E. A. Botulinum Neurotoxins Can Enter Cultured Neurons Independent of Synaptic Vesicle Recycling. *PLoS One* **10,** e0133737 (2015).
50. Keller, J. E., Neale, E. A., Oyler, G. & Adler, M. Persistence of botulinum neurotoxin action in cultured spinal cord cells. *FEBS Lett.* **456,** 137–142 (1999).
51. Eleopra, R., Tugnoli, V., Rossetto, O., De Grandis, D. & Montecucco, C. Different time courses of recovery after poisoning with botulinum neurotoxin serotypes A and E in humans. *Neurosci Lett* **256,** 135–138 (1998).
52. Meunier, F. r. A., Lisk, G., Sesardic, D. & Dolly, J. O. Dynamics of motor nerve terminal remodeling unveiled using SNARE-cleaving botulinum toxins: the extent and duration are dictated by the sites of SNAP-25 truncation. *Molecular and Cellular Neuroscience* **22,** 454–466 (2003).
53. Keller, J. E. Recovery from botulinum neurotoxin poisoning *in vivo*. *Neuroscience* **139,** 629–637 (2006).
54. Diril, M. K., Wienisch, M., Jung, N., Klingauf, J. & Haucke, V. Stonin 2 Is an AP-2-Dependent Endocytic Sorting Adaptor for Synaptotagmin Internalization and Recycling. *Developmental Cell* **10,** 233–244 (2006).
55. Sun, S., Tepp, W. H., Johnson, E. A. & Chapman, E. R. Botulinum neurotoxins B and E translocate at different rates and exhibit divergent responses to GT1b and low pH. *Biochemistry.* **51,** 5655–5662 (2012).
56. Willig, K. I., Rizzoli, S. O., Westphal, V., Jahn, R. & Hell, S. W. STED microscopy reveals that synaptotagmin remains clustered after synaptic vesicle exocytosis. *Nature* **440,** 935–939 (2006).
57. Peng, L., Tepp, W. H., Johnson, E. A. & Dong, M. Botulinum neurotoxin D uses synaptic vesicle protein SV2 and gangliosides as receptors. *PLoS Pathog.* **7,** e1002008 (2011).
58. Simpson, L. The life history of a botulinum toxin molecule. *Toxicon* **68,** 40–59 (2013).
59. Fagan, R. P., McLaughlin, J. B. & Middaugh, J. P. Persistence of botulinum toxin in patients' serum: Alaska, 1959-2007. *The Journal of infectious diseases* **199,** 1029–1031.(2009).
60. Sheth, A. N. *et al.* International outbreak of severe botulism with prolonged toxemia caused by commercial carrot juice. *Clinical infectious diseases: an official publication of the Infectious Diseases Society of America* **47,** 1245–1251 (2008).
61. Koepke, R., Sobel, J. & Arnon, S. S. Global occurrence of infant botulism, 1976-2006. *Pediatrics* **122,** e73–82 (2008).

Acknowledgements

We gratefully thank Dr. P. Caccin for performing and evaluating *ex vivo* experiments. This work was supported by the Italian Ministry of Defence (Progetto PNRM - NIB, Segretariato Generale della Difesa V Reparto), Fondazione CARIPARO "Synaptic Functions and Role of Glial Cells in Brain and Muscle Diseases" to C.M., and a grant from the Ministero dell'Universita e della Ricerca (Progetto PRIN) to O.R.

Author Contributions

C.M. conceived the project together with M.P., D.A.T., A.M., F.L. and C.P. A.M. performed the chemical synthesis. D.A.T. performed and evaluated *in vitro* experiments. G.Z. performed and evaluated *in vivo* experiments together with M.P., D.A.T. and C.M. C.C.S., T.B. and O.R. produced, purified and tested botulinum neurotoxins, and with S.F. provided advices. O.L. cloned, expressed and purified recombinant proteins. M.P., A.M. and C.M. wrote the paper with contributions of all co-authors.

Additional Information

Supplementary information accompanies this paper at http://www.nature.com/srep

Competing financial interests: The authors declare no competing financial interests.

How to cite this article: Azarnia Tehran, D. *et al.* A Novel Inhibitor Prevents the Peripheral Neuroparalysis of Botulinum Neurotoxins. *Sci. Rep.* **5**, 17513; doi: 10.1038/srep17513 (2015).

A Novel Inhibitor Prevents the Peripheral Neuroparalysis of Botulinum Neurotoxins

Domenico AZARNIA TEHRAN[1,†], Giulia ZANETTI[1,†], Oneda LEKA[1], Florigio LISTA[3], Silvia FILLO[3], Thomas BINZ[4], Clifford C. SHONE[5], Ornella ROSSETTO[1], Cesare MONTECUCCO[1,2], Cristina PARADISI[6], Andrea MATTAREI[6,*] and Marco PIRAZZINI[1,*]

Supplementary figures

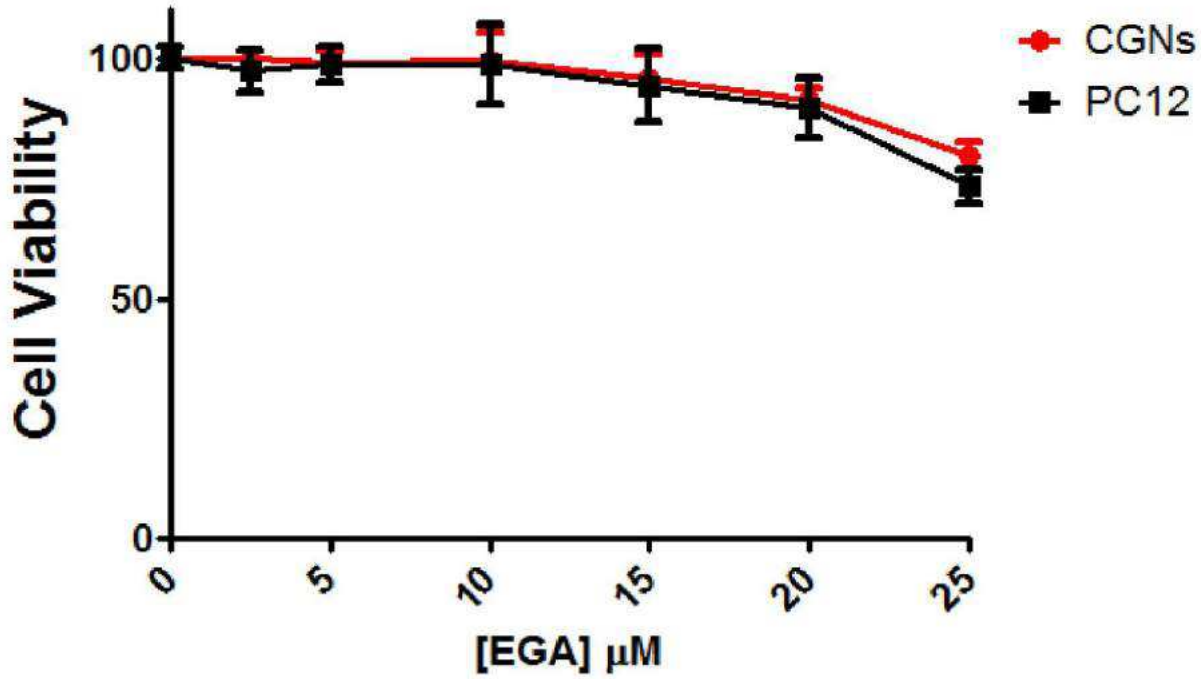

Figure S1. EGA does not affect cell viability of CGNs and PC12. CGNs and PC12 were treated with increasing concentration of EGA ranging from 2.5 to 25 µM or vehicle in culture medium at 37° C. After 24 hours, cell viability has been assayed with a MTS assay. Data are presented as a percentage with respect to cells treated with the vehicle, set as 100%. All data are presented as mean values and error bars indicated the deviation standard obtained from three independent experiments.

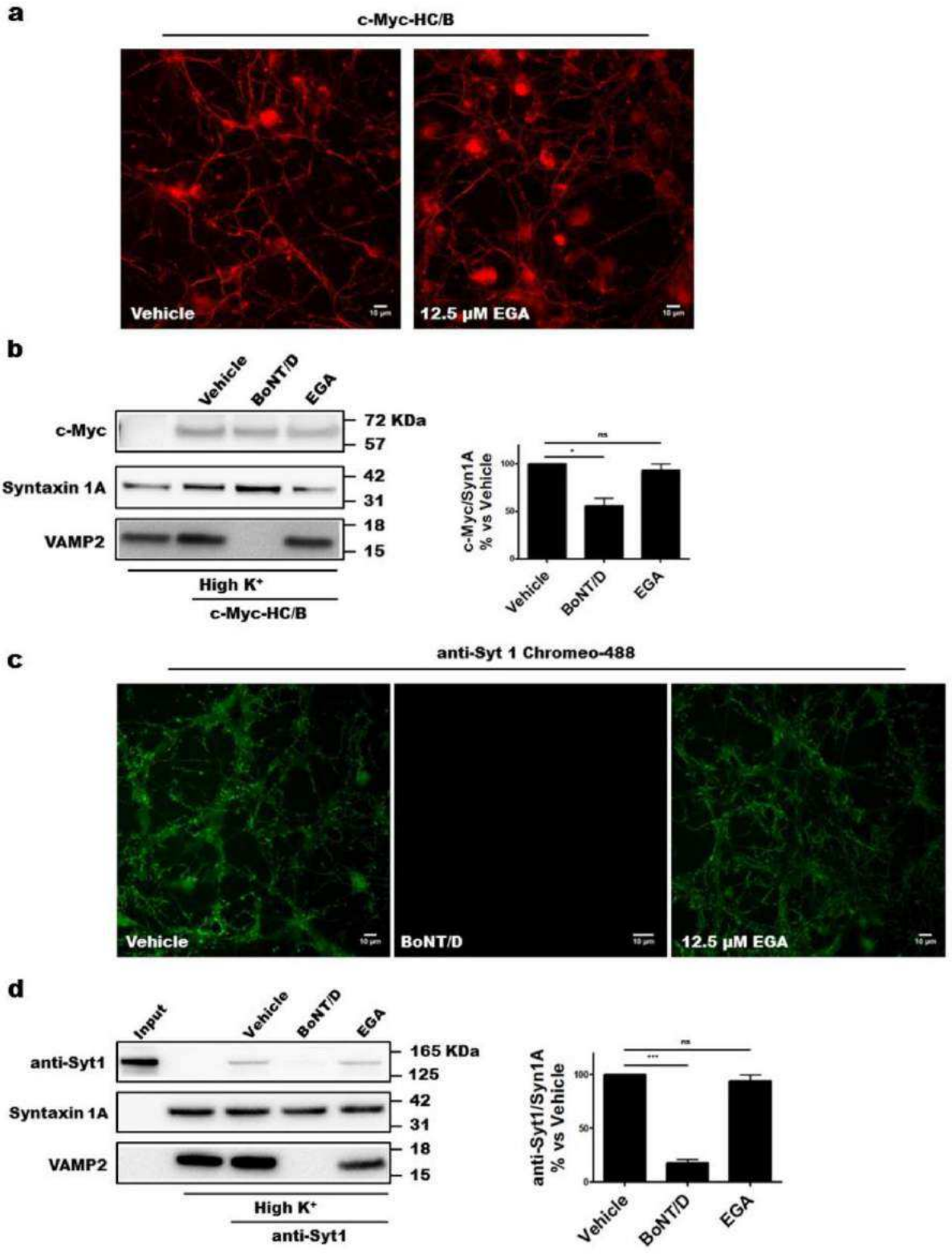
a
c-Myc-HC/B
Vehicle
12.5 µM EGA
b
Vehicle
BoNT/D
EGA
c-Myc
Syntaxin 1A
VAMP2
72 KDa
57
42
31
18
15
High K+
c-Myc-HC/B
c-Myc/Syn1A
% vs Vehicle
ns
*
100
50
0
Vehicle
BoNT/D
EGA
c
anti-Syt 1 Chromeo-488
Vehicle
BoNT/D
12.5 µM EGA
d
Input
Vehicle
BoNT/D
EGA
anti-Syt1
Syntaxin 1A
VAMP2
165 KDa
125
42
31
18
15
High K+
anti-Syt1
anti-Syt1/Syn1A
% vs Vehicle
ns
***
100
50
0
Vehicle
BoNT/D
EGA

Figure S2. EGA does not affect binding and synaptic vesicles dynamics in CGNs. (a) CGNs were treated with EGA (12.5 μM) or vehicle in culture medium at 37° C. After 30 min, 100 nM c-Myc-HC/B was added in high K^+ buffer for 1 h. Neurons were then washed, fixed, permeabilized and stained with a primary antibody specific for the c-Myc epitope. An Alexa Fluor 488 goat anti-mouse secondary antibody was used for detection. These images are representative of two independent sets of experiments. Scale bar, 10 μm. (b) CGNs were treated as in *(a)* with 250 nM of c-Myc-HC/B and then lysed. The c-Myc-HC/B content was estimated with specific antibodies against c-Myc epitope. Syntaxin 1A was used as loading control and VAMP2 to assess BoNT/D cleavage. The amount of c-Myc-HC/B was determined as a ratio to Syntaxin 1A staining taking the value in non-treated cells (vehicle) as 100%. All data are presented as mean values and error bars indicated the standard deviation obtained from two independent experiments (* $p<0.05$; ns – non significant). (c) CGNs were treated with EGA (12.5 μM) or vehicle at 37° C for 30 minutes. Where indicated, neurons were pre-treated with BoNT/D (10 nM) for 30 min. Cells were then incubated for 20 min with an antibody against the lumenal domain of Synaptotagmin-1 conjugated to Chromeo 488 in high K^+ buffer. At the end of the incubation, CGNs were washed twice, fixed and imaged by fluorescence microscopy. These images are representative of three independent sets of experiments. Scale bar, 10 μm. (d) CGNs were treated as in (c), using a non-fluorescent version of the same anti-Synaptotagmin-1 antibody. At the end of the incubation, neurons were washed twice and lysed in non-reducing Laemmli sample buffer. In the upper panel the internalized antibody was detected by immunoblotting, using an anti mouse HRP-conjugated secondary antibody. Blots were then stripped and incubated with specific antibodies against VAMP2 to assess BoNT/D cleavage and against Syntaxin 1A as loading control. In the first lane (input) 50 ng of the anti-Synaptotagmin 1 antibody were loaded as reference. The bottom panel reports the quantification. All data are presented as mean values and error bars indicated the

standard deviation obtained from three independent experiments (*** p<0.0001; ns – non significant).

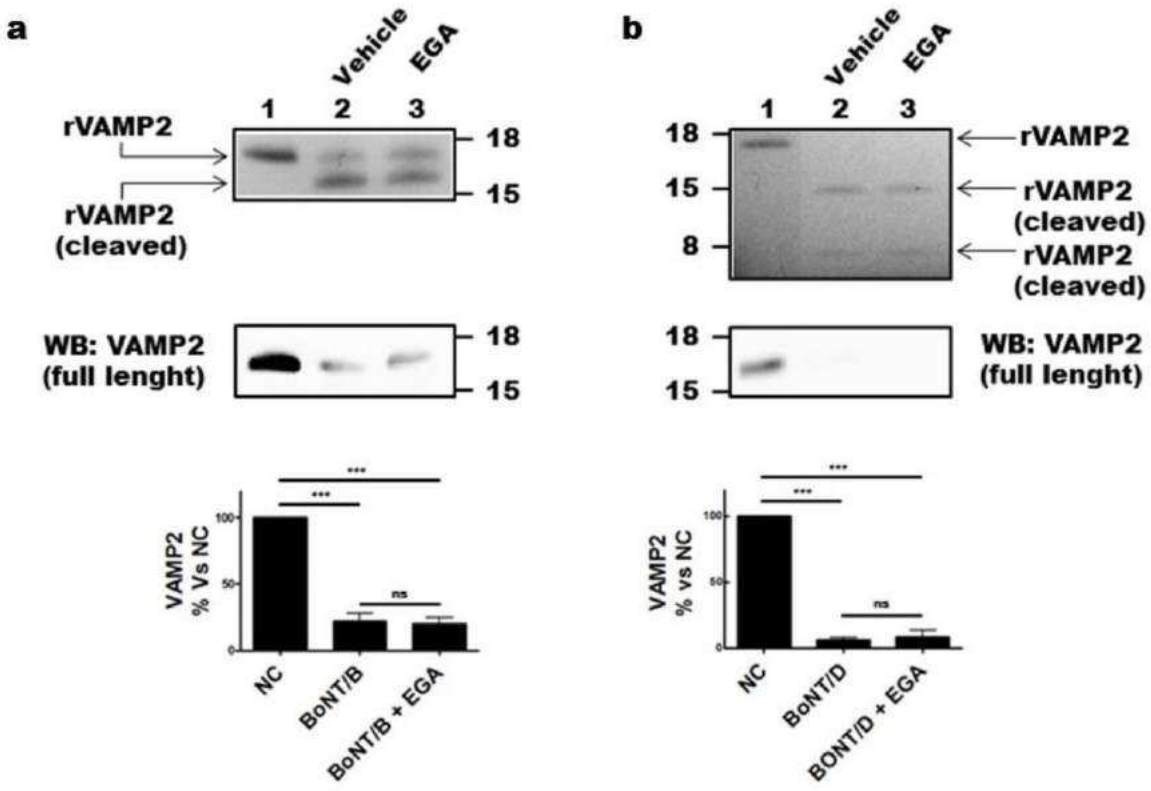

Figure S3. EGA does not affect BoNT/B and /D metalloprotease activity in vitro. (a) BoNT/B (1 µg) or (b) BoNT/D (0.25 µg) was reduced in the presence of EGA (12.5 µM) for 30 min at 37 °C. 1 µg of recombinant VAMP2 (rVAMP2) was then added, the concentration of inhibitor restored and the reaction carried out for 12 hours at 37 °C. VAMP2 cleavage was assessed by SDS-PAGE (top panels) or immunoblotting (middle panels) with an antibody that recognizes full length VAMP2. Lower panels show the densitometry analysis of western blots. All data are presented as mean values and error bars indicated the standard deviation obtained from three independent experiments (*** p<0.0001; ns – non significant).

	BoNT/A		BoNT/B		BoNT/D	
	DMSO	**EGA**	**DMSO**	**EGA**	**DMSO**	**EGA**
Lag phase (minutes)	36.3 ± 3.37	59.6 ± 0.9**	56.3 ± 2.4	82.0 ± 5.3*	29.0 ± 5.1	34.7 ± 2.4^{ns}
$t_{1/2}$ (minutes)	64.0 ± 2.6	146.3 ± 21.5*	99.0 ± 3.8	154.3 ± 11.9*	46.7 ± 4.1	67.7 ± 4.9*
Slope	2.1 ± 0.14	0.5 ± 0.09**	1.3 ± 0.11	0.6 ± 0.01**	2.4 ± 0.16	1.46 ± 0.09**
N	3	3	3	3	3	3

Table S1. Statistical analysis of the phrenic nerve-hemidiaphram twitch model. Given the variability of each muscle contraction, the data from BoNT/A, /B and /D intoxicated muscles treated with EGA or DMSO, were normalized and each single group was compared. The average values±SEM of lag phase, $t_{1/2}$ and slope derive from three independent experiments. Significance was calculated by Student's t test (unpaired, two-side). *P < 0.05; **P < 0.01. Only values below 0.05 were considered significant.

Supplementary experimental procedures

Reagents. BoNT/A was purified as previously described[1,2]. BoNT/B and BoNT/D were produced in *E. coli* as recombinant proteins[3,4]. LysoTracker® Red DND-99 was purchased from ThermoFischer Scientific (L-7528), instead, Bafilomycin A1 (sc-201550) from Santa Cruz Biotechnology. Cytosine β-D-arabinofuranoside hydrochloride (C6645), DNAse I from bovine pancreas (DN25), poly-L-lysine hydrobromide (P1274), solvents and reagents were purchased from Sigma Aldrich, and were used as received.

Chemical Synthesis. Phenyl (2,6-dimethylphenyl)carbamate (**2**): 2,6-dimethylaniline (1.00 g, 8.3 mmol, 1.0 eq) was dissolved in DCM (15 mL) and pyridine (0.73 g, 9.2 mmol, 1.1 eq) and cooled on ice-bath. Phenyl chloroformate (1.43 g, 9.2 mmol, 1.1 eq) in DCM (25 mL) was added dropwise. After addition the flask was brought to room temperature and stirred for 3 h. The reaction mixture was diluted with DCM (50 mL) and washed with 0.5 N HCl (5 × 100 mL). The organic layer was dried over MgSO4 and concentrated. The resulting crude product was purified by flash column chromatography on silica gel (eluent: Petroleum Ether/DCM/Acetone 60:35:5) to afford **2** as a bright white solid (1.92 g, 8.0 mmol, 96%). ^{1}H NMR (500 MHz, DMSO) δ 9.35 (s, 1H, -N*H*-), 7.43 (m, 2H, 2 × Ar-*H*), 7.24 (s, 1H, 1 × Ar-*H*), 7.22 (m, 2H, 2× Ar-*H*), 7.21 (m, 2H, 2 × Ar-*H*), 7.12 (m, 3H, 3 × Ar-*H*), 2.28 (s, 6H, 2 × -C*H3*); ^{13}C NMR (126 MHz, DMSO) δ 152.95, 151.56, 136.01, 134.76, 129.86, 128.38, 127.23, 125.56, 122.20, 18.47; ESI-MS: m/z = 242 = $[M+H]^+$; HRMS (ESI^+): m/z 242.1193 $[M+H]^+$, calculated for $C_{15}H_{16}NO_2$: 242.1181. 2-(4-Bromobenzylidene)-N-(2,6-dimethylphenyl)hydrazinecarboxamide (3, *EGA*): 2 (0.50 g, 2.1 mmol, 1.0 eq) was dissolved in DME (5 mL) and mixed with hydrazine monohydrate (50-60%, 0.13 g, 4.2 mmol, 2.0 eq) at 0°C. After addition the flask was brought to rt and stirred for 24 h. The reaction mixture was concentrated to give a crude white solid that was used

without further purification. This white solid was dissolved in chloroform (20 mL), mixed with 4-bromobenzaldehyde (0.77 g, 4.2 mmol, 2.0 eq) and vigorously stirred 15 h at room temperature. Solvent was removed under reduced pressure and the crude was purified by flash column chromatography on silica gel (eluent: DCM/EtOAc 85:15) to afford EGA (3) as a bright white solid (0.63 g, 1.8 mmol, 88%). ^{1}H NMR (500 MHz, DMSO) δ 10.65 (s, 1H, -N*H*-), 8.58 (s, 1H, -C*H*=N-), 7.88 (s, 1H, -N*H*-), 7.82-7.80 (d, 2H, 2 × Ar-*H*), 7.59-7.57 (d, 2H, 2 × Ar-*H*), 7.09 (m, 3H, 3 × Ar-*H*), 2.20 (s, 6H, 2 × -C*H*$_3$). ^{13}C NMR (126 MHz, DMSO) δ 154.20, 138.99, 136.71, 136.02, 134.59, 131.94, 129.24, 128.01, 126.67, 122.70, 18.68. ESI-MS: m/z = 346 = $[M+H]^+$; HRMS (ESI$^+$): m/z 346.0563 $[M+H]^+$, calcd for $C_{16}H_{17}BrN_3O$: 346.0555. TLCs were run on silica gel supported on plastic (Macherey-Nagel Polygram®SIL G/UV$_{254}$, silica thickness 0.2 mm) and visualized by UV detection. Flash chromatography was performed on silica gel (Macherey-Nagel 60, 230-400 mesh granulometry (0.063-0.040 mm)) under air pressure. The solvents were analytical or synthetic grade and were used without further purification. ^{1}H NMR spectra were recorded with a Bruker AVII500 spectrometer operating at 500 MHz. Chemical shifts (δ) are given in ppm relative to the signal of the solvent. Mass spectra were performed with a 1100 Series Agilent Technologies system, equipped with binary pump (G1312A) and MSD SL Trap mass spectrometer (G2445D SL) with ESI source. ESI-MS positive spectra of reaction intermediates and the final purified product were obtained from solutions in acetonitrile, eluting with a water:acetonitrile, 1:1 mixture containing 0.1% formic acid. High-resolution mass measurements were obtained using a Mariner ESI-TOF spectrometer (PerSeptive Biosystems). HPLC-MS analysis was used to confirm the purity (> 95%).

Cerebellar Granule Neurons (CGN) cultures. Primary cultures of rat cerebellar granule neurons (CGNs) were prepared from 6- to 8-days-old rats[5]. Cerebella were isolated, mechanically disrupted and then trypsinized in the presence of DNase I. Cells were then

plated into 24 well plates, pre-coated with poly-L-lysine (50 µg/mL), at a cell density of 4 x 10^5 cells per well. Cultures were maintained at 37 °C, 5% CO_2, 95% humidity in BME supplemented with 10% fetal bovine serum, 25 mM KCl, 2 mM glutamine and 50 µg/mL gentamicin (hereafter indicated as complete culture medium). To arrest growth of non-neuronal cells, cytosine arabinoside (10 µM) was added to the medium 18–24 h after plating.

Botulinum neurotoxin inhibition assay and immunocytochemistry. CGNs at 6–8 DIV were treated for 30 min with 12.5 µM of EGA or vehicle (DMSO) in complete culture medium at 37 °C and 5% CO_2. 0.3 nM BoNT/A or 5 nM BoNT/B or 0.025 pM BoNT/D was added and left for 12 hours at 37 °C and 5% CO_2. Neurons were then washed with PBS, fixed for 10 minutes at RT with 4% paraformaldehyde in PBS, quenched (50 mM NH_4Cl in PBS) for 20 minutes and permeabilized with 5% acetic acid in ethanol for 20 minutes at -20° C. CGNs were then incubated with indicated primary antibodies. BoNT/A cleavage was evaluated following the generation of the cleaved form of SNAP25, whereas the cleavage of BoNT/B and BoNT/D was evaluated following the disappearance of the staining due to a primary antibody recognizing the full-length form of VAMP2 (Synaptic System, 104 211). As internal control (not shown) it was used an anti SV2A (Santa Cruz, [E-8] sc376234) or anti SV2B (Synaptic System, 119 102), respectively. Primary antibodies were detected with Alexa Fluor 488 goat anti-mouse IgG (Life Technologies, A-11001) and Alexa Fluor 555 goat anti-rabbit IgG (Life Technologies, A-21428). Coverslips were mounted using Fluorescent Mounting Medium (Dako) and examined by epifluorescence (Leica CTR6000) microscopy. Images were collected with the same lamp intensity and exposure time.

For immunoblotting experiments, the neurons were treated with the same condition and the neurotoxicity was evaluated following the specific proteolytic activity of the toxin with

specific antibodies against their SNARE protein targets: anti BoNT/A-cleaved SNAP25[6], anti SNAP25 (SMI81: abcam, ab24737), anti VAMP2 (Synaptic System, 104 211) and anti BoNT/B-cleaved form of VAMP2[7]. The staining with anti Na^+/K^+ ATPase (abcam, ab7671) was used as loading control.

Immunoblotting. Cells were directly lysed with reducing Laemmli sample buffer containing protease inhibitors (complete Mini EDTA-free, Roche). Protein concentration was determined with the BCA test (Pierce BCA protein assay, Thermo Scientific), and equal amounts were loaded onto a 4-12% NuPage gel or 12% NuPage gel (Life technologies) and separated by electrophoresis in 1X MES buffer or 1X MOPS (Life technologies), respectively. Proteins were then transferred onto Protran nitrocellulose membranes (Whatman) and saturated for 1 h in PBST (PBS 0.1% Tween20) supplemented with 5% non-fatty milk. Incubation with primary antibodies was performed overnight at 4°C. The membranes were then washed three times with PBST and incubated with secondary HRP-conjugated antibodies (goat anti-mouse IgG, H&L chain specific peroxidase conjugate, Merk Millipore 401215 and goat anti-rabbit IgG, H&L chain specific peroxidase conjugate, Merk Millipore 401393). Finally, membranes were washed twice with PBST and once with PBS; visualization was carried out using Luminata Crescendo (Merck Millipore).

cpV-HC/A and c-Myc-HC/B expression, purification and binding assay. The HC of BoNT/B (nucleotides corresponding to residues 833-1291) with a N-terminus c-Myc tag was cloned into a pRSETa His-tag vector (Novagen) and expressed into BL21pLysS *E.coli* cells. Protein purification was achieved by affinity chromatography with a prepacked HisTrap Ni column (GE Healthcare) and then by size-exclusion chromatography using a Superdex 200, 10/300GL column (GE Healthcare). The purified c-Myc-HC/B fusion protein

were pooled and concentrated using a membrane filter with a cutoff of 30 kDa (Amicon Millipore).

The HC of BoNT/A (nucleotides corresponding residues 876-1296) fused with cpV (Circularly Permuted Venus) at the N-terminus was cloned into a pET28a His-tag vector (Novagen) and expressed in BL21 DE3 *E.coli* cells. Purification of cpV-HC/A fusion protein was achieved as described for c-Myc-HC/B.

In binding and internalization assay, CGNs were treated with EGA 12.5 μM or vehicle (DMSO) in culture medium at 37° C. After 30 minutes, 100 nM cpV-HC/A or c-Myc-HC/B was added in stimulating culture medium (complete culture medium, 57 mM KCl), for 1 hr. Neurons were then washed twice, fixed with 4% paraformaldehyde in PBS and directly imaged for cpV or permeabilized and stained with a primary antibody specific for the c-Myc epitope (Sigma Aldrich, M4439). An Alexa Fluor 488 goat anti-mouse (Life Technologies, A-11001) was used to detect the c-Myc primary antibody.

The same experiment was performed with 250 nM of cpV-HC/A or c-Myc-HC/B but neurons were then lysed and immunoblotted to obtain a quantitative result. Where indicated, neurons were pre-treated with 10 nM of BoNT/D for 30 minutes. Syntaxin 1A (Synaptic System, 110 111) staining was used as loading control, instead, VAMP2 (Synaptic System, 104 211) staining to assess BoNT/D cleavage. cpV-HC/A was detected with an anti-GFP antibody (Cell Signaling, #2956) whereas c-Myc-HC/B was detected with the aforementioned antibody.

Maturation of acidic compartment assay. CGNs at 6–8 DIV were treated for 30 min with the indicated concentrations of EGA or 10 nM Bafilomycin A1 in complete culture medium supplemented with 6.25 mM Hepes at 37 °C and 5% CO_2. 75 nM Lysotracker® Red DND-99 was added for 90 minutes. Cells were then washed with Krebs-Ringer buffer (KRH: 128 mM NaCl, 2.5 mM HEPES, 4.8 mM KCl, 1.3 mM $CaCl_2$, 1.2 mM $MgSO_4$ and 1.2 mM

K_2HPO_4) and images of living neurons were acquired with a Leica CTR6000 microscope. Fluorescence intensity was quantified using ImageJ software.

In vitro proteolytic activity. 0.25 µg BoNT/A or BoNT/D or 1 µg BoNT/B was incubated in reducing buffer (150 mM NaCl, 10 mM NaH2PO4, 15 mM DTT pH 7.4) in the presence of 12.5 µM of EGA for 30 min at 37 °C or DMSO. Then 1 µg of recombinant GST-SNAP25 or recombinant VAMP2 (1-96) was added to the reduced toxins, the concentration of inhibitor was restored, and the reaction was carried out for 12 hours at 37 °C. SNAP25 or VAMP2 cleavage was assessed by SDS-PAGE or immunoblotting using an anti-SNAP25 A-cleaved form or an anti-VAMP2 (Synaptic System, 104 211).

Low pH induced translocation of BoNT/B and BoNT/D across the plasma membrane. At a glance, 10^4 PC12-SYT N24Q were plated into 12-wells plates and maintained in RPMI supplemented with 10% HS, 5% FBS, 2 mM L-alanyl-L-glutamine (GlutaMAX), 100 U/ml penicillin, 100 µg/ml streptomycin, 250 ng/ml amphotericin B at 37 °C in a humid incubator. After adhesion, cells were incubated with a mixture of ganglioside (50 ug) for 24 hours. Cells were washed twice with culture medium and subsequently incubated with 10 nM of BoNT/B in ice-cooled medium (pH 7.4) and left at 4 °C for 15 minutes. After washing twice with the same cold medium, pre-warmed (37 °C) medium A (123 mM NaCl, 6 mM KCl, 0.8 mM $MgCl_2$, 1.5 mM $CaCl_2$, 5 mM NaP_i, 5 mM citric acid, 5.6 mM glucose, 10 mM NH_4Cl) - adjusted at indicated pH (7.4 or 4.5) with 1 M TRIS-base - was added and left for 10 minutes. Cells where then washed twice and further incubated in normal culture medium (pH 7.4) containing 50 nM Bafilomycin A1 for 24 hours. Where indicated, 12.5 µM EGA was pre-incubated with cells for 30 minutes and was then present in all solutions used along experiment. The same procedure was performed using CGNs, 2.5 pM of BoNT/D and after low pH assay the incubation was prolonged for 24 hr. Where indicated, 12.5 µM EGA was pre-incubated with cells for 30 minutes and was then present in all

solutions used along experiment. The translocation of BoNT/B or BoNT/D was assessed by following the metalloprotease activity against VAMP2 via western blot using an anti-VAMP2 (Synaptic System, 104211). The staining of SNAP25 (SMI81: abcam, ab24737), was used as loading control.

Mouse diaphragm and lethality assay. Muscles were mounted into two chambers filled with 4 ml of oxygenated (95% O_2, 5% CO_2) solution (139 mM NaCl, 12 mM $NaHCO_3$, 4 mM KCl, 2 mM $CaCl_2$, 1 mM $MgCl_2$, 1 mM KH_2PO_4 and 11 mM glucose, pH 7.4). The phrenic nerves were stimulated via two ring platinum electrodes with supramaximal stimuli of 3 V amplitude and 0.1 ms pulse duration, with a frequency of 0.1 Hz (Stimulator 6002, Harvard Apparatus, Massachusetts, USA). Muscle contraction was monitored with an isometric transducer (Harvard Apparatus); data was recorded and analysed via an i-WORX 118 system with Labscribe software (Harvard Apparatus). EGA was added directly to the oxygenated solution of one muscle to reach the final concentration of 12.5 µM of and the same volume of vehicle (DMSO) was added to the contralateral one for direct comparison. After 30 minutes of incubation, 10 pM BoNT/A or BoNT/B or 100 pM BoNT/D was added to both preparations and the twitch monitored until complete paralysis was achieved. Graphs show muscle twitching capability over time, reported as percentage with respect to the initial value obtained before toxin addition.

For lethality assay, EGA was dissolved in DMSO as a stock solution (12.5 mg/ml). Mice were conditioned for 3 days, with 12.5 mg/kg EGA or vehicle with intraperitoneal (i.p.) injections b.i.d. (every 12 hours). After the last injection of drug (or vehicle), mice were weighted and i.p. injected with 1 µl/g body weight of BoNT/A, /B or /D prepared as stock solutions (BoNT/A 0.5 pg/µl, BoNT/B 0.9 pg/µl and BoNT/D 0.045 pg/µl in 0.9% NaCl with 0.2% gelatin) roughly corresponding to $2XMLD_{50}$. Mice were monitored every 4 hr for 96

hr, after which the experiment was considered ended. Results are displayed as Kaplan-Meyer plots, and analysed with a Mantel-Cox test for statistical significance.

Synaptic vesicles dynamics assay. Experiment was performed as previously described [8]. Briefly, CGNs were conditioned in high K^+ buffer (70 mM NaCl, 2.5 mM HEPES, 57 mM KCl, 1.3 mM $CaCl_2$, 1.2 mM $MgSO_4$ and 1.2 mM K_2HPO_4) for 10 minutes. Hereafter, 5 µg/ml of Chromeo 488 (Synaptic System, 105 311CR1) was added for 20 min in the same buffer. Cells were then washed twice with PBS and fixed. Internalized antibodies were imaged using a Leica CTR6000 microscope. Where indicated, 10 nM BoNT/D or 12.5 µM of EGA (or DMSO) were pre-incubated in normal culture medium for 30 minutes. The same concentration of EGA is maintained during antibody incubation. In order to have a quantitative result, the same experiment was performed using as a read-out western blot. Accordingly, CGNs were lysed in non-reducing condition, blotted on nitrocellulose membrane saturated for 1 hr in PBST supplemented with 5% non-fatty milk and directly incubated with secondary antibody to detect the internalized anti-Synaptotagmin1 antibody (Synaptic System, 105 101). The staining of VAMP2 (Synaptic System, 104 211) was used to assess BoNT/D cleavage, instead, Syntaxin 1A (Synaptic System, 110 111) was used as loading control.

Viability test. CGNs or PC12-SYT N24Q were seeded in a 96 wells plates at a cell density 10^5 cells per well. Different concentration of EGA, ranging from 0 to 25 µM, were added and left for 24 hours. Neurons were then washed and MTS assay (Promega) performed according to manufacturer indication.

References

1 Schiavo, G. & Montecucco, C. Tetanus and botulism neurotoxins: isolation and assay. *Methods Enzymol* **248**, 643-652. (1995).

2 Shone, C. C. & Tranter, H. S. Growth of clostridia and preparation of their neurotoxins. *Curr Top Microbiol Immunol* **195**, 143-160. (1995).

3 Rummel, A., Mahrhold, S., Bigalke, H. & Binz, T. The HCC-domain of botulinum neurotoxins A and B exhibits a singular ganglioside binding site displaying serotype specific carbohydrate interaction. *Mol Microbiol.* **51**, 631-643. (2004).

4 Bade, S. *et al.* Botulinum neurotoxin type D enables cytosolic delivery of enzymatically active cargo proteins to neurones via unfolded translocation intermediates. *J Neurochem* **91**, 1461-1472. (2004).

5 Rigoni, M. *et al.* Snake presynaptic neurotoxins with phospholipase A2 activity induce punctate swellings of neurites and exocytosis of synaptic vesicles. *J Cell Sci.* **117**, 3561-3570. (2004).

6 Antonucci, F., Rossi, C., Gianfranceschi, L., Rossetto, O. & Caleo, M. Long-distance retrograde effects of botulinum neurotoxin A. *J Neurosci.* **28**, 3689-3696. (2008).

7 Mainardi, M., Pietrasanta, M., Vannini, E., Rossetto, O. & Caleo, M. Tetanus neurotoxin-induced epilepsy in mouse visual cortex. *Epilepsia* **53**, e132-136. (2012).

8 Kraszewski, K. *et al.* Synaptic vesicle dynamics in living cultured hippocampal neurons visualized with CY3-conjugated antibodies directed against the lumenal domain of synaptotagmin. *The Journal of Neuroscience* **15**, 4328-4342 (1995).

3.2 BoNT/C variants for clinical use

BoNT/C is a neuroparalytic toxin associated with outbreaks of animal botulism, particularly in birds. It is unique among BoNTs as it targets two intraneuronal substrates: SNAP-25 and syntaxins. BoNT/C has shown to be a good substitute for BoNT/A in therapy because of its long lasting effects. However, whether BoNT/C cleaves both SNAP-25 and syntaxins also *in vivo* and which proteolytical event accounts for its long duration is not known. Recently, two BoNT/C triple-mutants were reported to specifically cleave syntaxins[187], thus providing an advantageous tool to fill these gaps.

In collaboration with Dr. T. Binz (Hannover Medical School), BoNT/C L200W/M221W/I226W (BoNT/C α-3W) and BoNT/C S51T/R52N/N53P (BoNT/C α-51) were produced in *E. coli*, and their biochemical and toxicological features were studied with respect to recombinant wild-type BoNT/C (BoNT/C-wt).

I found that both mutants cleave syntaxin-1A/1B and that the extent of cleavage is similar to that of BoNT/C-wt, suggesting that mutations do not affect their capacity to enter neurons and the enzymatic efficiency of their L chains. Unexpectedly, and contrary to what reported in the original paper, I found that both mutants have a residual activity against SNAP-25, with BoNT/C α-3W being more active than BoNT/C α-51.

Interestingly, their potency is strictly related to the extent of SNAP-25 cleavage, as evaluated by in *ex vivo* and *in vivo* experiments. Surprisingly, the poorly potent BoNT/C α-51 produces a very long-lasting and reversible paralysis upon local injection of one LD_{50}. At the same time, one LD_{50} of the more potent BoNT/C α-3W has a very short duration. These results indicate that the duration of the neuroparalytic effects of BoNT/C mutants does not correlate with their respective potency. Remarkably, by staining intoxicated muscles for SNAP-25 and syntaxin, I found that neuroparalysis correlates with SNAP-25 cleavage, whereas syntaxin cleavage impairs but do not completely block neurotransmission.

Indeed, a low amount of BoNT/C α-51 (1/75 of its LD_{50}), which produces a nearly complete cleavage of syntaxin but no cleavage of SNAP-25, causes a substantial decrease of neurotransmission efficacy without paralyzing the injected muscle.

These results indicate that syntaxin-specific BoNTs have a further great therapeutic potential as they can attenuate nerve terminal activity without causing complete muscle paralysis.

3.2.1. Botulinum neurotoxin C mutant reveal different effects of syntaxin or SNAP-25 proteolysis on neuromuscular transmission

Molecular effects of BoNT/C substrate cleavage at NMJ

Giulia Zanetti[1], Stefan Sikorra[2], Andreas Rummel[3], Nadja Krez[3], Elisa Duregotti[1], Samuele Negro[1], Tina Henke[2], Ornella Rossetto[1], Thomas Binz[2] and Marco Pirazzini[1].

[1]Department of Biomedical Sciences, University of Padova, Italy

[2]Institut für Zellbiochemie, Medizinische Hochschule Hannover, Hannover, Germany

[3]Institut für Toxikologie, Medizinische Hochschule Hannover, Hannover, Germany

Zanetti G. *et al.* Botulinum Neurotoxin C Mutants reveal Different Effects of Syntaxin or SNAP-25 Proteolysis on Neuromuscular Transmission. *PLoS Pathog,* 13(8):e1006567.

doi: 10.1371/journal.ppat.1006567. eCollection (2017)

PLOS | PATHOGENS

RESEARCH ARTICLE

Botulinum neurotoxin C mutants reveal different effects of syntaxin or SNAP-25 proteolysis on neuromuscular transmission

Giulia Zanetti[1], Stefan Sikorra[2], Andreas Rummel[3], Nadja Krez[3], Elisa Duregotti[1], Samuele Negro[1], Tina Henke[2], Ornella Rossetto[1], Thomas Binz[2], Marco Pirazzini[1]*

1 Department of Biomedical Sciences, University of Padova, Padova, Italy, **2** Institut für Zellbiochemie, Medizinische Hochschule Hannover, Hannover, Germany, **3** Institut für Toxikologie, Medizinische Hochschule Hannover, Hannover, Germany

* marcopiraz@gmail.com

Citation: Zanetti G, Sikorra S, Rummel A, Krez N, Duregotti E, Negro S, et al. (2017) Botulinum neurotoxin C mutants reveal different effects of syntaxin or SNAP-25 proteolysis on neuromuscular transmission. PLoS Pathog 13(8): e1006567. https://doi.org/10.1371/journal.ppat.1006567

Editor: Bruce A. McClane, University of Pittsburgh School of Medicine, UNITED STATES

Received: April 28, 2017

Accepted: August 3, 2017

Published: August 11, 2017

Data Availability Statement: All relevant data are within the paper and its Supporting Information files.

Funding: This work was supported by grants from the University of Padova to OR (grant DOR1692572/16) and in part by the Bundesministerium für Wirtschaft und Technologie (BMWi) Zentrales Innovationsprogramm Mittelstand (KF2437603MD3) to AR. The funders had no role in study design, data collection and

Abstract

Botulinum neurotoxin serotype C (BoNT/C) is a neuroparalytic toxin associated with outbreaks of animal botulism, particularly in birds, and is the only BoNT known to cleave two different SNARE proteins, SNAP-25 and syntaxin. BoNT/C was shown to be a good substitute for BoNT/A1 in human dystonia therapy because of its long lasting effects and absence of neuromuscular damage. Two triple mutants of BoNT/C, namely BoNT/C *S51T/R52N/N53P* (BoNT/C α-51) and BoNT/C *L200W/M221W/I226W* (BoNT/C α-3W), were recently reported to selectively cleave syntaxin and have been used here to evaluate the individual contribution of SNAP-25 and syntaxin cleavage to the effect of BoNT/C *in vivo*. Although BoNT/C α-51 and BoNT/C α-3W toxins cleave syntaxin with similar efficiency, we unexpectedly found also cleavage of SNAP-25, although to a lesser extent than wild type BoNT/C. Interestingly, the BoNT/C mutants exhibit reduced lethality compared to wild type toxin, a result that correlated with their residual activity against SNAP-25. In spite of this, a local injection of BoNT/C α-51 persistently impairs neuromuscular junction activity. This is due to an initial phase in which SNAP-25 cleavage causes a complete blockade of neurotransmission, and to a second phase of incomplete impairment ascribable to syntaxin cleavage. Together, these results indicate that neuroparalysis of BoNT/C at the neuromuscular junction is due to SNAP-25 cleavage, while the proteolysis of syntaxin provides a substantial, but incomplete, neuromuscular impairment. In light of this evidence, we discuss a possible clinical use of BoNT/C α-51 as a botulinum neurotoxin endowed with a wide safety margin and a long lasting effect.

Author summary

The seven established Botulinum Neurotoxins serotypes (BoNT/A to G) and the many BoNT subtypes, the causative agents of botulism, are the most poisonous substances known (lethal doses in the low ng/kg range). Due to their toxicological properties, BoNTs are Janus-faced toxins: potent pathogenic factors and potential bioterrorism agents as well

analysis, decision to publish, or preparation of the manuscript.

Competing interests: The authors have declared that no competing interests exist.

as safe and efficacious therapeutics. BoNTs exert their neuroparalytic action by cleaving SNARE proteins, either SNAP-25 or synaptobrevin/VAMP, which mediate neurotransmitter release at the neuromuscular junction; BoNT/C is the only serotype shown to cleave SNAP-25 and syntaxin-1 *in vitro*. Our study shows for the first time that this parallel cleavage also occurs *in vivo*. By using mutated toxins reported to be syntaxin-selective, we found that SNAP-25 proteolysis at the neuromuscular junction is the key determinant of BoNT/C lethality as it completely blocks nerve-muscle transmission. Conversely, syntaxin-1 cleavage only attenuates nerve terminal activity without inactivating the synapse, leading to only a partial decrease of neuromuscular functionality. As a result, the BoNT/C mutants have dramatically reduced lethality, but still modulate neuromuscular junction activity upon intramuscular injection. This aspect is particularly relevant considering the possible use of syntaxin-specific BoNT/C derivatives to improve the present clinical utilization of BoNTs.

Introduction

Few species of the bacterial genus *Clostridium* produce botulinum neurotoxins (BoNTs), which cause the flaccid paralysis of botulism [1]. BoNTs are divided into at least seven different serotypes (BoNT/A to G) that comprise an increasing number of subtypes [1–3]. BoNTs are the most poisonous toxins known to date and display lethal doses in the low ng/kg range [4, 5]. This remarkable potency is due to their selective action within the peripheral nervous system, most notably at the neuromuscular junction (NMJ), where BoNTs inactivate the machinery responsible for neurotransmitter release, causing muscle paralysis and blockade of autonomic innervations [6]. Therefore, BoNTs are used to treat human diseases characterized by hyperactivity of peripheral nerve terminals of both the motor and autonomic nervous system [7]. This clinical use is almost exclusively restricted to BoNT/A1 as it produces the longest effect, and in very few circumstances to BoNT/B1, mainly to overcome BoNT/A1 resistance [5, 8].

The BoNT structure is composed of three domains that perform different functions [1]: a) the C-terminal part harbors two binding sites for two different receptors that mediate toxin anchoring and internalization within nerve terminals [9, 10]; b) an intermediate domain responsible for the translocation of the catalytic domain into the cytosol of nerve terminals [11, 12]; and c) the N-terminal catalytic domain, termed light chain (LC), which is a metalloprotease cleaving one of the three SNARE (Soluble NSF Attachment Protein Receptors) proteins, namely VAMP-1/2 (vesicle-associated membrane protein 1/2, also known as synaptobrevin-1/2), SNAP-25 (synaptosomal-associated protein of 25 kDa) and syntaxin-1A/1B (Stx) [13, 14]. These three proteins assemble into a complex, i.e. the SNARE complex, which mediates the fusion of synaptic vesicles with the presynaptic membrane [15], and their proteolysis is directly responsible for the pathogenicity of BoNTs [1, 6]. BoNT/B, /D, /F and /G cleave the vesicular SNARE protein VAMP-1/2 [16–19], whereas BoNT/A, and /E cleave the plasma membrane protein SNAP-25 [20, 21]. BoNT/C is the only toxin known to cleave two SNARE substrates, SNAP-25 and syntaxin-1A/1B, *in vitro* [22–24]. Each toxin cleaves its SNARE at a unique site thereby removing different portions of the respective substrates [13, 14]. Interestingly, while BoNTs cleaving VAMP cause a paralysis of intermediate duration, the three serotypes that cleave SNAP-25 provide the shortest and the longest persistence of action [25–28]: BoNT/E removes 26 amino acids from SNAP-25 C-terminus and produces a muscle paralysis of a few days. BoNT/A and BoNT/C remove

only nine and eight amino acids, respectively, and cause a paralysis that lasts for months in humans [29–31]. However, it is currently unknown whether BoNT/C cleaves syntaxins at the NMJ and to what extent this cleavage contributes to its long lasting paralysis.

Recently, two BoNT/C LC mutants were reported to display selective protease activity against syntaxins [32]. These mutants offer the unique opportunity of dissecting the contribution of syntaxin and SNAP-25 cleavage to BoNT/C-induced paralysis and duration of action. Therefore, we synthesized the respective full-length BoNT/C mutants and tested their potency *in vitro* and *in vivo*. Surprisingly, we found that the two mutant toxins are much less toxic than wild type BoNT/C and their respective toxicity correlates with an unexpected residual activity against SNAP-25. Our findings suggest that BoNT/C lethality is mainly due to SNAP-25 cleavage, while the proteolysis of syntaxin accounts for a prolonged and substantial, albeit incomplete, impairment of neuromuscular transmission.

Results

BoNT/C mutants retain a residual activity on SNAP-25

Based on the work of Wang *et al.* (2011) [32], we produced the full-length triple mutants BoNT/C *S51T/R52N/N53P* (hereafter referred to as BoNT/C α-51) and BoNT/C *L200W/M221W/I226W* (BoNT/C α-3W) in *Escherichia coli*, along with wild type BoNT/C (BoNT/C-wt). Amino acid substitutions are mapped in the crystal structure of BoNT/C-wt LC (PDB 2QN0) and shown in S1 Fig. Mutations are concentrated either in the S1' pocket of the LC (*L200W/M221W/I226W*, red spot), thus likely impinging on LC-substrate recognition around the active site (blue spot), or on a region outside the active site (*S51T/R52N/N53P*, green spot), which is possibly involved in LC-SNAREs interaction [32]. Recombinant toxins were expressed in *E. coli*, activated into di-chain toxins by host proteases, and one-step affinity-purified using StrepTactin-sepharose matrix. The level of purification was suitable for biochemical and toxicological characterization (S2 Fig).

We first tested the overall functionality of recombinant wild type and mutant BoNT/C in cerebellar granular neurons (CGNs), which are highly sensitive to BoNTs and provide a rapid and reliable method to assay the cleavage of SNARE proteins by western blot [28, 33]. We used two specific antibodies that recognize both the intact and the truncated form of SNAP-25 and syntaxin-1A/1B. After 12 hours of incubation, BoNT/C-wt cleaved both syntaxin-1A/1B (EC_{50} ~ 0.25 nM) and SNAP-25 (EC_{50} ~ 0.05 nM), the latter more efficiently (Fig 1A). Importantly, the extent of cleavage was similar to that of a "natural BoNT/C" purified from *Clostridium botulinum*, implying that production in *E. coli* provides BoNT/C-wt with identical biological properties, as previously reported for other recombinant toxins [28, 34–36]. The two mutant BoNT/C toxins cleaved syntaxin-1A/1B with similar efficiency (EC_{50} ~ 0.5 nM), which was only slightly lower compared to BoNT/C-wt, indicating that the mutations do not alter the mutant's capacity to enter neurons. Contrary to what was reported in the original paper by Wang *et al.* [32], we also detected cleavage of SNAP-25 (Fig 1A, middle and bottom panels), with BoNT/C α-3W being more active (EC_{50} ~ 2.5 nM) than BoNT/C α-51 (EC_{50} > 5 nM) indicating they are not specific for syntaxins. Notably, mutant BoNT/C toxins retained a 50-fold and >100-fold lower activity for SNAP-25 cleavage compared to BoNT/C-wt. This unexpected result may be due to the different methods used, i.e. Wang *et al.* virally transduced the gene encoding for mutant LCs while we exogenously added full-length toxins to the neuron culture medium allowing uptake of physiological amounts. We also noticed that a certain amount of syntaxin-1A/1B appears to be inaccessible to the three BoNT/Cs, even when toxins were used at high concentrations. This became particularly evident when the incubation time was extended to 24 hours (S3 Fig). Moreover, unlike BoNT/C-wt, the amount of SNAP-25

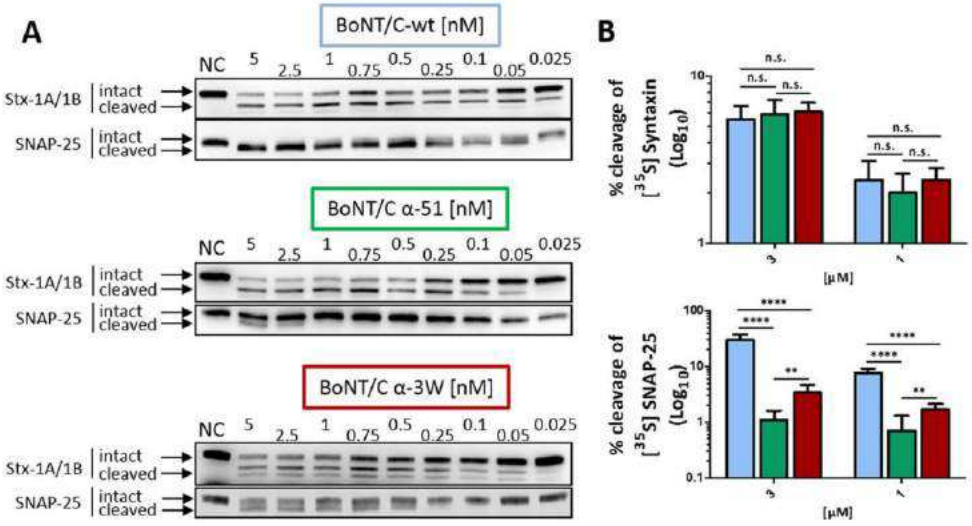

Fig 1. BoNT/C triple mutants retain a residual activity against SNAP-25. (A) Proteolytic activity of BoNT/C variants in cultured cerebellar granule neurons (CGNs). Full-length BoNT/C-wt or BoNT/C α-51 or BoNT/C α-3W were added to cultured CGNs at indicated concentrations for 12 hours. The cleavage of syntaxin-1A/1B and SNAP-25 was assayed in western blot by using two antibodies recognizing both the intact and the cleaved forms of the proteins. **(B)** Recombinant syntaxin 1A fusion protein (1 μM, upper panel) or SNAP-25 (10 μM, lower panel) spiked with the corresponding radiolabeled protein generated by *in vitro* transcription/translation in the presence of [^{35}S]-Met were incubated with various concentrations of LC/C-wt (cyan) or its mutants (α-51, green; α-3W, red) in toxin assay buffer. After 1 h of incubation at 37˚C, samples were analyzed by SDS-PAGE. Percentage of cleavage was quantified by means of the radiolabeled substrate by phosphorimaging. Data are mean values of three to six independent experiments. Statistical significance was determined by a Student's t-test comparing the mean values between groups (* p<0.05, ** p<0.01, *** p<0.001, **** p<0.0001, n.s. not significant).

https://doi.org/10.1371/journal.ppat.1006567.g001

cleaved by BoNT/C α-51 and BoNT/C α-3W did not increase significantly from 12 to 24 hours (Fig 1A and S3 Fig middle and bottom panels).

To further characterize the enzymatic properties of the mutated toxins, we assayed the proteolytic activity of their LCs *in vitro* against recombinant SNAP-25 and syntaxin1A. When applied at equal concentrations, LC/C-wt, LC/C α-51 and LC/C α-3W cleaved syntaxin to a similar extent (Fig 1B, upper panel), suggesting an overall similar enzymatic efficiency. On the other hand, the activity of LC/C α-51 and LC/C α-3W against SNAP-25 (bottom panel) was much lower (30-fold and 10-fold, respectively) than that of LC/C wt.

Collectively, these experiments demonstrate that mutant BoNT/C toxins are not specific for syntaxin-1A/1B, but maintain a residual activity against SNAP-25 which is higher for BoNT/C α-3W compared to BoNT/C α-51.

BoNT/C mutants have different neurodegenerative effects on neurons

To provide additional evidence on the proteolytic activity of BoNT/C mutants on SNAP-25, we used an antibody that recognizes SNAP-25 segment 185–197, which corresponds to the newly formed C-terminus generated upon cleavage by BoNT/A. This antibody recognizes BoNT/A-cleaved, and not intact, SNAP-25 both *in vitro* and *in vivo* (S4 Fig) [27, 37, 38]. Since BoNT/C cleaves SNAP-25 one amino acid downstream of the BoNT/A cleavage site [13, 31], we asked whether this antiserum would also recognize BoNT/C-cleaved SNAP-25. The antibody recognized SNAP-25 cleaved by BoNT/C-wt as it caused an accumulation of staining like that generated by BoNT/A1 (S4 Fig). Similar results were obtained upon treatment of CGNs with BoNT/C mutants (12 hours, 5 nM) (Fig 2). In agreement with the western blot analysis,

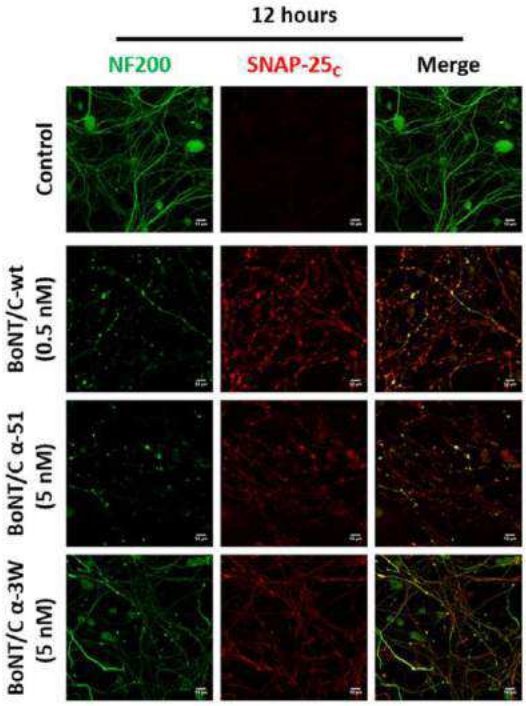

Fig 2. BoNT/C mutants display a different neurodegenerative effect on cultured neurons. CGNs were treated with the indicated concentrations of BoNT/C-wt or mutants for 12 hours. Neurons were then fixed and stained with an antibody against cleaved SNAP-25 (SNAP-25$_c$, in red) and neurofilament-200 (NF200, in green). Neurodegeneration was evaluated following the appearance of varicosities along neurites and the loss of NF200 staining. Images are representative of at least three independent experiments. Scale bar, 10 μm.

https://doi.org/10.1371/journal.ppat.1006567.g002

neurons treated with BoNT/C α-3W displayed a more prominent staining compared to those neurons treated with BoNT/C α-51, yet less intense than that arising from BoNT/C-wt treatment (12 hours, 0.5 nM). Moreover, prolonging the incubation time did not significantly increase the amount of cleaved SNAP-25 (S5 Fig).

BoNT/C is long known to cause neurodegeneration in neuronal cultures [39–41], and this effect can be monitored by staining neurofilament-200 (NF200), a major component of axon cytoskeleton. After 12 hours of incubation, BoNT/C-wt caused a substantial loss of NF200 and the formation of varicosities, also filled with cleaved SNAP-25, all along the neurites (Fig 2). BoNT/C α-51 induced a very similar phenotype and caused an evident degeneration of neurons. Intriguingly, neurons treated with BoNT/C α-3W neither displayed significant signs of degeneration nor loss of NF200. This was even more clear after 24 hours of intoxication when the detrimental effects of BoNT/C-wt and BoNT/C α-51 completely degenerated neurons (S5 Fig).

Together with the western blotting analyses, these results suggest that the three BoNT/C variants have different neurodegenerative activity on CGNs and that this effect may not depend on the proteolysis of SNAP-25 and syntaxin-1A/1B.

BoNT/C mutants are less toxic than wild type BoNT/C

Since the three toxins tested here have a similar activity against syntaxin-1A/1B and vary only for the extent of SNAP-25 cleavage, we evaluated the contribution of SNAP-25 cleavage to BoNT/C neuroparalysis. We first assessed the potency of the three toxins using the mouse

phrenic nerve hemidiaphragm (MPN) assay. This *ex vivo* assay mimics the respiratory failure of botulism by intoxicating an explanted hemidiaphragm and allows for the recording of muscle contraction capacity elicited by phrenic nerve stimulation [35, 42–45]. The addition of BoNTs to the organ bath impairs nerve-muscle transmission and causes progressive muscle neuroparalysis. The time needed to halve the initial twitch amplitude at a given concentration (T_{50}) is proportional to toxin potency [43] and can be used to provide very accurate comparisons of the activity of different BoNT preparations, including mutant toxins [35, 46]. The black trace of Fig 3A shows the T_{50} values obtained for different bath concentrations of a standard BoNT/C, and provides a dose-response calibration curve ($y = 148.95x^{-0.2089}$; $R^2 = 0.9806$) [45] which was used to compare the BoNT/C-wt and the two mutant toxins. BoNT/C-wt (100 pM; black diamond) displayed a potency similar to standard BoNT/C (Fig 3A), whereas to achieve a T_{50} value within the calibration curve, BoNT/C α-3W (empty square) and BoNT/C α-51 (filled square) were used at much larger concentrations (300 pM and 3000 pM, respectively). Their potency was calculated as 12.1% and 3.4% of the BoNT/C-wt, respectively (Fig 3B). Hemidiaphragms were then stained for cleaved SNAP-25 (Fig 3C). Cleaved SNAP-25 was detected in all muscles analyzed, suggesting that mutant toxins cleave SNAP-25 also at the NMJ. At the same time, we detected minute levels in hemidiaphragms treated with a concentration of BoNT/C α-51 (300 pM) which caused a very slow decline in muscle strength compared to the higher concentration. These experiments suggest a strict correlation between the potency of BoNT/C variants and their capacity to cleave SNAP-25.

We next assessed the potency of wild type and mutant BoNT/C toxins *in vivo* using the mouse bioassay [47], in which mice are injected intraperitoneally with different amounts of BoNTs and the dose causing death in the 50% of animals (i.e. 1 LD_{50}) is used as a parameter to estimate toxin lethality. BoNT/C-wt resulted in a LD_{50} = 0.75 ng/kg, whereas BoNT/C α-3W and BoNT/C α-51 displayed LD_{50} = 150 ng/kg and LD_{50} = 750 ng/kg, respectively (Fig 4A and Table 1). Similarly to BoNT/C-wt, both mutants induced the classical symptoms of botulism, i.e. the progressive collapse of flank musculature, ruffled fur, eye dryness, and labored breath until respiratory failure. Relative to BoNT/C-wt lethality (Fig 4B, top panel), botulism onset due to BoNT/C α-3W was very rapid as mice died very quickly (Fig 4B, middle panel). Conversely, BoNT/C α-51 induced botulism with a slower progression, with lethality occurring significantly later (Fig 4B, bottom panel). Taken together, these observations suggest that the lethality/potency of the three toxins are linked to their capacity to cleave SNAP-25.

Duration of neuroparalysis does not correlate with potency of mutant BoNT/C toxins

A fundamental feature of BoNT/C is the long lasting paralysis induced following local injection in sub-lethal amounts. Among the toxins tested to date, BoNT/A1 and BoNT/C have the longest persistence both in human and in mice [26, 48]. Accordingly, we tested the duration of paralysis by mutant toxins upon injection in the hind limb with the Digit Abduction Score (DAS) [49]. In this assay, animals are scored from 0 to 4, where 0 corresponds to normal mobility and 4 to complete block of digit abduction. One LD_{50} of BoNT/C-wt induced a severe paralysis within the first few days after administration, which was then progressively recovered (Fig 5A). Surprisingly, one LD_{50} of BoNT/C α-3W induced a very quick onset followed by a complete recovery within 48 hours. Even more surprisingly, one LD_{50} of BoNT/C α-51 had a very long persistence, also exceeding that of BoNT/C-wt. Interestingly, we detected an acute phase (days 1–5) of severe paralysis followed by a longer period of time characterized by a progressive, yet slow, recovery of function.

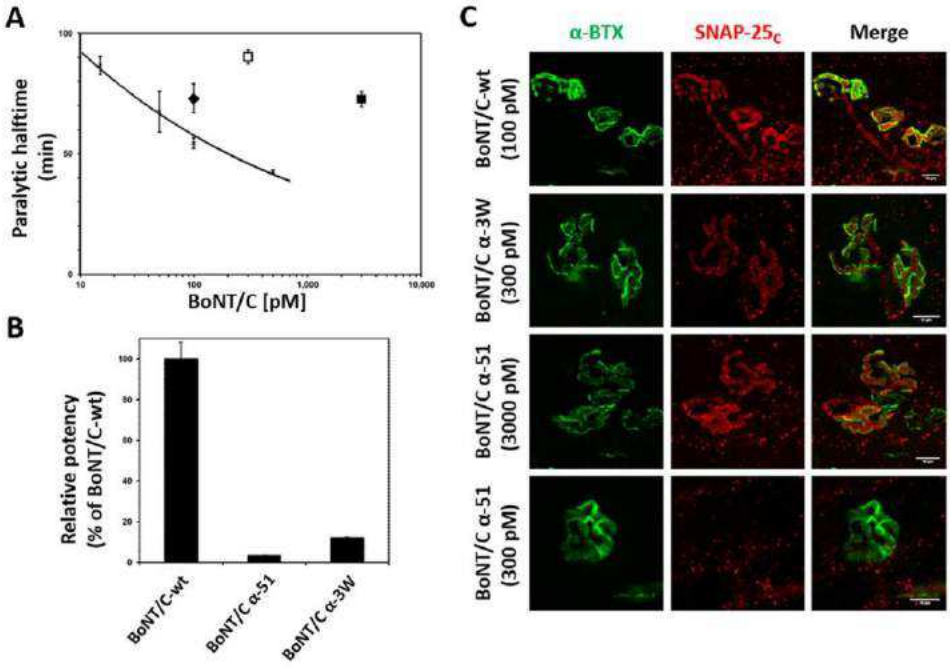

Fig 3. BoNT/C mutants display noticeable lower potency than wild type BoNT/C. (A) Activity of BoNT/C variants at the MPN hemidiaphragm assay. The black trace represents a dose-response calibration curve reporting the T_{50} value obtained at indicated bath concentration of a reference wild type BoNT/C [45]. Recombinant BoNT/C-wt (black diamond), tested at 100 pM displays a T_{50} comparable to the previous BoNT/C-wt used at the same concentration. BoNT/C α-3W (white square) and BoNT/C α-51 (black square) need much higher concentrations to achieve a T_{50} within the calibration curve. Error bars represent SD of n = 3–4 technical replicates. **(B)** Calculation of potency of BoNT/C mutants employing a power function fitted to the dose-response calibration curve in A. **(C)** Immunofluorescent analysis of hemidiaphragms derived from MPN assays. Hemidiaphragms treated with the indicated toxin and concentration were fixed immediately upon completion of paralysis and stained for cleaved SNAP-25 ($SNAP\text{-}25_c$, red). NMJs were spotted with α-Bungarotoxin (α-BTX, in green). Images shown are representative of at least three independent experiments. Scale bar, 10 μm.

https://doi.org/10.1371/journal.ppat.1006567.g003

To obtain a more quantitative time course of the paralyses, we measured the "evoked junction potential" (EJP). This electrophysiological analysis allows an accurate estimation of neurotransmitter release at the NMJ and can be used to monitor neurotransmission recovery in a quantitative way [27]. Muscles treated with BoNT/C α-3W were fully paralyzed 24 hours after injection, yet recovery was fast and nerve-muscle transmission reached control levels within two weeks (Fig 5B). Unlike BoNT/C α-3W, BoNT/C-wt and BoNT/C α-51 completely abrogated neurotransmission for at least one week and recovery was slow, being incomplete even after 5 weeks.

Altogether, these experiments indicate that the duration of the neuroparalytic effects of BoNT/C mutants does not correlate with their respective potency.

Cleavage of SNAP-25 or syntaxin-1B have different functional consequences on neuromuscular transmission

We hypothesized that lack of correlation between duration of paralysis and the relative potency of BoNT/C variants was due to different cleavage of SNAP-25 and syntaxin. To test this hypothesis, we stained soleus muscles of mice treated with wild type and mutant BoNT/C toxins for cleaved SNAP-25. BoNT/C-wt induced long-lasting SNAP-25 cleavage, which was reduced only at a later stage, when neurotransmission has significantly recovered (Fig 6A).

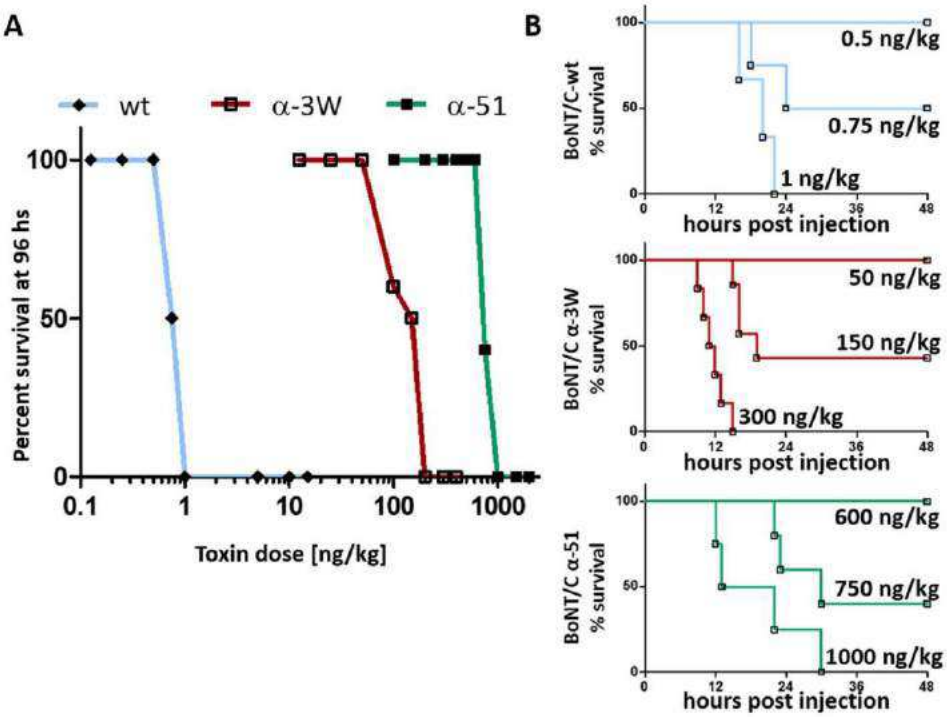

Fig 4. BoNT/C mutants are poorly lethal *in vivo*. (A) Mouse bioassay for BoNT/C variants. CD1 female mice weighting 20–24 grams were injected intraperitoneally with the indicated doses of BoNT/C-wt (cyan) or BoNT/C α-51 (green) or BoNT/C α-3W (red). Survival after 96 hours is reported as the percentage of mice survived with respect to the total group treated with the same amount of toxin. **(B)** Animals of the mouse bioassay were monitored every 4 hours and their survival reported as a Kaplan-Meier plot. Top panel shows BoNT/C-wt, middle panel is for BoNT/C α-3W and bottom panel is for BoNT/C α-51.

https://doi.org/10.1371/journal.ppat.1006567.g004

Two weeks after toxin treatment, we also observed NMJ fragmentation, extensive nerve terminal sprouting, and synaptic remodeling, as previously reported [50]. Interestingly, cleaved SNAP-25 was detected all along sprout membranes and within the presynaptic side of newly formed nerve-muscle contacts. Following BoNT/C α-3W treatment, cleaved SNAP-25 was clearly detectable 24 hours after injection, when neurotransmission is completely blocked, but disappeared within four days, indicating that SNAP-25 1–198 has a half-life of <4 days (Fig 7A). NMJs displayed neither signs of postsynaptic remodeling nor nerve sprouting. These results suggest that SNAP-25 cleavage is associated with a nerve terminal blockage and that muscle paralysis persists as long as SNAP-25 is cleaved. On the other hand, Fig 8A shows that in muscles treated with BoNT/C α-51, cleaved SNAP-25 is evident only at 24 hours after

Table 1. Summary of the lethality of the different BoNT/C variants used in this study.

	LD_{50}	Lethal amount*	Relative lethality
BoNT/C-wt	0.75 ng/kg	0.015 ng	1
BoNT/C α-3W	150 ng/kg	3 ng	1/200
BoNT/C α-51	750 ng/kg	15 ng	1/1000

A comparison of the lethal doses and the lethal amounts of BoNT/C-wt, BoNT/C α-3W and BoNT/C α-51, as estimated from the mouse bioassay. The relative lethality of BoNT/C α-3W and BoNT/C α-51 with respect to BoNT/C-wt is also shown.

(*) The lethal amount is calculated considering a mouse of 20 grams.

https://doi.org/10.1371/journal.ppat.1006567.t001

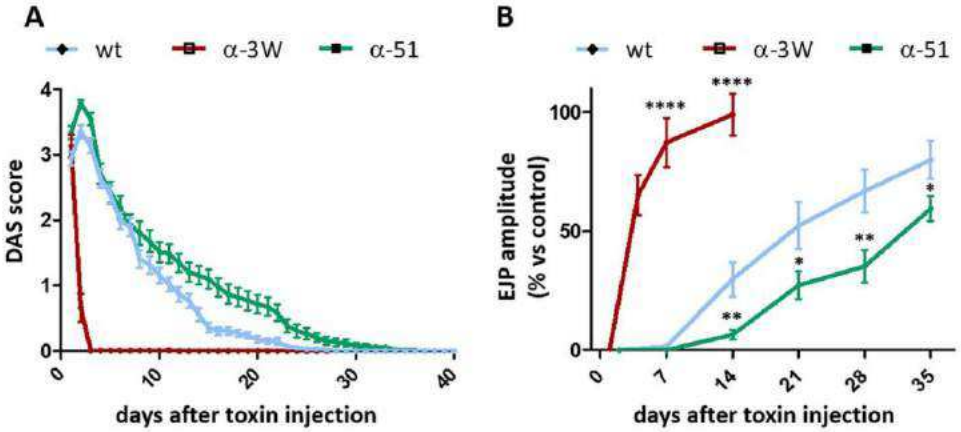

Fig 5. Time course of neuroparalysis recovery upon a local injection of BoNT/C variants in the mouse hind limb. (A) Digit Abduction Score (DAS) assay. 1 LD_{50} of BoNT/C-wt (cyan), or BoNT/C α-51 (green) or BoNT/C α-3W (red) were injected intramuscularly in the mice hind limb and neuroparalysis was evaluated according to [49]. The rescue from paralysis was monitored daily until complete recovery was attained. Traces are representative of three independent experiments with at least 5 mice per condition. Error bars represent SEM **(B)** Analysis of evoked post synaptic junction potentials (EJP) on injected soleus muscles. Mice were treated as in A and at indicated time points soleus muscles were collected and processed for recordings of EJPs, as previously reported [27]. Data are presented as a percentage of EJPs of control muscles. Each point represents an average EJP amplitude obtained from at least 45 muscle fibers from three different mice per condition. Statistical significance at each time point was determined by a Student's t-test comparing the mean values between either BoNT/C α-51 (green) or BoNT/C α-3W (red) compared to BoNT/C-wt (cyan) (* $p<0.05$, ** $p<0.01$, *** $p<0.001$, **** $p<0.0001$, n.s. not significant). Error bars represent SEM.

https://doi.org/10.1371/journal.ppat.1006567.g005

injection and barely detectable at one and two weeks after. This indicates that SNAP-25 proteolysis occurs only at the very beginning of the time course and, consequently, the long lasting neurotransmission impairment induced by BoNT/C α-51 cannot be ascribed to SNAP-25 cleavage. Therefore, we stained injected muscles for syntaxin-1A/1B. Control NMJs displayed an intense and widespread staining characterized by large puncta of syntaxin-1B, the isoform prevalently expressed at the NMJ [51] (Figs 6B, 7B and 8B). BoNT/C and mutant toxins caused a large, though incomplete, loss of signal and the complete disappearance of syntaxin-1B clusters. This effect, which we interpreted as syntaxin-1B cleavage, was prolonged for BoNT/C-wt and it was not recovered even five weeks after injection (Fig 6B). In the case of BoNT/C α-3W, loss of syntaxin-1B was obvious only 24 hours after toxin injection with return to control levels between 7 to 14 days, indicating re-synthesis of syntaxin within 4 days and absence of LC/C α-3W activity (Fig 7B). BoNT/C α-51 caused a loss of syntaxin-1B similar to BoNT/C-wt and even 35 days post-injection there were no signs of recovery (Fig 8B). Importantly, nerve terminals underwent remodeling with a time course and an intensity comparable to the BoNT/C-wt-treated muscles, indicating a long-term impairment of NMJs. Considering that syntaxin re-synthesis is rapid (Fig 7B), these results suggest that the long lasting effect of BoNT/C α-51 is due to a persistent cleavage of syntaxin-1B and that LC/C α-3W activity has a very short half-life *in vivo*. Moreover, it is interesting to note that syntaxin proteolysis by LC/C α-51 also occurs in a phase in which SNAP-25 is not cleaved anymore (Fig 8B) which might be ascribed to the >10-fold higher EC_{50} for SNAP-25 (EC_{50Stx} 0.5 nM vs $EC_{50SNAP\text{-}25}$ >5 nM).

Altogether, electrophysiological measurements and nerve terminal analyses indicate that the cleavage of SNAP-25 is necessary for a complete neuromuscular block and muscle paralysis, while the proteolysis of syntaxin-1B induces a significant, though incomplete, impairment of neurotransmission.

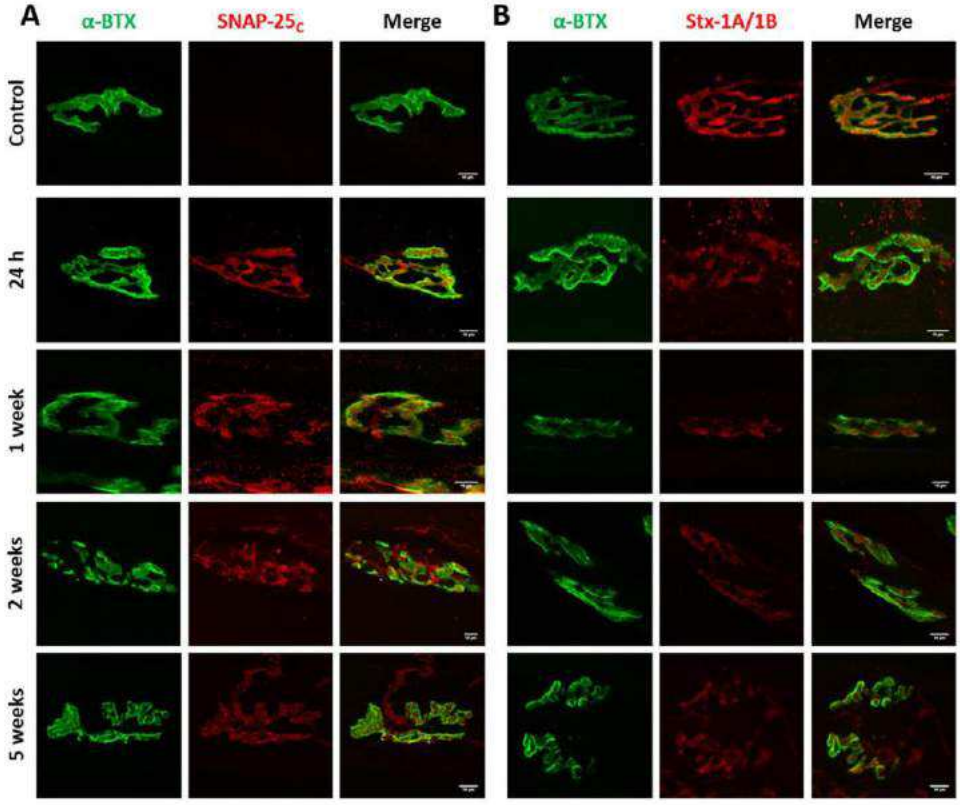

Fig 6. Imaging of cleaved SNAP-25 and syntaxin-1 in muscles treated with BoNT/C-wt. Soleus muscles of mice treated with BoNT/C-wt and used for the analysis of EJPs of Fig 5B were fixed immediately after the electrophysiological recordings and stained for **(A)** cleaved SNAP-25 (SNAP-25$_c$) or **(B)** Syntaxin-1A/1B (Stx-1A/1B), both shown in red. NMJs were spotted with α-Bungarotoxin (α-BTX, in green). The first row of panels represents the staining of a control muscle. Scale bar, 10 μm.

https://doi.org/10.1371/journal.ppat.1006567.g006

A low dose of BoNT/C α-51 accounts for a prolonged modulation of neurotransmission at the neuromuscular junction

Since the previous experiments showed that SNAP-25 cleavage occurs only with large amounts of mutant toxins, we reasoned that a low dose might induce exclusive proteolysis of syntaxin-1B. In this way, motor nerve activity should be attenuated without complete abrogation of neurotransmission. To test this hypothesis, we opted to use BoNT/C α-51 because of its low activity against SNAP-25 and its long half-life. Toxin was injected in the hind-limb at a dose of 10 ng/kg, which corresponds to about 1/75 of its LD_{50} and 13-fold LD_{50} of BoNT/C-wt. Interestingly, this "low dose" of BoNT/C α-51 did not result in a visible neuroparalysis (i.e., DAS score 0). Rather BoNT/C α-51 caused a substantial decrease of EJP amplitude in injected muscles, which lasted for almost one month before returning to control levels (Fig 9A). Importantly, no cleavage of SNAP-25 was detected during the entire time course (Fig 9B), while a significant loss of syntaxin-1B staining occurred, especially within the first two weeks after injection (Fig 9C). Thereafter, syntaxin-1B expression recovered together with neurotransmission, suggesting that nerve terminal activity (EJP amplitude) is proportional to the amount of syntaxin-1B. In addition, we found a reduced atrophy of muscles injected with the low dose of BoNT/C α-51 relative to muscles injected with either 1 LD_{50} of BoNT/C α-51 or 1 LD_{50} of BoNT/C-wt. These results indicate that BoNT/C α-51 can persistently modulate nerve terminal activity without compromising the overall activity of muscles.

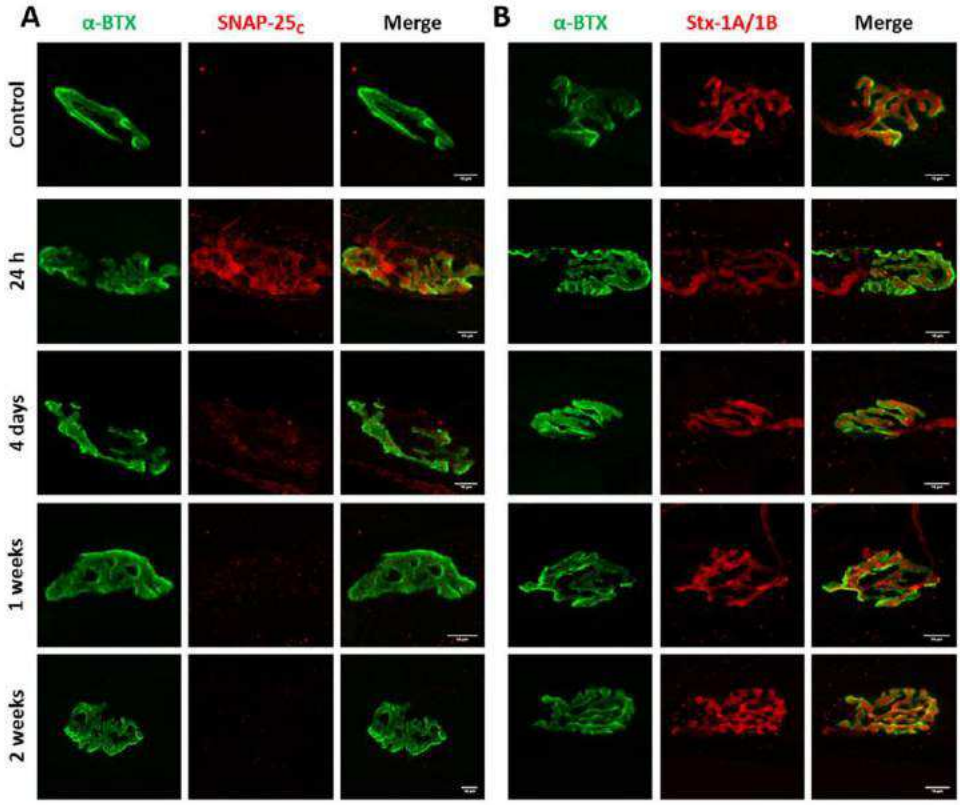

Fig 7. Imaging of cleaved SNAP-25 and syntaxin-1 in muscles treated with BoNT/C α-3W. Soleus muscles of mice treated with BoNT/C α-3W and used for the analysis of EJPs of Fig 5B were fixed immediately after the electrophysiological recordings and stained for **(A)** cleaved SNAP-25 (SNAP-25_c) or **(B)** Syntaxin-1A/1B (Stx-1A/1B), both shown in red. NMJs were spotted with α-Bungarotoxin (α-BTX, in green). The first row of panels represents the staining of a control muscle. Scale bar, 10 μm.

https://doi.org/10.1371/journal.ppat.1006567.g007

Discussion

Among the many botulinum neurotoxins characterized so far, BoNT/C is unique in that it cleaves two neuronal SNARE proteins, i.e. SNAP-25 and syntaxins. Although this parallel activity was demonstrated over 20 years ago in cultured neurons [24], it has never been reported at the NMJs nor was it clear which proteolytic event by BoNT/C causes neuroparalysis. Our results show that BoNT/C cleaves both substrates at the NMJ, and that the key determinant of potency and lethality is the proteolysis of SNAP-25 rather than syntaxin. We also report that the cleavage of syntaxin-1B (syntaxin-1A is not expressed at the NMJ [51]) does not cause complete block of the NMJ, although it accounts for a substantial impairment of neurotransmission efficiency. Such a result is surprising considering the current view of the SNARE-mediated mechanism of neuroexocytosis [52], but it is supported by previous reports showing that: i) BoNT/C paralysis at NMJ can be reversed by 3,4-diaminopyridine [50], consistent with a neuroparalytic effect lying on SNAP-25 cleavage rather than syntaxin, like for BoNT/A1 [53]; ii) Syntaxin-1B knock out mice have a very limited life span, yet they survive for a couple of weeks after birth, implying that neuromuscular transmission is viable [54, 55]; iii) Syntaxin-1B deficiency reduces but does not abolish NMJ capacity of neurotransmitter release [55]. A likely explanation is the compensation of syntaxin-1B knock out/proteolysis at the NMJ by other syntaxin isoforms. In knock out mice a minor expression of syntaxin-1A was reported, which might occur as a compensatory mechanism [55]. In the present study, this

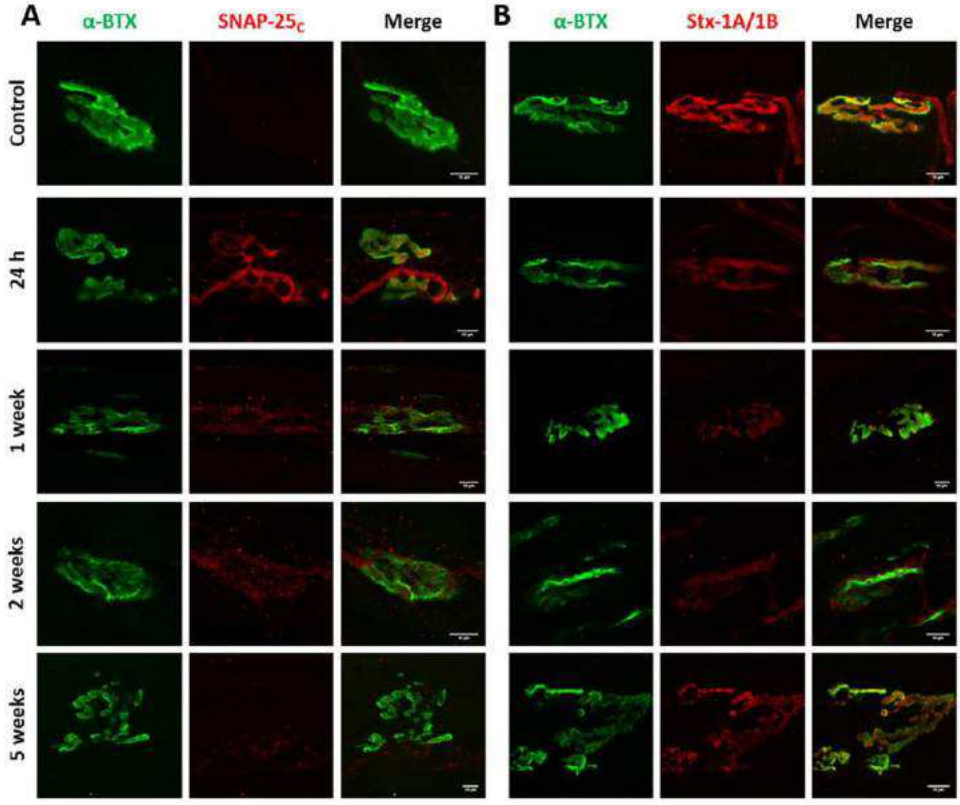

Fig 8. Imaging of cleaved SNAP-25 and syntaxin-1 in muscles treated with BoNT/C α-51. Soleus muscles of mice treated with BoNT/C α-51 and used for the analysis of EJPs of Fig 5B were fixed immediately after the electrophysiological recordings and stained for **(A)** cleaved SNAP-25 (SNAP-25$_c$) or **(B)** Syntaxin-1A/1B (Stx-1A/1B), both shown in red. NMJ were spotted with α-Bungarotoxin (α-BTX, in green). The first row of panels represents the staining of a control muscle. Scale bar, 10 μm.

https://doi.org/10.1371/journal.ppat.1006567.g008

possibility has to be discarded as syntaxin-1A would also be substrate of the toxins. On the other hand, many non-cleavable syntaxins exist [5], raising the possibility that a cognate isoform compensates for syntaxin-1 biochemical knock down, leading to a largely inefficient, yet functional neurotransmitter release.

As a general conclusion, syntaxin-1B proteolysis does not seem to be critical for the acute neuroparalytic action of BoNT/C, which instead relies on SNAP-25 cleavage. Nonetheless, syntaxin cleavage may contribute to delaying the recovery process. In fact, fusion of synaptic vesicles with the plasma membrane depends on the incorporation of multiple SNARE complexes into SNARE super-complexes [56]. Since cleavage by BoNT/C occurs at the very C-terminus and frees syntaxin from its transmembrane domain [5, 13, 14], it may be speculated that the SNARE motif of cleaved-syntaxins are incorporated within SNARE super-complexes, and negatively modulate vesicle fusion. This effect may be added to the long known effect of BoNT/C (and BoNT/A) cleaved-SNAP-25 in modulating neuroexocytosis [5, 56].

We were surprised to find that BoNT/C mutants exert different neurodegenerative effects in cultured neurons. This effect was previously attributed to cleavage of SNAP-25 and syntaxin-1A/1B, and to the complete elimination of one of them [40, 41]. However, we found that *in vitro* neurodegeneration triggered by BoNT/C-wt and BoNT/C α-51 occurs even if a small portion of syntaxin-1A/1B is resistant to cleavage. Moreover, BoNT/C α-3W is not cytotoxic even if it displays proteolytic activity against SNAP-25 and syntaxin-1A/1B to an extent equal,

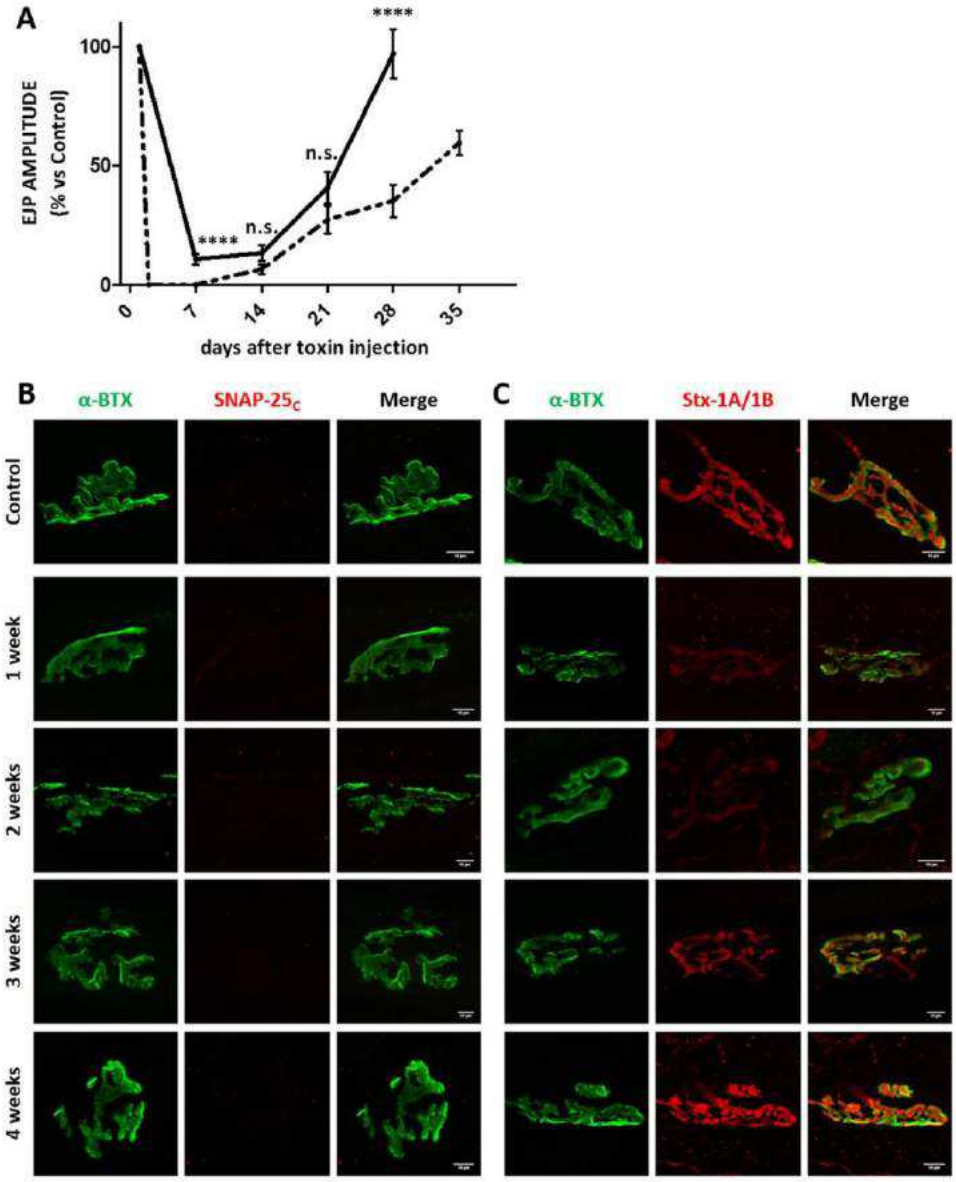

Fig 9. Time course of neurotransmission recovery in soleus muscles upon a local injection of a low dose of BoNT/C α-51. (A) The black trace shows the analysis of evoked post synaptic junction potentials (EJP) on soleus muscles injected intramuscularly with 10 ng/kg of BoNT/C α-51. At indicated time points soleus muscles were collected and processed for the electrophysiological recordings of EJPs, as previously reported [27]. Data are presented as a percentage of EJPs of control muscles. Each point represents an average EJP amplitude obtained from at least 45 muscle fibers from three different mice per condition. Error bars represent SEM. As a comparison, dotted trace shows the time course of EJP recovery obtained with 1 LD_{50} of BoNT/C α-51. Statistical significance at each time point was determined by a Student's t-test comparing the mean values (**** $p<0.0001$, n.s. not significant). Error bars represent SEM. **(B and C)** Soleus muscles coming from the EJP analyses were fixed and stained for (B) cleaved SNAP-25 ($SNAP\text{-}25_c$) or (C) Syntaxin-1A/1B (Stx-1A/1B), both shown in red. NMJ were spotted with α-Bungarotoxin (α-BTX, in green). The first row of panels represents the staining of a control muscle.

https://doi.org/10.1371/journal.ppat.1006567.g009

if not superior, to BoNT/C α-51. These results indicate that SNARE cleavage may be not directly implicated in BoNT/C-mediated neurodegeneration, at least in CGNs. An intriguing alternative explanation may be the proteolysis of an additional substrate, still recognized by BoNT/C-wt and BoNT/C α-51, but not by BoNT/C α-3W.

BoNT/C neurodegeneration does not occur at the NMJ *in vivo* in mice [50] and humans [48, 57, 58]. A plausible explanation as to why neurodegeneration occurs only in cell culture may be found in the different mode of entry of BoNT/C at the NMJ and in cultured neurons. *In vivo*, like the other BoNTs, BoNT/C entry is restricted to unmyelinated areas of the nerve terminals as axons are covered and protected by a tight nerve-blood-barrier. Neurons in culture are instead not myelinated and fully exposed to the action of all toxins residing in the culture medium. Accordingly, BoNT/C may affect neuronal compartments that are not accessible *in vivo*. In any case, we show here that poisoned nerve terminals do not degenerate at any time after toxin injection, a relevant finding considering that very high amounts of BoNT/C α-51 had been locally injected (1 $LD_{50} \geq 15$ ng/mouse). Rather, poisoned nerve terminals activate and set in motion a profound remodeling of the NMJ as an attempt to bypass the functional block of the synapse, similarly to what is observed upon BoNT/A1 and BoNT/B1 intoxication [25, 27, 50, 59]. Therefore, our results suggest that the use of BoNT/C in humans would be safe, and that BoNT/C α-51 may be a suitable candidate for this purpose. In fact, used at a dose comparable to BoNT/C-wt, this toxin provides a persistent modulation of nerve terminal activity without causing the complete paralysis of the muscle, a relevant finding for therapeutic and cosmetic applications. BoNT/C α-51 would likely be ideal for applications characterized by a narrow therapeutic window, when an optimal modulation of nerve terminal hyperactivity is usually difficult to achieve without causing significant muscle weakening, as in focal dystonia [5, 60]. Moreover, considering the low systemic toxicity in mice, this toxin may be suitable in clinical conditions requiring considerable amounts of BoNT, like the treatment of large muscles in post-stroke spasticity [5, 61, 62]. As for other BoNTs [29, 57, 58, 63], electrophysiological testing on human volunteers can be used to assess the time course of action and the susceptibility of human muscles to BoNT/C α-51 (or syntaxin-specific BoNTs). These preliminary analyses would reveal a dose-response window and may be essential in evaluating the therapeutic potential of the toxin as well as its safety margin and immunogenicity [5].

In conclusion, this work highlights that minimal changes can functionally impact BoNT biological activity, and suggests that inspection of structure-activity relationships may be used to generate tailor-made toxins with *ad hoc* pharmacological properties to improve the present applications and expand the clinical landscape of BoNT pharmacotherapy [41, 46, 64, 65].

Materials and methods

Reagents

Native BoNT/C and BoNT/A1 were purified as previously described [66, 67]. Cytosine β-D-arabinofuranoside hydrochloride (C6645), DNAse I from bovine pancreas (DN25), poly-L-lysine hydrobromide (P1274) and trypsin (T4799) were from Sigma Aldrich. μ-Conotoxin GIIIB is from Alomone, Jerusalem, Israel. Primary antibodies: anti-SNAP-25 (SMI81, ab24737) was from Abcam. Anti-SNAP-25 (cleaved) and syntaxin-1A/1B polyclonal antibodies were produced in our laboratory and previously characterized [37, 68]. Secondary antibodies conjugated to HRP were from Calbiochem; secondary antibodies for immunofluorescence conjugated to Alexa Fluorophores 488 or 555 and α-Bungarotoxin conjugated to Alexa 647 were from Thermo Scientific, Waltham, MA, USA.

Production of recombinant BoNT/C and SNARE substrates

Full-length BoNT/C (GenBank: X53751.1) and BoNT/C LC (aa 1–430) as well as the mutants thereof were produced, the former under biosafety level 2 containment (project number GAA A/Z 40654/3/57), in *E. coli* strain M15pREP4 (Qiagen, Hilden, Germany) during 15 h of induction at 21˚C and purified on StrepTactin-sepharose matrix (IBA GmbH, Göttingen, Germany)

and Ni^{2+}-nitrilotriacetic acid-agarose matrix (Qiagen), respectively, according to the manufacturers' instructions. Aliquots of BoNT/C derivatives (in 100 mM Tris, pH 8.0) and of BoNT/C LC derivatives (dialyzed against toxin assay buffer (150 mM potassium glutamate, 10 mM HEPES-KOH, pH 7.2), were frozen in liquid nitrogen, and kept at -70˚C.

Recombinant substrate proteins, rat SNAP-25His6 [69] and a syntaxin fusion protein comprising an N-terminal His6-tag followed by the Halo-tag, rat syntaxin 1A aa 183–259, luciferase, and a C-terminal Strep-tag, were produced using the *E. coli* strains M15 pREP4 and BL21-DE3 (Stratagene Europe, Ebsdorfergrund, Germany), respectively, purified via His6- or His6- and Strep-tag, dialyzed against toxin assay buffer or PBS, pH 7.4, supplemented with 7% (w/v) sucrose, and finally frozen in liquid nitrogen.

Radiolabeled substrates were generated by *in vitro* transcription/translation using the plasmids pSNAP-25his6 and pET29-HASyn(183–259)LS, the SP6/T7 coupled TNT reticulocyte lysate system (Promega), and [^{35}S]methionine (370 KBq/μL, >37 TBq/mmol, Hartmann Analytic, Braunschweig, Germany) according to the manufacturer´s instructions.

Concentrations of *E. coli* expressed proteins were determined subsequent to SDS-PAGE and Coomassie blue staining by using a LAS-3000 imaging system (Fuji Photo Film), the AIDA 3.51 program, and various known concentrations of BSA. The extent of hydrolytic activation of full-length BoNT/C by *E. coli* proteases was 81% (wild type), 73% (α-51), and 79% (α-3W).

In vitro proteolytic activity

Cleavage assays were conducted using 10 μM SNAP-25 or 1 μM syntaxin fusion protein, respectively, each 1 μL of transcription/translation mixture of the respective substrate as [^{35}S]-methionine-labeled protein, and purified LC/C derivative at 1 to 3 μM final concentrations in 10 μL. Incubation was done for 60 min at 37˚C in toxin assay buffer. Reactions were stopped by the addition of an equal volume of double-concentrated sample buffer (120 mM Tris-HCl, pH 6.75, 10% (v/v) β-mercaptoethanol, 4% (w/v) SDS, 20% (w/v) glycerol, 0.014% (w/v) bromphenol blue) and then subjected to SDS-PAGE using 10% or 15% tris/glycine gels (the latter using acrylamide/bis-acrylamide in 73.5:1 ratio). Subsequently, gels were dried and radiolabeled proteins were visualized employing a FLA-9000 phosphorimager (Fuji Photo Film, Co., Ltd., Tokyo, Japan). Quantification of cleavage was done by means of the radiolabeled substrates by phosphorimaging using the Multigauge 3.2 software (Fuji Photo Film).

Neuronal cultures and intoxication assay

Primary cultures of rat cerebellar granule neurons (CGNs) were prepared from 6- to 8-day-old rats as previously described [26]. Briefly, cerebella were isolated, mechanically disrupted and trypsinized in the presence of DNase I. Cells were then collected and plated into 24 well plates pre-coated with poly-L-lysine (50 μg/ml) at a cell density of $4x10^5$ cells per well. Cultures were maintained at 37˚C, 5% CO_2, 95% humidity in BME (Basal Medium Eagle) supplemented with 10% fetal bovine serum, 25 mM KCl, 2 mM glutamine and 50 μg/ml gentamicin (hereafter indicated as complete culture medium). To arrest growth of non-neuronal cells, cytosine arabinoside (10 μM) was added to the complete culture medium 18–24 h after plating.

CGNs at 6–8 days *in vitro* (DIV) were incubated with increasing concentrations (from 0.01 nM to 5 nM) of the indicated BoNT/C in complete culture medium for 12 or 24 hours at 37˚C. The specific proteolytic activity against SNAP-25 and syntaxin-1A/1B was evaluated via immunoblotting with antibodies that recognize both the intact and the truncated form of the two proteins.

Immunoblotting

Cells were directly lysed with Laemmli sample buffer containing protease inhibitors (Roche). Cell lysates were loaded onto NuPage 12% Bis-Tris gels (Life technologies) and separated by electrophoresis in MOPS buffer (Life technologies). Proteins were transferred onto Protran nitrocellulose membranes (Whatman) and saturated for 1 h in PBS-T (PBS, 0.1% Tween 20) supplemented with 5% non-fatty milk. Incubation with primary antibodies was performed overnight at 4˚C. The membranes were then washed three times with PBS-T and incubated with appropriate secondary antibodies for 1 h. Membranes were washed three times with PBS and proteins revealed either with an Odyssey imaging system (LI-COR Bioscience) or with an Uvitec gel doc system (Uvitec Cambridge).

Immunocytochemistry

CGNs were seeded onto 13 mm round glasses in 24-well plates at a cell density of $4x10^5$ cells per well. CGNs at 6–8 DIV were incubated for the indicated time and concentration of toxin in complete culture medium at 37˚C. After treatment, neurons were fixed for 10 min with 4% (w/v) paraformaldehyde in PBS and stained with an antibody against cleaved SNAP-25 and an antibody against neurofilament-200 (NF200). Coverslips were mounted using Fluorescent Mounting Medium (Dako) and examined with a Leica SP5 confocal microscope (Leica Microsystems, Wetzlar, Germany) equipped with 100X HCX PL APO NA 1.4 objective.

Mouse phrenic nerve (MPN) hemidiaphragm assay

The MPN assay was performed as described previously [43, 45]. To limit the consumption of mice, the left and right phrenic nerve hemidiaphragms were excised from female mice of strain RjHan:NMRI (18–25 g, Janvier, St Berthevin Cedex, France) and placed in an organ bath containing 4 ml of Earle's Balanced Salt Solution. The pH was adjusted to 7.4, and oxygen saturation was achieved by gassing with 95% O_2 and 5% CO_2. The phrenic nerve was continuously electro-stimulated at a frequency of 1 Hz with a pulse duration of 0.1 ms and a current of 25 mA to achieve maximal contraction amplitudes. Isometric contractions were recorded with a force transducer (Scaime, Annemasse, France) and the software VitroDat (Föhr Medical Instruments GmbH (FMI), Seeheim, Germany). The resting tension of the hemidiaphragm was approximately 10 mN. In each experiment, the preparation was first allowed to equilibrate for 15 min under control conditions. Then, the buffer was exchanged to 4 ml of Earle's Balanced Salt Solution supplemented with 0.1% BSA and varying BoNT/C dilutions. The previously reported calibration curve determined for recombinant, *E. coli* host activated BoNT/C (y (BoNT/C; 15, 50, 70, 100 and 233 pM) = $148.95x^{-0.2089}$; $R^2 = 0.9806$) was used to calculate the residual potency of BoNT/C mutants. The resulting paralytic half-times of BoNT/C mutants were converted to the corresponding concentrations of wild type BoNT/C, using the equation mentioned above. The toxicities were finally expressed relative to wild type BoNT/C.

Lethality assay

Swiss-Webster adult female CD1 mice (20–24 grams) were housed under controlled light/dark conditions, and food and water were provided *ad libitum*. All experiments were performed in accordance with the European Community Council Directive n˚ 2010/63/UE and approved by the Italian Ministry of Health. LD_{50} were determined by injecting different doses of BoNT/C-wt or BoNT/C α-3W or BoNT/C α-51 diluted in 0.9% NaCl 0.2% gelatin. Toxins were prepared at a given concentration and mice were injected intraperitoneally with different volumes

according to their body weight in order to reach the indicated doses. Mice were monitored every 4 hours for 96 hours, when the experiment was considered to be concluded.

Digit abduction score (DAS) assay

Swiss-Webster adult female CD1 mice weighing 20–24 g were injected in the left hind limb with 1xLD_{50} of BoNT/C-wt (0.75ng/kg) or BoNT/C α-3W (150 ng/kg) or BoNT/C α-51 (750 ng/kg) diluted in 0.9% NaCl with 0.2% gelatin. Neuroparalysis was assessed daily according to the Digit Abduction Score (DAS) assay scale, as previously reported [49].

Electrophysiological recordings of evoked junction potential

Mice were injected in the left hind limb as described for the DAS assay with indicated doses. At scheduled times, mice were sacrificed by anesthetic overdose coupled to cervical dislocation and the soleus muscle dissected. Electrophysiological recordings were performed in oxygenated Krebs-Ringer solution, using intracellular glass microelectrodes (WPI) filled with 1 M KCl and 2 M CH_3COOK. Evoked junction potentials (EJP) were recorded in current-clamp mode, starting from resting membrane potential of -70 mV, adjusted with direct current injection if needed. EJPs were elicited by supramaximal nerve stimulation at 0.5 Hz, using a suction microelectrode connected to a S88 stimulator (Grass, Warwick, RI, USA). Muscle contraction was prevented by 1 μM μ-Conotoxin GIIIB (Alomone, Jerusalem, Israel). Signals were amplified with intracellular bridge mode amplifier (BA-01X; NPI, Tamm, Germany), sampled using a digital interface (NI PCI-6221; National Instruments, Austin, TX, USA) and recorded by means of electrophysiological software (WinEDR; Strathclyde University, Glasgow, Scotland, UK). EJPs measurements were carried out with Clampfit software (Molecular Devices, Sunnyvale, CA, USA). EJPs represent the average value obtained analyzing at least three muscles (15 fibers/muscle) for each condition at each time-point and reported as a percentage with respect to control muscles.

Imaging of neuromuscular junctions

Immediately after electrophysiological recording, soleus muscles were fixed in 4% paraformaldehyde in PBS for 10 min at RT. Each muscle was then separated in bundles of about 20–40 fibers to facilitate the following steps, in particular antibody penetration. In the case of explanted and intoxicated hemidiaphragms, upon completion of paralysis, muscles were fixed for 30 minutes. Samples were quenched in 50 mM NH_4Cl in PBS and treated for 2 h with a blocking solution (15% v/v goat serum, 2% w/v BSA, 0.25% w/v gelatin, 0.2% w/v glycine in PBS, 0.5% Triton X-100) to saturate and permeabilize nerve terminals. Thereafter, incubation with the following primary antibodies was carried out for at least 48 h in blocking solution with either anti-cleaved SNAP-25 or anti-Syntaxin-1A/1B. Muscles were then extensively washed and incubated with a secondary antibody conjugated with Alexa-555 diluted in blocking solution supplemented with α-Bungarotoxin conjugated to Alexa 647 to counterstain postsynaptic nicotinic acetylcholine receptors. Images were collected with a Leica SP5 confocal microscope (Leica Microsystems, Wetzlar, Germany) equipped with 100X HCX PL APO NA 1.4 objective. Laser excitation line, power intensity, and emission range were chosen according to each fluorophore in different samples to minimize bleed-through.

Ethics statements

All experiments were performed in accordance with the Italian laws and policies (D.L. n°26 14th March 2014) and with the guidelines established by the European Community Council

Directive n° 2010/63/UE and approved by the veterinary services of the University of Padova (O.P.B.A.—Organismo Preposto al Benessere degli Animali) (protocol 359/2015).

Supporting information

S1 Fig. Mutations conferring to BoNT/C specificity for syntaxins. Space-filling representation of BoNT/C LC (PDB entry 2QN0) with highlighted triple mutations for syntaxin selectivity [32]: S51T/R52N/N53P (BoNT/C α-51) in green and L200W/M221W/I226W (BoNT/C 0078-3W) in red. Blue spot shows the metalloprotease active site.
(TIF)

S2 Fig. SDS-PAGE analysis of the different BoNT/C toxins used in the study. From left to right, 250 nanograms of either native BoNT/C-wt, or recombinant BoNT/C-wt, BoNT/C α-51 or BoNT/C α-3W were loaded in a 12% gel under reducing conditions and revealed by Coomassie staining. The extent of hydrolytic activation of full-length BoNT/C by *E. coli* proteases was 81% (wild type), 73% (α-51), and 79% (α-3W). The lower purity of α-51 does not compromise its biological activity as deduced by the very similar EC_{50Stx} of this toxin with respect to BoNT/C α-3W and BoNT/C-wt in cultured neurons.
(TIF)

S3 Fig. The cleavage of SNAP-25 by BoNT/C mutants in CGNs does not increase by prolonging the incubation time to 24 hours. CGNs were treated as in Fig 1 but incubation was prolonged to 24 hours. The cleavage of syntaxin-1A/1B and SNAP-25 was assayed by western blot using two antibodies recognizing both the intact and the cleaved forms of the proteins.
(TIF)

S4 Fig. SNAP-25 cleaved by BoNT/C is recognized by an antibody raised against SNAP-25 cleaved by BoNT/A1. CGNs were treated with BoNT/A1 (0.1 nM) or BoNT/C-wt (0.1 nM) in normal culture medium at 37˚C for 3 hours. Thereafter cells were fixed and stained with an antibody raised against SNAP-25 segment 185–197 (red) [37], corresponding to the C-terminus generated by BoNT/A1 cleavage (SNAP-25_c). The antibody against neurofilament-200 (NF200, in green) is used as control staining. Scale bar, 10 μm.
(TIF)

S5 Fig. BoNT/C mutants display a different cytotoxic effect on cultured neurons. CGNs were treated as in Fig 2 but incubation was prolonged to 24 hours. Neurons were then fixed and stained with an antibody against cleaved SNAP-25 (SNAP-25_c, in red) and neurofilament-200 (NF200, in green). Cytotoxicity was evaluated following the appearance of varicosities along neurites and the loss of NF200 staining. Images are representative of at least three independent experiments. Scale bar, 10 μm.
(TIF)

Acknowledgments

We thank Prof. C. Montecucco for comments and suggestions, Dr. Paola Caccin for technical assistance in experiments, Dr. Jasmin Weisemann for providing the syntaxin fusion protein and Dr. Lena Pernas and Prof. Maria Pennuto for editing of the manuscript.

Author Contributions

Conceptualization: Andreas Rummel, Thomas Binz, Marco Pirazzini.

Data curation: Giulia Zanetti, Stefan Sikorra, Andreas Rummel, Elisa Duregotti, Samuele Negro, Ornella Rossetto, Marco Pirazzini.

Formal analysis: Giulia Zanetti, Stefan Sikorra, Nadja Krez, Elisa Duregotti, Samuele Negro, Tina Henke, Ornella Rossetto, Marco Pirazzini.

Funding acquisition: Andreas Rummel, Ornella Rossetto.

Investigation: Giulia Zanetti, Thomas Binz, Marco Pirazzini.

Methodology: Andreas Rummel, Tina Henke, Ornella Rossetto, Thomas Binz, Marco Pirazzini.

Writing – original draft: Marco Pirazzini.

Writing – review & editing: Andreas Rummel, Ornella Rossetto, Thomas Binz, Marco Pirazzini.

References

1. Rossetto O, Pirazzini M, Montecucco C. Botulinum neurotoxins: genetic, structural and mechanistic insights. Nat Rev Microbiol. 2014; 12(8):535–49. https://doi.org/10.1038/nrmicro3295 PMID: 24975322
2. Montecucco C, Rasotto MB. On botulinum neurotoxin variability. MBio. 2015; 6(1).
3. Peck MW, Smith TJ, Anniballi F, Austin JW, Bano L, Bradshaw M, et al. Historical Perspectives and Guidelines for Botulinum Neurotoxin Subtype Nomenclature. Toxins (Basel). 2017; 9(1).
4. Gill DM. Bacterial toxins: a table of lethal amounts. Microbiol Rev. 1982; 46(1):86–94. PMID: 6806598
5. Pirazzini M, Rossetto O, Eleopra R, Montecucco C. Botulinum Neurotoxins: Biology, Pharmacology, and Toxicology. Pharmacol Rev. 2017; 69(2):200–235. https://doi.org/10.1124/pr.116.012658 PMID: 28356439
6. Johnson EA, Montecucco C. Botulism. Handb Clin Neurol. 2008; 91:333–68. https://doi.org/10.1016/S0072-9752(07)01511-4 PMID: 18631849
7. Bigalke H. Botulinum toxin: application, safety, and limitations. Curr Top Microbiol Immunol. 2013; 364:307–17. https://doi.org/10.1007/978-3-642-33570-9_14 PMID: 23239359
8. Lew MF, Adornato BT, Duane DD, Dykstra DD, Factor SA, Massey JM, et al. Botulinum toxin type B: a double-blind, placebo-controlled, safety and efficacy study in cervical dystonia. Neurology. 1997; 49 (3):701–7. PMID: 9305326
9. Binz T, Rummel A. Cell entry strategy of clostridial neurotoxins. J Neurochem. 2009; 109(6):1584–95. https://doi.org/10.1111/j.1471-4159.2009.06093.x PMID: 19457120
10. Rummel A. Two Feet on the Membrane: Uptake of Clostridial Neurotoxins. Curr Top Microbiol Immunol. 2016.
11. Montal M. Botulinum neurotoxin: a marvel of protein design. Annu Rev Biochem. 2010; 79:591–617. https://doi.org/10.1146/annurev.biochem.051908.125345 PMID: 20233039
12. Pirazzini M, Tehran DA, Leka O, Zanetti G, Rossetto O, Montecucco C. On the translocation of botulinum and tetanus neurotoxins across the membrane of acidic intracellular compartments. Biochim Biophys acta. 2016; 1858(3):467–74. https://doi.org/10.1016/j.bbamem.2015.08.014 PMID: 26307528
13. Binz T. Clostridial neurotoxin light chains: devices for SNARE cleavage mediated blockade of neurotransmission. Curr Top Microbiol Immunol. 2013; 364:139–57. https://doi.org/10.1007/978-3-642-33570-9_7 PMID: 23239352
14. Pantano S, Montecucco C. The blockade of the neurotransmitter release apparatus by botulinum neurotoxins. Cell Mol Life Sci. 2014; 71(5):793–811. https://doi.org/10.1007/s00018-013-1380-7 PMID: 23749048
15. Sudhof TC, Rizo J. Synaptic vesicle exocytosis. Cold Spring Harb Perspect Biol. 2011; 3(12).
16. Schiavo G, Benfenati F, Poulain B, Rossetto O, Polverino de Laureto P, DasGupta BR, et al. Tetanus and botulinum-B neurotoxins block neurotransmitter release by proteolytic cleavage of synaptobrevin. Nature. 1992; 359(6398):832–5. https://doi.org/10.1038/359832a0 PMID: 1331807
17. Schiavo G, Shone CC, Rossetto O, Alexander FC, Montecucco C. Botulinum neurotoxin serotype F is a zinc endopeptidase specific for VAMP/synaptobrevin. J Biol Chem. 1993; 268(16):11516–9. PMID: 8505288

18. Schiavo G, Rossetto O, Catsicas S, Polverino de Laureto P, DasGupta BR, Benfenati F, et al. Identification of the nerve terminal targets of botulinum neurotoxin serotypes A, D, and E. J Biol Chem. 1993; 268 (32):23784–7. PMID: 8226912

19. Schiavo G, Malizio C, Trimble WS, Polverino de Laureto P, Milan G, Sugiyama H, et al. Botulinum G neurotoxin cleaves VAMP/synaptobrevin at a single Ala-Ala peptide bond. J Biol Chem. 1994; 269 (32):20213–6. PMID: 8051110

20. Schiavo G, Santucci A, Dasgupta BR, Mehta PP, Jontes J, Benfenati F, et al. Botulinum neurotoxins serotypes A and E cleave SNAP-25 at distinct COOH-terminal peptide bonds. FEBS Lett. 1993; 335 (1):99–103. PMID: 8243676

21. Blasi J, Chapman ER, Link E, Binz T, Yamasaki S, Camilli PD, et al. Botulinum neurotoxin A selectively cleaves the synaptic protein SNAP-25. Nature. 1993; 365(6442):160–3. https://doi.org/10.1038/365160a0 PMID: 8103915

22. Blasi J, Chapman ER, Yamasaki S, Binz T, Niemann H, Jahn R. Botulinum neurotoxin C1 blocks neurotransmitter release by means of cleaving HPC-1/syntaxin. EMBO J. 1993; 12(12):4821–8. PMID: 7901002

23. Williamson LC, Halpern JL, Montecucco C, Brown JE, Neale EA. Clostridial neurotoxins and substrate proteolysis in intact neurons: botulinum neurotoxin C acts on synaptosomal-associated protein of 25 kDa. J Biol Chem. 1996; 271(13):7694–9. PMID: 8631808

24. Foran P, Lawrence GW, Shone CC, Foster KA, Dolly JO. Botulinum neurotoxin C1 cleaves both syntaxin and SNAP-25 in intact and permeabilized chromaffin cells: correlation with its blockade of catecholamine release. Biochemistry. 1996; 35(8):2630–6. https://doi.org/10.1021/bi9519009 PMID: 8611567

25. Meunier FrA, Lisk G, Sesardic D, Dolly JO. Dynamics of motor nerve terminal remodeling unveiled using SNARE-cleaving botulinum toxins: the extent and duration are dictated by the sites of SNAP-25 truncation. Mol Cell Neurosci. 2003; 22(4):454–66. PMID: 12727443

26. Pirazzini M, Azarnia Tehran D, Zanetti G, Megighian A, Scorzeto M, Fillo S, et al. Thioredoxin and its reductase are present on synaptic vesicles, and their inhibition prevents the paralysis induced by botulinum neurotoxins. Cell Rep. 2014; 8(6):1870–8. https://doi.org/10.1016/j.celrep.2014.08.017 PMID: 25220457

27. Duregotti E, Zanetti G, Scorzeto M, Megighian A, Montecucco C, Pirazzini M, et al. Snake and Spider Toxins Induce a Rapid Recovery of Function of Botulinum Neurotoxin Paralysed Neuromuscular Junction. Toxins (Basel). 2015; 7(12):5322–36.

28. Zanetti G, Azarnia Tehran D, Pirazzini M, Binz T, Shone CC, Fillo S, et al. Inhibition of botulinum neurotoxins interchain disulfide bond reduction prevents the peripheral neuroparalysis of botulism. Biochem Pharmacol. 2015; 98(3):522–30. https://doi.org/10.1016/j.bcp.2015.09.023 PMID: 26449594

29. Eleopra R, Tugnoli V, Rossetto O, De Grandis D, Montecucco C. Different time courses of recovery after poisoning with botulinum neurotoxin serotypes A and E in humans. Neurosci Lett. 1998; 256 (3):135–8. PMID: 9855358

30. Eleopra R, Tugnoli V, Quatrale R, Rossetto O, Montecucco C, Dressler D. Clinical use of non-A botulinum toxins: botulinum toxin type C and botulinum toxin type F. Neurotox Res. 2006; 9(2–3):127–31. PMID: 16785109

31. Vaidyanathan VV, Yoshino K, Jahnz M, Dorries C, Bade S, Nauenburg S, et al. Proteolysis of SNAP-25 isoforms by botulinum neurotoxin types A, C, and E: domains and amino acid residues controlling the formation of enzyme-substrate complexes and cleavage. J Neurochem. 1999; 72(1):327–37. PMID: 9886085

32. Wang D, Zhang Z, Dong M, Sun S, Chapman ER, Jackson MB. Syntaxin requirement for Ca2+-triggered exocytosis in neurons and endocrine cells demonstrated with an engineered neurotoxin. Biochemistry. 2011; 50(14):2711–3. https://doi.org/10.1021/bi200290p PMID: 21401123

33. Pirazzini M, Tehran DA, Zanetti G, Lista F, Binz T, Shone CC, et al. The thioredoxin reductase—Thioredoxin redox system cleaves the interchain disulphide bond of botulinum neurotoxins on the cytosolic surface of synaptic vesicles. Toxicon. 2015; 107(Pt A):32–6. https://doi.org/10.1016/j.toxicon.2015.06.019 PMID: 26130523

34. Bade S, Rummel A, Reisinger C, Karnath T, Ahnert-Hilger G, Bigalke H, et al. Botulinum neurotoxin type D enables cytosolic delivery of enzymatically active cargo proteins to neurones via unfolded translocation intermediates. J Neurochem. 2004; 91(6):1461–72. https://doi.org/10.1111/j.1471-4159.2004.02844.x PMID: 15584922

35. Pirazzini M, Henke T, Rossetto O, Mahrhold S, Krez N, Rummel A, et al. Neutralisation of specific surface carboxylates speeds up translocation of botulinum neurotoxin type B enzymatic domain. FEBS Lett. 2013; 587(23):3831–6. https://doi.org/10.1016/j.febslet.2013.10.010 PMID: 24157364

36. Weisemann J, Krez N, Fiebig U, Worbs S, Skiba M, Endermann T, et al. Generation and Characterization of Six Recombinant Botulinum Neurotoxins as Reference Material to Serve in an International Proficiency Test. Toxins (Basel). 2015; 7(12):5035–54.

37. Antonucci F, Rossi C, Gianfranceschi L, Rossetto O, Caleo M. Long-distance retrograde effects of botulinum neurotoxin A. J Neurosci. 2008; 28(14):3689–96. https://doi.org/10.1523/JNEUROSCI.0375-08.2008 PMID: 18385327

38. Azarnia Tehran D, Zanetti G, Leka O, Lista F, Fillo S, Binz T, et al. A Novel Inhibitor Prevents the Peripheral Neuroparalysis of Botulinum Neurotoxins. Sci Rep. 2015; 5:17513. https://doi.org/10.1038/srep17513 PMID: 26670952

39. Berliocchi L, Fava E, Leist M, Horvat V, Dinsdale D, Read D, et al. Botulinum neurotoxin C initiates two different programs for neurite degeneration and neuronal apoptosis. J Cell Biol. 2005; 168(4):607–18. https://doi.org/10.1083/jcb.200406126 PMID: 15716378

40. Peng L, Liu H, Ruan H, Tepp WH, Stoothoff WH, Brown RH, et al. Cytotoxicity of botulinum neurotoxins reveals a direct role of syntaxin 1 and SNAP-25 in neuron survival. Nat Commun. 2013; 4:1472. https://doi.org/10.1038/ncomms2462 PMID: 23403573

41. Rust A, Leese C, Binz T, Davletov B. Botulinum neurotoxin type C protease induces apoptosis in differentiated human neuroblastoma cells. Oncotarget. 2016; 7(22):33220–8. https://doi.org/10.18632/oncotarget.8903 PMID: 27121208

42. Rummel A, Hafner K, Mahrhold S, Darashchonak N, Holt M, Jahn R, et al. Botulinum neurotoxins C, E and F bind gangliosides via a conserved binding site prior to stimulation-dependent uptake with botulinum neurotoxin F utilising the three isoforms of SV2 as second receptor. J Neurochem. 2009; 110(6):1942–54. https://doi.org/10.1111/j.1471-4159.2009.06298.x PMID: 19650874

43. Bigalke H, Rummel A. Botulinum Neurotoxins: Qualitative and Quantitative Analysis Using the Mouse Phrenic Nerve Hemidiaphragm Assay (MPN). Toxins (Basel). 2015; 7(12):4895–905.

44. Rasetti-Escargueil C, Liu Y, Rigsby P, Jones RG, Sesardic D. Phrenic nerve-hemidiaphragm as a highly sensitive replacement assay for determination of functional botulinum toxin antibodies. Toxicon. 2011; 57(7–8):1008–16. https://doi.org/10.1016/j.toxicon.2011.04.003 PMID: 21513727

45. Strotmeier J, Gu S, Jutzi S, Mahrhold S, Zhou J, Pich A, et al. The biological activity of botulinum neurotoxin type C is dependent upon novel types of ganglioside binding sites. Mol Microbiol. 2011; 81(1):143–56. https://doi.org/10.1111/j.1365-2958.2011.07682.x PMID: 21542861

46. Kutschenko A, Reinert M- C, Krez N, Liebetanz D, Rummel A. BoNT/AB hybrid maintains similar duration of paresis as BoNT/A wild-type in murine running wheel assay. Neurotoxicology. 2017; 59:1–8. https://doi.org/10.1016/j.neuro.2016.12.008 PMID: 28043867

47. Pearce LB, Borodic GE, First ER, MacCallum RD. Measurement of botulinum toxin activity: evaluation of the lethality assay. Toxicol Appl Pharmacol. 1994; 128(1):69–77. https://doi.org/10.1006/taap.1994.1181 PMID: 8079356

48. Eleopra R, Tugnoli V, Quatrale R, Rossetto O, Montecucco C. Different types of botulinum toxin in humans. Mov Disord. 2004; 19 Suppl 8:S53–9.

49. Aoki KR. A comparison of the safety margins of botulinum neurotoxin serotypes A, B, and F in mice. Toxicon. 2001; 39(12):1815–20. PMID: 11600142

50. Morbiato L, Carli L, Johnson EA, Montecucco C, Molgo J, Rossetto O. Neuromuscular paralysis and recovery in mice injected with botulinum neurotoxins A and C. Eur J Neurosci. 2007; 25(9):2697–704. https://doi.org/10.1111/j.1460-9568.2007.05529.x PMID: 17561839

51. Aguado F, Majó G, Ruiz-Montasell B, Llorens J, Marsal J, Blasi J. Syntaxin 1A and 1B display distinct distribution patterns in the rat peripheral nervous system. Neuroscience. 1999; 88(2):437–46. PMID: 10197765

52. Sudhof TC. Neurotransmitter release: the last millisecond in the life of a synaptic vesicle. Neuron. 2013; 80(3):675–90. https://doi.org/10.1016/j.neuron.2013.10.022 PMID: 24183019

53. Molgo J, Lemeignan M, Thesleff S. Aminoglycosides and 3,4-diaminopyridine on neuromuscular block caused by botulinum type A toxin. Muscle Nerve. 1987; 10(5):464–70. https://doi.org/10.1002/mus.880100514 PMID: 3497343

54. Kofuji T, Fujiwara T, Sanada M, Mishima T, Akagawa K. HPC-1/syntaxin 1A and syntaxin 1B play distinct roles in neuronal survival. J Neurochem. 2014; 130(4):514–25. https://doi.org/10.1111/jnc.12722 PMID: 24666284

55. Wu YJ, Tejero R, Arancillo M, Vardar G, Korotkova T, Kintscher M, et al. Syntaxin 1B is important for mouse postnatal survival and proper synaptic function at the mouse neuromuscular junctions. J Neurophysiol. 2015; 114(4):2404–17. https://doi.org/10.1152/jn.00577.2015 PMID: 26203110

56. Montecucco C, Schiavo G, Pantano S. SNARE complexes and neuroexocytosis: how many, how close? Trends Biochem Sci. 2005; 30(7):367–72. https://doi.org/10.1016/j.tibs.2005.05.002 PMID: 15935678

57. Eleopra R, Tugnoli V, Rossetto O, Montecucco C, De Grandis D. Botulinum neurotoxin serotype C: a novel effective botulinum toxin therapy in human. Neurosci Lett. 1997; 224(2):91–4. PMID: 9086464

58. Eleopra R, Tugnoli V, Quatrale R, Gastaldo E, Rossetto O, De Grandis D, et al. Botulinum neurotoxin serotypes A and C do not affect motor units survival in humans: an electrophysiological study by motor units counting. Clin Neurophysiol. 2002; 113(8):1258–64. PMID: 12140005

59. de Paiva A, Meunier FA, Molgo J, Aoki KR, Dolly JO. Functional repair of motor endplates after botulinum neurotoxin type A poisoning: biphasic switch of synaptic activity between nerve sprouts and their parent terminals. Proc Natl Acad Sci U S A. 1999; 96(6):3200–5. PMID: 10077661

60. Karp BI. Botulinum toxin treatment of occupational and focal hand dystonia. Mov Disord. 2004; 19 Suppl 8:S116–9.

61. Dressler D, Saberi FA, Kollewe K, Schrader C. Safety aspects of incobotulinumtoxinA high-dose therapy. J Neural Transm (Vienna). 2015; 122(2):327–33.

62. Santamato A, Micello MF, Ranieri M, Valeno G, Albano A, Baricich A, et al. Employment of higher doses of botulinum toxin type A to reduce spasticity after stroke. J Neurol Sci. 2015; 350(1–2):1–6. https://doi.org/10.1016/j.jns.2015.01.033 PMID: 25684341

63. Eleopra R, Montecucco C, Devigili G, Lettieri C, Rinaldo S, Verriello L, et al. Botulinum neurotoxin serotype D is poorly effective in humans: an in vivo electrophysiological study. Clin Neurophysiol. 2013; 124 (5):999–1004. https://doi.org/10.1016/j.clinph.2012.11.004 PMID: 23245668

64. Masuyer G, Chaddock JA, Foster KA, Acharya KR. Engineered botulinum neurotoxins as new therapeutics. Annu Rev Pharmacol Toxicol. 2014; 54:27–51. https://doi.org/10.1146/annurev-pharmtox-011613-135935 PMID: 24016211

65. Sikorra S, Litschko C, Muller C, Thiel N, Galli T, Eichner T, et al. Identification and Characterization of Botulinum Neurotoxin A Substrate Binding Pockets and Their Re-Engineering for Human SNAP-23. J Mol Biol. 2016; 428(2 Pt A):372–84. https://doi.org/10.1016/j.jmb.2015.10.024 PMID: 26523682

66. Schiavo G, Montecucco C. Tetanus and botulism neurotoxins: isolation and assay. Methods Enzymol. 1995; 248:643–52. PMID: 7674951

67. Shone CC, Tranter HS. Growth of clostridia and preparation of their neurotoxins. Curr Top Microbiol Immunol. 1995; 195:143–60. PMID: 8542752

68. Schiavo G, Shone CC, Bennett MK, Scheller RH, Montecucco C. Botulinum neurotoxin type C cleaves a single Lys-Ala bond within the carboxyl-terminal region of syntaxins. J Biol Chem. 1995; 270 (18):10566–70. PMID: 7737992

69. Binz T, Bade S, Rummel A, Kollewe A, Alves J. Arg(362) and Tyr(365) of the botulinum neurotoxin type a light chain are involved in transition state stabilization. Biochemistry. 2002; 41(6):1717–23. PMID: 11827515

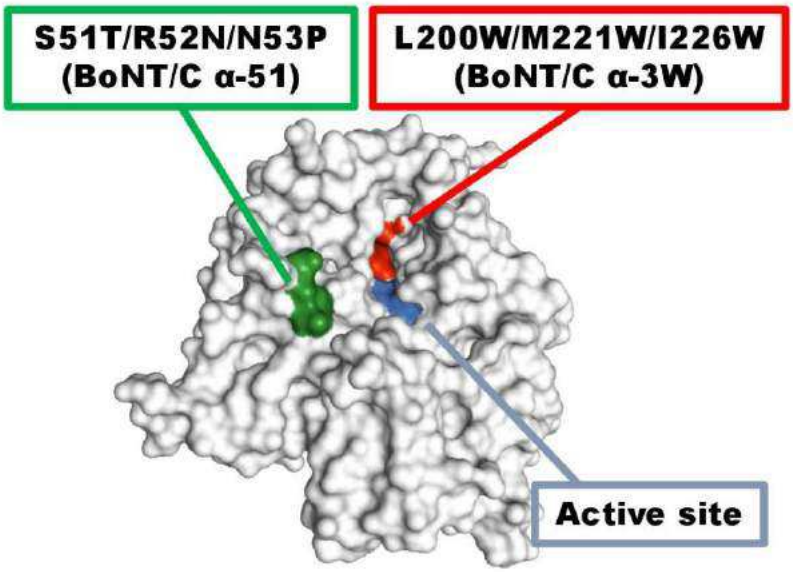

S1 Fig. Mutations conferring to BoNT/C specificity for syntaxins. Space-filling representation of BoNT/C light chain (PDB entry 2QN0) with highlighted triple mutations for syntaxin selectivity [32]: *S51T/R52N/N53P* (BoNT/C α-51) in green and *L200W/M221W/I226W* (BoNT/C α-3W) in red. Blue spot shows the metalloprotease active site.

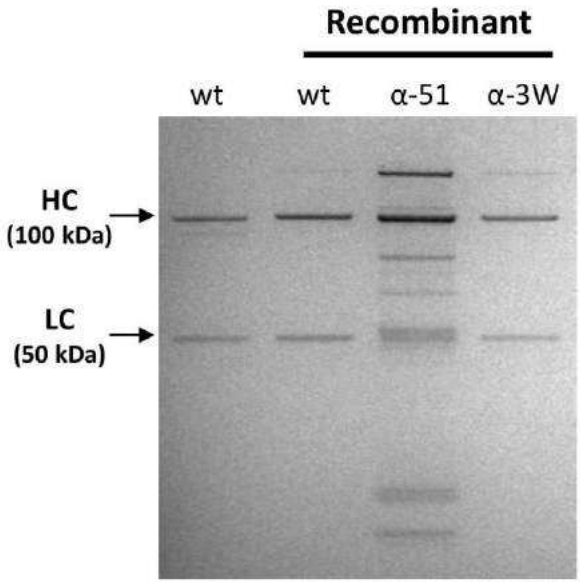

S2 Fig. SDS-PAGE analysis of the different BoNT/C toxins used in the study. From left to right, 250 nanograms of either native BoNT/C-wt, or recombinant BoNT/C-wt, BoNT/C α-51 or BoNT/C α-3W were loaded in a 12% gel under reducing conditions and revealed by Coomassie staining. The extent of hydrolytic activation of full-length BoNT/C by *E. coli* proteases was 81% (wild type), 73% (α-51), and 79% (α-3W). The lower purity of α-51 does not compromise its biological activity as deduced by the very similar EC_{50STX} of this toxin with respect to BoNT/C α-3W and BoNT/C-wt in cultured neurons.

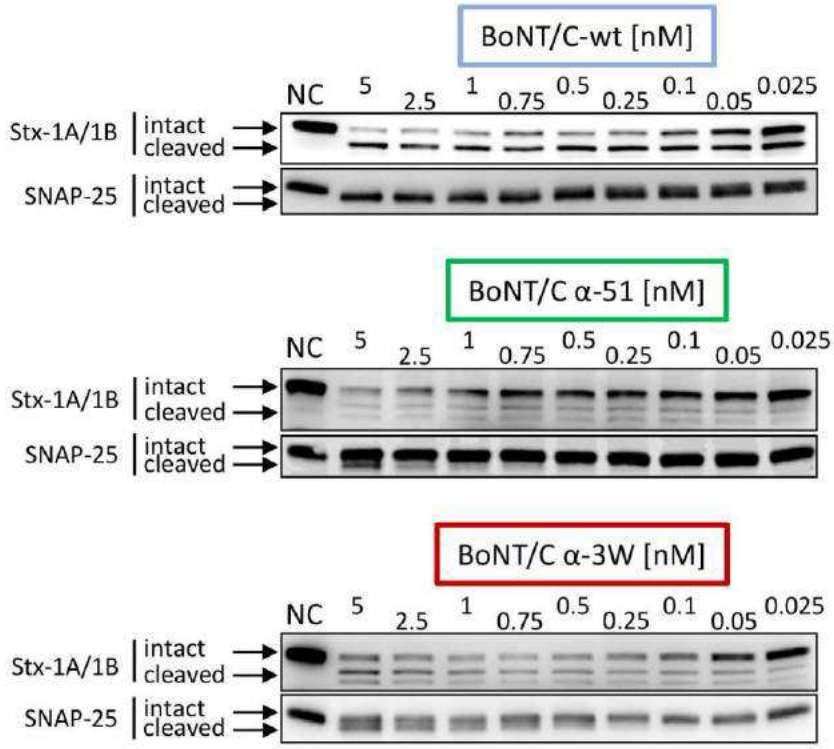

S3 Fig. The cleavage of SNAP-25 by BoNT/C mutants in CGNs does not increase prolonging the incubation time to 24 hours. CGNs were treated as in Figure 1 but incubation was prolonged to 24 hours. The cleavage of syntaxin-1A/1B and SNAP-25 was assayed by western blot using two antibodies recognizing both the intact and the cleaved forms of the proteins.

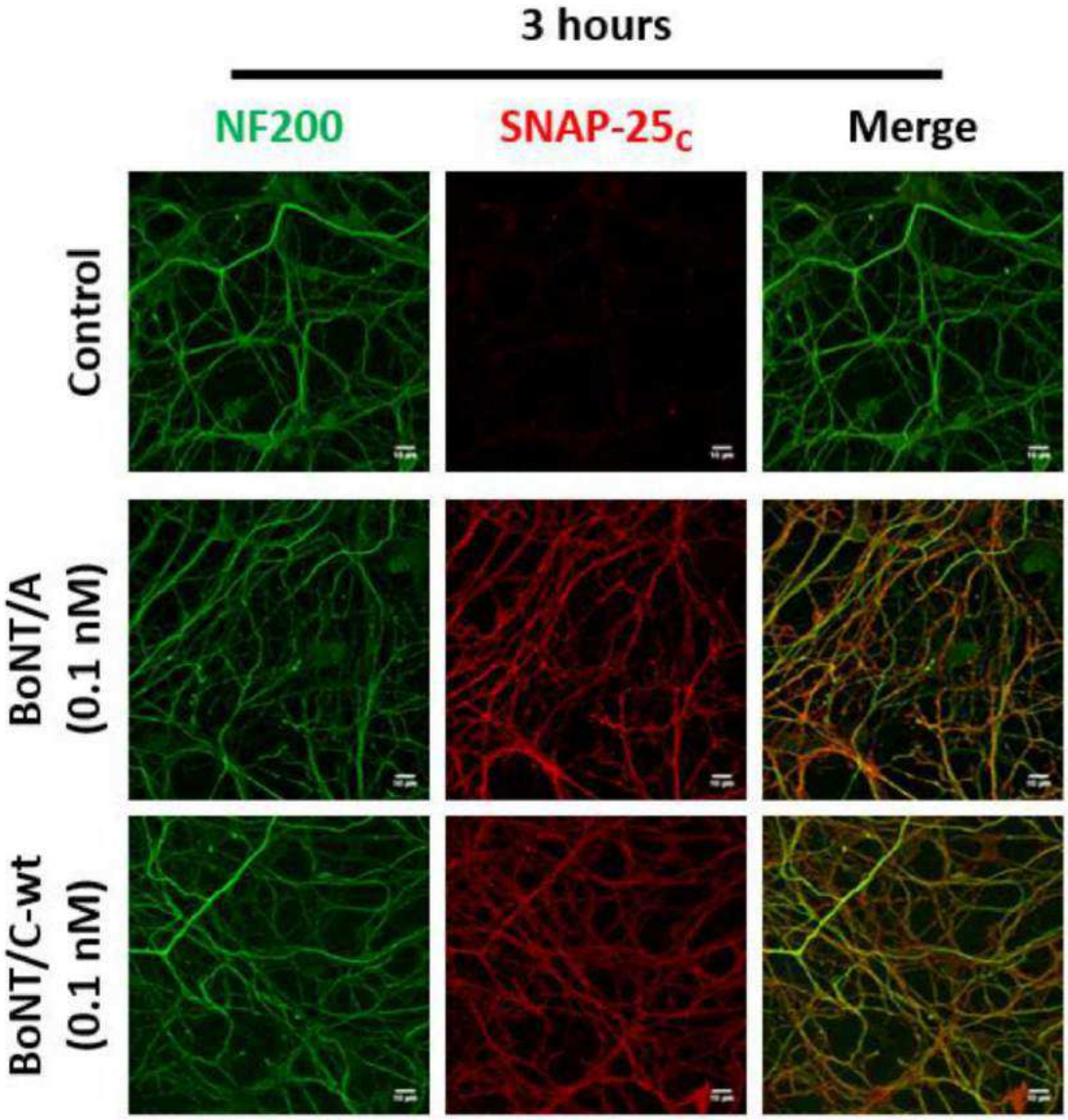

S4 Fig. SNAP-25 cleaved by BoNT/C is recognized by antibody raised against SNAP-25 cleaved by BoNT/A. CGNs were treated with BoNT/A (0.1 nM) or BoNT/C-wt (0.1 nM) in normal culture medium at 37 °C for 3 hours. Thereafter cells were fixed and stained with an antibody raised against SNAP-25 segment 185-197 (red) [37], corresponding to the C-terminus generated by BoNT/A cleavage (SNAP-25c). The antibody against neurofilament-200 (NF200, in green) is used as control staining. Scale bar, 10 µm.

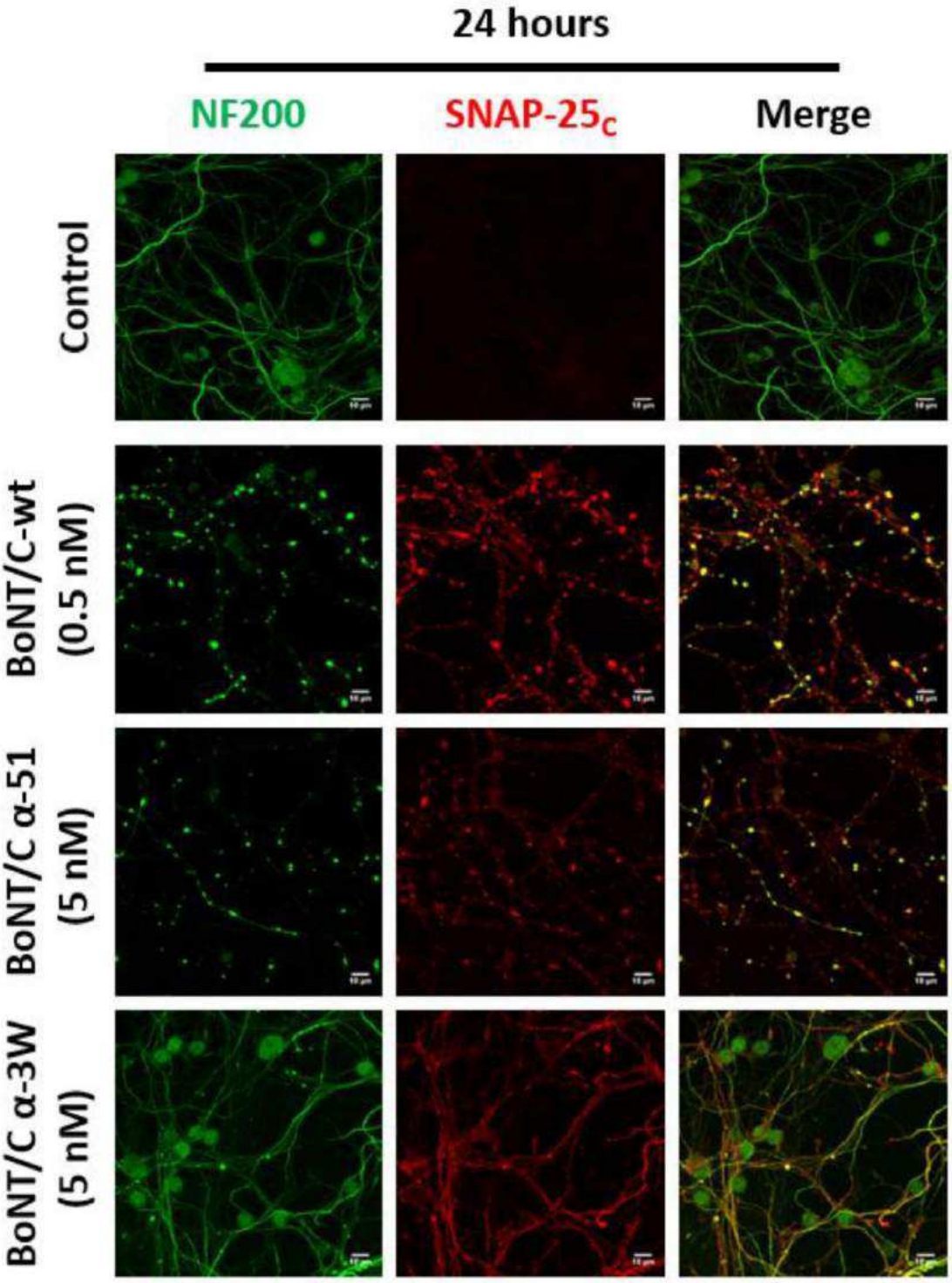

S5 Fig. BoNT/C mutants display a different cytotoxic effect on cultured neurons. CGNs were treated as in Figure 2 but incubation was prolonged to 24 hours. Neurons were then fixed and stained with an antibody against cleaved SNAP-25 (SNAP-25c, in red) and neurofilament-200 (NF200, in green). Cytotoxicity was evaluated following the appearance of varicosities along neurites and the loss of NF200 staining. Images are representative of at least three independent experiments. Scale bar, 10 μm.

Chapter 4

Discussion

During biological evolution, Clostridia have developed strategies aimed to survive and spread in the environment. They are anaerobic bacteria capable of sporulation to bypass nutrients scarcity and oxygen exposure. Under favorable environmental conditions they germinate and some Clostridia produce very potent neurotoxins. Despite the exact role of neurotoxins in Clostridia life cycle is not known, it is likely that they contribute in increasing the availability of a suitable anaerobic environment (cadaver and carcasses) which can support their further proliferation and dissemination[3,25].

BoNTs are efficient tools to achieve this purpose. Indeed, by blocking neurotransmission[11,135,137,138], which is essential physiological features for vertebrates' survival, they can kill hundreds of thousands individuals in a single outbreak[188,189].

Moreover, although the amount of toxin is not sufficient to cause death in the poisoned animal, even a small impairment in the functionality of the peripheral nervous system can significantly compromise animal viability in the wilderness (difficulty in eating, more susceptibility to predation and so on)[3].

BoNTs consist of two polypeptide chains (H and L) linked by a single disulphide bond[40] and have evolved to take advantage from essential features of nerve terminal physiology[50-52].

This suggests that BoNTs are the result of a co-evolution process with vertebrates[178]. In this respect, it is very meaningful that the seven antigenically different serotypes and the many subtypes, notwithstanding a significant variability in amino acid composition[3,16-18], intoxicate nerve terminals *via* a very sophisticated but conserved mechanism of action.

Despite botulism is essentially a disease of animals[190] with only very rare cases of human intoxication[158,190-192], the extreme potency and easy production on large scale, make BoNTs possible bioweapons[28,161]. To date, the only way to prevent intoxication is based on immunological approaches (toxin antisera)[25], but the existence of many different subtypes is a major safety problem: indeed, BoNT variants are neutralized to a different extent by existing serotype-specific antisera[16,18,25]. Moreover, this diversity questions the possibility of developing a vaccine covering all BoNTs[3]. This calls for implementing more studies aiming at the discovery of new inhibitors capable of blocking BoNTs regardless of their antigenic differences, hence useful even without knowing the particular variant involved in the intoxication[3].

The results presented in this PhD thesis are very relevant in this context. I found that by targeting a step of the intoxication mechanism shared by all BoNTs, it is possible to block their activity regardless of intertypic differences.

In this respect, the Trx-TrxR system represents an optimal pharmacological target as the activity of all BoNT serotypes and subtypes strictly depends from the reduction of the interchain disulphide bond, occurring after L translocation into the cytosol. The inhibition of this system is sufficient to completely abrogate BoNTs toxicity *in vitro* and, most important, to significantly reduce their lethality *in vivo* upon systemic injection. This last result is particularly relevant because it is obtained under conditions that recapitulate the human (and animal) botulism[3]. It is noteworthy that the scale of potency of the various inhibitors is closely similar for all BoNTs, indicating that these neurotoxins are similarly dependent on disulphide reduction.

Moreover, I found that another fundamental step in the intoxication mechanism of BoNTs is their trafficking into nerve terminals. I used EGA, a molecule which, although being characterized by unknown specific target, interferes with the

maturation of the endosomal pathway, thus inhibiting pathogens requiring a passage through an acidic environment[186].

Intriguingly, despite altering the neurotoxicity of all BoNTs tested, EGA provided a different degree of protection from BoNT/A, BoNT/B and BoNT/D, both *in vitro* and *in vivo*. This is an interesting finding because it revives the possibility that different serotypes may be trafficked through diverse routes inside nerve terminals, in keeping with their specific protein receptors. Of course, this aspect deserves further investigation as the study of the specific pathways undertaken by BoNTs may be linked to the discovery of unknown trafficking/endocytic pathways of organelles, SV in particular, inside nerve terminals[40].

Clearly, both the inhibitors of Trx-TrxR and EGA, are not effective if L has already translocated in the cytosol.

Nevertheless, it is known that in clinical botulism the neurotoxin remains in circulation for weeks after the initial symptoms[43,193,194], and these drugs may prevent further entry of BoNT L. This is even more relevant in infant botulism, where there is a continuous supply of BoNTs from the vegetative bacteria implanted into the intestine[3,24,26]. Accordingly, these drugs should be considered as preventive antidotes, similarly to antisera, but with the significant advantage of acting regardless of the toxin type responsible for poisoning. This is actually relevant as the diagnostic procedures necessary for toxin typization may require even days, whereas this strategies may be used immediately after diagnosis. Such a prompt treatment, by preventing the entry of circulating BoNTs[193], may contribute to significantly reduce the severity of the symptoms and shorten the period of hospitalization, associated with high costs of intensive care. This is also relevant to those cases of botulism caused by Clostridia able to produce more than one BoNT[195-198].

Importantly, by embarking on the study of BoNT inhibitors, I participated to the discovery that the Trx-TrxR system belongs to the protein inventory of SV. This result is very important as it shows for the first time that SVs bear a redox system on their cytosolic side. Intriguingly, Trx-TrxR is conspicuously enriched in the vesicles docked to the presynaptic membrane, suggesting that this redox system may play a physiological role in neuroexocytosis, possibly by regulating the redox

state of the many proteins present on SV[9,88]. In any case, from the point of view of BoNT mechanism of action, this result fits with the idea that BoNTs have evolved around essential feature of the host: SV are, in fact, the organelles exploited by the toxins[58,86,87] to enter nerve terminals and wherefrom the L chain is translocated in the cytosol. In such way, the L chain finds the redox system capable of reducing the interchain bond, thus enabling its protease activity immediately after its translocation.

As aforementioned, BoNTs are the most poisonous poison[139] but, at the same time, their neurospecificity and reversibility of action are critical features required for an ideal drug. Indeed BoNT/A1 and BoNT/B1 are largely used to treat a growing number of human diseases characterized by hyperfunctionality of cholinergic nerve terminals[141,167,168]. The clinical use is based on the intramuscular injection of a limited amount of toxin, exploiting the very limited diffusion which is particularly important when small muscles are treated[155,199].
Unfortunately, several case reports have shown how recurrent BoNT/A1 administration may trigger anti-BoNTs antibodies production, thus causing BoNT/A1 loss of efficacy. In addition, individuals have displayed unresponsiveness to BoNT/A1 even at the first injection[25,200].
To bypass this caveat, BoNT/B1 is largely used, being clinically effective as BoNT/A1 if used at appropriate doses. However, BoNT/B1 clinical use is characterized by painful injections, shorter efficacy and higher immunogenicity[201]. Moreover, frequent autonomic side effects have been reported[201]. These observations encouraged the use of a different BoNT[155,185]: recently, BoNT/C has been suggested as a novel effective botulinum neurotoxin serotype for the therapy of focal dystonia, with a general profile of action similar to that of BoNT/A[148,184].
Among the many botulinum neurotoxins, BoNT/C is unique because *in vitro* it is long known to cleave two substrates, SNAP-25 and syntaxins[25,133]. However, the single contribution of SNAP-25 cleavage and syntaxin cleavage in the mechanism of action of BoNT/C *in vivo* was not known. By comparing the activity of BoNT/C-wt and BoNT/C mutants reported to be selective for syntaxins [187], I found that

BoNT/C cleaves both substrates also *in vivo.* At the same time, I also found that the key determinant of the toxicity *in vivo* is the proteolysis of SNAP-25, while the cleavage of syntaxin accounts for a substantial impairment of neurotransmission efficiency without completely block neuron activity. This is actually a surprising result according to the centrality of the three SNARE proteins in regulated neuroexocytosis. A likely explanation is the compensation of syntaxin biochemical knock-down by other non-cleavable protein isoforms[25,202,203]. This situation is completely different for SNAP-25, whose action seems to be not vicariable by other isoforms, suggesting that this protein is a real master framework in neuron physiology.

Importantly, these results suggest that syntaxin-specific BoNT/C may be represent a suitable candidate for the development of engineered BoNTs endowed with very interesting features[148]. In fact, these toxins display a very low lethality in mice, suggesting that the range of concentrations usable for local injection in humans may be much wider than BoNT/A. In other words, these toxins may be featured by a dose-response with high safety margin. This possibility is reinforced by the finding that syntaxin-specific BoNTs provide a persistent modulation of nerve terminal activity without causing the complete blockage of the muscle. Accordingly, syntaxin-specific BoNTs would be very useful for applications requiring considerable amounts of BoNTs and where therapeutic efficiency is difficult to achieve without causing excessive muscle weakness[204,205].

In conclusion, these results highlight how minimal changes in the primary sequence (in this case three amino acids) can modify the biological activity of BoNTs[187,206], and how the relationship between primary structure and toxins pharmacological properties may represent a new avenue to engineer toxins endowed with specific features for tailor made applications.

Chapter 5

Extras

5.1 Other papers and reviews

During my PhD I participated also in the preparation of two reviews concerning mechanism of action of botulinum neurotoxins.

In the first one, we discussed about the development of pan-inhibitors and the necessity of expanding the efforts towards the discovery of new molecules that can block BoNTs regardless of their antigenic differences (see section 5.1.1).

In the second one, we proposed a novel model for BoNTs membrane translocation that consists of a concertized process instead of a sequential one, in which the H channel formation is a consequence of electrostatic attraction between BoNT molecule and lipid bilayers (see section 5.1.2).

Furthermore, I worked on other two side projects, whose common ground is the neurodegeneration, both toxin- and ageing-related. These collaborations resulted in the production of other two manuscripts (see section 5.1.3 and 5.1.4).

5.1.1 The thioredoxin reductase-thioredoxin redox system cleaves the interchain disulphide bond of botulinum neurotoxins on the cytosolic surface of synaptic vesicles

Marco Pirazzini[a], Domenico Azarnia Tehran[a], Giulia Zanetti[a], Florigio Lista[c], Thomas Binz[d], Clifford C. Shone[e], Ornella Rossetto[a], Cesare Montecucco[a,b]

[a]Dipartimento di Scienze Biomediche, Università di Padova, Via U. Bassi 58/B, 35121 Padova, Italy

[b]Istituto CNR di Neuroscienze, Università di Padova, Via U. Bassi 58/B, 35121 Padova, Italy

[c]Histology and Molecular Biology Section, Army Medical and Veterinary Research Center, Via Santo Stefano Rotondo 4, 00184 Rome, Italy

[d]Institut fur Biochemie, Medizinische Hochschule Hannover, 30623 Hannover, Germany

[e]Public Health England, Porton Down, Salisbury, Wiltshire, SP4 OJG, UK

Pirazzini M. *et al.* The thioredoxin reductase e Thioredoxin redox system cleaves the interchain disulphide bond of botulinum neurotoxins on the Cytosolic surface of synaptic vesicles. *Toxicon*. 107(Pt A):32-6.
doi: 10.1016/j.toxicon.2015.06.019 (2015).

Toxicon 107 (2015) 32–36

Contents lists available at ScienceDirect

Toxicon

journal homepage: www.elsevier.com/locate/toxicon

The thioredoxin reductase – Thioredoxin redox system cleaves the interchain disulphide bond of botulinum neurotoxins on the cytosolic surface of synaptic vesicles

Marco Pirazzini [a, *], Domenico Azarnia Tehran [a], Giulia Zanetti [a], Florigio Lista [c], Thomas Binz [d], Clifford C. Shone [e], Ornella Rossetto [a], Cesare Montecucco [a, b]

[a] Dipartimento di Scienze Biomediche, Università di Padova, Via U. Bassi 58/B, 35121 Padova, Italy
[b] Istituto CNR di Neuroscienze, Università di Padova, Via U. Bassi 58/B, 35121 Padova, Italy
[c] Histology and Molecular Biology Section, Army Medical and Veterinary Research Center, Via Santo Stefano Rotondo 4, 00184 Rome, Italy
[d] Institut fur Biochemie, Medizinische Hochschule Hannover, 30623 Hannover, Germany
[e] Public Health England, Porton Down, Salisbury, Wiltshire, SP4 OJG, UK

ARTICLE INFO

Article history:
Received 15 June 2015
Accepted 23 June 2015
Available online 27 June 2015

Keywords:
Thioredoxin reductase
Thioredoxin
Synaptic vesicles
Botulinum neurotoxins
Inhibitors

ABSTRACT

Botulinum neurotoxins (BoNTs) are Janus toxins, as they are at the same time the most deadly substances known and one of the safest drugs used in human therapy. They specifically block neurotransmission at peripheral nerves through the proteolysis of SNARE proteins, i.e. the essential proteins which are the core of the neuroexocytosis machinery. Even if BoNTs are traditionally known as seven main serotypes, their actual number is much higher as each serotype exists in many different subtypes, with individual biological properties and little antigenic relations. Since BoNTs can be used as biological weapons, and the only currently available therapy is based on immunological approaches, the existence of so many different subtypes is a major safety problem. Nevertheless, all BoNT isoforms are structurally similar and intoxicate peripheral nerve endings via a conserved mechanism. They consist of two chains linked by a unique disulphide bond which must be reduced to enable their toxicity. We found that thioredoxin 1 and its reductase compose the cell redox system responsible for this reduction, and its inhibition via specific chemicals significantly reduces BoNTs activity, *in vitro* as well as *in vivo*. Such molecules can be considered as lead compounds for the development of pan-inhibitors.

1. Introduction

Botulinum neurotoxins, together with Tetanus neurotoxin (TeNT), form the family of clostridial neurotoxins (CNTs). They are the most lethal bacterial toxins, so toxic that the lethal dose for humans is estimated to be around 1 ng per kg of body weight (Gill, 1982). Such potency can be ascribed to their specific inhibition of a fundamental physiologic event, that of neurotransmission. BoNTs specifically bind and intoxicate the neuromuscular junction, where they block neurotransmitter release, resulting in a progressive flaccid paralysis (Johnson and Montecucco, 2008; Rossetto et al., 2014). In contrast, TeNT binds to peripheral nerves, is retrogradely transported inside motor axons and taken up within inhibitory interneurons in the spinal cord. Here, it blocks neurotransmitter release with a molecular mechanism identical to BoNTs, but causing a spastic paralysis (Schiavo et al., 2000). Notably, CNTs do not cause the degeneration of poisoned nerve, and, if mechanical ventilation is timely performed, affected individuals survive and fully recover. Exploiting this feature, BoNTs have become extraordinary therapeutics for the treatment of many pathological conditions caused by the hyperactivity of cholinergic terminals, and one of the safest and most versatile drug available on the market (Hallett et al., 2013; Naumann et al., 2013; Rossetto et al., 2001). In addition, thanks to the comprehension of their mechanism of action, CNTs have become useful and sophisticated tools for the study of neuronal physiology (Pantano and Montecucco, 2013).

CNTs are produced by different species of the genus Clostridium (Rossetto et al., 2014). There is one single tetanus neurotoxin but many different botulinum neurotoxins. They have been

* Corresponding author.
E-mail address: marcopiraz@gmail.com (M. Pirazzini).

http://dx.doi.org/10.1016/j.toxicon.2015.06.019
0041-0101/

traditionally classified as seven main distinct toxins (BoNT/A-G), distinguished on the basis of their immunological properties (serotypes). Recently, the development of next generation sequencing has permitted the analysis of clinical cases of botulism accumulated over time. As a result, it has become rapidly clear that neurotoxigenic Clostridia have considerable genetic heterogeneity in terms of genome organization, toxin gene clusters, and most importantly, toxin sequences variability (Hill and Smith, 2013). Accordingly, the number of BoNT subtypes has dramatically grown, reaching more than forty molecules in a few years, and this number is continuously increasing (Montecucco and Rasotto, 2015). They have been categorized as subserotypes, i.e. toxins immunogenically related to the parental serotypes but with an aminoacidic composition difference higher than 2.6% (indicated as BoNT/A1, BoNT/A2, etc.) (Hill and Smith, 2013; Rossetto et al., 2014; Smith et al., 2007). At variance, some others are composed by the recombination of different serotypes: accordingly, they have been classified as mosaic toxins and indicated as BoNT/CD and/DC (Moriishi et al., 1996a, 1996b). Recently, a toxin isolated from a case of infant botulism was proposed to be a new serotype, but later analysis showed it to be a chimera of A1 and F5 (Kalb et al., 2015). Remarkably, this finding raised the issue of serotype definition, but, most importantly, this concretely embodies the limitation of using antisera for the treatment of botulism, and questions the possibility of developing a universal vaccine covering all the BoNTs. This is even more relevant as BoNTs can be employed as bioweapons (Centers for Disease Control and Prevention, 2012). This calls for implementing more studies aiming at the discovery of new inhibitors capable of blocking BoNTs regardless of their antigenic differences.

2. BoNTs mechanism of action as target for new inhibitors

The available crystallographic structures of BoNTs (Kumaran et al., 2009; Lacy et al., 1998; Swaminathan and Eswaramoorthy, 2000) show they share an overall highly conserved molecular architecture, which is functional to their mechanism of action. The structure, which is similar for TeNT too, is constituted by two main chains: L, 50 kDa and H, 100 kDa, held together by a single interchain disulphide bond and non-covalent interactions. The C-terminal part of H (HC) mediates the neurospecific binding and the internalization of the toxin into peripheral nerve terminals via a double receptor mechanism (Montecucco, 1986; Rummel, 2013). Firstly, BoNTs accumulate on the plasma membrane via the recognition of polysialogangliosides, molecules highly enriched in the neuronal plasma membrane (Binz and Rummel, 2009). Thereafter, BoNTs enter the nerve as a result of the interaction with the luminal domain of a synaptic vesicle protein, which may differ for the different BoNTs (Benoit et al., 2014; Dong et al., 2008, 2003, 2007, 2006; Mahrhold et al., 2006; Nishiki et al., 1994; Peng et al., 2012; Rummel et al., 2004). At variance, nidogen 1 and 2, two extracellular matrix proteins, have been suggested to be the peripheral receptor of TeNT (Bercsenyi et al., 2014), mediating its entry into vesicles undergoing retrograde axonal transport up to the spinal cord (Deinhardt et al., 2006). TeNT is then delivered to inhibitory interneurons where is internalized inside SV (Matteoli et al., 1996), as BoNTs do. Here, the HN domain of TeNT and BoNTs assist the membrane translocation of the L chain in a process driven by the luminal acidification (Fischer and Montal, 2007b; Montal, 2010). The L chain is a Zn^{2+} dependent metalloprotease that targets specifically the three SNARE proteins: BoNT/B,/D,/F,/G and TeNT cleave VAMP1/2 at different positions (Schiavo et al., 1992, 1993a, 1993c), BoNT/A and/E cleave two different peptide bonds away from the C-terminus of SNAP25 (Blasi et al., 1993; Schiavo et al., 1993b), BoNT/C is unique as it cleaves both SNAP25 and Syntaxin1A-1B (Pantano and Montecucco, 2013). SNAREs form a heterotrimeric complex (Sutton et al., 1998) that constitutes the core of the neuroexocytosis nanomachine and their proteolysis impairs its assembly and/or function (Pantano and Montecucco, 2013).

Remarkably, each molecule may exert the same toxic mechanism with its own specific features, i.e. different binding partners, different trafficking, different substrates and exclusive enzyme–substrate interactions. At the same time, it is even more surprising that despite of a great variability within their primary structure, CNTs have evolved to have a high similar mechanism to exploit nerve terminals: this offers the possibility to rationally design new molecules capable of inhibiting BoNTs, independently from their antigenic properties.

3. The interchain disulphide bond reduction as a rational target

Besides the structural role, the interchain disulphide bond plays a fundamental role in BoNTs toxicity. The first evidence was provided by the lack of toxicity *in vivo* of a previously reduced tetanus neurotoxin (Schiavo et al., 1990). Later, an elegant study of BoNT dynamics at single molecule resolution (Fisher and Montal, 2006) demonstrated that an intact disulphide linkage is an essential prerequisite for productive translocation across the channel arranged by HN, and that reduction occurs on the cytosolic side (Fischer and Montal, 2007a). Accordingly, it was later proposed that the positioning, the size and the high hydrophobicity of the two sulfur atoms, together with a group of conserved acidic and protonable aminoacids within the same surface of a BoNT molecule, are pivotal in initiating the translocation event (Pirazzini et al., 2011; Rossetto et al., 2014). Although the role of the disulfide bond during translocation is known in molecular details only for BoNT/A, none of the different serotypes display the protease activity unless the interchain disulphide is reduced (Schiavo et al., 1993b). Accordingly, the aforementioned mechanism for BoNT/A can be safely extended to all other toxin isoforms, leading to the more general deduction that the reduction of the interchain disulphide bond within nerve terminal cytosol is a "*conditio sine qua non*" to free the metalloprotease activity of botulinum neurotoxins, and therefore represents a rationale for the development of mechanism-based antitoxins.

4. Thioredoxin–thioredoxin reductase inhibitors as a new class of antitoxins

Cells possess many different redox systems and their presence within key compartments (nucleus, mitochondria, endoplasmic reticulum and cytosol) explains their cardinal role in managing redox reactions (Arner and Holmgren, 2000; Hanschmann et al., 2013; Holmgren, 1985; Powis and Kirkpatrick, 2007). Notably, the understanding of redox biochemistry has rapidly and radically evolved over the last few years. The initial picture of an overall redox balance that must be simply maintained to avoid pathological conditions, has turned into a complex network of specific, compartmentalized and reversible redox reactions regulating the activity of key proteins involved in many intracellular, as well as extracellular, physiologic events (Hanschmann et al., 2013). The reducing system responsible for the disulphide reduction of BoNTs was shown to act on the cytosolic side (Fischer and Montal, 2007a). The thioredoxin 1-thioredoxin reductase 1 (TrxR-Trx) and the glutathione–glutathione reductase systems are important redox systems in the cytosol and those involved in controlling protein disulphides. They act via the so called "dithiol mechanism" through which an electron flow is shuttled from NADPH to thioredoxin or

glutathione by means of their respective reductases, and finally consumed to reduce target disulfide bonds (Hanschmann et al., 2013). Notably, in the test tube, reconstituted TrxR-Trx was shown, in the presence of NADPH, to specifically reduce the interchain disulphide bond of tetanus neurotoxin and BoNT/A (Kistner and Habermann, 1992; Schiavo et al., 1990). Furthermore, TrxR-Trx is synthetized and transported along axons in peripheral neurons (Stemme et al., 1985) and is enriched in secretory cells (Rozell et al., 1985).

The first evidence that TrxR-Trx is involved *in vivo* in the reduction of the interchain disulfide bond of TeNT and BoNTs, was the finding that Auranofin, the most potent TrxR inhibitor identified so far (Omata et al., 2006), also prevented the toxicity of tetanus neurotoxin and botulinum neurotoxins B, C, D in cultured cerebellar granular neurons, in a concentration dependent manner (Pirazzini et al., 2013). On the other hand, buthionine sulfoximine, a compound capable to substantially reduce GSH intracellular levels (Griffith and Meister, 1979), had no inhibitory activity, indicating that the glutathione-glutaredoxin system is not involved in the entry of CNTs in the cytoplasm.

Alterations of the TrxR-Trx system in different tissues and organs are associated with many pathological conditions, including cancer. As a consequence, the identification of molecules capable of inhibiting thioredoxin and/or its reductase has become a primary goal in the field of redox biology (Cai et al., 2012; Mahmood et al., 2013; Mukherjee and Martin, 2008; Powis and Kirkpatrick, 2007). Accordingly, many molecules have become available, and some of them have already reached the evaluation stage for clinical use (Baker et al., 2013; Ramanathan et al., 2011; Yamaguchi et al., 1998) or are already on the market (Madeira et al., 2012). These compounds can be very different from a chemical point of view, but in general they are electrophiles targeting the active site of TrxR or are substrates that maintain Trx in the oxidized, unreactive form (Zhao et al., 2002). Using, some of these drugs, we found that all the molecules tested disrupted the toxicity of BoNT/A, C and E in neuronal cultures (Pirazzini et al., 2014). These compounds are shown in Fig. 1. Interestingly, each inhibitor blocked the different BoNTs tested within a very similar concentration range, suggesting

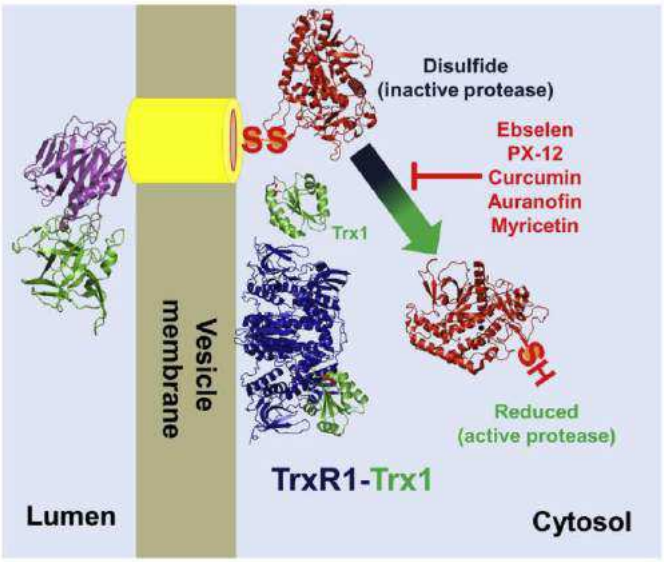

Fig. 1. Thioredoxin1-Thioredoxin Reductase 1 are extrinsic proteins of synaptic vesicles and enable BoNT proteolytic activity. TrxR-Trx system is bound on the cytosolic surface of SV and reduces the interchain disulphide bond of BoNTs after the delivery of L chain in the cytosol, thereby enabling its release from the membrane and the display of its metalloprotease activity.

that the molecular environment where reduction takes place and the relevance of the interchain disulfide reduction is closely similar for different BoNTs serotypes. These *in vitro* results were validated *in vivo* using the digit abduction score (DAS) assay, a well-established model to compare potency and duration of BoNTs (Aoki, 2001; Broide et al., 2013). All tested molecules were very effective in reducing the degree and duration of paralysis induced by the local injection of BoNT/A and BoNT/C. For the first time, it was shown that small molecules effectively prevent the paralytic activity of BoNTs. As a proof of concept, we also tested one of these inhibitors, Ebselen, a compound reported to target both TrxR and Trx (Zhao et al., 2002), in the lethality assay. Ebselen, preventively administered via intraperitoneal injection, was very effective in protecting animals from a lethal amount of BoNT/A, both as prolongation of the time to death and as reduction of the number of deaths (Pirazzini et al., 2014).

We also investigated the presence of the TrxR-Trx system within neuronal cultures and in nerve-muscle preparations and we found that both thioredoxin and its reductase are highly expressed within nerve terminals of cultured neurons as well as at the level of the neuromuscular junction. The latter result is particularly important because it demonstrates that TrxR-Trx is present at the site of action of BoNTs. In addition, using a well-established protocol for the purification of synaptic vesicles from rat cortices (De Camilli et al., 1983), we demonstrated that the TrxR-Trx system is bound to the cytosolic side of the SV membrane (Pirazzini et al., 2014), the organelle exploited by BoNTs to enter nerve terminals and where probably translocation takes place (Colasante et al., 2013; Harper et al., 2011). Notably, both proteins are enriched in the so called "docked vesicles" fraction, i.e. a portion of SV which are co-purified together with the presynaptic membrane (Morciano et al., 2009, 2005). This finding further suggests a possible active role of TrxR-Trx system in synaptic vesicles dynamics.

5. Conclusions

So far, the easier explanation for the existence of BoNTs (and TeNT) within Clostridia genomes is related to their strategic function in increasing the availability of a suitable anaerobic environment necessary to their growth and dissemination. BoNTs are indeed the most potent poisons found in nature and because of them a single and isolated outbreak of animal botulism can rapidly assume epidemic proportions, causing up to hundreds of thousands deaths (Friend, 1988). Such potency derives from the ability of these toxins to be efficiently delivered from one animal to the other (Rossetto et al., 2014) and to specifically target the neuromuscular junction, a compartment essential for the survival of BoNT principal hosts, the vertebrates. It is however remarkable that, beside such genetic and proteomic heterogeneity, their molecular architecture is very similar. As a consequence, the structure–activity relationship of BoNTs could be considered as the result of co-evolution to maximize their performance in intoxicating peripheral neurons. Each region of the toxin has in fact been shaped in order to exploit fundamental features and/or events of neuron physiology. Therefore, given the paramount importance of the redox status of the interchain disulphide bond before, during and after translocation, the finding that the TrxR-Trx system resides on SV membrane and mediates the detachment of the catalytic L chain by reducing the disulphide on the cytosolic side, could be seen again as an evolutionary choice exploited by BoNTs and TeNT to reach their final goal. This has been further proved recently, by using a non-toxic TeNT derivative as a reporter (Zuverink et al., 2015). Moreover, it must be remembered that, besides its redox activity, Trx has the fold of ancient chaperones (Arner and Holmgren, 2000; Berndt et al., 2008; Dekker et al., 2011; Ingles-Prieto et al., 2013), and

that the L chain has to unfold, at least partially, in order to cross the membrane (Cai et al., 2006; Kukreja and Singh, 2005; Montal, 2010; Montecucco et al., 1989). It is thus likely that Trx may also help the refolding of the L chain to reacquire a suitable conformation for SNARE cleavage. In light of this, we thus propose the reduction of the interchain disulphide bond as a new fundamental event of BoNTs and TeNT intoxication process (Fig. 1), accordingly recapitulated into 5 main steps: i) binding to polysialogangliosides for toxin accumulation on the target neurons, ii) interaction with the luminal domain of an SV protein for its internalization, iii) acidification of this "Trojan horse" to deliver the catalytically active part across the SV membrane, iv) reduction of the interchain disulphide bond by TrxR-Trx to complete the translocation and release the L chain on the cytosolic side, v) L chain-mediated cleavage of SNARE proteins and disruption of SV ability to fuse with the presynaptic plasma membrane.

Our results have important implications regarding the possible application of TrxR-Trx inhibitors as therapeutic agents to treat botulism. The most important point is that these inhibitors are active regardless of the subserotype causing intoxication. Such a pharmacological approach may be seen not as an alternative with respect to the use of antisera, rather as a synergistic treatment. Since these inhibitors are small molecules, they can affect toxin molecules which have already been taken up by the neurons, but cannot be blocked any longer by antibodies. Clearly, the toxicity of L chains that have already reached the neuronal cytosol cannot be blocked. However, it was shown that in clinical botulism, BoNTs can remain in the blood circulation and/or in interstitial fluids for many days (Fagan et al., 2009; Sheth et al., 2008; Simpson, 2013). Henceforth, the severity of BoNT intoxication may be substantially mitigated by blocking BoNT molecules that have not yet entered nerve terminals using these inhibitors.

Interestingly, most of the inhibitors used in our study are natural compounds, already sold as antioxidant agents and with an established safety profile. Other compounds are instead under clinical trials. Furthermore, the considerable interest around TrxR-Trx system has provided a rich source of compounds (Cai et al., 2012), which should be considered and investigated for this new field of application.

Acknowledgment

We thank Dr. M. Rigoni for comments and A. Geffner-Smith for careful editing of the manuscript. This work was supported by the Italian Ministry of Defence (Progetto PNRM – NIB, Segretariato Generale della Difesa V Reparto), Fondazione CARIPARO "Synaptic Functions and Role of Glial Cells in Brain and Muscle Diseases" (to C.M.), and a grant from the Ministero dell'Universita' e della Ricerca (Progetto PRIN) to O.R.

Transparency document

Transparency document related to this article can be found online at http://dx.doi.org/10.1016/j.toxicon.2015.06.019.

References

Aoki, K.R., 2001. A comparison of the safety margins of botulinum neurotoxin serotypes A, B, and F in mice. Toxicon 39, 1815–1820.
Arner, E.S., Holmgren, A., 2000. Physiological functions of thioredoxin and thioredoxin reductase. Eur. J. Biochem. 267, 6102–6109.
Baker, A.F., Adab, K.N., Raghunand, N., Chow, H.H.S., Stratton, S.P., Squire, S.W., Boice, M., Pestano, L.A., Kirkpatrick, D.L., Dragovich, T., 2013. A phase IB trial of 24-hour intravenous PX-12, a thioredoxin-1 inhibitor, in patients with advanced gastrointestinal cancers. Invest New. Drugs 31, 631–641.
Benoit, R.M., Frey, D., Hilbert, M., Kevenaar, J.T., Wieser, M.M., Stirnimann, C.U., McMillan, D., Ceska, T., Lebon, F., Jaussi, R., Steinmetz, M.O., Schertler, G.F.X., Hoogenraad, C.C., Capitani, G., Kammerer, R.A., 2014. Structural basis for recognition of synaptic vesicle protein 2C by botulinum neurotoxin A. Nature 505, 108–111.
Bercsenyi, K., Schmieg, N., Bryson, J.B., Wallace, M., Caccin, P., Golding, M., Zanotti, G., Greensmith, L., Nischt, R., Schiavo, G., 2014. Nidogens are therapeutic targets for the prevention of tetanus. Science 346, 1118–1123.
Berndt, C., Lillig, C.H., Holmgren, A., 2008. Thioredoxins and glutaredoxins as facilitators of protein folding. Biochim. Biophys. Acta 1783, 641–650.
Binz, T., Rummel, A., 2009. Cell entry strategy of clostridial neurotoxins. J. Neurochem. 109, 1584–1595.
Blasi, J., Chapman, E.R., Link, E., Binz, T., Yamasaki, S., Camilli, P.D., Sudhof, T.C., Niemann, H., Jahn, R., 1993. Botulinum neurotoxin A selectively cleaves the synaptic protein SNAP-25. Nature 365, 160–163.
Broide, R.S., Rubino, J., Nicholson, G.S., Ardila, M.C., Brown, M.S., Aoki, K.R., Francis, J., 2013. The rat Digit Abduction Score (DAS) assay: a physiological model for assessing botulinum neurotoxin-induced skeletal muscle paralysis. Toxicon 71, 18–24.
Cai, S., Kukreja, R., Shoesmith, S., Chang, T.W., Singh, B.R., 2006. Botulinum neurotoxin light chain refolds at endosomal pH for its translocation. Protein J. 25, 455–462.
Cai, W., Zhang, L., Song, Y., Wang, B., Zhang, B., Cui, X., Hu, G., Liu, Y., Wu, J., Fang, J., 2012. Small molecule inhibitors of mammalian thioredoxin reductase. Free Radic. Biol. Med. 52, 257–265.
Centers for Disease Control and Prevention, D.o.H.a.H.S., 2012. Possession, use, and transfer of select agents and toxins; biennial review. Final rule. Fed. Regist. 77, 61083–61115.
Colasante, C., Rossetto, O., Morbiato, L., Pirazzini, M., Molgo, J., Montecucco, C., 2013. Botulinum neurotoxin type A is internalized and translocated from small synaptic vesicles at the neuromuscular junction. Mol. Neurobiol. 48, 120–127.
De Camilli, P., Harris, S.M., Huttner, W.B., Greengard, P., 1983. Synapsin I (Protein I), a nerve terminal-specific phosphoprotein. II. Its specific association with synaptic vesicles demonstrated by immunocytochemistry in agarose-embedded synaptosomes. J. Cell Biol. 96, 1355–1373.
Deinhardt, K., Berninghausen, O., Willison, H.J., Hopkins, C.R., Schiavo, G., 2006. Tetanus toxin is internalized by a sequential clathrin-dependent mechanism initiated within lipid microdomains and independent of epsin1. J. Cell Biol. 174, 459–471.
Dekker, C., Willison, K.R., Taylor, W.R., 2011. On the evolutionary origin of the chaperonins. Proteins 79, 1172–1192.
Dong, M., Liu, H., Tepp, W.H., Johnson, E.A., Janz, R., Chapman, E.R., 2008. Glycosylated SV2A and SV2B mediate the entry of botulinum neurotoxin E into neurons. Mol. Biol. Cell 19, 5226–5237.
Dong, M., Richards, D.A., Goodnough, M.C., Tepp, W.H., Johnson, E.A., Chapman, E.R., 2003. Synaptotagmins I and II mediate entry of botulinum neurotoxin B into cells. J. Cell Biol. 162, 1293–1303.
Dong, M., Tepp, W.H., Liu, H., Johnson, E.A., Chapman, E.R., 2007. Mechanism of botulinum neurotoxin B and G entry into hippocampal neurons. J. Cell Biol. 179, 1511–1522.
Dong, M., Yeh, F., Tepp, W.H., Dean, C., Johnson, E.A., Janz, R., Chapman, E.R., 2006. SV2 is the protein receptor for botulinum neurotoxin A. Science 312, 592–596.
Fagan, R.P., McLaughlin, J.B., Middaugh, J.P., 2009. Persistence of botulinum toxin in patients' serum: Alaska, 1959–2007. J. Infect. Dis. 199, 1029–1031.
Fischer, A., Montal, M., 2007a. Crucial role of the disulfide bridge between botulinum neurotoxin light and heavy chains in protease translocation across membranes. J. Biol. Chem. 282, 29604–29611.
Fischer, A., Montal, M., 2007b. Single molecule detection of intermediates during botulinum neurotoxin translocation across membranes. Proc. Natl. Acad. Sci. USA 104, 10447–10452.
Fisher, A., Montal, M., 2006. Characterization of *Clostridial botulinum* neurotoxin channels in neuroblastoma cells. Neurotox. Res. 9, 93–100.
Friend, M., 1988. Avian Botulism: an International Perspective. Fort Collins, CO, pp. 290.
Gill, D.M., 1982. Bacterial toxins: a table of lethal amounts. Microbiol. Rev. 46, 86–94.
Griffith, O.W., Meister, A., 1979. Potent and specific inhibition of glutathione synthesis by buthionine sulfoximine (S-n-butyl homocysteine sulfoximine). J. Biol. Chem. 254, 7558–7560.
Hallett, M., Albanese, A., Dressler, D., Segal, K.R., Simpson, D.M., Truong, D., Jankovic, J., 2013. Evidence-based review and assessment of botulinum neurotoxin for the treatment of movement disorders. Toxicon 67, 94–114.
Hanschmann, E.M., Godoy, J.R., Berndt, C., Hudemann, C., Lillig, C.H., 2013. Thioredoxins, glutaredoxins, and peroxiredoxins-molecular mechanisms and health significance: from cofactors to antioxidants to redox signaling. Antioxid. Redox Signal 19, 1539–1605.
Harper, C.B., Martin, S., Nguyen, T.H., Daniels, S.J., Lavidis, N.A., Popoff, M.R., Hadzic, G., Mariana, A., Chau, N., McCluskey, A., Robinson, P.J., Meunier, F.A., 2011. Dynamin inhibition blocks botulinum neurotoxin type A endocytosis in neurons and delays botulism. J. Biol. Chem. 286, 35966–35976.
Hill, K.K., Smith, T.J., 2013. Genetic diversity within Clostridium botulinum serotypes, botulinum neurotoxin gene clusters and toxin subtypes. Curr. Top. Microbiol. Immunol. 364, 1–20.
Holmgren, A., 1985. Thioredoxin. Annu Rev. Biochem. 54, 237–271.
Ingles-Prieto, A., Ibarra-Molero, B., Delgado-Delgado, A., Perez-Jimenez, R., Fernandez, J.M., Gaucher, E.A., Sanchez-Ruiz, J.M., Gavira, J.A., 2013. Conservation of protein structure over four billion years. Structure 21, 1690–1697.

Johnson, E.A., Montecucco, C., 2008. Botulism. Handb. Clin. Neurol. 91, 333–368.
Kalb, S.R., Baudys, J., Raphael, B.H., Dykes, J.K., Lúquez, C., Maslanka, S.E., Barr, J.R., 2015. Functional characterization of botulinum neurotoxin serotype H as a hybrid of known serotypes F and A (BoNT F/A). Anal. Chem 87, 3911–3917.
Kistner, A., Habermann, E., 1992. Reductive cleavage of tetanus toxin and botulinum neurotoxin A by the thioredoxin system from brain. Evidence for two redox isomers of tetanus toxin. Naunyn Schmiedeb. Arch. Pharmacol. 345, 227–234.
Kukreja, R., Singh, B., 2005. Biologically active novel conformational state of botulinum, the most poisonous poison. J. Biol. Chem. 280, 39346–39352.
Kumaran, D., Eswaramoorthy, S., Furey, W., Navaza, J., Sax, M., Swaminathan, S., 2009. Domain organization in *Clostridium botulinum* neurotoxin type E is unique: its implication in faster translocation. J. Mol. Biol. 386, 233–245.
Lacy, D.B., Tepp, W., Cohen, A.C., DasGupta, B.R., Stevens, R.C., 1998. Crystal structure of botulinum neurotoxin type A and implications for toxicity. Nat. Struct. Biol. 5, 898–902.
Madeira, J.M., Gibson, D.L., Kean, W.F., Klegeris, A., 2012. The biological activity of auranofin: implications for novel treatment of diseases. Inflammopharmacology 20, 297–306.
Mahmood, D.F., Abderrazak, A., El Hadri, K., Simmet, T., Rouis, M., 2013. The thioredoxin system as a therapeutic target in human health and disease. Antioxid. Redox Signal 19, 1266–1303.
Mahrhold, S., Rummel, A., Bigalke, H., Davletov, B., Binz, T., 2006. The synaptic vesicle protein 2C mediates the uptake of botulinum neurotoxin A into phrenic nerves. FEBS Lett. 580, 2011–2014.
Matteoli, M., Verderio, C., Rossetto, O., Iezzi, N., Coco, S., Schiavo, G., Montecucco, C., 1996. Synaptic vesicle endocytosis mediates the entry of tetanus neurotoxin into hippocampal neurons. Proc. Natl. Acad. Sci. USA 93, 13310–13315.
Montal, M., 2010. Botulinum neurotoxin: a marvel of protein design. Annu Rev. Biochem. 79, 591–617.
Montecucco, C., 1986. How do tetanus and botulinum toxins bind to neuronal membranes? Trends Biochem. Sci. 11, 314–317.
Montecucco, C., Rasotto, M.B., 2015. On botulinum neurotoxin variability. MBio 6.
Montecucco, C., Schiavo, G., Dasgupta, B.R., 1989. Effect of pH on the interaction of botulinum neurotoxins A, B and E with liposomes. Biochem. J. 259, 47–53.
Morciano, M., Beckhaus, T., Karas, M., Zimmermann, H., Volknandt, W., 2009. The proteome of the presynaptic active zone: from docked synaptic vesicles to adhesion molecules and maxi-channels. J. Neurochem. 108, 662–675.
Morciano, M., Burré, J., Corvey, C., Karas, M., Zimmermann, H., Volknandt, W., 2005. Immunoisolation of two synaptic vesicle pools from synaptosomes: a proteomics analysis. J. Neurochem. 95, 1732–1745.
Moriishi, K., Koura, M., Abe, N., Fujii, N., Fujinaga, Y., Inoue, K., Ogumad, K., 1996a. Mosaic structures of neurotoxins produced from *Clostridium botulinum* types C and D organisms. Biochim. Biophys. Acta 1307, 123–126.
Moriishi, K., Koura, M., Fujii, N., Fujinaga, Y., Inoue, K., Syuto, B., Oguma, K., 1996b. Molecular cloning of the gene encoding the mosaic neurotoxin, composed of parts of botulinum neurotoxin types C1 and D, and PCR detection of this gene from *Clostridium botulinum* type C organisms. Appl. Environ. Microbiol. 62, 662–667.
Mukherjee, A., Martin, S.G., 2008. The thioredoxin system: a key target in tumour and endothelial cells. Br. J. Radiol. 81, 57–68.
Naumann, M., Dressler, D., Hallett, M., Jankovic, J., Schiavo, G., Segal, K.R., Truong, D., 2013. Evidence-based review and assessment of botulinum neurotoxin for the treatment of secretory disorders. Toxicon 67, 141–152.
Nishiki, T., Kamata, Y., Nemoto, Y., Omori, A., Ito, T., Takahashi, M., Kozaki, S., 1994. Identification of protein receptor for *Clostridium botulinum* type B neurotoxin in rat brain synaptosomes. J. Biol. Chem. 269, 10498–10503.
Omata, Y., Folan, M., Shaw, M., Messer, R.L., Lockwood, P.E., Hobbs, D., Bouillaguet, S., Sano, H., Lewis, J.B., Wataha, J.C., 2006. Sublethal concentrations of diverse gold compounds inhibit mammalian cytosolic thioredoxin reductase (TrxR1). Toxicol. In Vitro 20, 882–890.
Pantano, S., Montecucco, C., 2013. The blockade of the neurotransmitter release apparatus by botulinum neurotoxins. Cell Mol. Life Sci. 71, 793–811.
Peng, L., Berntsson, R.P., Tepp, W.H., Pitkin, R.M., Johnson, E.A., Stenmark, P., Dong, M., 2012. Botulinum neurotoxin D-C uses synaptotagmin I and II as receptors, and human synaptotagmin II is not an effective receptor for type B, D-C and G toxins. J. Cell Sci. 125, 3233–3242.
Pirazzini, M., Azarnia Tehran, D., Zanetti, G., Megighian, A., Scorzeto, M., Fillo, S., Shone, C.C., Binz, T., Rossetto, O., Lista, F., Montecucco, C., 2014. Thioredoxin and its reductase are present on synaptic vesicles, and their inhibition prevents the paralysis induced by botulinum neurotoxins. Cell Rep. 8, 1870–1878.
Pirazzini, M., Bordin, F., Rossetto, O., Shone, C.C., Binz, T., Montecucco, C., 2013. The thioredoxin reductase-thioredoxin system is involved in the entry of tetanus and botulinum neurotoxins in the cytosol of nerve terminals. FEBS Lett. 587, 150–155.
Pirazzini, M., Rossetto, O., Bolognese, P., Shone, C.C., Montecucco, C., 2011. Double anchorage to the membrane and intact inter-chain disulfide bond are required for the low pH induced entry of tetanus and botulinum neurotoxins into neurons. Cell Microbiol. 13, 1731–1743.
Powis, G., Kirkpatrick, D.L., 2007. Thioredoxin signaling as a target for cancer therapy. Curr. Opin. Pharmacol. 7, 392–397.
Ramanathan, R.K., Abbruzzese, J., Dragovich, T., Kirkpatrick, L., Guillen, J.M., Baker, A.F., Pestano, L.A., Green, S., Von Hoff, D.D., 2011. A randomized phase II study of PX-12, an inhibitor of thioredoxin in patients with advanced cancer of the pancreas following progression after a gemcitabine-containing combination. Cancer Chemother. Pharmacol. 67, 503–509.
Rossetto, O., Pirazzini, M., Montecucco, C., 2014. Botulinum neurotoxins: genetic, structural and mechanistic insights. Nat. Rev. Microbiol. 12, 535–549.
Rossetto, O., Seveso, M., Caccin, P., Schiavo, G., Montecucco, C., 2001. Tetanus and botulinum neurotoxins: turning bad guys into good by research. Toxicon 39, 27–41.
Rozell, B., Hansson, H.A., Luthman, M., Holmgren, A., 1985. Immunohistochemical localization of thioredoxin and thioredoxin reductase in adult rats. Eur. J. Cell Biol. 38, 79–86.
Rummel, A., 2013. Double receptor anchorage of botulinum neurotoxins accounts for their exquisite neurospecificity. Curr. Top. Microbiol. Immunol. 364, 61–90.
Rummel, A., Karnath, T., Henke, T., Bigalke, H., Binz, T., 2004. Synaptotagmins I and II act as nerve cell receptors for botulinum neurotoxin G. J. Biol. Chem. 279, 30865–30870.
Schiavo, G., Benfenati, F., Poulain, B., Rossetto, O., Polverino de Laureto, P., DasGupta, B.R., Montecucco, C., 1992. Tetanus and botulinum-B neurotoxins block neurotransmitter release by proteolytic cleavage of synaptobrevin. Nature 359, 832–835.
Schiavo, G., Matteoli, M., Montecucco, C., 2000. Neurotoxins affecting neuroexocytosis. Physiol. Rev. 80, 717–766.
Schiavo, G., Papini, E., Genna, G., Montecucco, C., 1990. An intact interchain disulfide bond is required for the neurotoxicity of tetanus toxin. Infect. Immun. 58, 4136–4141.
Schiavo, G., Rossetto, O., Catsicas, S., Polverino de Laureto, P., DasGupta, B.R., Benfenati, F., Montecucco, C., 1993a. Identification of the nerve terminal targets of botulinum neurotoxin serotypes A, D, and E. J. Biol. Chem. 268, 23784–23787.
Schiavo, G., Santucci, A., Dasgupta, B.R., Mehta, P.P., Jontes, J., Benfenati, F., Wilson, M.C., Montecucco, C., 1993b. Botulinum neurotoxins serotypes A and E cleave SNAP-25 at distinct COOH-terminal peptide bonds. FEBS Lett. 335, 99–103.
Schiavo, G., Shone, C.C., Rossetto, O., Alexander, F.C., Montecucco, C., 1993c. Botulinum neurotoxin serotype F is a zinc endopeptidase specific for VAMP/synaptobrevin. J. Biol. Chem. 268, 11516–11519.
Sheth, A.N., Wiersma, P., Atrubin, D., Dubey, V., Zink, D., Skinner, G., Doerr, F., Juliao, P., Gonzalez, G., Burnett, C., Drenzek, C., Shuler, C., Austin, J., Ellis, A., Maslanka, S., Sobel, J., 2008. International outbreak of severe botulism with prolonged toxemia caused by commercial carrot juice. Clin. Infect. Dis. 47, 1245–1251.
Simpson, L., 2013. The life history of a botulinum toxin molecule. Toxicon 68, 40–59.
Smith, T.J., Hill, K.K., Foley, B.T., Detter, J.C., Munk, A.C., Bruce, D.C., Doggett, N.A., Smith, L.A., Marks, J.D., Xie, G., Brettin, T.S., 2007. Analysis of the neurotoxin complex genes in *Clostridium botulinum* A1-A4 and B1 strains: BoNT/A3,/Ba4 and/B1 clusters are located within plasmids. PLoS One 2, e1271.
Stemme, S., Hansson, H.A., Holmgren, A., Rozell, B., 1985. Axoplasmic transport of thioredoxin and thioredoxin reductase in rat sciatic nerve. Brain Res. 359, 140–146.
Sutton, R.B., Fasshauer, D., Jahn, R., Brunger, A.T., 1998. Crystal structure of a SNARE complex involved in synaptic exocytosis at 2.4 A resolution. Nature 395, 347–353.
Swaminathan, S., Eswaramoorthy, S., 2000. Structural analysis of the catalytic and binding sites of *Clostridium botulinum* neurotoxin B. Nat. Struct. Biol. 7, 693–699.
Yamaguchi, T., Sano, K., Takakura, K., Saito, I., Shinohara, Y., Asano, T., Yasuhara, H., 1998. Ebselen in acute ischemic stroke: a placebo-controlled, double-blind clinical trial. Ebselen Study Group. Stroke 29, 12–17.
Zhao, R., Masayasu, H., Holmgren, A., 2002. Ebselen: a substrate for human thioredoxin reductase strongly stimulating its hydroperoxide reductase activity and a superfast thioredoxin oxidant. Proc. Nat. Acad. Sci. USA 99, 8579–8584.
Zuverink, M., Chen, C., Przedpelski, A., Blum, F.C., Barbieri, J.T., 2015. A heterologous reporter defines the role of the tetanus toxin inter-chain disulfide in light chain translocation. Infect Immun. http://dx.doi.org/10.1128/IAI.00477–15.

5.1.2 On the translocation of botulinum and tetanus neurotoxins across the membrane of acidic intracellular compartments

Marco Pirazzini[a], Domenico Azarnia Tehran[a], Oneda Leka[a], Giulia Zanetti[a], Ornella Rossetto[a], Cesare Montecucco[a,b]

[a]Dipartimento di Scienze Biomediche, Università di Padova, Via U. Bassi 58/B, 35121 Padova, Italy

[b]Istituto CNR di Neuroscienze, Università di Padova, Via U. Bassi 58/B, 35121 Padova, Italy

Pirazzini M. *et al.* On the translocation of botulinum and tetanus neurotoxins across the membrane of acidic intracellular compartments. *Biochim Biophys Acta*. 2016 Mar;1858(3):467-74.
doi: 10.1016/j.bbamem.2015.08.014. Epub 2015 Aug 22.

Biochimica et Biophysica Acta 1858 (2016) 467–474

Contents lists available at ScienceDirect

Biochimica et Biophysica Acta

journal homepage: www.elsevier.com/locate/bbamem

Review

On the translocation of botulinum and tetanus neurotoxins across the membrane of acidic intracellular compartments☆

Marco Pirazzini [a], Domenico Azarnia Tehran [a], Oneda Leka [a], Giulia Zanetti [a], Ornella Rossetto [a], Cesare Montecucco [a,b,*]

[a] Dipartimento di Scienze Biomediche, Università di Padova, Via U. Bassi 58/B, 35121 Padova, Italy
[b] Istituto CNR di Neuroscienze, Università di Padova, Via U. Bassi 58/B, 35121 Padova, Italy

ARTICLE INFO

Article history:
Received 3 July 2015
Received in revised form 4 August 2015
Accepted 17 August 2015
Available online 22 August 2015

Keywords:
Botulinum neurotoxin isoforms
Clostridia
Duration of neuroparalysis
Endocytosis
Presynaptic binding
Translocation

ABSTRACT

Tetanus and botulinum neurotoxins are produced by anaerobic bacteria of the genus *Clostridium* and are the most poisonous toxins known, with 50% mouse lethal dose comprised within the range of 0.1–few nanograms per Kg, depending on the individual toxin. Botulinum neurotoxins are similarly toxic to humans and can therefore be considered for potential use in bioterrorism. At the same time, their neurospecificity and reversibility of action make them excellent therapeutics for a growing and heterogeneous number of human diseases that are characterized by a hyperactivity of peripheral nerve terminals. The complete crystallographic structure is available for some botulinum toxins, and reveals that they consist of four domains functionally related to the four steps of their mechanism of neuron intoxication: 1) binding to specific receptors of the presynaptic membrane; 2) internalization via endocytic vesicles; 3) translocation across the membrane of endocytic vesicles into the neuronal cytosol; 4) catalytic activity of the enzymatic moiety directed towards the SNARE proteins.

Despite the many advances in understanding the structure–mechanism relationship of tetanus and botulinum neurotoxins, the molecular events involved in the translocation step have been only partially elucidated. Here we will review recent advances that have provided relevant insights on the process and discuss possible models that can be experimentally tested. This article is part of a Special Issue entitled: Pore-Forming Toxins edited by Mauro Dalla Serra and Franco Gambale.

Contents

1. Introduction

Tetanus and botulinum neurotoxins (TeNT and BoNT, respectively) are produced by neurotoxigenic spore-forming *Clostridia*. These bacteria have a considerable genetic heterogeneity, both in terms of genome organization and, most importantly, in toxin gene clusters, with a remarkable variability in their toxin sequences [1]. BoNTs have been traditionally classified as seven distinct toxin serotypes (BoNT/A–G), but recently, thanks to faster and cheaper sequencing technology, many toxin subtypes within each serotype have been discovered. They are commonly considered as subserotypes (indicated with numerical designations following the toxin serotype, for example BoNT/A1 or BoNT/A2…). Their number has reached several dozens of BoNTs in a few years, and many more will be released in the near future [1–3].

☆ This article is part of a Special Issue entitled: Pore-Forming Toxins edited by Mauro Dalla Serra and Franco Gambale.

* Corresponding author.
E-mail address: cesare.montecucco@gmail.com (C. Montecucco).

http://dx.doi.org/10.1016/j.bbamem.2015.08.014
0005-2736/

TeNT acts in the spinal cord causing a spastic paralysis, whereas all the BoNTs cause peripheral neuroparalysis of the skeletal and autonomic nervous systems [4]. BoNTs have become very useful therapeutics for the treatment of many pathological conditions caused by the hyperactivity of cholinergic terminals [5–9].

1.1. Structure and cellular mechanism of action

Despite the amino acid sequence variability among the TeNT and BoNT variants, they share a very similar architecture which is related to a similar mechanism of nerve intoxication. They consist of a light chain (L, 50 kDa) and a heavy chain (H, 100 kDa) linked by a strictly conserved interchain disulfide bond. Fig. 1 shows the crystal structures of BoNT/A1 and of BoNT/E1; BoNT/B1 is very similar to BoNT/A1 (not shown) [10–12]. They consist of four domains: HC-C (25 kDa, in green in Fig. 1) involved in nerve terminal binding; HC-N (25 kDa purple in Fig. 1) of unknown function, though there is evidence that it binds to membrane lipids [13,14]; L (red in Fig. 1); HN (50 kDa, yellow in Fig. 1), assists the translocation of L from the lumen of an intracellular acidic compartment into the cytosol; L is a metalloprotease that cleaves the SNARE proteins within the nerve terminal cytosol thus blocking the release of neurotransmitters causing a reversible neuroparalysis [15,16].

HC-C mediates the neurospecific binding of the toxin to the presynaptic membrane via two independent receptors: a polysialoganglioside (PSG) and the luminal domain of a synaptic vesicles (SV) membrane protein [2,15,17]. There appears to be no interaction or mutual interference between the two receptors binding sites [2,18]. Such a binding is preliminary to the following step of internalization inside the nerve. TeNT and BoNT/A1 exploit the endocytosis of SV to penetrate into neurons [19–21]. Information on the nature of the endocytic vesicle involved in the uptake of the other neurotoxins is still lacking. However, the fact that BoNT/B, /CD, /E and /G interact with a SV protein receptor suggests that their internalization may be SV-mediated as well [22]. After endocytosis is completed, the SV lumen and the lumen of synaptic endosomes with which SV may have fused is acidified by the proton pumping action of the v-ATPase present on the SV membrane. This action lowers the luminal pH to a value estimated to be around 5.8 [23,24]. This pH gradient drives the uptake of neurotransmitters from the cytosol into SV and it is used by TeNT and BoNTs to translocate their L domain from the SV interior, or synaptic endosome interior, into the cytosol [25,26]. This process is made possible by the HN domain, also known as translocation domain (yellow in Fig. 1). The main structural feature of HN is the presence of two long amphipathic α-helices (~110 A) and four shorter ones, running parallel to each other, which are linked to the L domain via the aforementioned SS bond and by a long unstructured belt (orange and blue, respectively, in Fig. 1) that encircles the L domain.

1.2. Models for the membrane translocation of the L chain of tetanus and botulinum neurotoxins

Of the various steps of the cellular mechanism of intoxication, the membrane translocation of the L chain from intracellular acidic compartments into the cytosol is the least understood in terms of molecular mechanism. It was long known that BoNTs form ion channel of low conductance in planar lipid bilayers at low pH values [27–29]. More recently, Koriazova and Montal showed that transmembrane ion channel formation in planar lipid bilayers is associated with translocation of the L chain of BoNT/A1 with cleavage of its target protein SNAP-25 [30]. A major step forward was made by using the patch clamp technique in Neuro2A cells [25,26,31–33] and in PC12 cells [34–36]. This experimental approach is close to the in vivo situation and permits a single molecule analysis [26]. The main conclusions derived from these studies are:

1) Upon lowering the pH of the cis side of the membrane (the one corresponding to the SV lumen), and the application of a negative membrane potential, BoNT/A1 and /E1 induce increasing transmembrane currents across the plasma membrane that begin with low values (~10 pS) and raise within ~10 min to a single channel conductance of ~65 pS (Neuro2A, Fig. 2A) or ~110 pS (PC12); although there is no direct correspondence between conductance and internal diameter of an ion channel, these figures indicate an internal channel diameter of 15–20 Å [37] which compares well with the value

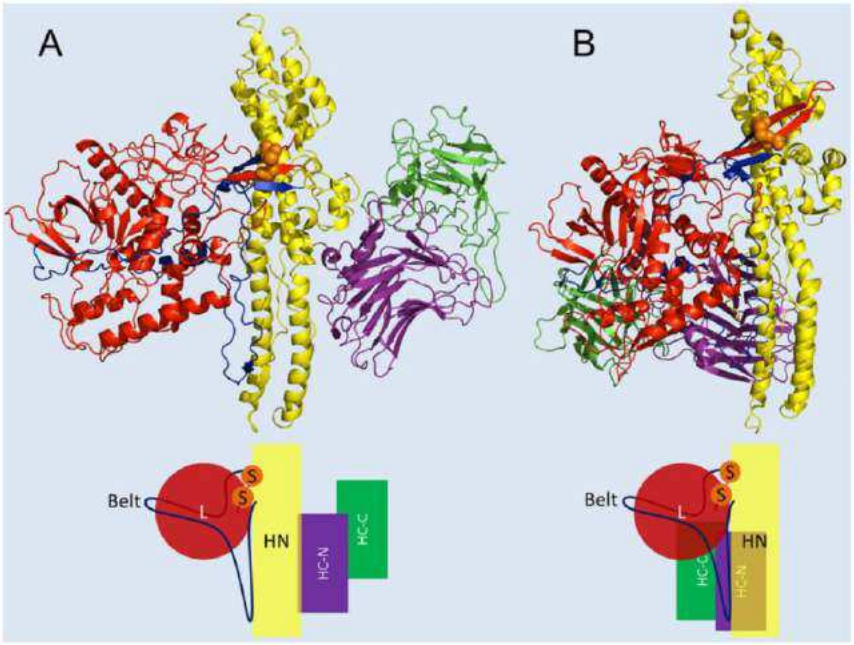

Fig. 1. Structure of BoNT and of its complexes. The crystallographic structures of BoNT/A (PDB 3BTA) and of BoNT/E (PDB 3FFZ) are shown in panel A and B, respectively. The lower panels show simplified schematic molecular organizations of the four domains that compose these neurotoxins, labelled with the same colours found in the crystals: L (red) indicates the metalloprotease domain, HN (yellow) the membrane translocating domain, HC-N (pink), whose role is not known and of HC-C (green). HN and L are connected by the disulphide bond (orange) and by the belt (blue).

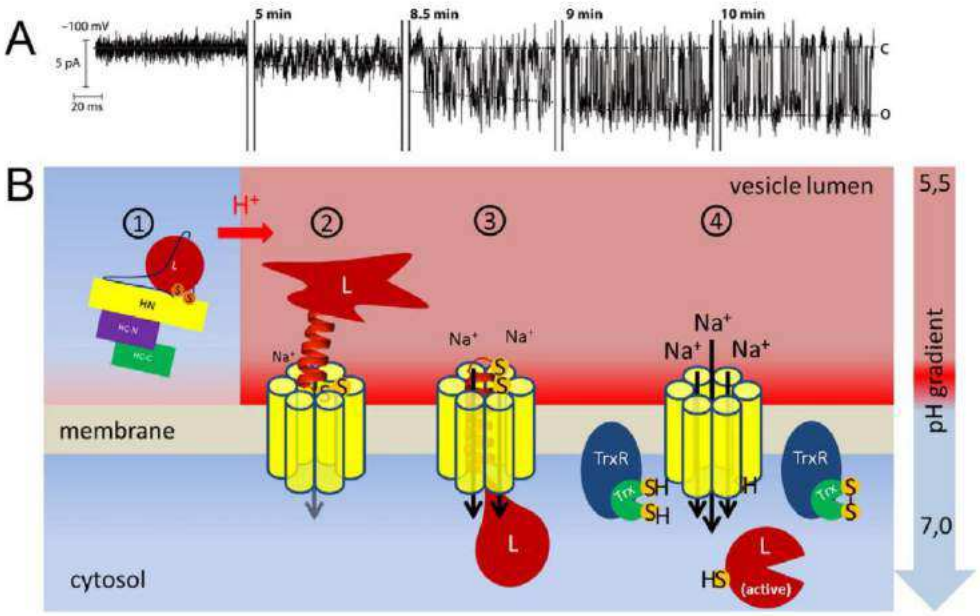

Fig. 2. Membrane translocation of BoNTs. This figure is elaborated on the basis of ref. [25]. A) The upper panel shows the conductance increase of a portion of the plasma membrane of a Neuro2A cell induced by BoNT/A at low pH. The toxin causes subsequent increases in conductance from low values to attain ~65 pS within few minutes. B) Based on an elegant and consistent series of biophysical studies [25,26,88], the sequence of molecular events depicted in the cartoon are proposed to be involved in the membrane translocation of the L chain (blue). 1) Shows a schematic structure of the toxin in the lumen of an acidic vesicle within the nerve terminal; 2) shows the HN domain inserted into the membrane at acidic pH forming a transmembrane channel, hypothetically made of six α-helices (represented by yellow cylinders), that operates as a chaperone for the unfolding of the L chain and its translocation inside the channel [30]; 3) the translocation of L from the acidic lumen into the neutral cytosol proceeds and this is accompanied by a higher conductance; 4) the L chain is almost completely translocated in the cytosol where it refolds. This is accompanied by the translocation of the interchain disulphide bond shown in green; 5) the SS bond is reduced by the Thioredoxin reductase (TrxR)–thioredoxin (Trx) protein disulphide reducing system, leading to the detachment of the L domain from the membrane with freeing of its metalloprotease activity.

obtained by measuring dextrane permeability [38]. Such a channel allows the passage of α-helices but not of tertiary structure elements, indicating that some unfolding of the L chain has to take place before and/or during its membrane translocation. In agreement with this observation, mAbs preventing L chain unfolding precluded channel formation [39].

2) HN alone, or HN–belt, or HN–belt–HC form at neutral pH ion channels with the same conductance, the same opening probability and voltage dependence of the one formed by BoNT/A1 at low pH [40]. This indicates that the transmembrane ion channel consists of the HN domain with little, if any, contribution of other parts of the toxin molecule.
3) The interchain disulfide bond has to be reduced once it reaches the trans side of the membrane (corresponding to the cytosolic side) to allow L to leave the channel; pre-reduced BoNT does not form channels and reduction at any stage before reaching the trans side aborts channel formation [26,33]. These findings are in agreement with the fact that only reduced TeNT and BoNTs can hydrolyse their substrates [41] and explain why this disulfide bridge is essential for neurotoxicity [17,42,43]. Other experiments showed that cargo molecules capable of unfolding at low pH, attached to the N-terminus of BoNT/D, are transported in an active form in the neuronal cytosol unless unfolding is prevented [44]. On the basis of these data, the model schematically shown in Fig. 2B was generated [25]. This model posits that upon acidification, the BoNT molecules change structure and penetrate the membrane. The initial low conductance states are taken as an indication of the low pH-driven membrane insertion of the H chain forming a transmembrane chaperone that assists the translocation of a partially unfolded L domain. Translocation of the L chain is accompanied by an increase in conductance. As the L chain moves through the pore and progressively empties the channel, ion conductance increases. Transfer of the SS bond is suggested to occur at the end of the L translocation process and is concluded by its reduction taking place on the cytosolic face of the membrane; this final event opens the pore, which attains its full conductance [25].

However, a consistent set of data suggests that this model requires revision and integration. In fact: a) BoNT/B1 and the L or HN domains of BoNT/A1 do not change structure at low pH in solution [45,46]; b) BoNT/A1 and /B1 change structure at low pH in the presence of a membrane or PSG [35,46–48]; c) membrane photolabelling studies employing photoactivatable radioactive phospholipids showed that both the L and H chains of TeNT, BoNT/A1, /B1 and /E1 enter in contact with the hydrocarbon chain of phospholipids in model membranes at low pH [49,50] and this is not accounted for by the model of Fig. 2, as the L chain is protected from the contact with lipid by the H channel; d) ion conductance along the "paradigmatic" toxin transmembrane channel, i.e. the anthrax protective antigen channel, is blocked even by fragments of transported protein [51–53] and this is at variance from what proposed in the model of Fig. 2; e) more recently, using an experimental approach that bypasses the endocytosis step and induces the translocation of the L chain from the cell surface, it was found that BoNTs have to be anchored to the membrane via two receptors and that translocation occurs in the pH range 4.5–6 [17]. Considering the properties of the different experimental setup used, a parallel study led to the same conclusions [35]; f) membrane translocation of L is accomplished within few minutes at 37 °C and has a strong temperature dependence with very little translocation taking place at 20 °C [54]; g) the pH dependence of membrane translocation of the L chains of different BoNTs and TeNT was found to be very similar, suggesting that the overall mechanism involves similar molecular events [17].

The above data can be reconciled by a new model depicted in Fig. 3B. BoNT is envisaged to be bound to its two receptors inside the lumen of nerve terminal acidic compartments. There are no conserved histidines in BoNTs, apart from those coordinating the active site Zn^{2+}, but there are conserved carboxylate residues predicted to have a high pKa [17]. Table 1 lists the conserved Asp and Glu residues (with BoNT/A1 and

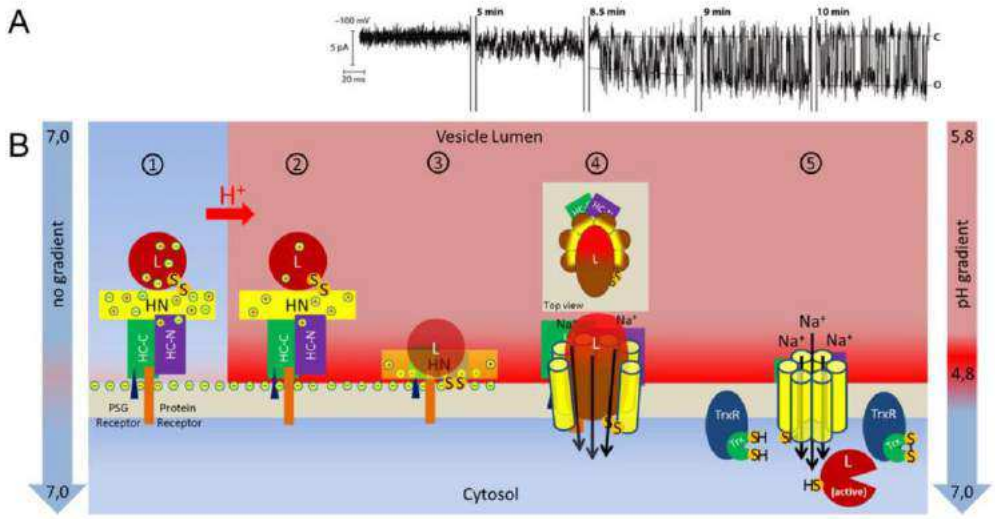

Fig. 3. A revised model of membrane binding and translocation of BoNT. The starting point is the binding of BoNT to its two receptors present on the presynaptic membrane (1). The four domains of the toxin are depicted schematically in different colours and with some conserved charged residues: L (red), HN (yellow), HC-N (purple) and HC-C in green bound to its two receptors, i.e. the polysialoganglioside (PSG, blue triangle) and protein (orange rectangle). (2) Following the operation of the v-ATPase proton pump, the vesicle lumen acidifies (represented by the pink colour) and the high pKa carboxylate residues, which are mainly localized on the face of the protein including the interchain disulphide bond and the membrane interacting segment (see text). This face of the protein acquires a net positive charge and will eventually fall down on the anionic membrane surface (3) following electrostatic attraction. (4) It should be considered that the negative membrane surface attracts protons creating a locally lower pH (horizontal red stripe) that leads to further protonation of the BoNT laying down on the lumenal surface of the synaptic vesicle membrane. Low pH and lipid interactions cause a concerted and sequential structural change involving at the same time the L and HN domains and lipids. Some major events can be posited to occur (see text), the major ones being; i) the destabilization and breakage of the long HN α-helices at selected conserved peptide bonds with ensuing membrane insertion of 20–24 residues long α-helices with their exterior facing lipids and their internal part interacting with the L chain perhaps in the form of a molten globule. Notice that hydrophobic parts of L can interact with the lipids. This membrane penetration of L and HN makes the membrane leaky because of mismatching among the protein surface and lipids accounting for the increased membrane conductance shown in the corresponding upper panel. (5) L moves to the cytosolic side, refolds and is released upon reduction of the interchain disulphide bond by thioredoxin (Trx, green), a protein disulphide reducing enzyme which is reconverted in its reduced form by the thioredoxin reductase (TrxR, blue). At the same time, additional segments of HN become membrane inserted in such a way that ion channel is assembled. This channel is shown here six transmembrane α-helices, though no structural data are available. The α-helices are suggested to be amphipathic with a hydrophobic external part interacting with lipids and a hydrophilic interior.

BoNT/B1 numbering), as deduced by comparison of the BoNT sequences deposited in the Gene Data Bank and in the UniProt data base. There are nineteen completely conserved carboxylates: three in the L chain, five in the belt, ten in HN and 1 in HC-N (Fig. 4). It is noteworthy that all these residues occupy almost identical spatial positions in the two neurotoxins, and that some of these residues are at the interface among domains or on the belt region (Fig. 4). Such a distribution suggests that there is no single pH sensor in BoNT. These residues become protonated, partially or entirely, in a sequential way, depending on their pKa, as the intravesicular pH lowers to its final value (Fig. 3B step 2). Three of these residues are predicted to have a high pKa (encircled in Table 1) by the propka 3.0 software [55] (http://nbcr-222.ucsd.edu/pdb2pqr_2.0.0/). This property allows their protonation, with charge neutralization, at mildly acidic pH values. Partially protonated BoNT has a net positive charge that favours its interaction with the negatively charged membrane surface. Remarkably, all the conserved carboxylates of high pKa are located within the BoNT face containing the interchain SS bond and the segment 637–688 (BoNT/B1 numbering) identified by Eswaramoorthy et al. [45] as a membrane interacting segment; the opposite face has no carboxylates of appropriate pKa value. On the other hand, the two extremities of the long α-helices of the HN, previously proposed to be the first part of HN inserting into the lipid bilayer, are not conserved. The proposal that conserved carboxylate of high pKa play an important role in the process was tested by mutagenesis of three high pKa conserved carboxylates of BoNT/B1 (Glu-47, Glu-652 and Asp-876) into the corresponding amides [56]. The prediction was that the presence of the amide residues, not requiring protonation to become neutral as the corresponding carboxylates do, should have increased toxicity. Indeed the triple mutant was more neurotoxic in vitro and in vivo than BoNT/B1, following a more rapid delivery of the enzymatic domain into the cytosol of neurons in culture [56]. Moreover it was found that membrane translocation of the triple amide mutant BoNT/B1 could take place at less acidic pH [56]. These findings indicate that neutralisation of specific Glu and Asp residues promotes the membrane interaction of BoNTs. This is suggested to begin with an electrostatic attraction between the anionic membrane surface and the positively charged toxin surface (Fig. 3B step 3), which induces the transfer of BoNT towards the membrane surface. Such a movement is not prevented by receptor interactions because either binding is weakened by low pH or the two receptors are flexible as it is the case with PSG and synaptotagmin [2,18]. These three initial steps integrate the model of Fig. 2B.

Table 1
Carboxylate residues conserved among TeNT and all BoNT types and subtypes are listed with the numbering of BoNT/A1 and BoNT/B1 and the corresponding estimated pKa values. The three high pKa carboxylates are in red.

Residue BoNT/A1	Residue BoNT/B1	Domain position	pKa BoNT/A1	pKa BoNT/B1
GLU46	GLU47	L chain	6.33	6.54
ASP73	ASP74	L chain	2.97	4.3
GLU82	ASP82	L chain	3.49	4.04
ASP460	ASP452	Belt	3.46	4.3
GLU467	ASP458	Belt	5.06	2.6
ASP473	ASP465	Belt	4.63	4.14
ASP496	GLU489	Belt	3.63	4.88
GLU534	GLU521	Belt	4.68	4.47
GLU573	ASP560	HN	4.66	4.12
ASP612	ASP599	HN	4.36	5.16
ASP624	ASP611	HN	3.92	8.5
ASP628	ASP615	HN	5.88	1.9
GLU665	GLU652	HN (putative transmembrane)	6.85	6.95
GLU669	GLU656	HN (putative transmembrane)	4.52	4.5
GLU707	ASP694	HN	5.21	5.71
GLU757	GLU744	HN	4.69	4.11
ASP809	ASP796	HN	4.89	4
ASP811	ASP798	HN	6.13	4.85
ASP889	ASP876	HC-N	4.42	5.02

Synaptic vesicles and endosomes have a transmembrane electrical potential positive inside, owing to the electrogenic operation of the v-ATPase proton pump, whilst the BoNT/A1 and /E1 channels were found to be closed at positive membrane voltages [33]. This discrepancy stimulates the elaboration of alternative models for the membrane translocation of the L chain. In the absence of experimental results that throw light on the molecular events that follow the initial phase depicted in Fig. 3B (steps 1 to 3), to contribute to the debate on toxin membrane translocation and to stimulate ad hoc experiments, we discuss here a more comprehensive model that is in keeping with current knowledge on protein–lipid interactions and accounts for all available experimental results.

As shown in Fig. 3B step 3, the layer of solvent above the membrane surface is more acidic (red layer) than the lumen (pink) because of the Guy-Chapman effect due to the negatively charge of the luminal surface carried by anionic lipids and the sialic acid residues of gangliosides and glycoproteins [57–59]. It is difficult to evaluate the pH value of the membrane surface, but it could be as much as one unit lower than in the lumen, as indicated in Fig. 3B. Such low pH would cause the protonation of additional carboxylates, whilst positively charged segments could form ionic couples with acidic lipids which can enter the hydrophobic core of the membrane in this form [60]. In addition, other segments of the BoNT molecules could interact with lipids via hydrogen bonding and van der Waals interactions [60]. The ensemble of these interactions is expected to cause a gross and concerted structural rearrangement involving three players at the same time: the L chain, the HN and the lipids. It can be envisaged that the hydrophobic and polarizable disulphide bond inserts into the lipid bilayer drawing the L chain from its C terminus. The L chain may become a "molten globule", i.e. a protein form with native secondary structure and increased hydrophobicity that renders it capable of inserting and moving across membranes [48,61–64]. In this view, the initial, low conductance, transmembrane currents of Fig. 3A are accounted for by mismatches among the HN and L protein surfaces and the lipids which render the membrane leaky. The long α-helices of HN may break generating amphipathic helices with the length of 20–24 residues. It is suggested that, together with the other amphipathic helices of the HN domain, a laterally open transmembrane channel is formed and that it partially surrounds the L molten globule, whilst the remaining surface of L interacts with lipids. In this way, hydrophilic and hydrophobic surfaces and interactions are matched (Fig. 3B, step 4 lateral and top views). The arch-shaped membrane inserted HN may act as a chaperone for the translocation of the L chain, as suggested by Koriazova and Montal [30]. Facing the neutral pH of the cytosol, the L chain deprotonates and refolds into the metalloprotease domain whilst the membrane inserted HN forms closes laterally to form a stable ion channel. The process is terminated by the reduction of the interchain SS bond by thioredoxin which releases the L chain and its protease activity and the HN channel attains its full conductance.

It should be noted that the two models diverge in a major aspect: in the model of Fig. 2, the membrane penetration with channel formation by HN is an early event and a prerequisite for the membrane translocation of L; at variance, in the model of Fig. 3, the channel formation is a consequence of the L translocation process. A prediction intrinsic to the first model is that the HN channel should be capable of translocating distinct L chains one after the other, as it is the case for the anthrax protective antigen channel [51–53]. This can be tested using N- or C-terminal segments of the L chain, but not tandems of chains linked one to the other as recently achieved [65] because such an experimental system cannot discriminate among the two models. On the contrary, the model of Fig. 3 envisages a single membrane translocation event which follows a concerted structural change of both the L and the H chains together with lipids. In both cases, the translocation of L leaves behind the HN channel inserted in the membrane making the SV unable to sustain a pH gradient.

Another important open question is the direction of the L polypeptide chain translocation (Fig. 3), i.e. from the N to the C terminus or vice versa; though very important, its determination will not allow one to discriminate between the two models because both of them can accommodate the two possibilities. The translocation process is expected in both cases to be driven and directed from the low pH membrane side to the neutral one by the reversible protonation/deprotonation of carboxylate residues. At least the initial part of the process should be reversible, but not after channel formation and L translocation with refolding at the neutral pH side. In fact, several events would render it irreversible: i) the exposure of protonated carboxylates to the neutral pH of the cytosol where they return negatively charged, ii) the refolding of the polypeptide chain facing the neutral environment of the cytosol and iii) the likely assistance of cytosolic chaperones for L chain refolding, as it occurs with several other bacterial toxins [66–68].

A major open question is the number of BoNT molecules involved in membrane translocation. The finding that one SV contains one or two molecules of BoNT/A leaves open the possibility that one molecule of BoNT/A is sufficient [20,21]. In other words, BoNT/A may have an in built membrane translocating system as it is the case for the bacterial SecY system [69]. Additional similarities between BoNT and SecY are their high content of α-helices and the fact that the SecY channel may open laterally to the lipid bilayer to release membrane spanning segment of a nascent protein. Also, the diphtheria toxin translocating domain is mainly α-helical and there is evidence that a single molecule is involved in the process with few transmembrane helices forming an ion channel [70,71]. At variance, it was recently reported that a BoNT/B trimer forms the protein conducting transmembrane channel in PC12 cells [35]. Clearly, further investigations are needed to clarify this essential aspect of the process.

The molecular mechanism of the membrane translocation of TeNT and of the BoNTs can be nowadays tackled by available techniques. The present article may help in designing an extensive mutagenesis project whose effects can be monitored using different read-outs, including the kinetics of the paralysis of the neuromuscular junction [72,73], the electrophysiological properties of excised patch [26] and of planar lipid bilayers [74] and the assay of L chain translocation from the plasma membrane [17,35]. However, it should be considered that planar lipid bilayers and plasma membranes differ significantly in terms of lipid composition, lipid packing and membrane curvature from the membrane of synaptic vesicles and endosomes. These parameters may play an essential role in the process.

1.3. The interchain disulphide bond reduction terminates the translocation process

Fischer and Montal demonstrated that for a productive translocation, the L domain has to remain attached to H via the interchain SS bridge and that its reduction is the concluding event which releases the L metalloprotease activity [33]. Consistently, the premature reduction of this bond, at any stage before its exposure to the cytosol, aborts the L chain translocation [33], indicating that it plays a fundamental role in the process and that it has to reach intact the cytosolic side of the membrane for a productive L chain delivery. The SV lumen of most intracellular organelles is oxidant, whilst the cell cytosol has a reducing potential, which is kept by a large number of redox couples. The reduction of protein disulfides is catalysed in the cell by different enzymatic systems [75–77]. A pharmacologic approach has led to the identification of the NADPH–Thioredoxin reductase (TrxR)–Thioredoxin (Trx) system being responsible for the cytosolic release of L in the cytosol [78] and this has led to the discovery that both TrxR and Trx are extrinsic proteins of the cytosolic side of SV [79]. Consequently, several inhibitors of the TrxR–Trx redox couple were found to prevent the L chain of BoNTs from displaying their metalloprotease activity versus the SNARE proteins in cultured neurons. Importantly, these inhibitors prevent the BoNT induced paralysis. This observation made originally on BoNT/A, /C and /E has been extended to all BoNT serotypes (Zanetti

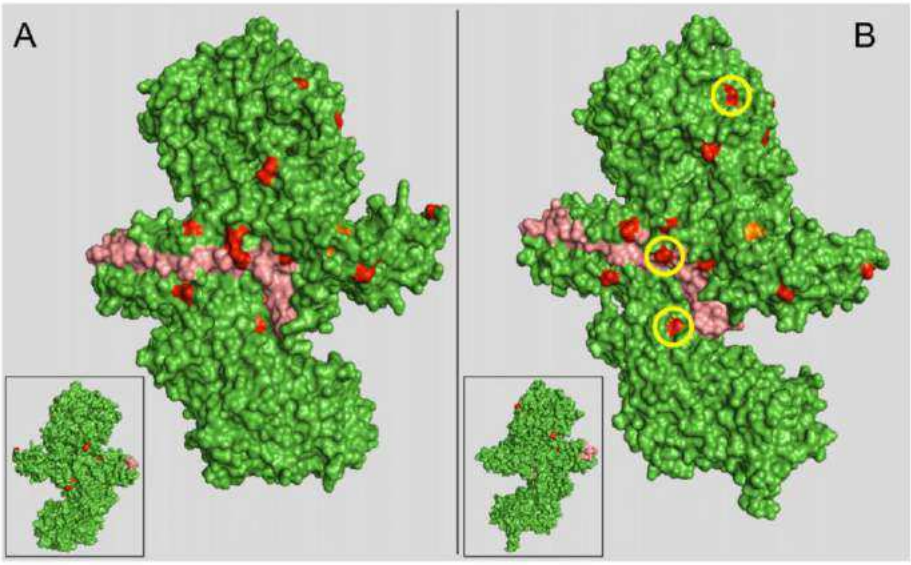

Fig. 4. Location of conserved carboxylate residues in the BoNT structure. The pictures shows in red the Asp or Glu residues conserved among all the available BoNT sequences in the structures of BoNT/A1 (PDB ID: 3BTA, panel A) and BoNT/B1 (PDB ID: 1EPW, panel B), represented as space filling models; those mutated in the corresponding amide residues on BoNT/B1 (see text) are encircled. The pink segment indicates the high membrane interaction segment (see text). Insets show the BoNT/A1 and BoNT/B1 opposite face with respect to the face harbouring the disulphide bond (orange).

et al., submitted) and therefore, the reduction of the single interchain disulphide bond of BoNTs taking place on the cytosolic surface of the organelle wherefrom they translocate is a general and fundamental aspect of BoNT and TeNT mechanism of nerve terminal intoxication. Interestingly, the TrxR–Trx redox system is also present on the endosomal membrane wherefrom diphtheria toxin enters the cytosol [66], and it is responsible for the interchain disulfide bond reduction [80] of this toxin, which was previously shown to be the rate limiting step of the entire cell intoxication process [81]. Together, these data suggest that the couple TrxR–Trx is the reducing system involved in the release of the catalytic part of all A–SS–B toxins in the cytosol.

1.4. The L chains of BoNTs are metalloproteases specific for the SNARE proteins

The L chains of all the presently known BoNTs are metalloproteases specific for one or another of the three SNARE proteins: VAMP/synaptobrevin, SNAP-25 and syntaxin which are cleaved at single sites (BoNT/C cleaves two SNAREs). This is the strongest evidence that the three SNARE proteins form the core of the neuroexocytosis nanomachine [16,82,83]. No additional substrates are presently known and this is related to the unique model of recognition of VAMP, SNAP-25 or syntaxin by the L domain, which is based on an extended interaction including the cleavage site and exosites dispersed along the substrate sequence [16,84,85]. As a consequence of this extensive interaction of the L chain with their substrates, the seven BoNT serotypes exhibit exclusive specificities with respect to the different isoforms of the three SNARE proteins present within different neurons and within different animal species [16,86]. Therefore, the TeNT and BoNTs can be used as simple tools to determine the effect of knocking-out specific SNAREs in cell physiology [16]. The metalloprotease enzymatic activity of the L chain is at the basis of the high toxicity of the BoNTs because, in principle, one single L molecule can cleave, one after the other, all its substrate molecules present within one nerve terminal. This aspect of BoNT action has been reviewed in depth recently [16,85,87]. The cleavage of a SNARE protein prevents the assembly of the SNARE complex which is a prerequisite for the fusion of the neurotransmitter containing vesicle with the presynaptic membrane [83], and, as long as the L remains active, the nerve terminal remains paralysed.

2. Conclusions and future perspectives

The very high potency of botulinum neurotoxins is the result of an elaborate molecular mechanism of action, which impairs a physiological function essential to the life of vertebrates. This mechanism includes the membrane translocation of the L metalloprotease domain from the lumen of synaptic vesicles or of other acidic compartments of the nerve terminals. This is the least known of the multi-steps process of nerve terminal intoxication and paralysis caused by these neurotoxins. Novel biophysical approaches that allow one to follow the action of single molecules coupled to extensive mutagenesis are expected to throw light on the molecular mechanism underlying this process. These studies should include TeNT and several BoNT serotypes as relevant differences may be found among them. These studies are likely to lead to the identification of novel toxins of therapeutic potential and novel inhibitors of these neurotoxins.

Conflict of interest

On behalf of all co-authors, I testify that our article submitted to Toxicon, entitled "On the translocation of botulinum and tetanus neurotoxins across the membrane of acidic intracellular compartments", is an original work composed without conflict of interest.

Acknowledgements

Work in authors' laboratory is supported by Fondazione CARIPARO Project "Synaptic Functions and Role of Glial Cells in Brain and Muscle Diseases", by the Italian Ministry of Defence (Progetto PNRM - NIB, Segretariato Generale della Difesa V Reparto) and by grant from the University of Padova (Progetto PRIN) to OR.

References

[1] K.K. Hill, T.J. Smith, Genetic diversity within *Clostridium botulinum* serotypes, botulinum neurotoxin gene clusters and toxin subtypes, Curr. Top. Microbiol. Immunol. 364 (2013) 1–20.
[2] O. Rossetto, M. Pirazzini, C. Montecucco, Botulinum neurotoxins: genetic, structural and mechanistic insights, Nat. Rev. Microbiol. 12 (2014) 535–549.
[3] C. Montecucco, M.B. Rasotto, On botulinum neurotoxin variability, MBio 6 (2015).
[4] E.A. Johnson, C. Montecucco, Botulism, Handb. Clin. Neurol. 91 (2008) 333–368.

[5] B. Davletov, M. Bajohrs, T. Binz, Beyond BOTOX: advantages and limitations of individual botulinum neurotoxins, Trends Neurosci. 28 (2005) 446–452.
[6] C. Montecucco, J. Molgo, Botulinal neurotoxins: revival of an old killer, Curr. Opin. Pharmacol. 5 (2005) 274–279.
[7] D. Dressler, Clinical applications of botulinum toxin, Curr. Opin. Microbiol. 15 (2012) 325–336.
[8] G. Masuyer, J.A. Chaddock, K.A. Foster, K.R. Acharya, Engineered botulinum neurotoxins as new therapeutics, Annu. Rev. Pharmacol. Toxicol. 54 (2014) 27–51.
[9] M. Hallett, A. Albanese, D. Dressler, K.R. Segal, D.M. Simpson, D. Truong, J. Jankovic, Evidence-based review and assessment of botulinum neurotoxin for the treatment of movement disorders, Toxicon 67 (2013) 94–114.
[10] D.B. Lacy, W. Tepp, A.C. Cohen, B.R. DasGupta, R.C. Stevens, Crystal structure of botulinum neurotoxin type A and implications for toxicity, Nat. Struct. Biol. 5 (1998) 898–902.
[11] S. Swaminathan, S. Eswaramoorthy, Structural analysis of the catalytic and binding sites of *Clostridium botulinum* neurotoxin B, Nat. Struct. Biol. 7 (2000) 693–699.
[12] D. Kumaran, S. Eswaramoorthy, W. Furey, J. Navaza, M. Sax, S. Swaminathan, Domain organization in *Clostridium botulinum* neurotoxin type E is unique: its implication in faster translocation, J. Mol. Biol. 386 (2009) 233–245.
[13] L. Muraro, S. Tosatto, L. Motterlini, O. Rossetto, C. Montecucco, The N-terminal half of the receptor domain of botulinum neurotoxin A binds to microdomains of the plasma membrane, Biochem. Biophys. Res. Commun. 380 (2009) 76–80.
[14] Y. Zhang, S.M. Varnum, The receptor binding domain of botulinum neurotoxin serotype C binds phosphoinositides, Biochimie 94 (2012) 920–923.
[15] T. Binz, A. Rummel, Cell entry strategy of clostridial neurotoxins, J. Neurochem. 109 (2009) 1584–1595.
[16] S. Pantano, C. Montecucco, The blockade of the neurotransmitter release apparatus by botulinum neurotoxins, Cell. Mol. Life Sci. 71 (2013) 739–811.
[17] M. Pirazzini, O. Rossetto, P. Bolognese, C.C. Shone, C. Montecucco, Double anchorage to the membrane and intact inter-chain disulfide bond are required for the low pH induced entry of tetanus and botulinum neurotoxins into neurons, Cell. Microbiol. 13 (2011) 1731–1743.
[18] R.A. Kammerer, R.M. Benoit, Botulinum neurotoxins: new questions arising from structural biology, Trends Biochem. Sci. 39 (2014) 517–526.
[19] M. Matteoli, C. Verderio, O. Rossetto, N. Iezzi, S. Coco, G. Schiavo, C. Montecucco, Synaptic vesicle endocytosis mediates the entry of tetanus neurotoxin into hippocampal neurons, Proc. Natl. Acad. Sci. U. S. A. 93 (1996) 13310–13315.
[20] C.B. Harper, S. Martin, T.H. Nguyen, S.J. Daniels, N.A. Lavidis, M.R. Popoff, G. Hadzic, A. Mariana, N. Chau, A. McCluskey, P.J. Robinson, F.A. Meunier, Dynamin inhibition blocks botulinum neurotoxin type A endocytosis in neurons and delays botulism, J. Biol. Chem. 286 (2011) 35966–35976.
[21] C. Colasante, O. Rossetto, L. Morbiato, M. Pirazzini, J. Molgo, C. Montecucco, Botulinum neurotoxin type A is internalized and translocated from small synaptic vesicles at the neuromuscular junction, Mol. Neurobiol. 48 (2013) 120–127.
[22] A. Rummel, Double receptor anchorage of botulinum neurotoxins accounts for their exquisite neurospecificity, Curr. Top. Microbiol. Immunol. 364 (2013) 61–90.
[23] G. Miesenbock, D.A. De Angelis, J.E. Rothman, Visualizing secretion and synaptic transmission with pH-sensitive green fluorescent proteins, Nature 394 (1998) 192–195.
[24] S. Sankaranarayanan, T.A. Ryan, Real-time measurements of vesicle-SNARE recycling in synapses of the central nervous system, Nat. Cell Biol. 2 (2000) 197–204.
[25] M. Montal, Botulinum neurotoxin: a marvel of protein design, Annu. Rev. Biochem. 79 (2010) 591–617.
[26] A. Fischer, M. Montal, Molecular dissection of botulinum neurotoxin reveals interdomain chaperone function, Toxicon 75 (2013) 101–107.
[27] D.H. Hoch, M. Romero-Mira, B.E. Ehrlich, A. Finkelstein, B.R. DasGupta, L.L. Simpson, Channels formed by botulinum, tetanus, and diphtheria toxins in planar lipid bilayers: relevance to translocation of proteins across membranes, Proc. Natl. Acad. Sci. U. S. A. 82 (1985) 1692–1696.
[28] J.J. Donovan, J.L. Middlebrook, Ion-conducting channels produced by botulinum toxin in planar lipid membranes, Biochemistry 25 (1986) 2872–2876.
[29] C. Montecucco, G. Schiavo, Structure and function of tetanus and botulinum neurotoxins, Q. Rev. Biophys. 28 (1995) 423–472.
[30] L.K. Koriazova, M. Montal, Translocation of botulinum neurotoxin light chain protease through the heavy chain channel, Nat. Struct. Biol. 10 (2003) 13–18.
[31] A. Fischer, M. Montal, Single molecule detection of intermediates during botulinum neurotoxin translocation across membranes, Proc. Natl. Acad. Sci. U. S. A. 104 (2007) 10447–10452.
[32] A. Fischer, Y. Nakai, L.M. Eubanks, C.M. Clancy, W.H. Tepp, S. Pellett, T.J. Dickerson, E.A. Johnson, K.D. Janda, M. Montal, Bimodal modulation of the botulinum neurotoxin protein-conducting channel, Proc. Natl. Acad. Sci. U. S. A. 106 (2009) 1330–1335.
[33] A. Fischer, M. Montal, Crucial role of the disulfide bridge between botulinum neurotoxin light and heavy chains in protease translocation across membranes, J. Biol. Chem. 282 (2007) 29604–29611.
[34] R.E. Sheridan, Gating and permeability of ion channels produced by botulinum toxin types A and E in PC12 cell membranes, Toxicon 36 (1998) 703–717.
[35] S. Sun, S. Suresh, H. Liu, W.H. Tepp, E.A. Johnson, J.M. Edwardson, E.R. Chapman, Receptor binding enables botulinum neurotoxin B to sense low pH for translocation channel assembly, Cell Host Microbe 10 (2011) 237–247.
[36] S. Sun, W.H. Tepp, E.A. Johnson, E.R. Chapman, Botulinum neurotoxins B and E translocate at different rates and exhibit divergent responses to GT1b and low pH, Biochemistry 51 (2012) 5655–5662.
[37] M. Dalla Serra, I. Bernhart, P. Nordera, D. Di Giorgio, A. Ballio, G. Menestrina, Conductive properties and gating of channels formed by syringopeptin 25A, a bioactive lipodepsipeptide from *Pseudomonas syringae* pv. *syringae*, in planar lipid membranes, Mol. Plant Microbe, Interactions 12 (1999) 401–409.
[38] S. Parikh, B.R. Singh, Comparative membrane channel size and activity of botulinum neurotoxins A and E, Protein J. 26 (2007) 19–28.
[39] A. Fischer, C. Garcia-Rodriguez, I. Geren, J. Lou, J.D. Marks, T. Nakagawa, M. Montal, Molecular architecture of botulinum neurotoxin E revealed by single particle electron microscopy, J. Biol. Chem. 283 (2008) 3997–4003.
[40] A. Fischer, D.J. Mushrush, D.B. Lacy, M. Montal, Botulinum neurotoxin devoid of receptor binding domain translocates active protease, PLoS Pathog. 4 (2008), e1000245.
[41] G. Schiavo, F. Benfenati, B. Poulain, O. Rossetto, P. Polverino de Laureto, B.R. DasGupta, C. Montecucco, Tetanus and botulinum-B neurotoxins block neurotransmitter release by proteolytic cleavage of synaptobrevin, Nature 359 (1992) 832–835.
[42] G. Schiavo, E. Papini, G. Genna, C. Montecucco, An intact interchain disulfide bond is required for the neurotoxicity of tetanus toxin, Infect. Immun. 58 (1990) 4136–4141.
[43] A. de Paiva, B. Poulain, G.W. Lawrence, C.C. Shone, L. Tauc, J.O. Dolly, A role for the interchain disulfide or its participating thiols in the internalization of botulinum neurotoxin A revealed by a toxin derivative that binds to ecto-acceptors and inhibits transmitter release intracellularly, J. Biol. Chem. 268 (1993) 20838–20844.
[44] S. Bade, A. Rummel, C. Reisinger, T. Karnath, G. Ahnert-Hilger, H. Bigalke, T. Binz, Botulinum neurotoxin type D enables cytosolic delivery of enzymatically active cargo proteins to neurones via unfolded translocation intermediates, J. Neurochem. 91 (2004) 1461–1472.
[45] S. Eswaramoorthy, D. Kumaran, J. Keller, S. Swaminathan, Role of metals in the biological activity of *Clostridium botulinum* neurotoxins, Biochemistry 43 (2004) 2209–2216.
[46] M. Galloux, H. Vitrac, C. Montagner, S. Raffestin, M.R. Popoff, A. Chenal, V. Forge, D. Gillet, Membrane Interaction of botulinum neurotoxin A translocation (T) domain. The belt region is a regulatory loop for membrane interaction, J. Biol. Chem. 283 (2008) 27668–27676.
[47] F.N. Fu, D.D. Busath, B.R. Singh, Spectroscopic analysis of low pH and lipid-induced structural changes in type A botulinum neurotoxin relevant to membrane channel formation and translocation, Biophys. Chem. 99 (2002) 17–29.
[48] A. Puhar, E.A. Johnson, O. Rossetto, C. Montecucco, Comparison of the pH-induced conformational change of different clostridial neurotoxins, Biochem. Biophys. Res. Commun. 319 (2004) 66–71.
[49] C. Montecucco, G. Schiavo, J. Brunner, E. Duflot, P. Boquet, M. Roa, Tetanus toxin is labeled with photoactivatable phospholipids at low pH, Biochemistry 25 (1986) 919–924.
[50] C. Montecucco, G. Schiavo, B.R. Dasgupta, Effect of pH on the interaction of botulinum neurotoxins A, B and E with liposomes, Biochem. J. 259 (1989) 47–53.
[51] S. Zhang, A. Finkelstein, R.J. Collier, Evidence that translocation of anthrax toxin's lethal factor is initiated by entry of its N terminus into the protective antigen channel, Proc. Natl. Acad. Sci. U. S. A. 101 (2004) 16756–16761.
[52] T. Neumeyer, F. Tonello, F. Dal Molin, B. Schiffler, F. Orlik, R. Benz, Anthrax lethal factor (LF) mediated block of the anthrax protective antigen (PA) ion channel: effect of ionic strength and voltage, Biochemistry 45 (2006) 3060–3068.
[53] D. Basilio, L.D. Jennings-Antipov, K.S. Jakes, A. Finkelstein, Trapping a translocating protein within the anthrax toxin channel: implications for the secondary structure of permeating proteins, J. Gen. Physiol. 137 (2011) 343–356.
[54] M. Pirazzini, O. Rossetto, C. Bertasio, F. Bordin, C.C. Shone, T. Binz, C. Montecucco, Time course and temperature dependence of the membrane translocation of tetanus and botulinum neurotoxins C and D in neurons, Biochem. Biophys. Res. Commun. 430 (2013) 38–42.
[55] H. Li, A.D. Robertson, J.H. Jensen, Very fast empirical prediction and rationalization of protein pKa values, Proteins 61 (2005) 704–721.
[56] M. Pirazzini, T. Henke, O. Rossetto, S. Mahrhold, N. Krez, A. Rummel, C. Montecucco, T. Binz, Neutralisation of specific surface carboxylates speeds up translocation of botulinum neurotoxin type B enzymatic domain, FEBS Lett. 587 (2013) 3831–3836.
[57] J.W. Deutsch, R.B. Kelly, Lipids of synaptic vesicles: relevance to the mechanism of membrane fusion, Biochemistry 20 (1981) 378–385.
[58] R.W. Ledeen, M.F. Diebler, G. Wu, Z.H. Lu, H. Varoqui, Ganglioside composition of subcellular fractions, including pre- and postsynaptic membranes, from Torpedo electric organ, Neurochem. Res. 18 (1993) 1151–1155.
[59] P. Nordera, M.D. Serra, G. Menestrina, The adsorption of *Pseudomonas aeruginosa* exotoxin A to phospholipid monolayers is controlled by pH and surface potential, Biophys. J. 73 (1997) 1468–1478.
[60] A. van Dalen, B. de Kruijff, The role of lipids in membrane insertion and translocation of bacterial proteins, Biochim. Biophys. Acta 1694 (2004) 97–109.
[61] V.E. Bychkova, R.H. Pain, O.B. Ptitsyn, The 'molten globule' state is involved in the translocation of proteins across membranes? FEBS Lett. 238 (1988) 231–234.
[62] O.B. Ptitsyn, R.H. Pain, G.V. Semisotnov, E. Zerovnik, O.I. Razgulyaev, Evidence for a molten globule state as a general intermediate in protein folding, FEBS Lett. 262 (1990) 20–24.
[63] F.G. van der Goot, J.M. Gonzalez-Manas, J.H. Lakey, F. Pattus, A 'molten-globule' membrane-insertion intermediate of the pore-forming domain of colicin A, Nature 354 (1991) 408–410.
[64] R. Kukreja, B. Singh, Biologically active novel conformational state of botulinum, the most poisonous poison, J. Biol. Chem. 280 (2005) 39346–39352.
[65] J. Wang, T.H. Zurawski, J. Meng, G. Lawrence, W.M. Olango, D.P. Finn, L. Wheeler, J.O. Dolly, A dileucine in the protease of botulinum toxin A underlies its long-lived neuroparalysis: transfer of longevity to a novel potential therapeutic, J. Biol. Chem. 286 (2011) 6375–6385.
[66] R. Ratts, H. Zeng, E.A. Berg, C. Blue, M.E. McComb, C.E. Costello, J.C. vanderSpek, J.R. Murphy, The cytosolic entry of diphtheria toxin catalytic domain requires a host cell cytosolic translocation factor complex, J. Cell Biol. 160 (2003) 1139–1150.

[67] A.E. Lang, K. Ernst, H. Lee, P. Papatheodorou, C. Schwan, H. Barth, K. Aktories, The chaperone Hsp90 and PPIases of the cyclophilin and FKBP families facilitate membrane translocation of *Photorhabdus luminescens* ADP-ribosyltransferases, Cell. Microbiol. 16 (2014) 490–503.
[68] K. Ernst, S. Langer, E. Kaiser, C. Osseforth, J. Michaelis, M.R. Popoff, C. Schwan, K. Aktories, V. Kahlert, M. Malesevic, C. Schiene-Fischer, H. Barth, Cyclophilin-facilitated membrane translocation as pharmacological target to prevent intoxication of mammalian cells by binary clostridial actin ADP-ribosylated toxins, J. Mol. Biol. 427 (2015) 1224–1238.
[69] E. Park, T.A. Rapoport, Bacterial protein translocation requires only one copy of the SecY complex in vivo, J. Cell Biol. 198 (2012) 881–893.
[70] A. Finkelstein, K.J. Oh, L. Senzel, M. Gordon, R.O. Blaustein, R.J. Collier, The diphtheria toxin channel-forming T-domain translocates its own NH2-terminal region and the catalytic domain across planar phospholipid bilayers, Int. J. Med. Microbiol.IJMM 290 (2000) 435–440.
[71] M. Gordon, A. Finkelstein, The number of subunits comprising the channel formed by the T domain of diphtheria toxin, J. Gen. Physiol. 118 (2001) 471–480.
[72] K. Wohlfarth, H. Goschel, J. Frevert, R. Dengler, H. Bigalke, Botulinum A toxins: units versus units, Naunyn Schmiedebergs Arch. Pharmakol. 355 (1997) 335–340.
[73] C. Rasetti-Escargueil, Y. Liu, P. Rigsby, R.G. Jones, D. Sesardic, Phrenic nerve-hemidiaphragm as a highly sensitive replacement assay for determination of functional botulinum toxin antibodies, Toxicon 57 (2011) 1008–1016.
[74] D. Rodriguez-Larrea, H. Bayley, Protein co-translocational unfolding depends on the direction of pulling, Nat. Commun. 5 (2014) 4841.
[75] E.S. Arner, A. Holmgren, Physiological functions of thioredoxin and thioredoxin reductase, Eur. J. Biochem. 267 (2000) 6102–6109.
[76] Y. Meyer, B.B. Buchanan, F. Vignols, J.P. Reichheld, Thioredoxins and glutaredoxins: unifying elements in redox biology, Annu. Rev. Genet. 43 (2009) 335–367.
[77] E.M. Hanschmann, J.R. Godoy, C. Berndt, C. Hudemann, C.H. Lillig, Thioredoxins, glutaredoxins, and peroxiredoxins—molecular mechanisms and health significance: from cofactors to antioxidants to redox signaling, Antioxid. Redox Signal. 19 (2013) 1539–1605.
[78] M. Pirazzini, F. Bordin, O. Rossetto, C.C. Shone, T. Binz, C. Montecucco, The thioredoxin reductase-thioredoxin system is involved in the entry of tetanus and botulinum neurotoxins in the cytosol of nerve terminals, FEBS Lett. 587 (2013) 150–155.
[79] M. Pirazzini, D. Azarnia Tehran, G. Zanetti, A. Megighian, M. Scorzeto, S. Fillo, C.C. Shone, T. Binz, O. Rossetto, F. Lista, C. Montecucco, Thioredoxin and its reductase are present on synaptic vesicles, and their inhibition prevents the paralysis induced by botulinum neurotoxins, Cell Rep. 8 (2014) 1870–1878.
[80] L. Schnell, L. Dmochewitz-Kück, P. Feigl, C. Montecucco, H. Barth, Thioredoxin reductase inhibitor auranofin prevents membrane transport of diphtheria toxin into the cytosol and protects human cells from intoxication, Toxicon (2015)http://dx.doi.org/10.1016/j.toxicon.2015.04.012 pii: S0041-0101(15)00109-9 [Epub ahead of print].
[81] E. Papini, R. Rappuoli, M. Murgia, C. Montecucco, Cell penetration of diphtheria toxin. Reduction of the interchain disulfide bridge is the rate-limiting step of translocation in the cytosol, J. Biol. Chem. 268 (1993) 1567–1574.
[82] R.B. Sutton, D. Fasshauer, R. Jahn, A.T. Brunger, Crystal structure of a SNARE complex involved in synaptic exocytosis at 2.4 A resolution, Nature 395 (1998) 347–353.
[83] T.C. Sudhof, J. Rizo, Synaptic vesicle exocytosis, Cold Spring Harb. Perspect. Biol. 3 (2011).
[84] A.T. Brunger, A. Rummel, Receptor and substrate interactions of clostridial neurotoxins, Toxicon 54 (2009) 550–560.
[85] T. Binz, Clostridial neurotoxin light chains: devices for SNARE cleavage mediated blockade of neurotransmission, Curr. Top. Microbiol. Immunol. 364 (2013) 139–157.
[86] Y. Humeau, F. Doussau, N.J. Grant, B. Poulain, How botulinum and tetanus neurotoxins block neurotransmitter release, Biochimie 82 (2000) 427–446.
[87] T. Binz, S. Sikorra, S. Mahrhold, Clostridial neurotoxins: mechanism of SNARE cleavage and outlook on potential substrate specificity reengineering, Toxins 2 (2010) 665–682.
[88] A. Fischer, Synchronized chaperone function of botulinum neurotoxin domains mediates light chain translocation into neurons, Curr. Top. Microbiol. Immunol. 364 (2013) 115–137.

5.1.3 Snake and spider toxins induce a rapid recovery of function of botulinum neurotoxin paralysed neuromuscular junction

Elisa Duregotti[1], Giulia Zanetti[1], Michele Scorzeto[1], Aram Megighian[1], Cesare Montecucco[1,2], Marco Pirazzini[1] and Michela Rigoni[1]

[1]Department of Biomedical Sciences, University of Padua, Via U. Bassi 58/B, 35131 Padova, Italy;

[2]Institute for Neuroscience, National Research Council, Via U. Bassi 58/B, 35131 Padova, Italy

Duregotti E. *et al.* Snake and Spider Toxins Induce a Rapid Recovery of Function of Botulinum Neurotoxin Paralysed Neuromuscular Junction.
Toxins (Basel), 7(12):5322-36. doi: 10.3390/toxins7124887 (2015).

toxins

MDPI

Article

Snake and Spider Toxins Induce a Rapid Recovery of Function of Botulinum Neurotoxin Paralysed Neuromuscular Junction

Elisa Duregotti [1], Giulia Zanetti [1], Michele Scorzeto [1], Aram Megighian [1], Cesare Montecucco [1,2], Marco Pirazzini [1,*] and Michela Rigoni [1,*]

Received: 23 October 2015; Accepted: 30 November 2015; Published: 8 December 2015
Academic Editor: Wolfgang Wüster

[1] Department of Biomedical Sciences, University of Padua, Via U. Bassi 58/B, 35131 Padova, Italy; elisa.duregotti@gmail.com (E.D.); gzanetti89@gmail.com (G.Z.); scorzeto.michele@gmail.com (M.S.); aram.megighian@unipd.it (A.M.); cesare.montecucco@gmail.com (C.M.)
[2] Institute for Neuroscience, National Research Council, Via U. Bassi 58/B, 35131 Padova, Italy
* Correspondence: marcopiraz@gmail.com (M.P.); rigonimic@gmail.com (M.R.); Tel.: +39-049-827-6057 (M.P.); +39-049-827-6077 (M.R.); Fax: +39-049-827-6049 (M.P. & M.R.)

Abstract: Botulinum neurotoxins (BoNTs) and some animal neurotoxins (β-Bungarotoxin, β-Btx, from elapid snakes and α-Latrotoxin, α-Ltx, from black widow spiders) are pre-synaptic neurotoxins that paralyse motor axon terminals with similar clinical outcomes in patients. However, their mechanism of action is different, leading to a largely-different duration of neuromuscular junction (NMJ) blockade. BoNTs induce a long-lasting paralysis without nerve terminal degeneration acting via proteolytic cleavage of SNARE proteins, whereas animal neurotoxins cause an acute and complete degeneration of motor axon terminals, followed by a rapid recovery. In this study, the injection of animal neurotoxins in mice muscles previously paralyzed by BoNT/A or /B accelerates the recovery of neurotransmission, as assessed by electrophysiology and morphological analysis. This result provides a proof of principle that, by causing the complete degeneration, reabsorption, and regeneration of a paralysed nerve terminal, one could favour the recovery of function of a biochemically- or genetically-altered motor axon terminal. These observations might be relevant to dying-back neuropathies, where pathological changes first occur at the neuromuscular junction and then progress proximally toward the cell body.

Keywords: botulinum neurotoxins; animal neurotoxins; nerve terminals degeneration; mouse; DAS assay; paralysis; neuroexocytosis

1. Introduction

Botulinum neurotoxins (BoNTs) produced by Clostridia are responsible for the flaccid paralysis of botulism [1,2]. Many different BoNTs are known and are grouped into seven serotypes (BoNT/A to BoNT/G). They include a metalloprotease domain that specifically cleaves three essential components of the synaptic vesicle fusion machinery leading to a persistent, but reversible, blockade of neurotransmission with no morphological alterations of the neuromuscular junction (NMJ) [2–4]. Indeed, most botulism patients survive if their respiration is mechanically supported. The duration of BoNTs-induced neuroparalysis depends on the BoNT serotype and on the toxin dose [5]. BoNT/A and BoNT/C induce the longest paralysis (up to many months), whilst BoNT/E and /F cause the shortest one (few weeks) [6–8]. The same occurs in rats and mice, although functional recovery is 3–4 times faster than in humans [5,9,10].

A similar peripheral neuroparalysis is also caused by some animal neurotoxins which induce a reversible degeneration of motor axon terminals. Their use provides a relevant model for the molecular characterization of the neurorepair process after injury [11]. These animal presynaptic neurotoxins include α-Latrotoxin (α-Ltx), a pore-forming toxin contained in the black widow spider venom (genus Latrodectus) [12,13], and β-Bungarotoxin (β-Btx, from the Taiwan krait *Bungarus multinctus* venom) [14]. β-Btx belongs to a family of snake neurotoxins endowed with phospholipase A2 activity, named SPANs [15,16]. Despite their different biochemical activities, intoxication by these animal neurotoxins results in a calcium overload inside motor axon terminals that, in turn, triggers a massive neuroexocytosis of synaptic vesicles and the progressive degeneration of the nerve endings [17,18]. Very remarkably, such an effect is strictly limited to the unmyelinated end-plate and is characterized by mitochondria failure and cytoskeletal fragmentation [11,19,20]. Nevertheless, the consequent neuromuscular paralysis is completely reversible: in rodents, nerve terminal regeneration and functional re-innervation are fully restored within a few days [21,22], in a process orchestrated by muscle, Schwann cells, and the basal membrane [23,24]. In humans, the peripheral neuroparalysis induced by the envenomation with snake venoms containing SPANs is functionally reversed within 3–6 weeks [25,26].

Despite the fact that these animal neurotoxins cause a complete disappearance of motor axon terminals, whereas BoNTs do not, the functional recovery in the first case is much faster than in the latter [21,22,27–30].

Based on these premises, we decided to investigate whether the local administration of α-Ltx or β-Btx could rapidly reverse the otherwise long-lasting effect induced by BoNTs in mice, leading to functional recovery from botulism paralysis. Functional and biochemical read-outs clearly indicate that a single injection of animal neurotoxins switches the kinetics of recovery from several weeks to few days, providing a proof of principle that any form of biochemically/genetically dysfunctional motor axon terminal can be restored by inducing a degeneration/regeneration process.

2. Results

2.1. α -Latrotoxin or β–Bungarotoxin Injection Accelerates the Recovery from BoNTs-Induced Paralysis

As a first approach to evaluate the effect of animal neurotoxins on the functional recovery of the BoNTs-poisoned NMJs, we took advantage of a well-established model for assessing the kinetics of rescue from BoNTs-induced muscular paralysis: the Digit Abduction Score (DAS) assay. This method is widely used to evaluate the severity and duration of local muscle weakening following the intramuscular injection of BoNTs into mouse hind limbs. We used the two BoNT serotypes most frequently associated to human botulism and that are commercially available for human therapy: BoNT/A and BoNT/B [2,31,32].

As shown by the black trace in Figure 1A, a minimal amount of BoNT/A induces a long lasting paralysis of mice hind limbs. Notably, the effect has a maximum severity (DAS $\geqslant$ 3.5) for at least five days, with the subsequent recovery—characterized by a slow, though progressive, increase in the capability of toes to abduct—taking more than 20 days to be substantially completed (DAS $\leqslant$ 0.5). The other two traces show that α-Ltx (light gray) and β-Btx (dark gray), injected when BoNT/A has reached its maximum effect (three days after injection, indicated as day zero), significantly shorten the time needed to rescue from paralysis: recovery (DAS $\leqslant$ 0.5) is indeed achieved well within nine days. Furthermore, the severity of paralysis drops very quickly from the maximum score, at the time of animal toxin injection, to a very low value (DAS $\leqslant$ 1), where hind-limb muscles are still weak but no longer paralyzed, allowing an almost normal control of toe movements. Figure 1B shows that a very similar outcome was obtained using BoNT/B: in this case, even though the maximum severity is likewise achieved, the paralysis lasts much shorter, being substantially extinguished (DAS $\leqslant$ 0.5) within seven days. Nevertheless, DAS scores of double-injected mice (α-Ltx or β-Btx 24 h after BoNT/B, indicated as day zero) return to baseline in three days, showing again a significantly faster

recovery. The difference between single- and double-injected animals is less remarkable in the case of BoNT/B treated animals with respect to those treated with BoNT/A, but this is the immediate consequence of the different duration of action of the two BoNT serotypes. In fact, BoNT/B-induced paralysis is about three times shorter than that caused by BoNT/A [32].

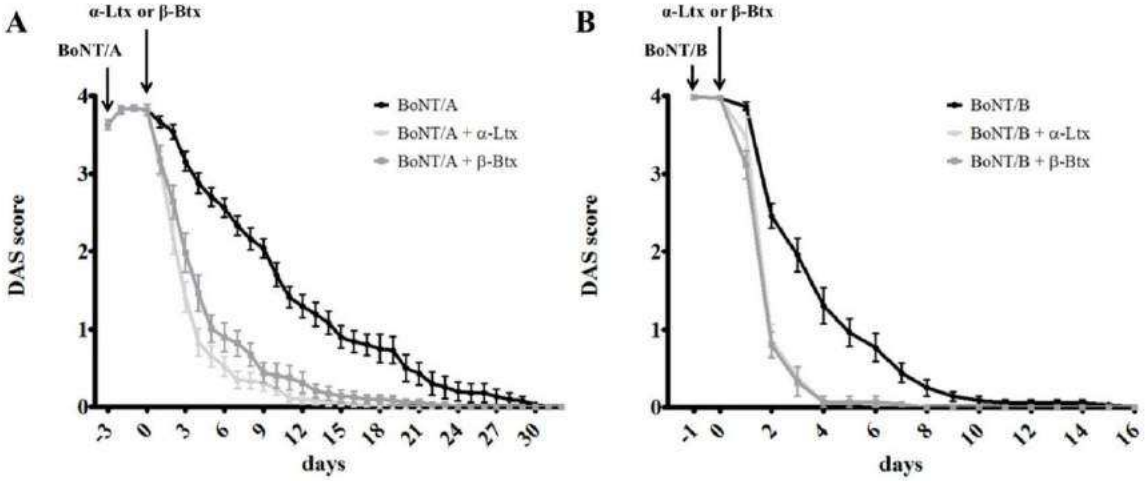

Figure 1. Digit Abduction Score (DAS) assay on single- or double-injected mice. Sub-lethal doses of BoNT/A (**A**) or BoNT/B (**B**) were i.m. injected in mice hind limbs; once complete paralysis was achieved (within 12 h from injection, DAS = 4), two groups of mice received a second i.m. injection of α-Ltx or β-Btx (three days after BoNT/A and 24 h after BoNT/B administration). The rescue from paralysis was monitored over time, until complete recovery was attained (DAS = 0). Representative experiments, $N = 10$ mice for each condition. Error bars represent s.e.m.

2.2. *Synaptic Activity of BoNT-Paralyzed Muscles is Restored Earlier Following α-Latrotoxin or β-Bungarotoxin Injection*

Though very reliable, DAS assay provides a more qualitative than quantitative read-out of muscle paralysis. Therefore, to monitor the functional recovery of BoNTs-poisoned nerve terminals in a more quantitative way, we performed electrophysiological recordings (ER) on soleus NMJs of single- or double-poisoned mice at different time points after treatments. The experiment was conducted as in the case of DAS assay, but at indicated times soleus muscles were collected and evoked junction potentials (EJPs) were recorded *ex vivo* in order to determine the functional state of single NMJs.

Figure 2 reports that, upon a supramaximal electric stimulation, neuroexocytosis occurs, as assessed by the recorded post synaptic depolarization (white bar). As expected, and in agreement with the DAS assay, BoNT/A inhibits the release of acetylcholine (Ach) soon after administration, indeed poisoned solei do not generate EJPs (day one, black bar). The same effect is observed at day one in double-injected muscles, as well as in those treated with the sole animal neurotoxins (Figure 2C), and is fully consistent with their degenerating effect on peripheral nerve endings [11]. However, four days after the injection of the animal toxins, which is a time window sufficient for degeneration/regeneration of nerve terminals to occur (Figure 2C), double-injected muscles display a partial restoration of the synaptic activity. The same is not observed in muscles injected with only BoNT/A, which at the same time point are still completely paralyzed (Figure 2A). Importantly, such a profile is maintained in the following time points, where double-injected muscles show EJPs of higher amplitudes compared to those of single-injected ones. Notably, 30 days after animal toxin administration, the functionality of double-injected muscles is substantially restored, while solei treated with only BoNT/A respond to nerve stimulation with an average depolarization which is only about 50% with respect to control ones. This faster recovery of NMJs functionality is not restricted to

muscles paralyzed by BoNT/A, but can be extended also to BoNT/B-poisoned ones (Figure 2B), even though in this case the overall rescue profile is faster, as BoNT/B-induced paralysis has, in itself, a shorter duration [32].

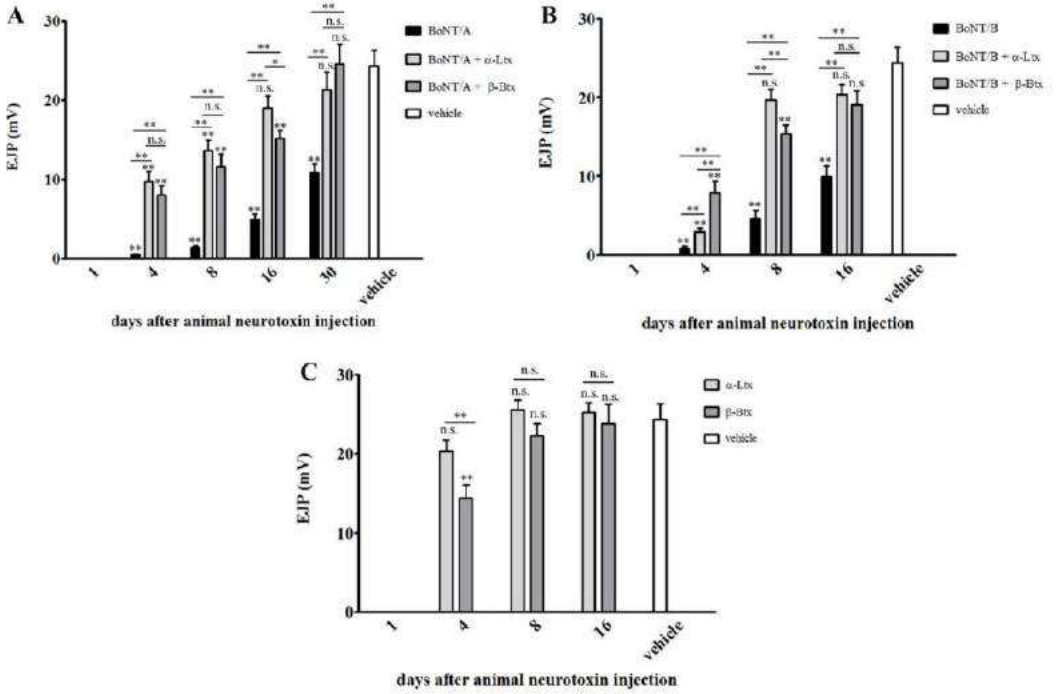

Figure 2. Electrophysiological recordings on single- or double-injected soleus muscles. Sub-lethal doses of α-Ltx or β-Btx were administered i.m. in mice hind limbs previously injected at the same site with BoNT/A (**A**, three days earlier) or BoNT/B (**B**, 24 h earlier). Soleus muscles were collected at different time points and processed for electrophysiological recordings. Muscles injected with BoNTs plus animal neurotoxins recover faster than BoNTs-treated ones. The same analysis was performed on solei injected with animal neurotoxins only (**C**). Bars represent the average EJP amplitude of 45 muscle fibers from three different mice per condition; paired *t*-test, * $p < 0.01$, ** $p < 0.001$ *versus* control (vehicle) or other conditions of the same time point; error bars represent s.e.m. n.s.= not significative.

As a control, ER were also performed on muscles injected with α-Ltx or β-Btx alone: as shown in Figure 2C, the complete recovery from paralysis is achieved more rapidly than in double-injected muscles (Figure 2A,B). This could be due to some residual activity of BoNTs, which might diffuse away from the site of injection to reach the blood circulation, being therefore able to re-affect regenerated nerve terminals, slightly impairing neurotransmission. This is consistent with the fact that BoNTs can be found in the general circulation of botulism patients for many days after the onset of symptoms development [33,34].

2.3. *Fluorescence Microscopy Analysis of SNAP25 and VAMP1 Turn-Over at Single- or Double-Poisoned NMJs*

It is now well documented that BoNT-induced neuroparalysis is a direct consequence of the specific cleavage of different SNARE proteins by the metalloprotease activity of the toxins. Specifically, BoNT/B removes a large cytosolic fragment of VAMP, thus preventing the formation of the SNARE complex, whereas BoNT/A cleaves few residues from the *C*-terminal of SNAP25: the resulting truncated SNAP25 (t-SNAP25) can still form stable SNARE complexes, which are although unable to mediate neuroexocytosis [3,5]. This can be ascribed to the inability of t-SNAP25 to correctly

interact with other SNARE complexes, preventing the assembly of the SNARE super-complex necessary to mediate synaptic vesicles fusion [5,35,36].

Being the blockade of neurotransmission by BoNTs the result of SNARE components proteolysis, we followed the kinetics of SNARE proteins cleavage by means of immunohistochemistry, using appropriate antibodies in order to characterize at a molecular level the effects of animal neurotoxins on BoNTs-poisoned NMJs. Importantly, this analysis was performed on muscles previously processed for ER, permitting a direct comparison of their functional state with SNARE proteins cleavage. For this purpose, in the case of BoNT/A-poisoned muscles we took advantage of a well characterized antibody that only recognizes the BoNT/A-cleaved form of SNAP25 [31], whereas BoNT/B-poisoned ones were labelled with an antibody which only binds the intact form of VAMP1 [37], as this is the main VAMP isoform present at NMJ [38]. As a control of their integrity state, presynaptic nerve terminals were also stained for neurofilaments (NF) and SNAP25 (using an antibody which recognizes both intact and truncated SNAP25, indicated as $SNAP25_{total}$), whereas fluorescent α-Bungarotoxin (α-BTX) was used to visualize post-synaptic specializations.

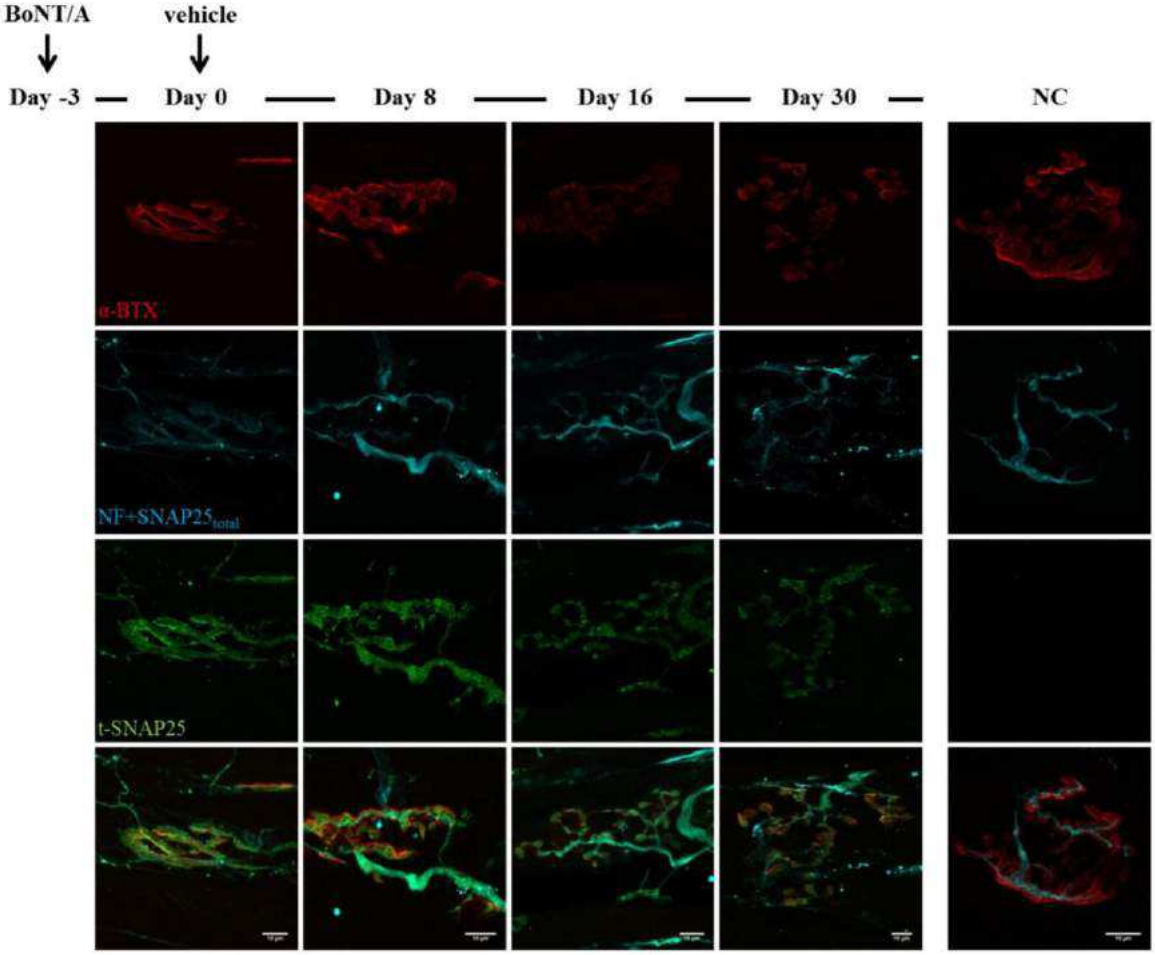

Figure 3. Time course of SNAP25 cleavage by BoNT/A. Soleus muscles injected with BoNT/A were dissected at different time points, analysed by electrophysiology and then processed for indirect immunohistochemistry. Day zero refers to NMJs treated for three days with BoNT/A (at day zero a second injection with animal neurotoxins was performed, see Figures 4 and 5). A strong staining of BoNT/A-cleaved SNAP25 (t-SNAP25) is detectable at NMJs from the very beginning of the analysis, and persists, though with decreasing intensity, until day 30. In untreated muscles, t-SNAP25 is undetectable (NC: negative control, NF: neurofilaments). Bar = 10 μm.

As shown in Figure 3, soon after BoNT/A injection t-SNAP25 starts accumulating at poisoned NMJs, and the staining persists until the end of the kinetics, although slowly decreasing its intensity. As expected, t-SNAP25 antibody does not cross-react with intact SNAP25, since no staining is detectable at untreated NMJs. As previously reported, chemically denervated NMJs sprout terminal and nodal processes (see Figure 3, day zero), that become longer and widespread over time [39]; in addition, paralyzed NMJs lose their typical and well-defined shape, and the post-synaptic staining of Ach receptors becomes progressively weaker and fragmented. A different scenario arises in double-injected muscles (Figures 4 and 5): 24 h after animal neurotoxins administration (injected three days after BoNT/A), NMJs have degenerated, as proven by the disappearance of neurofilaments, intact SNAP25 and t-SNAP25. Importantly, by day eight all motor axon terminals have regenerated, as shown by the staining of newly-synthetized SNAP25 and NF. Noteworthy, here t-SNAP25 is completely absent, suggesting that the degeneration "cleared" nerve terminals from BoNT/A L chains, neutralizing its poisonous effects. Moreover, the post-synaptic staining of NMJs is much more preserved than in muscles injected with only BoNT/A: this might be due to the trophic effect of Ach, whose release is earlier restored in double-injected solei (Figure 2), thus preventing the disassembly of Ach receptors-clusters forming post-synaptic specializations.

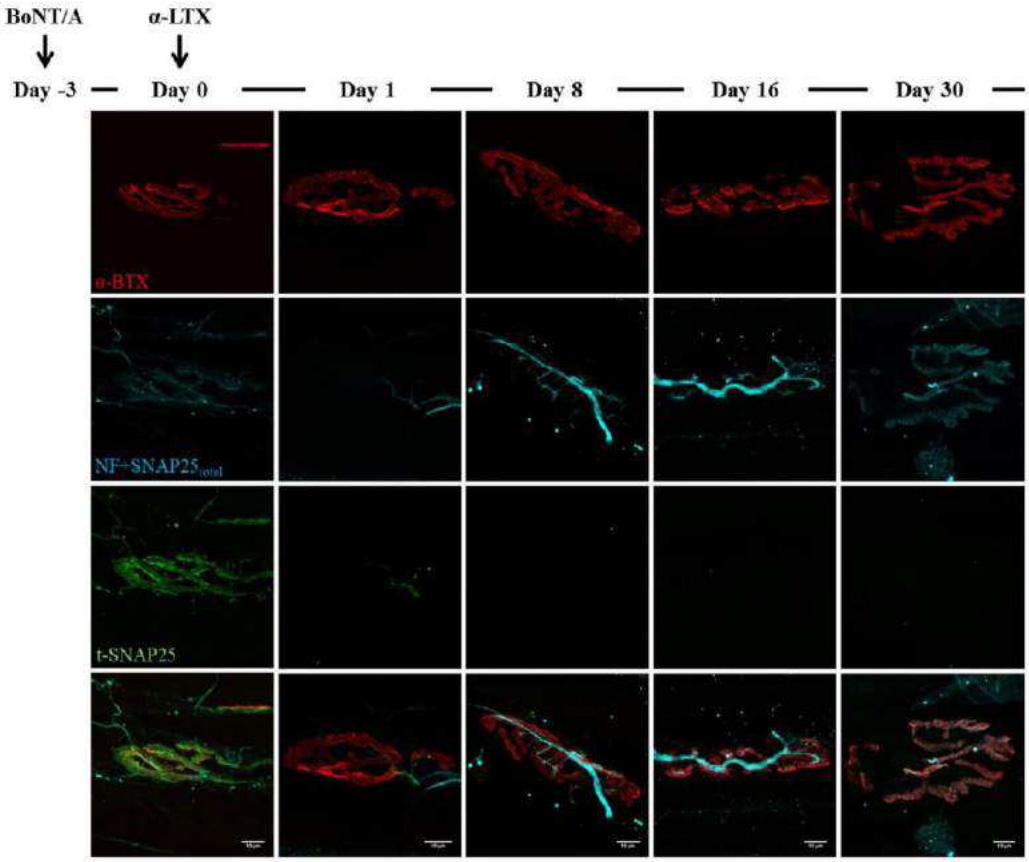

Figure 4. BoNT/A-cleaved SNAP25 turn-over at α-Ltx-injected NMJ. α-Ltx was administered i.m. in mice hind limbs 3 days after the injection of BoNT/A at the same site (day zero). Immunohistochemistry was then performed at different time points on soleus muscles previously processes for electrophysiology. As shown in the panel, the acute degeneration of nerve terminals is induced within 24 h from α-Ltx injection; at day eight, regeneration is achieved as demonstrated by the re-appearance of the $SNAP25_{total}$ and neurofilaments (NF) staining. However, no t-SNAP25 is detectable at regenerated NMJs throughout the time-course of the experiment. Bar = 10 μm.

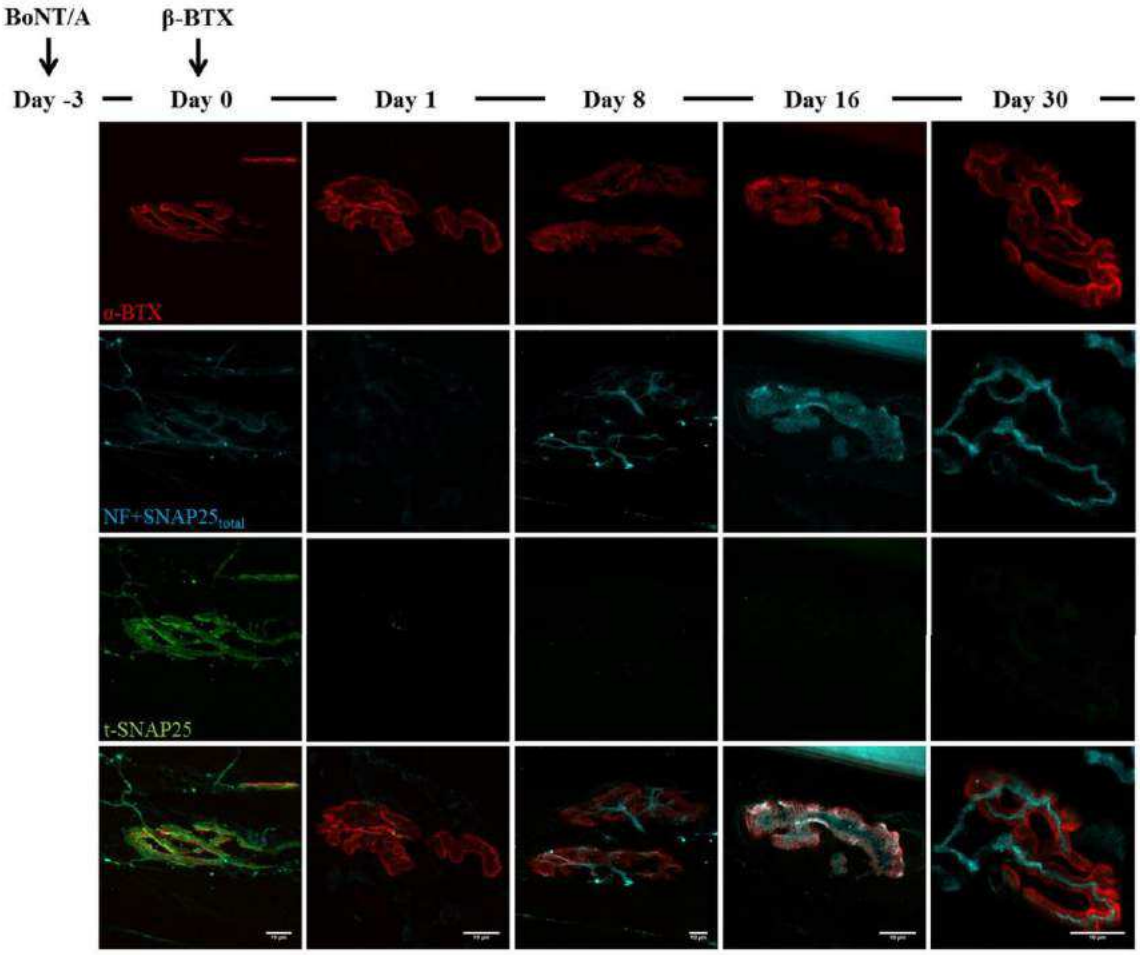

Figure 5. BoNT/A-cleaved SNAP25 turn-over at β-Btx-injected NMJ. β-Btx was administered i.m. in mice hind limbs three days after a first injection of BoNT/A at the same site. Immunohistochemistry was then performed at different time points on soleus muscles previously processes for electrophysiology. Similarly to α-Ltx, β-Btx induces an acute degeneration of nerve terminals within 24 h, followed by a complete regeneration. Again, the staining of t-SNAP25 in no more detectable at regenerated motor axon terminals. Bar = 10 μm.

Similar outcomes are observed in BoNT/B-treated mice: as expected, VAMP1 staining disappears soon after BoNT/B injection, and newly synthetized VAMP1 starts to be detectable starting from day 16 (Figure 6). Again, many neuronal sprouts can be seen at late time points, when paralyzed NMJs also become elongated and shapeless, though to a lesser extent than those treated with BoNT/A. When α-Ltx or β-Btx are administered, nerve terminals degenerate, and only the post-synaptic labelling is detectable at NMJs (Figures 7 and 8 day one). However, a rapid and complete regeneration takes place by day four, as assessed by the reappearance of the presynaptic markers SNAP25 and neurofilaments, as well as of VAMP1. Notably, the synaptic activity recovery parallels the reappearance of VAMP1 staining, which becomes more and more brilliant over time reaching control level by day 16, when NMJs perform indistinguishably from that of control muscles (Figure 2B).

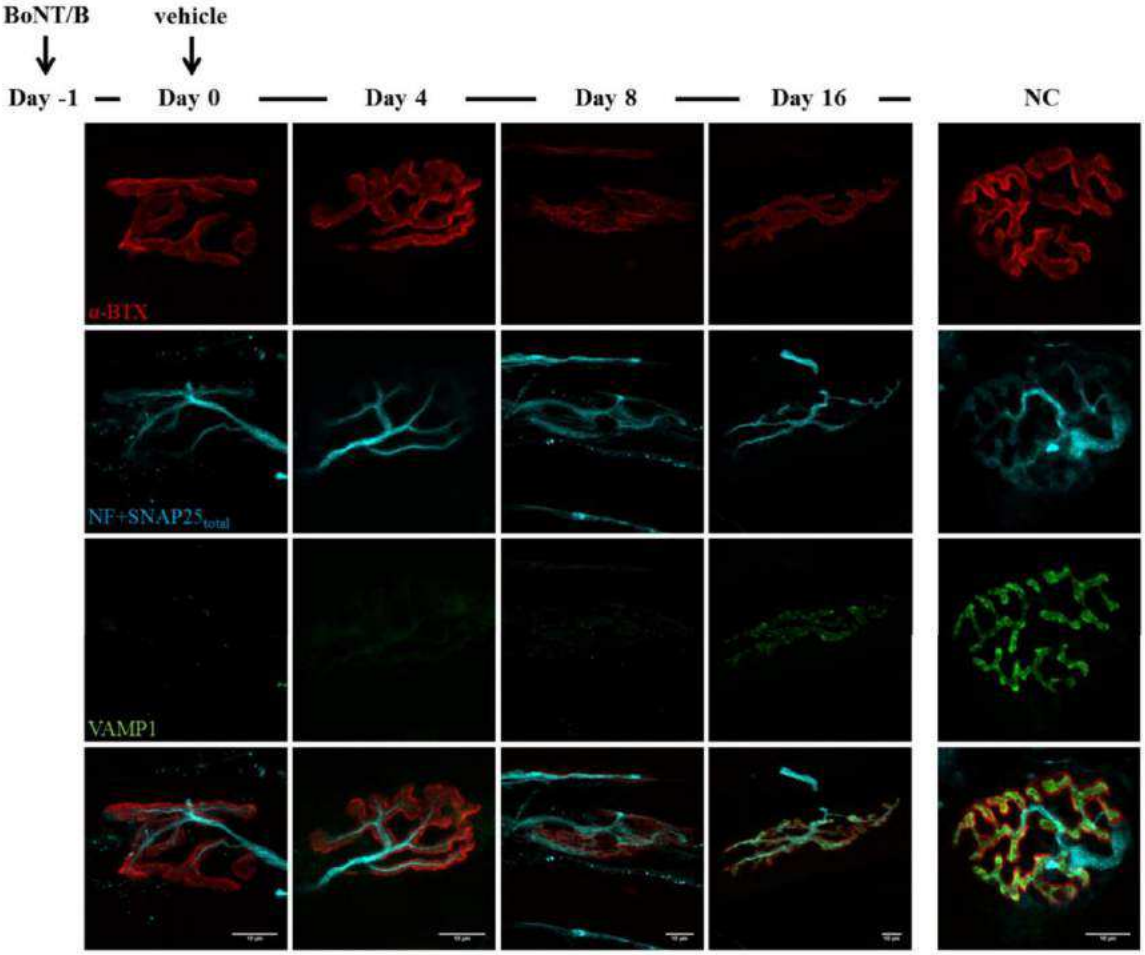

Figure 6. Time course of VAMP1 cleavage by BoNT/B. Soleus muscles injected with BoNT/B were dissected at different time points, analysed by electrophysiology and then processed for indirect immunohistochemistry. Day zero refers to NMJs treated for 24 h with BoNT/B (at day zesro a second injection with animal neurotoxins was performed, see Figures 7 and 8). VAMP1 staining, which is brightly present at untreated NMJs, disappears soon after BoNT/B injection and starts reappearing by day 16. Bar = 10 μm.

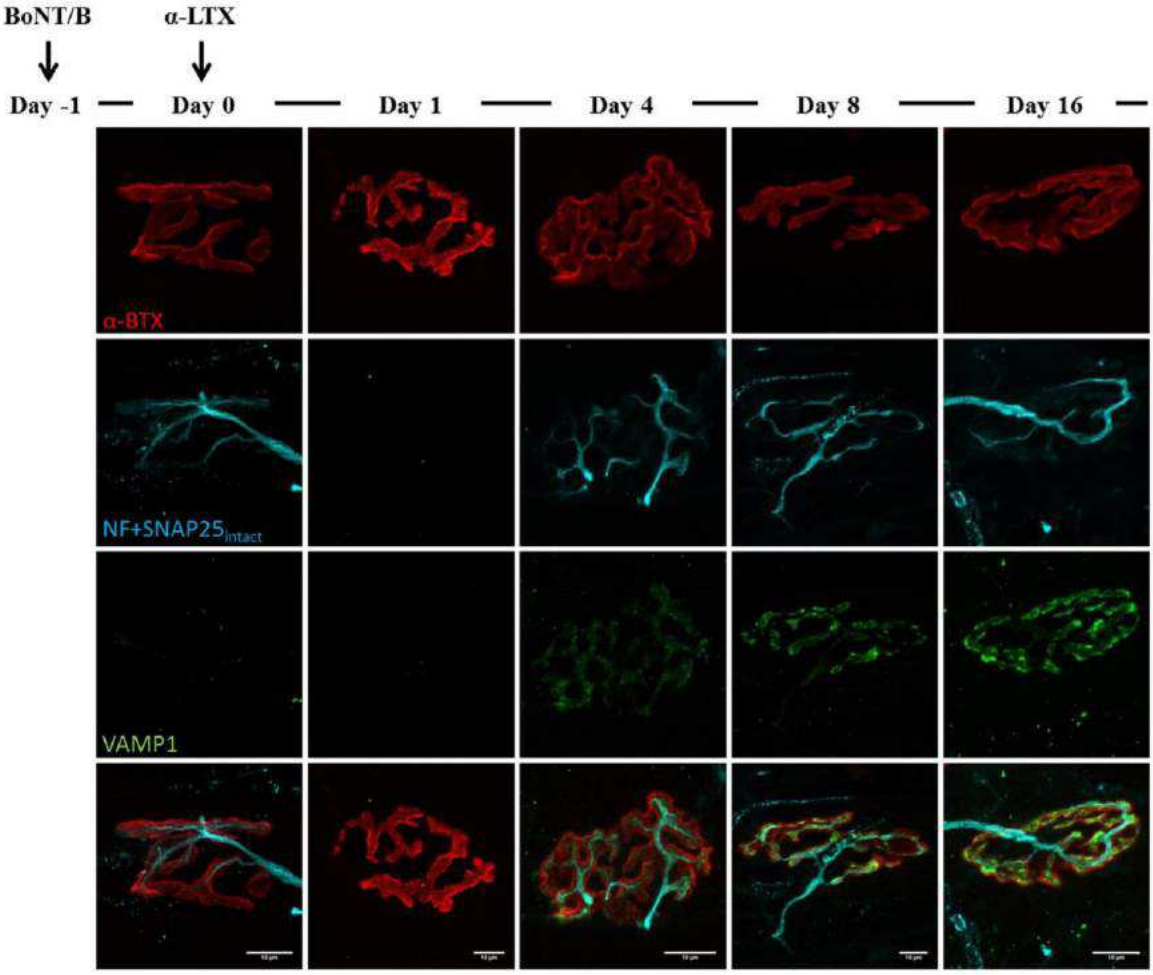

Figure 7. VAMP1 reappearance following α-Ltx injection at BoNT/B-poisoned NMJs. α-Ltx was administered i.m. in mice hind limbs 24 h after BoNT/B injection. Soleus muscles were then processed for immunohistochemistry after electrophysiology. Within 24 h from α-Ltx injection, nerve terminals completely degenerate, as demonstrated by the disappearance of $SNAP25_{total}$ and neurofilaments (NF) stainings; however, by day four newly-regenerated axon terminals show a clear labelling of VAMP1, which becomes more brilliant and defined over time. Bar = 10 μm.

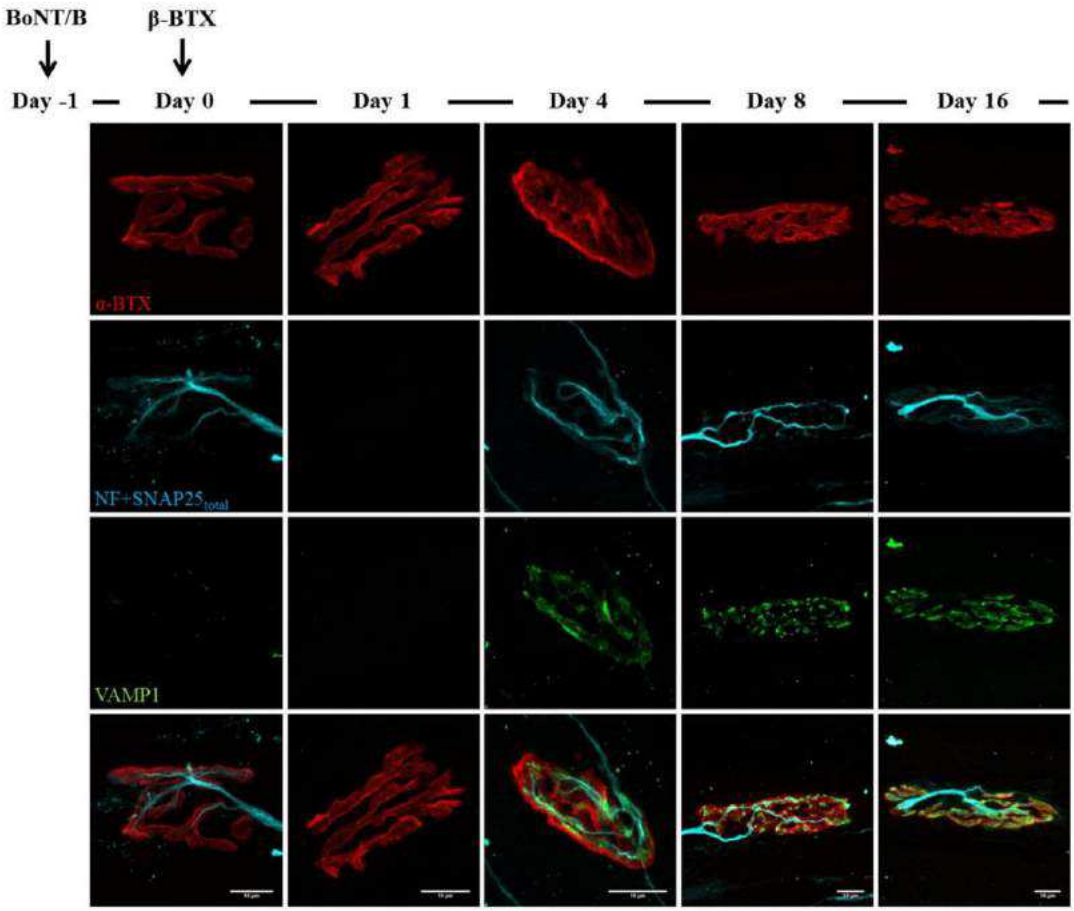

Figure 8. VAMP1 reappearance following β-Btx injection at BoNT/B-poisoned NMJs. β-Btx was administered i.m. in mice hind limbs 24 h after BoNT/B injection. Soleus muscles were then processed for immunohistochemistry after electrophysiological recordings. Similarly to α-Ltx, regeneration of nerve terminals takes place by day four and is paralleled by the re-appearance of VAMP1 staining at NMJs. Bar = 10 μm.

3. Discussion

Several peripheral human pathologies are due to biochemical lesions of motor axon terminals, caused by a genetic alteration or by exogenous agents. In non-cell autonomous and dying-back axonopathies such as ALS (amyotrophic lateral sclerosis) and autoimmune neuropathies, many molecular changes influencing motor neurons degeneration occur at the NMJ at the very early stages of the disease, and then progress along the axon leading to denervation and irreversible paralysis [40–43]. Here, we aimed at providing a proof of principle that a NMJ, biochemically-lesioned in its motor axon terminal, can be returned to functionality by operating a surgical removal of the terminal itself, followed by its re-growth under the stimulus and guidance of the basal membrane, the perisynaptic Schwann cells and the muscle fibre. As a biochemical damage, we chose one which has been well defined in the last 20 years, *i.e.*, the cleavage of a SNARE protein by a BoNT, which leads to long lasting but totally reversible paralysis of peripheral nerve terminals [2]. We have extended the study to the two BoNT serotypes that are the main responsible of human botulism and, at the same time, are used in the therapy of human pathological conditions characterized by hyperfunctionality of peripheral nerve terminals [32,44–46]. BoNT/A cleaves the C-terminus of SNAP25, whilst BoNT/B removes the major part of the cytosolic domain of the integral synaptic vesicle protein VAMP [3,16]. Both proteins are essential components of the SNARE complex, the nanomachine which mediates neurotransmitter release: for this reason, their cleavage leads to the

persistent paralysis that is the hallmark of botulism [5,47,48]. To perform the surgical removal of the motor axon terminals, we used two neurotoxins that bind specifically to the presynaptic plasma membrane, altering its permeability and allowing rapid influx of calcium to the cytosol; this in turn triggers a series of events, only partially known, leading to a complete degeneration which is spatially-restricted to nerve terminals only, with no evident damage of the axon [11,13,15,22,49].

Double poisoning with black widow spider venom and partially-purified preparations of BoNT/A was performed before in experiments aimed at understanding their mechanism of action, which was only partially known at that time [50,51]. In two other studies, the reversibility of BoNT/A induced paralysis was studied by inducing NMJ regeneration upon crushing the nerve terminal [52,53]. A similar approach was also extended to some *in vitro* experiments, in which α-Ltx was found to restore SNAP25 by elimination of the SNAP25 cleaved by BoNT/A. Nevertheless, this study did not include *in vivo* observations, therefore not providing any information about the effect of the spider toxin on the functional recovery of BoNTs-paralyzed NMJs [54].

The present work takes advantage of the actual wider knowledge of the mechanism of action of all the neurotoxins used here [2,11,12,15,16], including PLA2 neurotoxins (SPANs) and BoNT/B, which have never been tested in such double poisoning experiments before.

The remarkable finding described here is that, notwithstanding the target cleaved by the BoNTs, both α-Ltx and β-Btx are capable of effectively shorten the duration of the paralysis caused by BoNTs in mice, at doses that exclude a systemic effect. The progressive disappearance of the peripheral paralysis is accompanied by a recovery of the NMJ function, as assessed by electrophysiological measurements. In addition, we documented by fluorescence microscopy with specific antibodies that BoNT/A paralysis and recovery are paralleled by appearance and disappearance of the truncated form of SNAP25; a similar relation was found between VAMP1 staining and blockade of the motor axon terminals in BoNT/B treated animals. Moreover, to the best of our knowledge, this is the first time that the direct effect of BoNT/B on its substrate VAMP1 has been immunohistochemically characterized in terms of onset and resolution.

The general and relevant conclusion that can be drawn by the present study is that biochemical lesions of motor axon terminals, associated with a loss of synaptic functionality, can be overcome by treatments that cause a reversible degeneration of the terminals themselves. As the NMJ is one of the few anatomical structures whose regeneration capacity has been retained through evolution [23,24], the degeneration and removal of the motor axon terminal is followed by its regeneration and repositioning on the basal membrane, with complete regain of function. In the light of these observations, it would be interesting and relevant to extend the present approach to diseases characterized by a chronic and severe dysfunction of the motor axon terminals, such as ALS and some autoimmune neuropathies.

4. Experimental Section

4.1. Animals and Toxins

Experiments were performed on Swiss-Webster adult male CD1 mice (Plaisant Srl) in accordance with the Council Directive 2010/63/EU of the European Parliament, the Council of 22 September 2010 on the protection of animals used for scientific purposes, and approved by the Italian Ministry of Health (authorization number 359/2015, 11 May 2015).

BoNT/A was prepared and purified as previously described [55,56], BoNT/B was produced in *E. coli* via recombinant methods [57]. α-Ltx and β-Btx were purchased from Alomone (Jerusalem, Israel) and Sigma-Aldrich (St.Louis, MO, USA), respectively. Their purity was checked by SDS page and their potency tested in *ex vivo* hemidiaphragm preparations [15].

BoNT/A and BoNT/B were diluted with physiological saline (0.9% NaCl plus 0.2% gelatine) to a final concentration of 0.25 pg/μL and 0.5 pg/μL respectively, and locally injected in the left mouse hind-limb (1 μL/g of weight), in order to reach the final intramuscular dose of 0.25 ng/kg

(BoNT/A) or 0.5 ng/kg (BoNT/B). Similarly, at indicated time, α-Ltx (5 μg/kg) or β-Btx (10 μg/kg) were injected at the same site. Control animals were injected with saline. All injections were performed upon isofluorane anaesthetization of two months-old mice weighting around 20–25 g. Treated mice underwent DAS score evaluation and electrophysiological recordings at defined time points, as described in the following sections.

4.2. Digit Abduction Score Assay (DAS)

Swiss–Webster adult male CD1 mice were housed under controlled light/dark conditions, and food and water were provided *ad libitum*. The degree of hind limb paralysis was evaluated by the Digit Abduction Score Assay (DAS), which measures the local muscle weakening following BoNTs injection into mouse hind-limb [58,59]. Briefly, the local paralysis was scored on a five point scale, with 0 corresponding to a normal abduction of all digits of the hind limbs and four corresponding to the maximum degree of paralysis, *i.e.*, none of the toes can abduct. Ten mice for each condition were employed. Treated mice were checked once per day until the complete recovery of abduction capability.

4.3. Electrophysiological Recordings (ER)

Treated mice were sacrificed at scheduled times by anesthetic overdose followed by cervical dislocation, soleus muscles were dissected, subjected to electrophysiological measurements and then fixed for immunohistochemistry. Three mice were used for each condition at each time-point. Electrophysiological recordings (ER) were performed in oxygenated Krebs-Ringer solution on sham or neurotoxins-injected soleus muscles, using intracellular glass microelectrodes (WPI) filled with one part 3 M KCl and two parts 3 M CH3COOK. Evoked junction potentials (EJP) were recorded in current-clamp mode, starting from resting membrane potential of −70 mV, adjusted with direct current injection when needed. EJPs were elicited by supramaximal nerve stimulation at 0.5 Hz, using a suction microelectrode connected to a S88 stimulator (Grass, Warwick, RI, USA). To prevent muscle contraction after dissection, samples were incubated for 10 min with 1 μM μ-Conotoxin GIIIB (Alomone, Jerusalem, Israel). Signals were amplified with intracellular bridge mode amplifier (BA-01X; NPI, Tamm, Germany), sampled using a digital interface (NI PCI-6221; National Instruments, Austin, TX, USA) and recorded by means of electrophysiological software (WinEDR; Strathclyde University, Glasgow, Scotland, UK). EJPs measurements were carried out with Clampfit software (Molecular Devices, Sunnyvale, CA, USA).

4.4. NMJ Immunohistochemistry (IHC)

At the end of ER, soleus muscles were immediately fixed in 4% (*wt/vol*) PFA in PBS for 30 min at RT. Samples were quenched in 50 mM NH4Cl in PBS, then permeabilized and saturated for 2 h in blocking solution (15% *vol/vol* goat serum, 2% *wt/vol* BSA, 0.25% *wt/vol* gelatin, 0.2% *wt/vol* glycine in PBS), containing 0.5% Triton X-100. Incubation with the following primary antibodies was carried out for at least 48 h in blocking solution: anti-SNAP25 (SMI81 mouse monoclonal, 1:100, BioLegend, San Diego, CA, USA), anti-neurofilaments (mouse monoclonal, anti-NF200, 1:200, Sigma-Aldrich, St. Loius, MO, USA), anti-VAMP1 (rabbit polyclonal 1:200, generated as described in [37], and anti-SNAP25 BoNT/A-cleaved (t-SNAP25, rabbit polyclonal 1:200, generated as described in [31]. Muscles were then extensively washed and incubated with the appropriate secondary antibodies (Alexa-conjugated, 1:200 in PBS, Thermo Scientific, Waltham, MA, USA) supplemented with Alexa555-conjugated α-Btx (1:200, Thermo Scientific, Waltham, MA, USA) to counterstain post-synaptic nicotinic acetylcholine (Ach) receptors. Images were collected with a Leica SP5 confocal microscope (Leica Microsystems, Wetzlar, Germany) equipped with 100X HCX PL APO NA 1.4 objective. Laser excitation line, power intensity, and emission range were chosen according to each fluorophore in different samples to minimize bleed-through.

Acknowledgments: This work was supported by the Cariparo Foundation and the University of Padua.

Author Contributions: M.P., M.R., C.M., A.M. and E.D. conceived and designed the experiments; E.D., G.Z., M.S. and M.P. performed the experiments; E.D., G.Z. and M.S. analyzed the data; M.P., M.R, C.M. and E.D. wrote the paper; all authors have read and approved the final version of the manuscript.

Conflicts of Interest: The authors declare no conflict of interest. The founding sponsor had no role in the design of the study; in the collection, analysis, or interpretation of data; in the writing of the manuscript, and in the decision to publish the results.

References

1. Johnson, E.A.; Montecucco, C. Botulism. *Handb. Clin. Neurol.* **2008**, *91*, 333–368. [PubMed]
2. Rossetto, O.; Pirazzini, M.; Montecucco, C. Botulinum neurotoxins: Genetic, structural and mechanistic insights. *Nat. Rev. Microbiol.* **2014**, *12*, 535–549. [CrossRef] [PubMed]
3. Binz, T.; Sikorra, S.; Mahrhold, S. Clostridial neurotoxins: Mechanism of snare cleavage and outlook on potential substrate specificity reengineering. *Toxins* **2010**, *2*, 665–682. [CrossRef] [PubMed]
4. Keller, J.E.; Neale, E.A.; Oyler, G.; Adler, M. Persistence of botulinum neurotoxin action in cultured spinal cord cells. *FEBS Lett.* **1999**, *456*, 137–142. [CrossRef]
5. Pantano, S.; Montecucco, C. The blockade of the neurotransmitter release apparatus by botulinum neurotoxins. *Cell Mol. Life Sci.* **2014**, *71*, 793–811. [CrossRef] [PubMed]
6. Eleopra, R.; Tugnoli, V.; Rossetto, O.; Montecucco, C.; de Grandis, D. Botulinum neurotoxin serotype C: A novel effective botulinum toxin therapy in human. *Neurosci. Lett.* **1997**, *224*, 91–94. [CrossRef]
7. Eleopra, R.; Tugnoli, V.; Rossetto, O.; de Grandis, D.; Montecucco, C. Different time courses of recovery after poisoning with botulinum neurotoxin serotypes A and E in humans. *Neurosci. Lett.* **1998**, *256*, 135–138. [CrossRef]
8. Eleopra, R.; Tugnoli, V.; Quatrale, R.; Rossetto, O.; Montecucco, C. Different types of botulinum toxin in humans. *Mov. Disord.* **2004**, *19* (Suppl. 8), S53–S59. [CrossRef] [PubMed]
9. Meunier, F.A.; Lisk, G.; Sesardic, D.; Dolly, J.O. Dynamics of motor nerve terminal remodeling unveiled using snare-cleaving botulinum toxins: The extent and duration are dictated by the sites of SNAP-25 truncation. *Mol. Cell Neurosci.* **2003**, *22*, 454–466. [CrossRef]
10. Torii, Y.; Goto, Y.; Takahashi, M.; Ishida, S.; Harakawa, T.; Sakamoto, T.; Kaji, R.; Kozaki, S.; Ginnaga, A. Quantitative determination of biological activity of botulinum toxins utilizing compound muscle action potentials (cmap), and comparison of neuromuscular transmission blockage and muscle flaccidity among toxins. *Toxicon* **2010**, *55*, 407–414. [CrossRef] [PubMed]
11. Duregotti, E.; Negro, S.; Scorzeto, M.; Zornetta, I.; Dickinson, B.C.; Chang, C.J.; Montecucco, C.; Rigoni, M. Mitochondrial alarmins released by degenerating motor axon terminals activate perisynaptic schwann cells. *Proc. Natl. Acad. Sci. USA* **2015**, *112*, E497–E505. [CrossRef] [PubMed]
12. Ushkaryov, Y.A.; Rohou, A.; Sugita, S. Alpha-latrotoxin and its receptors. *Handb. Exp. Pharmacol.* **2008**, *184*, 171–206.
13. Südhof, T.C. Alpha-latrotoxin and its receptors: Neurexins and cirl/latrophilins. *Annu. Rev. Neurosci.* **2001**, *24*, 933–962. [CrossRef] [PubMed]
14. Dixon, R.W.; Harris, J.B. Nerve terminal damage by beta-bungarotoxin: Its clinical significance. *Am. J. Pathol.* **1999**, *154*, 447–455. [CrossRef]
15. Rigoni, M.; Caccin, P.; Gschmeissner, S.; Koster, G.; Postle, A.D.; Rossetto, O.; Schiavo, G.; Montecucco, C. Equivalent effects of snake PLA2 neurotoxins and lysophospholipid-fatty acid mixtures. *Science* **2005**, *310*, 1678–1680. [CrossRef] [PubMed]
16. Schiavo, G.; Matteoli, M.; Montecucco, C. Neurotoxins affecting neuroexocytosis. *Physiol. Rev.* **2000**, *80*, 717–766. [PubMed]
17. Tedesco, E.; Rigoni, M.; Caccin, P.; Grishin, E.; Rossetto, O.; Montecucco, C. Calcium overload in nerve terminals of cultured neurons intoxicated by alpha-latrotoxin and snake PLA2 neurotoxins. *Toxicon* **2009**, *54*, 138–144. [PubMed]
18. Pungercar, J.; Krizaj, I. Understanding the molecular mechanism underlying the presynaptic toxicity of secreted phospholipases A2. *Toxicon* **2007**, *50*, 871–892. [CrossRef] [PubMed]

19. Rigoni, M.; Pizzo, P.; Schiavo, G.; Weston, A.E.; Zatti, G.; Caccin, P.; Rossetto, O.; Pozzan, T.; Montecucco, C. Calcium influx and mitochondrial alterations at synapses exposed to snake neurotoxins or their phospholipid hydrolysis products. *J. Biol. Chem.* **2007**, *282*, 11238–11245. [CrossRef] [PubMed]
20. Duregotti, E.; Tedesco, E.; Montecucco, C.; Rigoni, M. Calpains participate in nerve terminal degeneration induced by spider and snake presynaptic neurotoxins. *Toxicon* **2013**, *64*, 20–28. [CrossRef] [PubMed]
21. Kularatne, S.A.; Senanayake, N. Venomous snake bites, scorpions, and spiders. *Handb. Clin. Neurol.* **2014**, *120*, 987–1001. [PubMed]
22. Duchen, L.W.; Gomez, S.; Queiroz, L.S. The neuromuscular junction of the mouse after black widow spider venom. *J. Physiol.* **1981**, *316*, 279–291. [CrossRef] [PubMed]
23. Nguyen, Q.T.; Sanes, J.R.; Lichtman, J.W. Pre-existing pathways promote precise projection patterns. *Nat. Neurosci.* **2002**, *5*, 861–867. [CrossRef] [PubMed]
24. Son, Y.J.; Trachtenberg, J.T.; Thompson, W.J. Schwann cells induce and guide sprouting and reinnervation of neuromuscular junctions. *Trends Neurosci.* **1996**, *19*, 280–285. [CrossRef]
25. Pearn, J.H. Survival after snake-bite with prolonged neurotoxic envenomation. *Med. J. Aust.* **1971**, *2*, 259–261. [PubMed]
26. Trevett, A.J.; Lalloo, D.G.; Nwokolo, N.C.; Naraqi, S.; Kevau, I.H.; Theakston, R.D.; Warrell, D.A. Electrophysiological findings in patients envenomed following the bite of a papuan taipan (oxyuranus scutellatus canni). *Trans R. Soc. Trop. Med. Hyg.* **1995**, *89*, 415–417. [CrossRef]
27. Connolly, S.; Trevett, A.J.; Nwokolo, N.C.; Lalloo, D.G.; Naraqi, S.; Mantle, D.; Schofield, I.S.; Fawcett, P.R.; Harris, J.B.; Warrell, D.A. Neuromuscular effects of papuan taipan snake venom. *Ann. Neurol.* **1995**, *38*, 916–920. [CrossRef] [PubMed]
28. Kularatne, S.A. Common krait (bungarus caeruleus) bite in anuradhapura, sri lanka: A prospective clinical study, 1996–1998. *Postgrad. Med. J.* **2002**, *78*, 276–280. [CrossRef] [PubMed]
29. Montecucco, C.; Molgó, J. Botulinal neurotoxins: Revival of an old killer. *Curr. Opin. Pharmacol.* **2005**, *5*, 274–279. [CrossRef] [PubMed]
30. Rossetto, O.; Morbiato, L.; Caccin, P.; Rigoni, M.; Montecucco, C. Presynaptic enzymatic neurotoxins. *J. Neurochem.* **2006**, *97*, 1534–1545. [CrossRef] [PubMed]
31. Antonucci, F.; Rossi, C.; Gianfranceschi, L.; Rossetto, O.; Caleo, M. Long-distance retrograde effects of botulinum neurotoxin A. *J. Neurosci.* **2008**, *28*, 3689–3696. [CrossRef] [PubMed]
32. Roger Aoki, K. Botulinum neurotoxin serotypes A and B preparations have different safety margins in preclinical models of muscle weakening efficacy and systemic safety. *Toxicon* **2002**, *40*, 923–928. [CrossRef]
33. Simpson, L. The life history of a botulinum toxin molecule. *Toxicon* **2013**, *68*, 40–59. [CrossRef] [PubMed]
34. Fagan, R.P.; McLaughlin, J.B.; Middaugh, J.P. Persistence of botulinum toxin in patients' serum: Alaska, 1959–2007. *J. Infect. Dis.* **2009**, *199*, 1029–1031. [CrossRef] [PubMed]
35. Megighian, A.; Zordan, M.; Pantano, S.; Scorzeto, M.; Rigoni, M.; Zanini, D.; Rossetto, O.; Montecucco, C. Evidence for a radial snare super-complex mediating neurotransmitter release at the drosophila neuromuscular junction. *J. Cell Sci.* **2013**, *126*, 3134–3140. [CrossRef] [PubMed]
36. Montecucco, C.; Schiavo, G.; Pantano, S. Snare complexes and neuroexocytosis: How many, how close? *Trends Biochem. Sci.* **2005**, *30*, 367–372. [CrossRef] [PubMed]
37. Rossetto, O.; Gorza, L.; Schiavo, G.; Schiavo, N.; Scheller, R.H.; Montecucco, C. Vamp/synaptobrevin isoforms 1 and 2 are widely and differentially expressed in nonneuronal tissues. *J. Cell Biol.* **1996**, *132*, 167–179. [CrossRef] [PubMed]
38. Li, J.Y.; Edelmann, L.; Jahn, R.; Dahlström, A. Axonal transport and distribution of synaptobrevin I and II in the rat peripheral nervous system. *J. Neurosci.* **1996**, *16*, 137–147. [PubMed]
39. de Paiva, A.; Meunier, F.A.; Molgó, J.; Aoki, K.R.; Dolly, J.O. Functional repair of motor endplates after botulinum neurotoxin type A poisoning: Biphasic switch of synaptic activity between nerve sprouts and their parent terminals. *Proc. Natl. Acad. Sci. USA* **1999**, *96*, 3200–3205. [CrossRef] [PubMed]
40. Vinsant, S.; Mansfield, C.; Jimenez-Moreno, R.; del Gaizo Moore, V.; Yoshikawa, M.; Hampton, T.G.; Prevette, D.; Caress, J.; Oppenheim, R.W.; Milligan, C. Characterization of early pathogenesis in the SOD1(G93A) mouse model of als: Part II, results and discussion. *Brain Behav.* **2013**, *3*, 431–457. [CrossRef] [PubMed]

41. Moloney, E.B.; de Winter, F.; Verhaagen, J. Als as a distal axonopathy: Molecular mechanisms affecting neuromuscular junction stability in the presymptomatic stages of the disease. *Front. Neurosci.* **2014**, *8*, 252. [CrossRef] [PubMed]
42. Plomp, J.J.; Willison, H.J. Pathophysiological actions of neuropathy-related anti-ganglioside antibodies at the neuromuscular junction. *J. Physiol.* **2009**, *587*, 3979–3999. [CrossRef] [PubMed]
43. Kaida, K.; Kusunoki, S. Antibodies to gangliosides and ganglioside complexes in guillain-barré syndrome and fisher syndrome: Mini-review. *J. Neuroimmunol.* **2010**, *223*, 5–12. [CrossRef] [PubMed]
44. Brashear, A.; Lew, M.F.; Dykstra, D.D.; Comella, C.L.; Factor, S.A.; Rodnitzky, R.L.; Trosch, R.; Singer, C.; Brin, M.F.; Murray, J.J.; *et al*. Safety and efficacy of neurobloc (botulinum toxin type B) in type A-responsive cervical dystonia. *Neurology* **1999**, *53*, 1439–1446. [CrossRef] [PubMed]
45. Abrams, S.B.; Hallett, M. Clinical utility of different botulinum neurotoxin preparations. *Toxicon* **2013**, *67*, 81–86. [CrossRef] [PubMed]
46. Dressler, D. Clinical applications of botulinum toxin. *Curr. Opin. Microbiol.* **2012**, *15*, 325–336. [CrossRef] [PubMed]
47. Sutton, R.B.; Fasshauer, D.; Jahn, R.; Brunger, A.T. Crystal structure of a snare complex involved in synaptic exocytosis at 2.4 Å resolution. *Nature* **1998**, *395*, 347–353. [PubMed]
48. Jahn, R.; Fasshauer, D. Molecular machines governing exocytosis of synaptic vesicles. *Nature* **2012**, *490*, 201–207. [CrossRef] [PubMed]
49. Gutiérrez, J.M.; Lomonte, B. Phospholipases A2: Unveiling the secrets of a functionally versatile group of snake venom toxins. *Toxicon* **2013**, *62*, 27–39. [CrossRef] [PubMed]
50. Stern, R.; Valjevac, K.; Dursum, K.; Ducic, V. Increased survival time in botulinum toxin poisoning by treatment with a venom gland extract from the black widow spider. *Toxicon* **1975**, *13*, 197–198. [CrossRef]
51. Gomez, S.; Queiroz, L.S. The effects of black widow spider venom on the innervation of muscles paralysed by botulinum toxin. *Q. J. Exp. Physiol.* **1982**, *67*, 495–506. [CrossRef] [PubMed]
52. Thesleff, S.; Zelena, J.; Hofmann, W.W. Restoration of function in botulinum paralysis by experimental nerve regeneration. *Proc. Soc. Exp. Biol. Med.* **1964**, *116*, 19–20. [CrossRef] [PubMed]
53. Duchen, L.W. The effects in the mouse of nerve crush and regneration on the innervation of skeletal muscles paralysed by clostridium botulinum toxin. *J. Pathol.* **1970**, *102*, 9–14. [CrossRef] [PubMed]
54. Mesngon, M.; McNutt, P. Alpha-latrotoxin rescues SNAP-25 from BoNT/A-mediated proteolysis in embryonic stem cell-derived neurons. *Toxins* **2011**, *3*, 489–503. [CrossRef] [PubMed]
55. Schiavo, G.; Montecucco, C. Tetanus and botulism neurotoxins: Isolation and assay. *Methods Enzymol.* **1995**, *248*, 643–652. [PubMed]
56. Shone, C.C.; Tranter, H.S. Growth of clostridia and preparation of their neurotoxins. *Curr. Top. Microbiol. Immunol.* **1995**, *195*, 143–160. [PubMed]
57. Rummel, A.; Mahrhold, S.; Bigalke, H.; Binz, T. The hcc-domain of botulinum neurotoxins A and B exhibits a singular ganglioside binding site displaying serotype specific carbohydrate interaction. *Mol. Microbiol.* **2004**, *51*, 631–643. [CrossRef] [PubMed]
58. Aoki, K.R. A comparison of the safety margins of botulinum neurotoxin serotypes A, B, and F in mice. *Toxicon* **2001**, *39*, 1815–1820. [CrossRef]
59. Broide, R.S.; Rubino, J.; Nicholson, G.S.; Ardila, M.C.; Brown, M.S.; Aoki, K.R.; Francis, J. The rat digit abduction score (DAS) assay: A physiological model for assessing botulinum neurotoxin-induced skeletal muscle paralysis. *Toxicon* **2013**, *71*, 18–24. [CrossRef] [PubMed]

5.1.4 The ablation of S1P3 receptor protects mouse soleus from age related drop of muscle mass, force and regenerative capacity

Michela Bondì[1], Elena Germinario[1,2], Marco Pirazzini[1], Giulia Zanetti[1], Francesca Cencetti[2,3], Chiara Donati[2,3], Luisa Gorza[1], Romeo Betto[2,4], Paola Bruni[2,3], Daniela Danieli-Betto[1,2]

[1]Department of Biomedical Sciences, University of Padova, Italy,

[2]IIM, Interuniversity Institute of Myology, Italy,

[3]Department of Biomedical, Experimental and Clinical Sciences, Mario Serio, University of Firenze, Italy,

[4]C.N.R. - Institute for Neuroscience, Padova, Italy

Bondì M. *et al.* The ablation of S1P3 receptor protects mouse soleus from age Related drop of muscle mass, force and regenerative capacity. *Am J Physiol Cell Physiol*. 2017 Jul 1;313(1):C54-C67.

doi: 10.1152/ajpcell.00027.2017. Epub 2017 Apr 26.

Am J Physiol Cell Physiol 313: C54–C67, 2017.
First published April 26, 2017; doi:10.1152/ajpcell.00027.2017.

RESEARCH ARTICLE

Ablation of $S1P_3$ receptor protects mouse soleus from age-related drop in muscle mass, force, and regenerative capacity

Michela Bondì,[1]* Elena Germinario,[1,2]* Marco Pirazzini,[1] Giulia Zanetti,[1] Francesca Cencetti,[2,3] Chiara Donati,[2,3] Luisa Gorza,[1] Romeo Betto,[2,4] Paola Bruni,[2,3] and Daniela Danieli-Betto[1,2]

[1]*Department of Biomedical Sciences, University of Padova, Padua, Italy;* [2]*Interuniversity Institute of Myology, Italy;* [3]*Department of Biomedical, Experimental and Clinical Sciences, Mario Serio, University of Firenze, Florence, Italy; and* [4]*National Research Council-Institute for Neuroscience, Padua, Italy*

Submitted 2 February 2017; accepted in final form 19 April 2017

Bondì M, Germinario E, Pirazzini M, Zanetti G, Cencetti F, Donati C, Gorza L, Betto R, Bruni P, Danieli-Betto D. Ablation of $S1P_3$ receptor protects mouse soleus from age-related drop in muscle mass, force, and regenerative capacity. *Am J Physiol Cell Physiol* 313: C54–C67, 2017. First published April 26, 2017; doi:10.1152/ajpcell.00027.2017.—We investigated the effects of $S1P_3$ deficiency on the age-related atrophy, decline in force, and regenerative capacity of soleus muscle from 23-mo-old male (old) mice. Compared with muscle from 5-mo-old (adult) mice, soleus mass and muscle fiber cross-sectional area (CSA) in old wild-type mice were reduced by ~26% and 24%, respectively. By contrast, the mass and fiber CSA of soleus muscle in old $S1P_3$-null mice were comparable to those of adult muscle. Moreover, in soleus muscle of wild-type mice, twitch and tetanic tensions diminished from adulthood to old age. A slowing of contractile properties was also observed in soleus from old wild-type mice. In $S1P_3$-null mice, neither force nor the contractile properties of soleus changed during aging. We also evaluated the regenerative capacity of soleus in old $S1P_3$-null mice by stimulating muscle regeneration through myotoxic injury. After 10 days of regeneration, the mean fiber CSA of soleus in old wild-type mice was significantly smaller (−28%) compared with that of regenerated muscle in adult mice. On the contrary, the mean fiber CSA of regenerated soleus in old $S1P_3$-null mice was similar to that of muscle in adult mice. We conclude that in the absence of $S1P_3$, soleus muscle is protected from the decrease in muscle mass and force, and the attenuation of regenerative capacity, all of which are typical characteristics of aging.

aging; sarcopenia; soleus muscle; regeneration; $S1P_3$ receptor

AGING OF SKELETAL MUSCLE is associated with the gradual loss of skeletal muscle mass and strength, a condition known as sarcopenia. Multiple phenomena, not totally understood, contribute to the development of sarcopenia, including intrinsic factors such as hormonal imbalance, inflammation, denervation, oxidative stress, mitochondrial dysfunction, and impaired satellite cell (SC) function; and extrinsic factors such as reduced physical activity and inadequate nutrition (48).

The reduction of muscle mass in old humans was demonstrated to be secondary to the loss of α-motoneurons and motor units, and to an incomplete reinnervation of previously denervated muscle fibers, evidence confirmed in rat-aging models (36, 37). Diversely, little or no neuronal death was evidenced in aged mice (14). On the other hand, oxidative stress and decreased release of trophic factors seem to influence neuromuscular junction (NMJ) integrity and contribute to denervation of the oldest muscle fibers (11, 14, 15). Large evidence was also accumulated demonstrating that altered intracellular and/or metabolic conditions lead to dysfunctional mitochondria; these conditions include impaired mitochondrial energetics, decreased rate of synthesis of mitochondrial proteins, increased mitochondrial-mediated apoptosis, and decreased autophagy, and therefore mitophagy (45). Therefore, defective autophagy increases sarcopenia by causing NMJ degeneration, and accumulation of large mitochondria and carbonylated proteins (11). Importantly, the latter seems to contribute to the reduced specific tension generated by old muscle fibers. In fact, the decrease in muscle force-generating capacity with age appears to be larger than the reduced muscle mass (1). The age-dependent fast-to-slow phenotype transformation could contribute to the reduction in muscle force (1), as fast fibers are stronger than slow fibers (9).

Aging is also characterized by a gradual decline in the regenerative efficiency of skeletal muscle (4), though recent evidence indicates that the process appears just delayed and completely fulfilled (2, 58). Whether this is due to extrinsic changes in the environment and/or to cell-intrinsic mechanisms associated with aging is still debated. Adult muscle regeneration involves activation of SCs, a stem cell population located between the basal lamina and plasma membrane. Activated SCs undergo proliferation and generate myoblasts, which fuse to each other or to injured myofibers to promote repair and regeneration. There was no significant difference in SC number between young and old muscle (18), but it is reported that with age, the systemic environment is less effective in maintaining the myogenic fate of muscle stem cells and facilitates the conversion to fibrogenic fate (12).

The bioactive sphingolipid sphingosine 1-phosphate (S1P) exerts important functions in almost all tissues and organs, and particularly in vascular and immune systems (46, 60). S1P acts by autocrine/paracrine mechanisms as a ligand of five distinct S1P receptors, ($S1P_{1–5}$) coupled to multiple heterotrimeric G proteins that activate distinct signaling pathways (46, 60). Three S1P receptor subtypes ($S1P_{1–3}$) are expressed in adult skeletal muscle. $S1P_1$ and $S1P_3$ receptors are localized both in the cell and nuclear membranes of adult fibers (67). In addition, $S1P_1$ was also detected in the neuromuscular junction (67). $S1P_1$ and $S1P_3$ are expressed by quiescent satellite cells of

* M. Bondì and E. Germinario contributed equally to this work.

Address for reprint requests and other correspondence: D. Danieli-Betto, Dept. of Biomedical Sciences, Univ. of Padova, Via Marzolo 3, 35131 Padova, Italy (e-mail: daniela.danieli@unipd.it).

adult muscle, whereas $S1P_2$ is only transiently expressed in activated SCs (21, 26, 33).

Studies of the role of S1P signaling in skeletal muscle are carried out in skeletal muscle cellular models, in in vivo experiments by modulating S1P signaling, and in transgenic mice lacking individual S1P receptors, demonstrating on the whole that S1P has pleiotropic effects on muscle functions (22). Our previous results indicate that exogenous S1P administration makes extensor digitorum longus (EDL) muscle more resistant to fatigue (20). Moreover, exogenous application of S1P counteracts the reduction in rat muscle mass caused by denervation, whereas neutralization of the extracellular lipid with a specific anti-S1P monoclonal antibody accelerated the atrophy caused by denervation in mice (67). It was then demonstrated that S1P stimulates quiescent SCs to enter the cell cycle, and muscle regeneration is compromised when S1P biosynthesis is inhibited (47). In addition, exogenous administration of S1P at the moment of myotoxic injury favors the growth of regenerating fibers in both rat and mouse (21). Moreover, reduced S1P catabolism improves muscle regeneration in mdx mice (33, 41). The role played by single S1P receptors in skeletal muscle is only partly revealed, and divergent evidence is reported. Previous results suggest that $S1P_3$ may positively control muscle trophism, because its expression dramatically drops in denervated rat soleus muscle (67). However, in $S1P_3$-null mice, denervation atrophy is reduced in the EDL muscle (27). In vivo pharmacological data suggest that $S1P_1$ negatively regulates the growth of regenerating rat soleus fibers, whereas $S1P_3$ seems to have an opposite, positive action (21). However, it has been recently demonstrated in vivo that in the absence of $S1P_3$, acute regeneration is enhanced both after a single cycle and repeated cycles of muscle injury in mouse tibialis anterior muscle (26). Moreover, it was suggested that signaling through $S1P_3$ may contribute to control the quiescence of SCs (26), whereas signaling that operates through $S1P_2$ may then drive S1P-mediated proliferation and/or differentiation in myogenic C2C12 cells (41). Finally, the lack of $S1P_2$ resulted in a delay of regenerating muscle fiber growth (29, 41).

In the present work, we explored the effects produced by the absence of $S1P_3$ on the characteristics of aged soleus muscle using $S1P_3$-null mice. The absence of $S1P_3$ receptor in old soleus muscle seems to favor the preservation of muscle mass, muscle force, NMJ integrity, and regenerating capacity.

MATERIALS AND METHODS

The Italian Health Ministry approved all animal experimental protocols. C57BL/6J (wild type) and $S1P_3$-null mice, generated by Jerold Chun (Scripps Institute, La Jolla, CA) (34) and kindly provided by Dr. Bodo Levkau, University of Essen, Essen, Germany (the genotype of $S1P_3$-null mouse was confirmed by PCR), were housed under a 12:12-h light-dark cycle in an air-conditioned room with ad libitum access to a standard chow and water diet. Male mice aged 5 and 23 mo were used. Throughout the experimental work, a total of 22 adult and 18 old, wild-type mice, and 24 adult and 20 old, $S1P_3$-null mice were used.

Muscle contractile properties of old soleus muscle. The experiments were performed in vitro in a vertical muscle apparatus (300B; Aurora Scientific, Aurora, ON, Canada) containing a Ringer solution of the following composition: 120 mM NaCl, 4.7 mM KCl, 2.5 mM $CaCl_2$, 3.15 mM $MgCl_2$, 1.3 mM NaH_2PO_4, 25 mM $NaHCO_3$, 11 mM glucose, and 30 μM d-tubocurarine, pH 7.2–7.4, 30°C, bubbled with 95% O_2/5% CO_2. Muscles were stretched to the optimal length (i.e., the length that allowed maximal tension development in response to a single pulse) and electrically stimulated via two parallel electrodes with supramaximal pulses (0.5 ms duration) delivered by a Grass S44 electronic stimulator through a stimulus isolation unit (Grass SIU5). Muscle response was recorded through an isometric force transducer (Grass FT03) connected to an AT-MIO 16AD acquisition card (National Instruments). Data were analyzed using LabView software (National Instruments) (27). Time to peak of the twitch, half relaxation time of the twitch and of the tetanus, and the maximum rate of rise of the tension were measured. Twitch and tetanic tensions were normalized to the muscle wet weight (specific tension, N/g). Force-frequency curve was determined by stimulating soleus muscle at 1, 20, 30, 40, 60, 80, 100, 120, and 150 Hz. Muscles were weighed at the end of each experiment.

Histological and immunofluorescence analysis. Muscles were isolated and quickly frozen in liquid nitrogen in a slightly stretched position. Serial cross sections (8 μm thick) were cut in a cryostat microtome (Slee, London, UK) set at −24 ± 1°C. Hematoxylin & eosin and succinate dehydrogenase (SDH) staining were performed on transverse muscle sections to examine the general morphology and overall mitochondrial content (27). To evaluate the extension of fibrosis, muscle cryostat sections were subjected to PicroSirius Red staining (31). Laminin staining was carried out to determine the cross-sectional area (CSA) of individual fibers (21, 67). Muscle sections were incubated for 1 h at 37°C with the polyclonal antibody specific for laminin (L9393; Sigma, St. Louis, MO) diluted 1:150 in 5% fetal bovine serum. Laminin was revealed with an anti-rabbit Alexa Fluor 488 (goat anti-rabbit IgG; Invitrogen, Carlsbad, CA) diluted 1:200 in PBS incubated for 1 h at 37°C. Nuclei were evidenced with DAPI staining. Muscle sections were examined in a Leica RD100 fluorescence microscopy equipped with a digital camera. Muscle fiber CSA was measured on digital photographs using ImageJ software (National Institutes of Health, Bethesda, MD). Type 1 and type 2A fibers were identified, respectively, with BA-F8 (diluted 1:100) and SC-71 (diluted 1:10) monoclonal antibodies (University of Iowa, Developmental Studies Hybridoma Bank). The secondary antibodies were Alexa Fluor goat anti-mouse IgG2b 488 conjugate for type 1 and IgG1 568 conjugate for type 2A, diluted 1:200.

Neuromuscular junction immunohistochemistry. Immediately after isolation, soleus muscle was fixed in 4% (wt/vol) paraformaldehyde (PFA) in PBS for 30 min at room temperature. Samples were then quenched in 50 mM NH_4Cl in PBS (NH_4Cl was used to quench residual active aldehydes after PFA fixation), permeabilized and saturated for 2 h in blocking solution (15% vol/vol goat serum, 2% wt/vol BSA, 0.25% wt/vol gelatin, and 0.2% wt/vol glycine in PBS), containing 0.5% Triton X-100. Bundles of 5 to 6 muscle fibers were dissected and incubated for at least 48 h with primary antibodies specific for the vesicle-associated membrane protein 1/synaptobrevin-1 (VAMP1; rabbit polyclonal, diluted 1:200), generated as described (54), or syntaxin 1A1B (rabbit polyclonal, diluted 1:200), generated as described (57). Muscles were then extensively washed and incubated with an anti-rabbit secondary antibody (Alexa 488-conjugated, diluted 1:200 in PBS, catalog no. A11008; Invitrogen by Thermo Scientific, Waltham, MA) supplemented with Alexa 555-conjugated α-Btx (diluted 1:200, B35451; Molecular Probes by Thermo Scientific, Waltham, MA) to counterstain postsynaptic nicotinic acetylcholine receptors. Images were collected with a Leica SP5 confocal microscope (Leica Microsystems, Wetzlar, Germany) equipped with a ×100 HCX PL APO NA 1.4 objective. Laser excitation line, power intensity, and emission range were chosen according to each fluorophore in different samples to minimize bleed-through.

Surgical procedures. Surgical procedures were performed while the mice were under general anesthesia via intraperitoneal injection of tiletamine and zolazepam (7 mg/kg, Virbac, Carros) and xylazine (14 mg/kg, Bayer). C576J and $S1P_3$-null mice aged 5 and 23 mo were

used. Acute degeneration was induced in the left soleus muscles by injecting 0.075 ml of the myotoxic drug notexin (0.5%, Sigma) as previously published (29). Shortly thereafter, soleus muscle was exposed by making a small, lateral incision and then gently detaching it from the covering muscles with the tip of a surgical scissor. Notexin was injected by inserting the tip of the needle longitudinally into the muscle until it slightly swelled up, to avoid leaking out of the toxin and the injury of surrounding muscles. Mice were euthanized 10 days after degeneration by neck dislocation, and the soleus muscle of both legs was removed.

Western blotting and SDS-PAGE analysis. Western immunoblotting was performed on muscle fragments dissolved in SDS-PAGE buffer supplemented with Complete protease (04693132001; Roche, Basel, Switzerland) and phosphatase (P0044 and P5726; Sigma) inhibitor cocktail, diluted as suggested. Muscle lysates (25–30 μg each) were electrophoresed on 10% SDS-PAGE gels. Electroblotting was performed as previously described (67). Nitrocellulose filters were probed with the selected primary antibody incubated overnight at 4°C at the conditions described below.

The following rabbit antibodies were used: phospho(Ser^{473})-Akt, 1:1,000 in 5% BSA and 0.1% Tween-20 in TBS (catalog no. 4060; Cell Signaling Technology); Akt, 1:500 in 5% BSA and 0.1% Tween-20 in TBS (9272; Cell Signaling Technology); phospho-(Ser$^{240/244}$)-S6, 1:1,000 in 5% BSA and 0.1% Tween-20 in TBS (5364; Cell Signaling Technology); phospho(Ser$^{423/425}$)Smad3, 1:1,000 in 5% BSA and 0.1% Tween-20 in TBS (Ab52903; Abcam); GAPDH, 1:5,000 in 2% BSA, 0.2% Tween-20 in TBS (GTX100118; GenTex); LC-3, 1:1,000 in 5% low-fat milk, 0.1% Tween-20 in TBS (L7543; Sigma); P62, 1:1,000 in 5% low-fat milk, 0.1% Tween-20 in TBS (P0067; Sigma); PGC-1α, 1:1,000 in 5% low-fat milk, 0.1% Tween-20 in TBS (ab54481; Abcam); MuRF-1, 1:500 in 5% low-fat milk, 0.04% Tween-20 in TBS (MP3401; ECMBioscience); Tom20, 1:500 in 5% BSA, 0.05% Tween-20 in TBS (sc11415; Santa Cruz Biotechnology); and Bcl2, 1:1,000 in 5% BSA, 0.1% Tween-20 in TBS (2876S; Cell Signaling Technology). The secondary antibody was an anti-rabbit peroxidase-conjugated antibody (P0448; Dako) diluted 1:5,000 in the same buffer as the cognate primary antibody and incubated for 1 h. A goat polyclonal antibody anti-SERCA2 (1:1,000 in 5% low-fat milk, 0.05% Tween-20 in TBS) (sc8094; Santa Cruz Biotechnology) was used. The secondary antibody was an anti-goat peroxidase-conjugated antibody (A5420; Sigma) diluted 1:10,000 in the same buffer as the cognate primary antibody and incubated for 1 h. Moreover, the following mouse monoclonal antibodies were used: Smad3, 1:2,500 in 5% BSA and 0.1% Tween-20 in TBS (Ab75512, Abcam); SERCA1 (D1G8), 1:3,000 in 1% BSA in TBS, generated as described (28); myogenin, 1:100 in 10% low-fat milk, 0.1% Tween-20 in TBS (F5D; Developmental Studies Hybridoma Bank); MyoD1, 1:1,500 in 5% low-fat milk, 0.05% Tween-20 in TBS (M3512; Dako); and embryonic MyHC isoform (1:500, in 2% BSA, 0.2% Tween-20 in TBS) (F1.652; Developmental Studies Hybridoma Bank). The secondary antibody was an anti-mouse peroxidase-conjugated (P0447; Dako) at 1:10,000 dilution (in the same buffer as the cognate primary antibody), incubated for 1 h. Visualization of reaction bands was performed either via tetramethylbenzidine staining or enhanced chemiluminescence (Amersham Pharmacia Biotech, Buckinghamshire, UK). Signal intensities were evaluated by densitometry. Analysis of oxidatively modified proteins was performed by detecting carbonylated proteins using an OxyBlot Protein Oxidation Detection kit (Millipore, Billerica, MA).

Analysis of MyHC isoforms was performed by the SDS-PAGE method previously described (26). Small muscle fragments were weighed, ground with a ceramic pestle in liquid nitrogen, and extracted at 2 mg/ml in SDS-PAGE sample buffer (62.5 mM Tris·HCl pH 6.8, 2.3% SDS, 5% 2-mercaptoethanol, and 10% glycerol). Muscle protein samples (10 μg each) were electrophoresed on 8% SDS-PAGE slab gels. MyHC protein bands were revealed with Coomassie brilliant blue staining. MyHC isoform percentage composition was determined by densitometry of gels by using a Bio-Rad Imaging Densitometer (GS-670).

Real-time PCR. Total RNA of soleus from old (age, 23 mo) S1P$_3$-null and wild-type mice was purified by TRI-Reagent, 1 μg of which was used for reverse transcription, using the SuperScript IV first-strand synthesis system, according to the manufacturer's instructions (Life Technologies, Carlsbad, CA). Quantification of S1P receptors (S1P$_1$, S1P$_2$, and S1P$_3$) and CTGF mRNA level was performed via real-time PCR employing *Taq*Man Gene Expression Assays (S1P$_1$, Mm00514644_m1; S1P$_2$, Mm01177794_m1; S1P$_3$, Mm00515669_m1; and CTGF, Mm01192933_g1). Each measurement was carried out in triplicate using an automated ABI Prism 7500 Sequence Detector System (Life Technologies) as described previously (23) by simultaneous amplification of the target sequence together with the housekeeping gene β-actin, whose expression was highly stable across all the groups. Results were analyzed using ABI Prism Sequence Detection Systems software, version 1.7 (Life Technologies), the $2^{-\Delta\Delta Ct}$ method was applied as a comparative method of quantification (40), and data were normalized to β-actin expression.

Statistical analysis. All values are expressed as means ± SE. The mean CSA values from individual muscles were pooled and the resulting mean was compared. More than 600 fibers from each muscle were measured. Data were analyzed with one-way between-subjects ANOVA followed by a Newman-Keuls post hoc test. For real-time PCR experiments, results are expressed as means ± SE of fold changes according to the $2^{-\Delta\Delta Ct}$ method, with 18S rRNA in each specimen used for housekeeping and the S1P$_1$ receptor in wild-type soleus as a calibrator. Statistical significance of real-time PCR data was assessed with two-way ANOVA followed by a Bonferroni post hoc test. Differences were considered significant at $P < 0.05$.

RESULTS

Aging of S1P$_3$-null soleus. Skeletal muscle aging is characterized by the loss of muscle mass and strength, generally termed sarcopenia. We evaluated the effects produced by the absence of S1P$_3$ receptor on aging of soleus muscle by using adult (5 mo old) and old (23 mo old) wild-type and S1P$_3$-null mice (34).

First, the body mass of wild-type mice was similar (+2%) in adult and old age mice, whereas that of S1P$_3$-null mice was substantially increased by ~14% (Fig. 1*A*). Soleus muscle mass of old wild-type mice was largely smaller (−26%) than that of adult mice (Fig. 1*B*), confirming the atrophy observed in old skeletal muscle (1). Consistently, the ratio between soleus mass and body weight was markedly decreased in wild-type mice (Fig. 1*C*). Soleus muscle mass of S1P$_3$-null mice decreased only slightly during aging (Fig. 1*B*). As a consequence, the ratio between soleus mass and body weight also decreased in S1P$_3$-null mice. Preservation of muscle mass during aging in S1P$_3$-null mice is also observed in EDL (10.7 ± 0.6 mg, n = 8, vs. 9.9 ± 0.9 mg, n = 7) and in tibialis anterior, the mass of which increased compared with that of adult animals (50.8 ± 2.9 mg, n = 8, vs. 37.9 ± 3.3 mg, n = 3, $P < 0.03$). On the other hand, laminin staining evidenced that old wild-type soleus fibers were clearly smaller than those of adult wild-type mice and adult and old S1P$_3$-null mice (Fig. 1*D*), confirming the loss of mass of old wild-type soleus. Analysis of the mean CSA of soleus fibers shows evidence that old wild-type soleus fibers are 24% smaller than adult soleus fibers, whereas the mean CSA of old S1P$_3$-null fibers is similar to that of adult animals (Fig. 1*E*). Fiber CSA distribution (Fig. 1*F*) demonstrates that old wild-type soleus contains a higher number of smaller fibers than old S1P$_3$-null mice. Finally, the

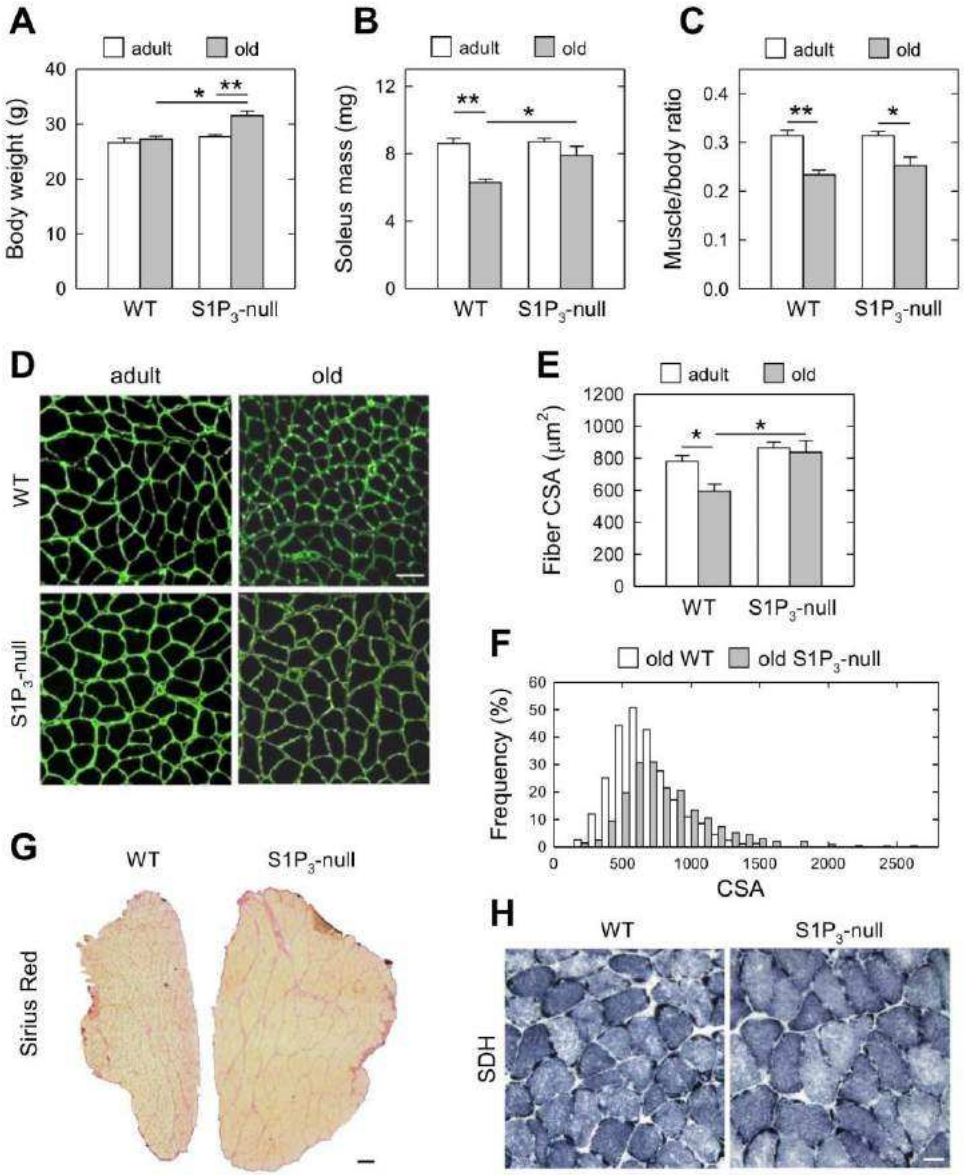

Fig. 1. Characteristics of old S1P$_3$-null soleus muscle. Values are means ± SE for 13 adult and 9 old wild-type (WT) and 15 adult and 14 old S1P$_3$-null mice. *A*: body weight of adult (age, 5 mo) and old (age, 23 mo) WT and S1P$_3$-null mice. *B*: soleus wet muscle mass of adult and old WT and S1P$_3$-null mice. *C*: muscle-to-body mass ratio in adult and old WT and S1P$_3$-null mice. *D*: laminin staining of soleus muscles from adult and old WT and S1P$_3$-null mice. Bar = 50 μm. *E*: soleus muscle fiber cross-sectional area (CSA) of adult and old WT and S1P$_3$-null mice. *F*: soleus muscle fiber CSA distribution in old WT and S1P$_3$-null mice. *G*: PicroSirius Red staining for collagen determination in old WT and S1P$_3$-null soleus muscle. Bar = 100 μm. *H*: succinate dehydrogenase (SDH) staining for mitochondrial content in old WT and S1P$_3$-null soleus muscle. Bar = 20 μm. $^*P < 0.05$, $^{**}P < 0.001$.

total number of fibers was comparable in adult and old wild-type and S1P$_3$-null soleus (916 ± 30, $n = 6$, and 899 ± 31, $n = 6$, in adult and old wild-type, respectively; 906 ± 24, $n = 5$, and 845 ± 35, $n = 7$, in adult and old S1P$_3$-null, respectively).

Histological analysis of adult and old soleus muscles from wild-type and S1P$_3$-null mice did not reveal overt morphological or pathological signs, however, some interesting differences emerged. The extent of collagen/fibrosis in old S1P$_3$-null mice was significantly lower ($P < 0.05$) compared with that in wild-type animals (8.3 ± 0.4%, $n = 6$, and 12.5 ± 1.8%, $n = 6$, respectively) (Fig. 1*G*), whereas adult muscles did not show any difference (not shown). Consistent with the lower amount of fibrosis in old S1P$_3$-null soleus, mRNA expression of CTGF (CCN2), a molecular marker and a mediator of fibrosis, was significantly ($P < 0.05$) lower in old S1P$_3$-null soleus (0.57 ± 0.09) compared with that of wild-type soleus (1.00 ± 0.10). In addition, we carried out an analysis of phosphorylated Smad3, a downstream effector of TGF-β, which through S1P$_3$, regulates muscle fibrosis (13). The P-Smad3-to-Smad3 ratio did not change during aging either in wild-type soleus (0.98 ± 0.38, $n = 5$, and 1.60 ± 0.48, $n = 4$, adult and old, respectively) or in S1P$_3$-null soleus (1.19 ± 0.38, $n = 5$, and 1.14 ± 0.30, $n = 5$, adult and old, respectively). Finally, the intensity of SDH staining did not show evident differences between old S1P$_3$-null and wild-type soleus fibers, with both muscles exhibiting in many fibers the presence of subsarcolemmal mitochondria aggregates (Fig. 1*H*).

Old wild-type and S1P$_3$-null soleus display a similar low number of fibers with central nuclei (likely a sign of regeneration) (3.7 ± 0.4%, $n = 5$ and 5.9 ± 1.3%, $n = 7$, respectively) and did not show angular fibers (a sign of denervation). Despite the apparent absence of denervation, myogenin protein expression level, usually high in denervated muscles (26, 61), was fivefold higher in old wild-type soleus compared with adult wild-type soleus (2.5 ± 0.59 vs. 0.59 ± 0.08; $n = 4$, $P < 0.02$). Myogenin was unchanged in old S1P$_3$-null soleus compared with that of adult soleus (1.26 ± 0.44 vs. 1.26 ± 0.25; $n = 4$).

A hallmark of aging atrophy is the progressive deterioration of NMJ integrity, which also accounts for the reduced performance of aged muscles. Figure 2, *A* and *D*, shows NMJs from a young soleus muscle stained either for VAMP1 or syntaxin 1A1B, respectively, two markers of the motor axon terminal, and for the ionotropic acetylcholine receptors, for the postsynaptic apparatus on the muscle fiber. Notably, the latter appears like a continuous and sinuous wavy line, assuming the classical pretzel-like shape that is perfectly matched by the presynaptic terminals. In agreement with previous reports (14, 15, 62), the morphology of the aged NMJ is characterized by a significant loss of the pretzel-like structure, which becomes highly fragmented and accompanied by a more complex branching of the presynaptic elements (Fig. 2, *B* and *E*). Remarkably, this alteration is significantly restrained in the age-matched S1P$_3$-null NMJ, which still displays a continuous and curvy architecture, more similar to that displayed by adult mice, though in some cases slightly less elaborated (Fig. 2, *C* and *F*).

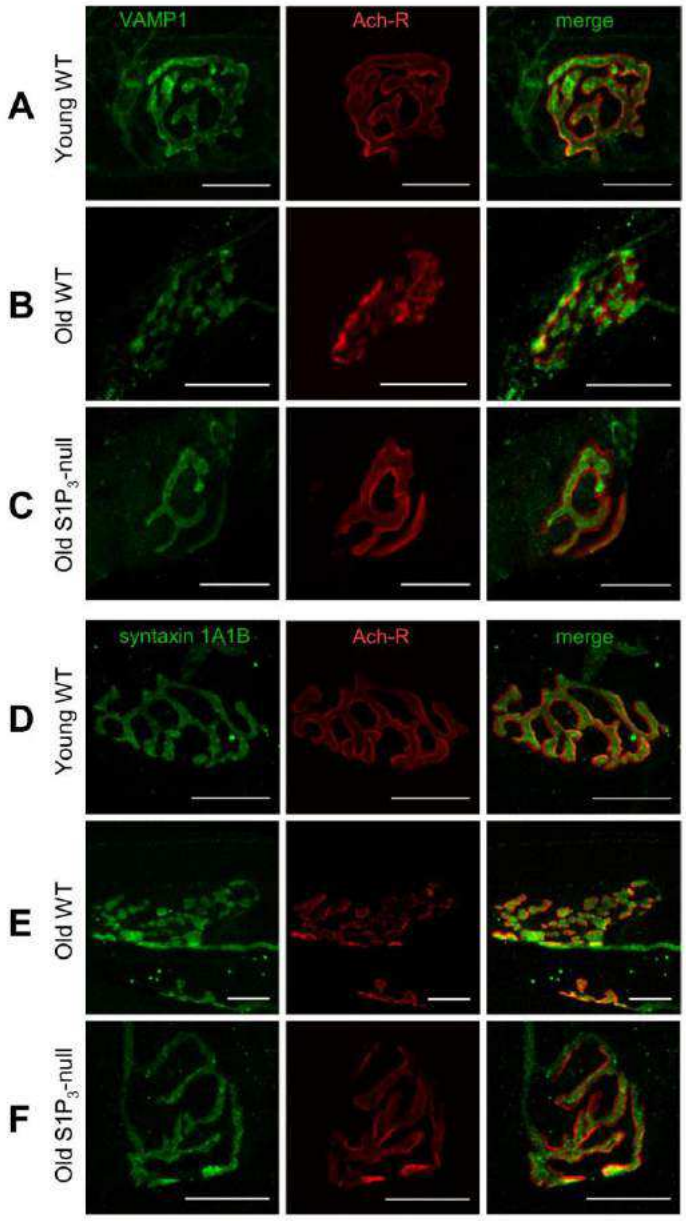

Fig. 2. Integrity of neuromuscular junctions (NMJs) is preserved during aging in S1P$_3$-null mice. Soleus muscles from adult (age, 5 mo) and old (age, 23 mo) WT mice or old S1P$_3$-null mice were dissected, fixed, and stained for a NMJ presynaptic marker, either VAMP1 (*A–C*) or syntaxin-1A1B (*D–F*), shown in green, and for the postsynaptic nicotinic acetylcholine receptors labeled in red, as described in MATERIALS AND METHODS. Adult NMJs (*A* and *D*) present the typical pretzel-like shape, which is largely lost in old WT muscle (*B* and *E*), which display a fragmented organization. NMJs from old S1P$_3$-null muscles (*C* and *F*) still exhibit a continuous and curvy pattern, similar to the pattern found in young mice. Photographs show a representative NMJ from at least two soleus muscles. Bar = 20 μm.

Aging of skeletal muscle is known to be associated with a progressive decline in muscle function (1). To evaluate whether the absence of S1P$_3$ may affect age-related changes in soleus performance, we compared the contractile properties of adult and old wild-type and S1P$_3$-null soleus. The absolute twitch and tetanic tensions of wild-type soleus were largely lower (−40.2 and −41%, respectively) in old compared with adult mice. On the contrary, no difference in absolute tension was observed between old and adult soleus of S1P$_3$-null mice (Fig. 3, *A* and *B*). Moreover, the specific twitch and tetanic tensions of old S1P$_3$-null soleus were higher compared with adult and old wild-type muscles (Fig. 3, *A* and *B*). Old wild-type soleus showed a significant lengthening of twitch contraction time, which was not evident in old S1P$_3$-null soleus. The maximal rate of tetanus rise was dramatically reduced (−55%) in old wild-type soleus compared with adult muscle, but unchanged in old S1P$_3$-null soleus. The half-relaxation time of the twitch is similar in the four muscles, whereas the half-relaxation time of the tetanus increased in old wild-type soleus only (Fig. 3, *A* and *B*).

The smaller tension developed by the twitch and tetanus of old wild-type soleus is also confirmed by the force-frequency curves, in which the absolute tension developed at each stimulation frequency tested was clearly smaller in old wild-type soleus than adult wild-type soleus (Fig. 3*C*). Therefore, old S1P$_3$-null soleus displays a similar absolute force-frequency curve (Fig. 3*C*) and a larger specific force-frequency curve to that of adult muscle at all stimulation frequencies (Fig. 3*D*).

Thus, aging produces a slowing of contractile properties in wild-type but not in S1P$_3$-null soleus. To evaluate whether the lengthening of contraction and relaxation times are associated with a reduced reaccumulation of myoplasmic calcium by the sarcoplasmic reticulum calcium pump (SERCA), we measured the expression level of fast and slow SERCA isoforms. In the soleus of old S1P$_3$-null mice the expression level of the fast SERCA1 isoform was lower than that in wild-type muscles (Fig. 4*A*). On the contrary, expression levels of the slow SERCA2 isoform were similar in adult and old soleus muscles (Fig. 4*B*).

The slowing of contractile properties could also be the consequence of fast-to-slow changes in the proportion of myosin isoforms. To evaluate possible changes in muscle phenotype we examined the composition of MyHC isoforms in adult and old soleus muscles. First, S1P$_3$-null adult soleus has a slower phenotype compared with that of wild-type muscle, showing a higher content of type 1 MyHC isoform and a lower content of type 2A and 2X isoforms (Table 1). Aging of wild-type soleus is characterized by a significant increase in type 1 fibers to the detriment of type 2A and 2X MyHC isoforms (Table 1), whereas no changes were observed when adult and old S1P$_3$-null soleus were compared.

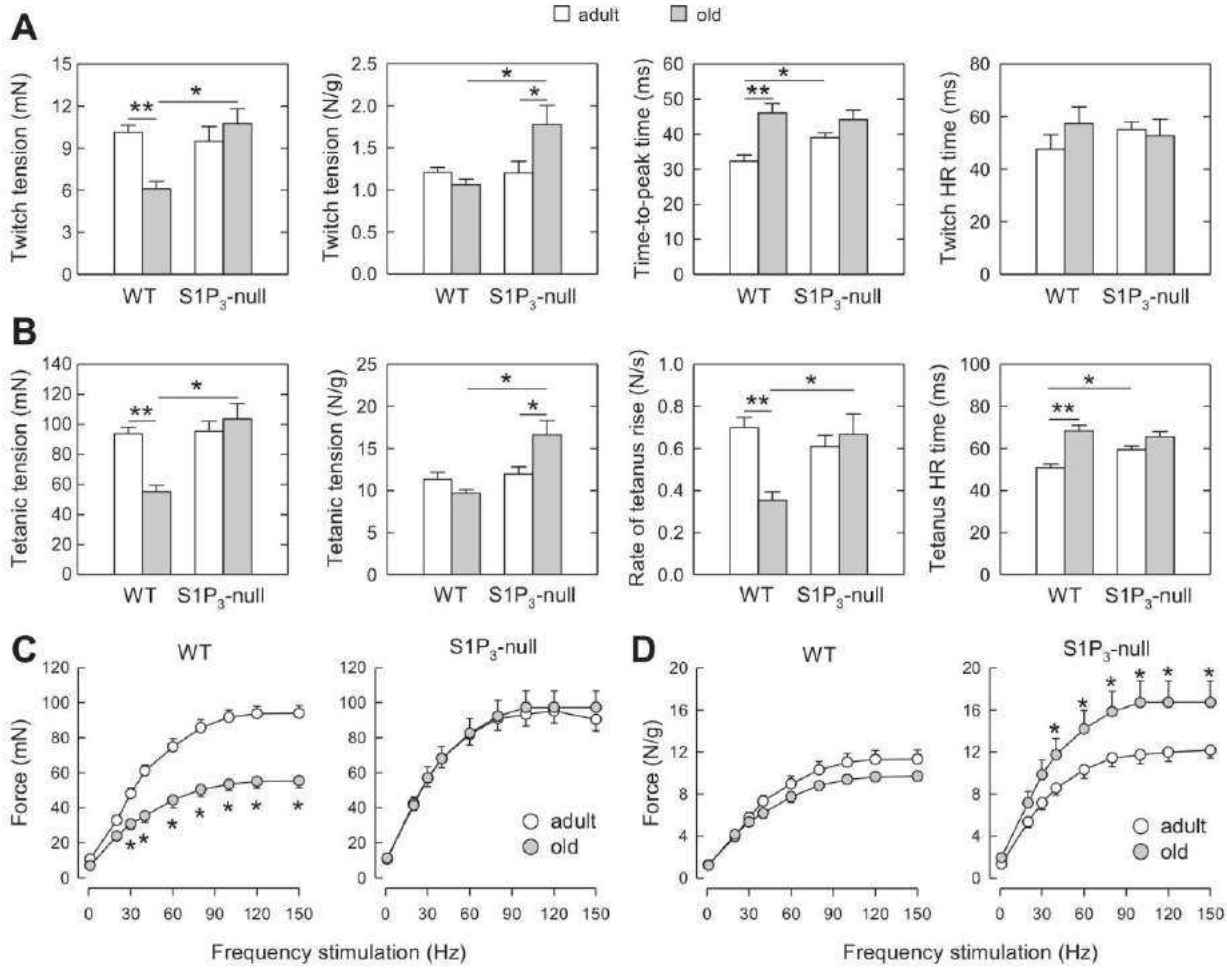

Fig. 3. Contractile properties of adult and old soleus muscle from WT and S1P$_3$-null mice. *A*: twitch characteristics of WT and S1P$_3$-null soleus. The absolute (mN) and specific (N/g) twitch tensions, time-to-peak time (ms), and the half-relaxation (HR) time (ms) of the twitch are shown. *B*: tetanus characteristics of WT and S1P$_3$-null soleus. The absolute and specific tetanic tensions, the maximal rate of rise of tension (N/s), and the half-relaxation time (ms) of the tetanus are shown. *C*: absolute force-frequency curves of adult and old WT and S1P$_3$-null soleus. *D*: specific force-frequency curves of adult and old WT and S1P$_3$-null soleus. Number of soleus muscles examined: adult WT (n = 8), old WT (n = 6), adult S1P$_3$-null (n = 9), and old S1P$_3$-null (n = 7). *$P < 0.05$, **$P < 0.001$.

Moreover, because the number of hybrid fibers (i.e., fibers expressing two or even more MyHC isoforms) has been reported during aging (52), we analyzed the fiber type composition of old soleus muscles. Results indicate that both old wild-type and S1P$_3$-null soleus possess a very low number of hybrid fibers (i.e., fibers expressing both type 1 and type 2A MyHC) (4.0 ± 1.4 vs. 5.0 ± 2.1% for old wild-type and S1P$_3$-null soleus, respectively).

Oxidative stress contributes, at least in part, to the progressive loss of muscle mass and function, leading to accumulation of oxidatively modified (carbonylated) proteins, including regulatory and contractile proteins (38, 49, 51). We investigated whether the extent of carbonylated proteins could explain the higher specific tension of old S1P$_3$-null soleus muscle. The results show that the amount of total carbonylated proteins was significantly lower in old S1P$_3$-null muscle compared with adult S1P$_3$ muscles, but not compared with adult or old wild-type muscles (Fig. 4*C*).

We next examined the consequences of the lack of S1P$_3$ on the expression of proteins involved in age-related atrophy. PGC-1α is a key regulator of mitochondria biogenesis (37) that could protect the S1P$_3$-null soleus muscle during aging. However, the expression level of PGC-1α did not change during aging either in wild-type soleus or in S1P$_3$-null soleus (Fig. 5*A*), which is in agreement with the similar SDH staining intensity (Fig. 1*H*) and the amount of Tom20, a component of the translocase receptor complex of the mitochondrial outer membrane, and an index of mitochondria content (Fig. 5*B*). The expression level of MuRF1, the E3 ligase involved in the proteolytic events of muscle atrophy (5) was comparable both in wild-type and S1P$_3$-null muscles (Fig. 5*C*). Moreover, the expression level of whole Akt and activated Akt (P-Akt), as well as the ratio between P-Akt and Akt, whose increase is related to muscle growth (6), did not change with age in wild-type or in S1P$_3$-null soleus. However, levels of P-Akt in adult muscle and that of whole Akt in old S1P$_3$-null muscles were higher than those in cognate wild-type muscles (Fig. 5*D*). We also examined the level of phosphorylated S6, the ribosomal protein marker of mammalian target of rapamycin (mTOR) and protein synthesis activation. No difference in the level of P-S6 was observed in the four conditions (Fig. 5*E*). Next, we measured the amount of p62, a protein involved in the recognition of autophagy substrates, and the LC3-II/LC3-I ratio, which is important in autophagosome formation (7).

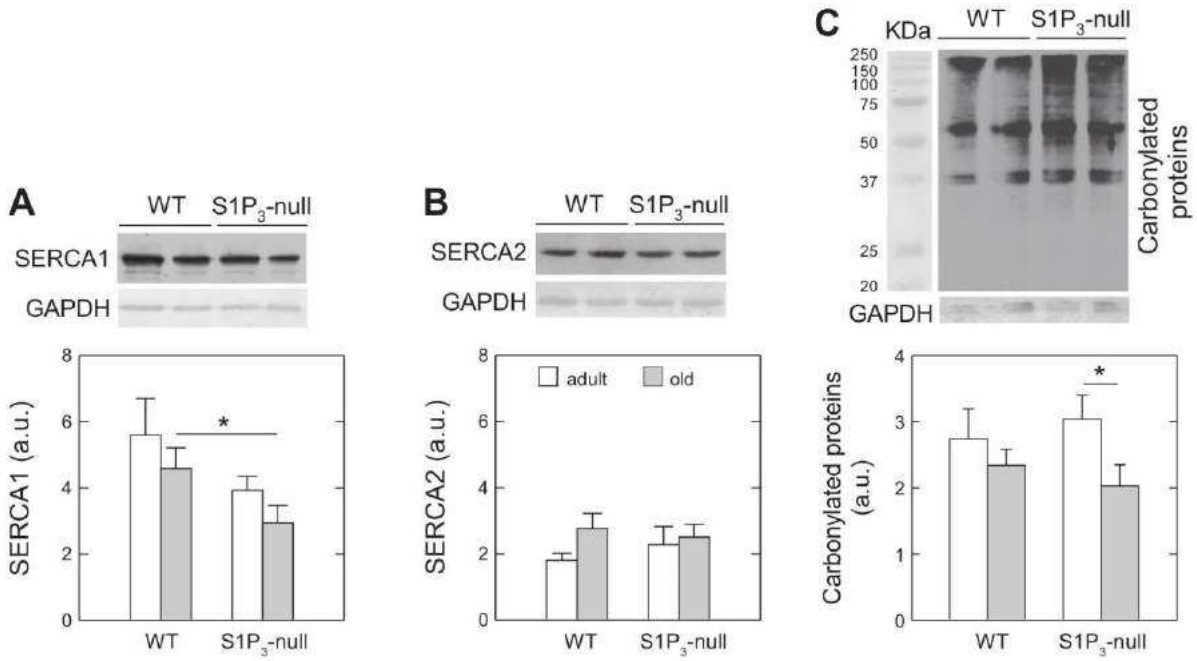

Fig. 4. Expression of SERCA protein isoforms and total level of carbonylated proteins in soleus muscle of adult and old WT and S1P$_3$-null mice. *A*: SERCA1 isoform expression level in adult and old WT and S1P$_3$-null soleus as determined by Western blotting (see example plot, *top*) as described in MATERIALS AND METHODS. The amount of SERCA1 was compared with that of GAPDH. *B*: SERCA2 isoform in adult and old WT and S1P$_3$-null soleus as determined by Western blotting (see example plot, *top*) as described in MATERIALS AND METHODS. The amount of SERCA2 was compared with that of GAPDH. *C*: carbonylated proteins in whole soleus muscle homogenates from adult and old WT and S1P$_3$-null mice. On the *left*, molecular mass (kDa) of protein markers is given. Carbonylated proteins were revealed by Western blotting (see example plot, *top*) as described in MATERIALS AND METHODS. GAPDH was used as a protein loading control. Number of soleus muscles examined: adult WT (n = 8), old WT (n = 6), adult S1P$_3$-null (n = 10), and old S1P$_3$-null (n = 6). *$P < 0.05$.

During aging, the expression level of p62 protein did not change in wild-type soleus, whereas it was significantly decreased in S1P$_3$-null muscle (Fig. 5*F*). Conversely, the LC3-II/LC3-I ratio did not change during aging either in wild-type or S1P$_3$-null soleus (Fig. 5*G*). Finally, to evaluate possible apoptotic events, we measured the expression level of Bcl-2, which, however, did not change (Fig. 5*H*).

We recently reported that expression of S1P$_1$ and S1P$_2$ transcripts, which are physiologically expressed in skeletal muscle, increases in the fast-twitch EDL muscle of S1P$_3$-null mice (27). Thus, we examined whether the absence of S1P$_3$ affects the expression level of the other S1P receptors in the slow-twitch soleus muscle. Using real-time PCR, we quantitated the transcript level of S1P$_1$ and S1P$_2$ receptors in soleus muscle. The data show that S1P$_3$ deficiency does not modify the expression level of S1P$_1$ or S1P$_2$ receptors either in adult or in old soleus muscle (Fig. 6).

Table 1. *Myosin heavy chain composition of soleus muscle from wild-type and S1P$_3$-null soleus muscle*

	Wild Type		S1P$_3$-Null	
MyHC Isoform	Adult (n = 8)	Old (n = 6)	Adult (n = 10)	Old (n = 6)
Type I	40.3 ± 1.7	48.6 ± 3.2*	49.3 ± 3.1*	48.9 ± 3.3
Type 2A	37.8 ± 1.6	33.6 ± 2.6	33.1 ± 1.3*	32.4 ± 1.5
Type 2X	20.2 ± 1.0	15.3 ± 1.1*	13.2 ± 0.8*	14.8 ± 0.9
Type 2B	1.7 ± 1.7	4.9 ± 1.7	4.3 ± 2.2	3.9 ± 3.9

Values are means ± SE (n = no. of muscles examined). MyHC, myosin heavy chain. *$P < 0.05$ vs. adult wild type.

Regeneration of old S1P$_3$-null soleus. We next examined the role of the S1P$_3$ receptor on the regenerative capacity of soleus muscle during aging. Regeneration of soleus muscle was induced by myotoxic injury (21, 29) to both adult and old soleus muscles from wild-type and S1P$_3$-null mice. Only muscles almost entirely regenerated were examined. Regenerating fibers were identified by the presence of centrally located nuclei after DAPI staining (Fig. 7*A*).

After 10 days of regeneration, adult wild-type soleus fibers had a mean CSA similar to that of age-matched S1P$_3$-null soleus (Fig. 7, *A* and *B*), indicating that regeneration progressed similarly in the two muscles and that the absence of the receptor does not seem to influence the regenerative process of adult soleus muscle.

The mean CSA of old wild-type soleus after 10 days of regeneration was significantly smaller (−28%) compared with that of adult regenerated muscle (Figs. 7, *A* and *B*), suggesting that regeneration of old wild-type soleus either proceeds more slowly or is impaired compared with that of adult muscle. On the contrary, regeneration of old S1P$_3$-null soleus was apparently as vigorous as in adult muscle, with a mean fiber CSA similar to that of adult muscle, and consequently, significantly larger (+ 27%) compared with that of old wild-type muscle (Fig. 7, *A* and *B*). Analysis of CSA distribution demonstrates that compared with old wild-type soleus, the larger mean CSA of S1P$_3$-null muscle derives from the presence of larger fibers and the absence/reduction of smaller ones (Fig. 7*C*).

The extent of fibrotic areas, as evidenced by PicroSirius Red staining, was not statistically different in old S1P$_3$-null soleus

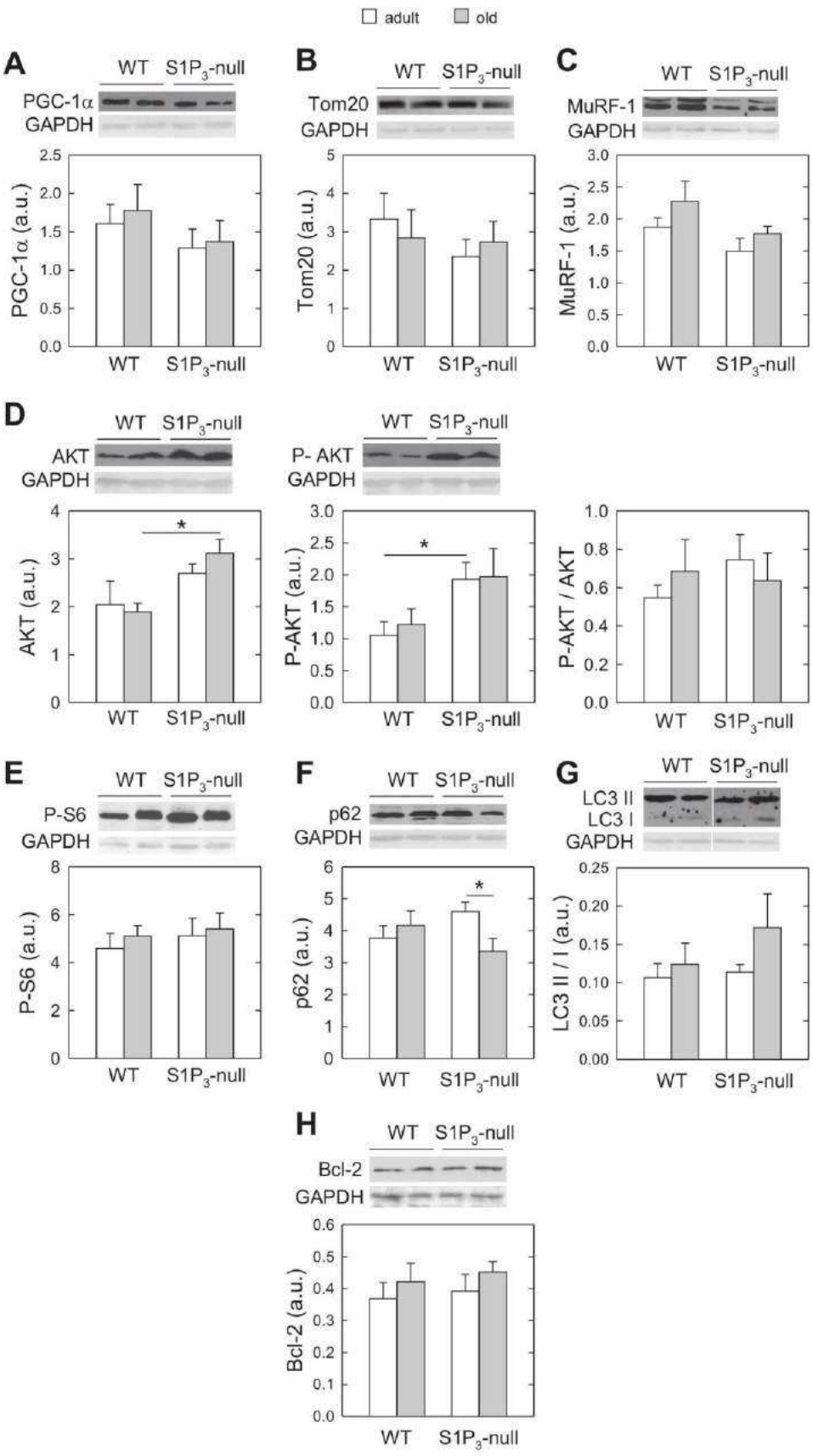

Fig. 5. Protein expression in adult and old WT and S1P$_3$-null soleus muscle. *A*: PGC-1α, peroxisome proliferator-activated receptor-γ coactivator 1α. *B*: Tom20, a component of the translocase receptor complex of mitochondrial outer membrane, an index of mitochondria content. *C*: MuRF1, E3 ligase involved in the proteolytic events of muscle atrophy. *D*: Akt, P-Akt, and P-Akt/Akt ratio. *E*: P-S6, phosphorylated ribosomal protein S6, a marker of mTOR and protein synthesis activation. *F*: p62, a protein involved in recognition of autophagy substrates. *G*: LC3 II/I ratio, an index of autophagosome formation. *H*: Bcl-2, an antiapoptotic factor. *Top*: all plots are examples of the relative Western blots carried out as described in MATERIALS AND METHODS. GAPDH was used as an internal control. Number of soleus muscles examined: adult WT (n = 7), old WT (n = 5), adult S1P$_3$-null (n = 9), and old S1P$_3$-null (n = 8). *$P < 0.05$.

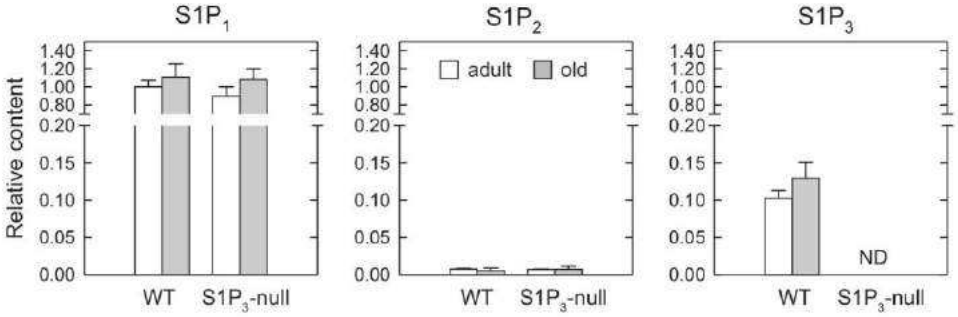

Fig. 6. Expression of S1P receptor transcripts in adult and old WT and S1P$_3$-null soleus. Expression of S1P receptors in each muscle was measured via real-time PCR. ND, not detected. Values are means ± SE of three independent experiments performed in triplicate.

(12.8 ± 1.4%, $n = 5$) compared with wild-type regenerating soleus (18.6 ± 2.5%, $n = 4$) (Fig. 7*D*).

Finally, we measured the myogenic transcription factors usually involved in muscle regeneration. The expression level of MyoD, a marker of cell proliferation (44), was significantly lower in old S1P$_3$-null soleus compared with adult transgenic muscle, whereas no difference was evident in wild-type muscles (Fig. 8*A*). MyoD levels in old regenerating S1P$_3$-null soleus were also lower than those of old wild-type regenerating muscle. The level of myogenin, a muscle differentiation marker (44), was larger in old wild-type soleus than in the adult muscle. Moreover, the level of myogenin was lower in old S1P$_3$-null soleus than in old wild-type soleus and was unchanged compared with that of adult transgenic muscle (Fig. 8*B*). Finally, the expression level of embryonic myosin, which was used to evaluate the progression of differentiation, was similar in the four regenerating muscles (Fig. 8*C*).

DISCUSSION

In this work, we evaluated whether and how S1P$_3$ receptor ablation influences the effects produced by age on soleus muscle. The study compared the morphological and functional characteristics, as well as the regenerative capacity of adult and old soleus muscle of wild-type and S1P$_3$-null mice. Some significant differences emerged in old animals: *1*) old S1P$_3$-null mice were heavier than age-matched wild-type mice; *2*) soleus muscles of S1P$_3$-null mice were protected from the

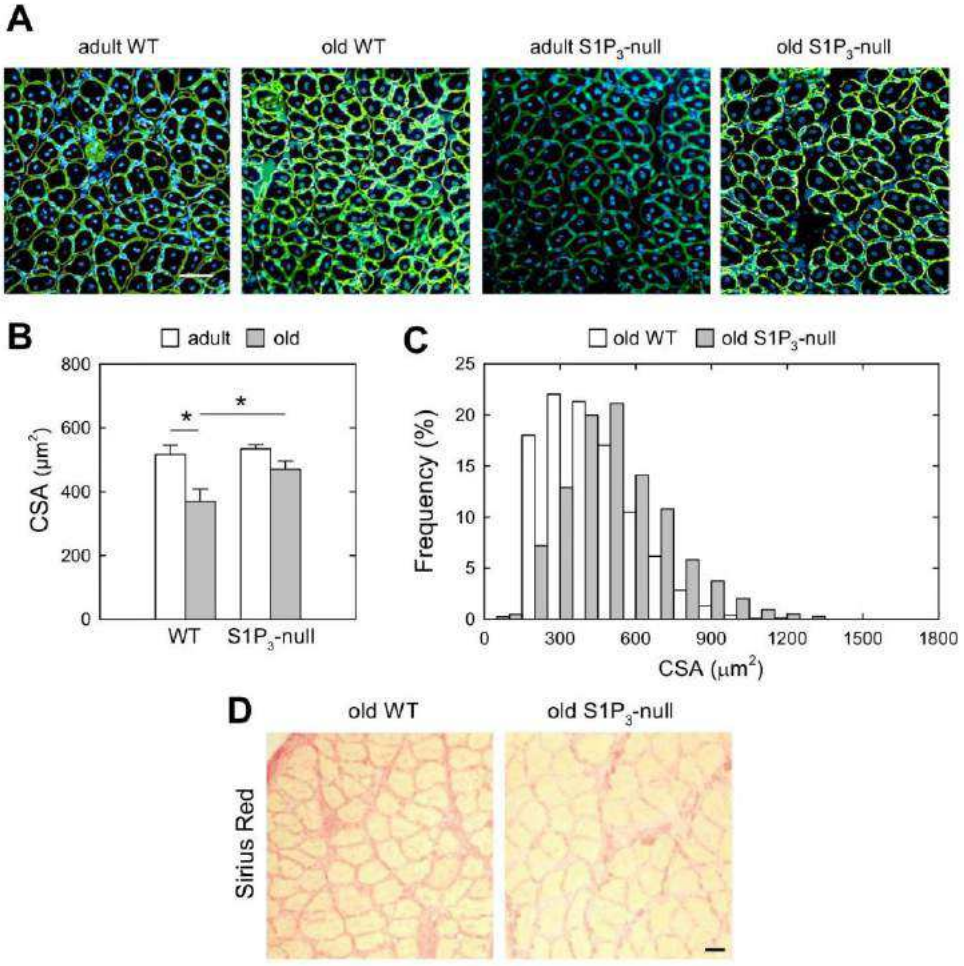

Fig. 7. Regeneration capacity is preserved in old S1P$_3$-null soleus muscle. Regeneration was induced in adult and old WT and S1P$_3$-null soleus by notexin, as described in MATERIALS AND METHODS. *A*: laminin staining of cryostat sections of soleus muscle from adult and old WT and S1P$_3$-null mice. Muscle sections were counterstained with DAPI to reveal centrally located nuclei in regenerating fibers. Bar = 50 μm. *B*: soleus muscle fiber CSA of adult and old, 10-day regenerated muscle from WT ($n = 5$) and S1P$_3$-null mice ($n = 5$), $^*P < 0.05$. *C*: soleus muscle fiber CSA distribution in old WT and old S1P$_3$-null mice. *D*: PicroSirius Red staining reveals the extent of collagen/fibrosis of old WT and S1P$_3$-null regenerated soleus muscle. Bar = 20 μm.

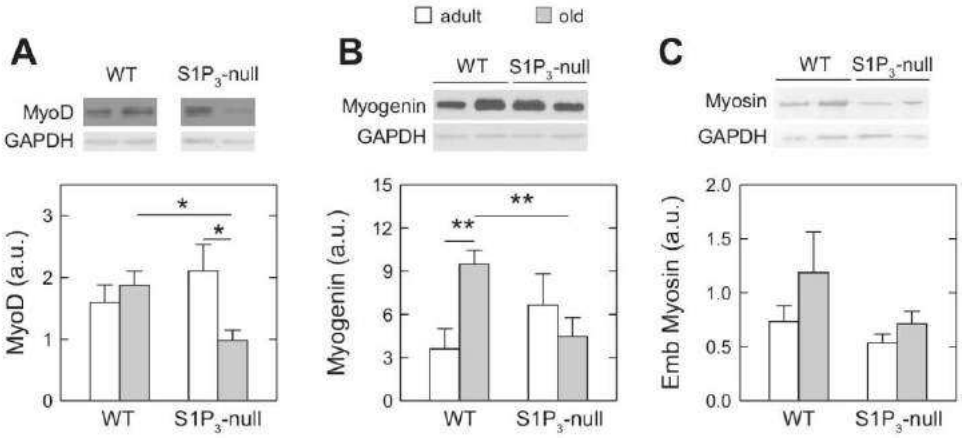

Fig. 8. Expression of muscle regeneration protein markers. *A*: MyoD expression level in 10-day regenerating adult (n = 5) and old (n = 5) WT and adult (n = 4) and old (n = 5) S1P$_3$-null soleus muscle. The expression level refers to that of GAPDH. *B*: myogenin expression level in 10-day regenerating adult (n = 5) and old (n = 6) WT and adult (n = 5) and old (n = 6) S1P$_3$-null soleus muscle. *C*: embryonic myosin in 10-day regenerating adult (n = 5) and old (n = 5) WT and adult (n = 4) and old (n = 5) S1P$_3$-null soleus muscle. *Top*: all plots are examples of the relative Western blots carried out as described in MATERIALS AND METHODS. The expression level refers to that of GAPDH. $*P < 0.05$, $**P < 0.025$.

age-related drop in muscle mass; *3*) the soleus muscles of old S1P$_3$-null mice were stronger and faster than those of wild-type mice; *4*) NMJs of old S1P$_3$-null mice are less deteriorated than those of wild-type mice; and *5*) the regenerative capacity of old S1P$_3$-null soleus is as efficient as it is in adulthood and is more efficient than it is in old wild-type soleus.

First, it is worth mentioning that the absence of S1P$_3$ appears to have different effects in fast and slow muscles. We recently characterized 3-mo-old S1P$_3$-null EDL (27). A common response to the absence of S1P$_3$ is a higher content of type 1 fibers that, only in soleus, is compensated by a decrease in type 2A and 2X fibers. Vice versa, the expression level of S1P$_1$ and S1P$_2$ in S1P$_3$-null EDL muscle is higher than in wild-type EDL muscle but it did not differ in soleus. Moreover, contractile properties of EDL were affected by the absence of S1P$_3$ (for example, lower twitch and tetanic tensions) but were mostly unaffected in soleus (27). Thus, the absence of S1P$_3$ seems to produce some fiber type-dependent differences.

Adult wild-type and S1P$_3$-null mice exhibited similar body weight, soleus muscle mass, and force. Diversely, old S1P$_3$-null mice were heavier than old wild-type mice. Wild-type mice usually grow up to approximately 16–18 mo of age and then slowly lose their body mass (62). The larger body mass of old S1P$_3$-null mice suggests a lower body mass reduction during aging compared with that in wild-type mice. Although there was no difference in body weight between adult and old wild-type mice, soleus mass, mean muscle fiber CSA, and ratio between soleus mass and body weight (a sarcopenia index) (24) were all significantly diminished during aging. Differently, soleus mass and the mean soleus fiber CSA of old S1P$_3$-null mice diminished much less (−9% and −3%, respectively) than they did in wild-type mice (−26% and −24%, respectively). Thus, compared with adult mice, old S1P$_3$-null mice showed an increased body weight and unchanged muscle weight, so that the muscle-to-body mass ratio was decreased as it is in wild-type mice (−19% and −25%, respectively), implying that the growth of other tissues and organs contributes to the heavier body, an intriguing aspect that deserves further investigation. Nonetheless, we propose that the larger body weight is in part dependent on the lower atrophic response of transgenic muscles. Our results indeed show that in the absence of S1P$_3$, the masses of old soleus, EDL, and tibialis anterior were the same size as they were in adult-age muscles.

To understand the reason for the minor atrophy of S1P$_3$-null soleus, we evaluated the expression of diverse muscle atrophy-related markers. An important factor in muscle loss is the prevalence of protein degradation over protein synthesis (7). The major component responsible for the degradation of contractile proteins in skeletal muscle is the ubiquitin-proteasome system (UPS), with MuRF-1 and atrogin-1 being the main E3 ubiquitin ligases activated during several forms of acute atrophy (5, 7). Here we found that, compared with adult soleus, the expression level of MuRF-1 protein was not changed either in old wild-type or in S1P$_3$-null soleus. Of note, during aging, MuRF-1 is reported to be either unchanged (32, 64), increased (17), or even decreased (24), suggesting that in the long term, the role of E3 ligases in age-related atrophy is apparently less definite than in acute atrophy.

Diminished protein synthesis in acute atrophy is associated with downregulation of Akt/mTOR signaling (3, 6, 7, 43), although even this correlation was not observed in the age-related atrophy of wild-type soleus (56, 64). In agreement, here we found that the level of total Akt and activated P-Akt did not change during aging either in wild-type or in S1P$_3$-null soleus. However, the expression levels of Akt and P-Akt were higher in adult and old S1P$_3$-null soleus than in wild-type soleus, a condition that could contribute to the maintenance of muscle mass in aged transgenic soleus. However, MuRF1 and P-S6, both downstream of Akt, did not change in transgenic soleus. Nevertheless, it is not surprising that the absence of S1P$_3$ may perturb Akt signaling. In fact, P-Akt and total Akt increase after denervation in S1P$_3$-null EDL (27). Moreover, it is known that S1P$_1$ and S1P$_2$ have opposite actions on cell proliferation through the stimulation and inhibition, respectively, of signaling pathways, including Akt (60).

The UPS and the lysosomal-autophagy system are coordinately activated in atrophying muscles (7, 43). We measured the amount of p62, a protein involved in the recognition of autophagy substrates (for example, mitochondria), and the LC3-II/LC3-I ratio, to evaluate the extent of autophagy. At variance with recent reports (11, 65), but in agreement with others (55, 64), in wild-type and S1P$_3$-null old soleus muscle, the LC3-II/LC3-I ratio did not change during aging compared with the ratio in adult-age muscle. During aging, the level of p62 did not change in wild-type soleus, whereas it significantly decreased in old S1P$_3$-null muscle. The reduced level of p62 protein could indicate a reduced autophagy in old S1P$_3$-null soleus, and therefore, a reduced atrophy. However, reduced or defective autophagy are reported to compromise mitochondrial homeostasis (11, 45) and mitochondrial-mediated apoptosis in

old muscles (65), eventually worsening sarcopenia (25). Instead, our results show that mitochondrial homeostasis seems preserved in old S1P$_3$-null soleus, as indicated by SDH staining, constitutive Tom20 protein, and PGC-1α levels that were comparable to those of adult-age muscle. Finally, the expression level of the antiapoptotic Bcl-2, reported to increase in fast but not in slow old rat muscles (53), was similar in adult and old wild-type and S1P$_3$-null soleus.

Another possible element contributing to the reduced sarcopenia in the knockout mice could be the better preservation of the architecture of their neuromuscular junctions. Indeed, it is long known that motor nerve terminals and their interactions with myofibers are greatly altered during aging (14, 15, 62). Even though we cannot establish whether reduced NMJ deterioration is a cause or an effect of the reduced muscle mass loss in S1P$_3$-null mice, it is, however, conceivable that the improved maintenance of acetylcholine receptor clusters in these animals may result in a more efficient and reliable stimulation of muscle fibers, which is trophic by itself. Obviously, this may in turn trigger a positive feedback toward nerve endings through the release of neurotrophic factors from the muscle fiber, thus leading to an overall endurance of the neuromuscular system. Vice versa, NMJ deterioration in old wild-type soleus could contribute to the progressive atrophy of the muscle, however, without the appearance of small and angular fibers and/or the reduction in total number of muscle fibers, which are clear signs of denervation.

Old S1P$_3$-null soleus was not only protected from age-related loss of mass but also from the loss of force. The literature (1) and our results show a significant drop in absolute force only in old wild-type soleus muscle, mainly attributable to the loss of muscle mass. By contrast, in old S1P$_3$-null soleus, not only was the absolute force unchanged, but it is evident of a significant increase in specific force. The results also show a slowing of contractile properties in old compared with adult wild-type soleus, a change, however, that was not observed in old S1P$_3$-null soleus. Different factors could modulate muscle force development and contraction speed: a greater relative number of slow-type fibers (19, 59), the oxidative damage to proteins involved in cross-bridge cycling (38), or alterations in excitation-contraction coupling (50). It is known that slow fibers have lower specific force than fast fibers (8, 9), so the fast-to-slow shift in old wild-type soleus could be responsible, at least in part, for the reduced force and contraction speed. However, compared with wild-type soleus, adult S1P$_3$-null soleus displays a slower phenotype (more type 1 and fewer type 2A and 2X fibers) but not varied contractile properties, a characteristic that did not change during aging. Slowing of contractile properties could also be due to the changes in the total amount of SERCA isoforms. Because SERCA1 and SERCA2 isoforms have the same enzymatic activity (42), the speed of calcium reaccumulation into the sarcoplasmic reticulum is related to the total amount of SERCA isoforms in a muscle. Our data did not show overt differences in adult muscles, and SERCA1 content was significantly reduced only in old S1P$_3$-null soleus. So, preservation of contractile properties in old S1P$_3$-null soleus does not seem to be related either to a fiber type switch or to a higher content of SERCA isoforms. An additional possibility is that the absence of S1P$_3$ could maintain a more favorable microenvironment in old animals compared with adult animals. Accordingly, myofibrillar protein carbonylation, an index of oxidative stress, was substantially decreased in old S1P$_3$-null soleus. Intriguingly, reactive oxygen species were found to be involved in S1P$_3$-mediated pathological cardiac remodeling in mice (61).

Morphologically, we did not observe a major difference between wild-type and S1P$_3$-null soleus. However, we noted that old wild-type soleus had a higher fibrosis level than old S1P$_3$-null soleus as confirmed by a lower level of CTGF (CCN2) mRNA in the transgenic muscle. Recent findings show that the concentration of collagen and of fibrosis in old mice is almost twice that in young mice (66). Because CTGF expression in adult tissues is a clinically relevant molecular marker of fibrosis (10), this result indicates that a less fibrotic phenotype is maintained in old soleus in the absence of S1P$_3$ receptor. It is worth mentioning that the reduced expression of CTGF and the related lower extent of fibrosis in S1P$_3$-null compared with wild-type old soleus are in agreement with recent data demonstrating a correlation between S1P$_3$ and activation of Yes-associated protein (YAP) (16). YAP is a transcriptional regulator that acts through the TEA domain family (TEAD) transcription factor, a recognized early activator of CTGF expression (68). Therefore, we can hypothesize that the lower extent of skeletal muscle fibrosis in S1P$_3$-null old soleus could be ascribed to decreased YAP/TEAD activation, which is responsible for CTGF expression. Moreover, S1P$_3$ is the dominant signaling receptor upon TGF-β1 challenge and seems to be implicated in the transdifferentiation of myoblasts into myofibroblasts (13). In agreement, the structural analogue of S1P, FTY720 phosphate, has been reported to elicit myofibroblast differentiation of fibroblasts via S1P$_3$, as its effect was abrogated in S1P$_3$-null mice (35). Activation of Smad3 signaling is also important for myofibroblast transdifferentiation (35). However, we did not observe significant changes in the P-Smad3/Smad3 ratio either in old wild-type or in S1P$_3$-null soleus. The absence of S1P$_3$ seems to be beneficial in the age-related accumulation of collagen in old soleus, which is consistent with the finding that S1P$_3$ ablation represses cardiac fibrosis (61).

Regeneration is less efficient or at least delayed in old muscles (4, 30). The lower regenerative capacity of aged muscle is associated with several factors, including the decrease of resident muscle stem cells and/or to a less favorable environment for stem cell activation and function (2, 12). Our data indicate that the absence of S1P$_3$ facilitates the growth of regenerating fibers. Multiple findings support the notion that S1P$_3$ may play a critical role in muscle regeneration. Indeed, quiescent SCs display very high levels of S1P$_3$ compared with proliferating SCs (26), suggesting that the drop in receptor level promotes proliferation. As a confirmation, SCs isolated from young (6–8 wk of age) S1P$_3$-null mice exhibited enhanced proliferative ability and more extensively differentiated into myotubes (26). Moreover, regeneration of tibialis anterior, the fast muscle of young S1P$_3$-null mice, was transiently enhanced compared with that of wild-type mice (26).

During regeneration, MyoD is related to proliferation of SCs, whereas myogenin is related to muscle differentiation. And whereas in young muscles myogenin and MyoD mRNA levels return to baseline after regeneration, in old muscles they remain upregulated (44), suggesting a more prolonged need for myogenic factors in old muscles. Ten-day-old regenerating S1P$_3$-null soleus contains less MyoD and myogenin proteins

than old wild-type soleus. Therefore, the reduced levels of MyoD and myogenin in old $S1P_3$-null regenerating muscle suggests a more efficient regeneration compared with that of wild-type muscle; however, it is not paralleled by a reduction in embryonic MyHC isoform. Because myogenin increases during muscle denervation (27, 63), the altered functional innervation observed in old wild-type muscle could contribute to the elevated myogenin expression of regenerating muscle.

Sarcopenia is a progressive, multifactorial impairment of skeletal muscle. Present results show that the absence of $S1P_3$ protects soleus from the decrease in muscle mass and force, and attenuation of regenerative capacity, all of which are typical characteristics of aging. The lack of $S1P_3$ seems to modulate the aging process without, apparently, affecting obvious molecular targets, most likely by modulating critical signaling pathways. During aging, the progressive adaptation of soleus muscle to the absence of $S1P_3$ and related signals probably produces a condition that allows a better resistance to sarcopenia. In conclusion, our results identify $S1P_3$ and its signaling as candidate targets for controlling the effects of aging on skeletal muscle. Because various novel molecules have been identified to modulate S1P signaling (60), our findings represent the basis for the development of treatments for sarcopenia.

GRANTS

Support for this work was provided by MIUR-PRIN 2009 to P. Bruni and D. Danieli-Betto, by funds from the National Research Council of Italy to R. Betto, and by PRAT University of Padova 2015 grants to L. Gorza and D. Danieli-Betto.

DISCLOSURES

No conflicts of interest, financial or otherwise, are declared by the authors.

AUTHOR CONTRIBUTIONS

D.D.-B. conceived and designed research; M.B., E.G., M.P., G.Z., F.C., and C.D. performed experiments; M.B., E.G., M.P., G.Z., F.C., C.D., and D.D.-B. analyzed data; M.B., E.G., M.P., G.Z., F.C., C.D., and D.D.-B. interpreted results of experiments; M.B., E.G., M.P., G.Z., F.C., C.D., and R.B. prepared figures; R.B. and D.D.-B. drafted manuscript; L.G., R.B., P.B., and D.D.-B. edited and revised manuscript; M.B., E.G., M.P., G.Z., F.C., C.D., L.G., R.B., P.B., and D.D.-B. approved final version of manuscript.

REFERENCES

1. **Ballak SB, Degens H, de Haan A, Jaspers RT.** Aging related changes in determinants of muscle force generating capacity: a comparison of muscle aging in men and male rodents. *Ageing Res Rev* 14: 43–55, 2014. doi:10.1016/j.arr.2014.01.005.
2. **Barberi L, Scicchitano BM, De Rossi M, Bigot A, Duguez S, Wielgosik A, Stewart C, McPhee J, Conte M, Narici M, Franceschi C, Mouly V, Butler-Browne G, Musarò A.** Age-dependent alteration in muscle regeneration: the critical role of tissue niche. *Biogerontology* 14: 273–292, 2013. doi:10.1007/s10522-013-9429-4.
3. **Bilodeau PA, Coyne ES, Wing SS.** The ubiquitin proteasome system in atrophying skeletal muscle: roles and regulation. *Am J Physiol Cell Physiol* 311: C392–C403, 2016. doi:10.1152/ajpcell.00125.2016.
4. **Blau HM, Cosgrove BD, Ho AT.** The central role of muscle stem cells in regenerative failure with aging. *Nat Med* 21: 854–862, 2015. doi:10.1038/nm.3918.
5. **Bodine SC, Baehr LM.** Skeletal muscle atrophy and the E3 ubiquitin ligases MuRF1 and MAFbx/atrogin-1. *Am J Physiol Endocrinol Metab* 307: E469–E484, 2014. doi:10.1152/ajpendo.00204.2014.
6. **Bodine SC, Stitt TN, Gonzalez M, Kline WO, Stover GL, Bauerlein R, Zlotchenko E, Scrimgeour A, Lawrence JC, Glass DJ, Yancopoulos GD.** Akt/mTOR pathway is a crucial regulator of skeletal muscle hypertrophy and can prevent muscle atrophy in vivo. *Nat Cell Biol* 3: 1014–1019, 2001. doi:10.1038/ncb1101-1014.
7. **Bonaldo P, Sandri M.** Cellular and molecular mechanisms of muscle atrophy. *Dis Model Mech* 6: 25–39, 2013. doi:10.1242/dmm.010389.
8. **Bottinelli R, Canepari M, Reggiani C, Stienen GJ.** Myofibrillar ATPase activity during isometric contraction and isomyosin composition in rat single skinned muscle fibres. *J Physiol* 481: 663–675, 1994. doi:10.1113/jphysiol.1994.sp020472.
9. **Bottinelli R, Reggiani C.** Human skeletal muscle fibres: molecular and functional diversity. *Prog Biophys Mol Biol* 73: 195–262, 2000. doi:10.1016/S0079-6107(00)00006-7.
10. **Bradham DM, Igarashi A, Potter RL, Grotendorst GR.** Connective tissue growth factor: a cysteine-rich mitogen secreted by human vascular endothelial cells is related to the SRC-induced immediate early gene product CEF-10. *J Cell Biol* 114: 1285–1294, 1991. doi:10.1083/jcb.114.6.1285.
11. **Carnio S, LoVerso F, Baraibar MA, Longa E, Khan MM, Maffei M, Reischl M, Canepari M, Loefler S, Kern H, Blaauw B, Friguet B, Bottinelli R, Rudolf R, Sandri M.** Autophagy impairment in muscle induces neuromuscular junction degeneration and precocious aging. *Cell Reports* 8: 1509–1521, 2014. doi:10.1016/j.celrep.2014.07.061.
12. **Carosio S, Berardinelli MG, Aucello M, Musarò A.** Impact of ageing on muscle cell regeneration. *Ageing Res Rev* 10: 35–42, 2011. doi:10.1016/j.arr.2009.08.001.
13. **Cencetti F, Bernacchioni C, Nincheri P, Donati C, Bruni P.** Transforming growth factor-β1 induces transdifferentiation of myoblasts into myofibroblasts via up-regulation of sphingosine kinase-1/$S1P_3$ axis. *Mol Biol Cell* 21: 1111–1124, 2010. doi:10.1091/mbc.E09-09-0812.
14. **Chai RJ, Vukovic J, Dunlop S, Grounds MD, Shavlakadze T.** Striking denervation of neuromuscular junctions without lumbar motoneuron loss in geriatric mouse muscle. *PLoS One* 6: e28090, 2011. doi:10.1371/journal.pone.0028090.
15. **Cheng A, Morsch M, Murata Y, Ghazanfari N, Reddel SW, Phillips WD.** Sequence of age-associated changes to the mouse neuromuscular junction and the protective effects of voluntary exercise. *PLoS One* 8: e67970, 2013. doi:10.1371/journal.pone.0067970.
16. **Cheng JC, Chang HM, Liu PP, Leung PC.** Sphingosine-1-phosphate induces COX-2 expression and PGE2 production in human granulosa cells through a $S1P_{1/3}$-mediated YAP signaling. *Cell Signal* 28: 643–651, 2016. doi:10.1016/j.cellsig.2016.03.006.
17. **Clavel S, Coldefy AS, Kurkdjian E, Salles J, Margaritis I, Derijard B.** Atrophy-related ubiquitin ligases, atrogin-1 and MuRF1 are up-regulated in aged rat tibialis anterior muscle. *Mech Ageing Dev* 127: 794–801, 2006. doi:10.1016/j.mad.2006.07.005.
18. **Conboy IM, Conboy MJ, Smythe GM, Rando TA.** Notch-mediated restoration of regenerative potential to aged muscle. *Science* 302: 1575–1577, 2003. doi:10.1126/science.1087573.
19. **Danieli-Betto D, Betto R, Megighian A, Midrio M, Salviati G, Larsson L.** Effects of age on sarcoplasmic reticulum properties and histochemical composition of fast- and slow-twitch rat muscles. *Acta Physiol Scand* 154: 59–64, 1995. doi:10.1111/j.1748-1716.1995.tb09886.x.
20. **Danieli-Betto D, Germinario E, Esposito A, Megighian A, Midrio M, Ravara B, Damiani E, Dalla Libera L, Sabbadini RA, Betto R.** Sphingosine 1-phosphate protects mouse EDL skeletal muscle during fatigue. *Am J Physiol Cell Physiol* 288: C1367–C1373, 2005. doi:10.1152/ajpcell.00246.2004.
21. **Danieli-Betto D, Peron S, Germinario E, Zanin M, Sorci G, Franzoso S, Sandonà D, Betto R.** Sphingosine 1-phosphate signaling is involved in skeletal muscle regeneration. *Am J Physiol Cell Physiol* 298: C550–C558, 2010. doi:10.1152/ajpcell.00072.2009.
22. **Donati C, Cencetti F, Bruni P.** Sphingosine 1-phosphate axis: a new leader actor in skeletal muscle biology. *Front Physiol* 4: 338, 2013. doi:10.3389/fphys.2013.00338.
23. **Donati C, Cencetti F, Nincheri P, Bernacchioni C, Brunelli S, Clementi E, Cossu G, Bruni P.** Sphingosine 1-phosphate mediates proliferation and survival of mesoangioblasts. *Stem Cells* 25: 1713–1719, 2007. doi:10.1634/stemcells.2006-0725.
24. **Edström E, Altun M, Hägglund M, Ulfhake B.** Atrogin-1/MAFbx and MuRF1 are downregulated in aging-related loss of skeletal muscle. *J Gerontol A Biol Sci Med Sci* 61: 663–674, 2006. doi:10.1093/gerona/61.7.663.
25. **Fan J, Kou X, Jia S, Yang X, Yang Y, Chen N.** Autophagy as a potential target for sarcopenia. *J Cell Physiol* 231: 1450–1459, 2016. doi:10.1002/jcp.25260.

26. **Fortier M, Figeac N, White RB, Knopp P, Zammit PS.** Sphingosine-1-phosphate receptor 3 influences cell cycle progression in muscle satellite cells. *Dev Biol* 382: 504–516, 2013. doi:10.1016/j.ydbio.2013.07.006.
27. **Germinario E, Bondì M, Cencetti F, Donati C, Nocella M, Colombini B, Betto R, Bruni P, Bagni MA, Danieli-Betto D.** S1P$_3$ receptor influences key physiological properties of fast-twitch extensor digitorum longus muscle. *J Appl Physiol (1985)* 120: 1288–1300, 2016. doi:10.1152/japplphysiol.00345.2015.
28. **Germinario E, Esposito A, Midrio M, Betto R, Danieli-Betto D.** Expression of sarco(endo)plasmic reticulum Ca^{2+}-ATPase slow (SERCA2) isoform in regenerating rat soleus skeletal muscle depends on nerve impulses. *Exp Physiol* 87: 575–583, 2002. doi:10.1113/eph8702436.
29. **Germinario E, Peron S, Toniolo L, Betto R, Cencetti F, Donati C, Bruni P, Danieli-Betto D.** S1P$_2$ receptor promotes mouse skeletal muscle regeneration. *J Appl Physiol (1985)* 113: 707–713, 2012. doi:10.1152/japplphysiol.00300.2012.
30. **Grounds MD.** Therapies for sarcopenia and regeneration of old skeletal muscles: more a case of old tissue architecture than old stem cells. *Bioarchitecture* 4: 81–87, 2014. doi:10.4161/bioa.29668.
31. **Hadi AM, Mouchaers KT, Schalij I, Grunberg K, Meijer GA, Vonk-Noordegraaf A, van der Laarse WJ, Beliën JA.** Rapid quantification of myocardial fibrosis: a new macro-based automated analysis. *Anal Cell Pathol (Amst)* 33: 257–269, 2010. doi:10.1155/2010/858356.
32. **Hwee DT, Baehr LM, Philp A, Baar K, Bodine SC.** Maintenance of muscle mass and load-induced growth in Muscle RING Finger 1 null mice with age. *Aging Cell* 13: 92–101, 2014. doi:10.1111/acel.12150.
33. **Ieronimakis N, Pantoja M, Hays AL, Dosey TL, Qi J, Fischer KA, Hoofnagle AN, Sadilek M, Chamberlain JS, Ruohola-Baker H, Reyes M.** Increased sphingosine-1-phosphate improves muscle regeneration in acutely injured mdx mice. *Skelet Muscle* 3: 20, 2013. doi:10.1186/2044-5040-3-20.
34. **Ishii I, Friedman B, Ye X, Kawamura S, McGiffert C, Contos JJ, Kingsbury MA, Zhang G, Brown JH, Chun J.** Selective loss of sphingosine 1-phosphate signaling with no obvious phenotypic abnormality in mice lacking its G protein-coupled receptor, LP$_{B3}$/EDG-3. *J Biol Chem* 276: 33697–33704, 2001. doi:10.1074/jbc.M104441200.
35. **Keller CD, Rivera Gil P, Tölle M, van der Giet M, Chun J, Radeke HH, Schäfer-Korting M, Kleuser B.** Immunomodulator FTY720 induces myofibroblast differentiation via the lysophospholipid receptor S1P$_3$ and Smad3 signaling. *Am J Pathol* 170: 281–292, 2007. doi:10.2353/ajpath.2007.060485.
36. **Larsson L.** Motor units: remodeling in aged animals. *J Gerontol A Biol Sci Med Sci* 50: 91–95, 1995.
37. **Lexell J.** Human aging, muscle mass, and fiber type composition. *J Gerontol A Biol Sci Med Sci* 50: 11–16, 1995.
38. **Li M, Ogilvie H, Ochala J, Artemenko K, Iwamoto H, Yagi N, Bergquist J, Larsson L.** Aberrant post-translational modifications compromise human myosin motor function in old age. *Aging Cell* 14: 228–235, 2015. doi:10.1111/acel.12307.
39. **Lin J, Wu H, Tarr PT, Zhang CY, Wu Z, Boss O, Michael LF, Puigserver P, Isotani E, Olson EN, Lowell BB, Bassel-Duby R, Spiegelman BM.** Transcriptional co-activator PGC-1 α drives the formation of slow-twitch muscle fibres. *Nature* 418: 797–801, 2002. doi:10.1038/nature00904.
40. **Livak KJ, Schmittgen TD.** Analysis of relative gene expression data using real-time quantitative PCR and the $2^{-\Delta\Delta CT}$ method. *Methods* 25: 402–408, 2001. doi:10.1006/meth.2001.1262.
41. **Loh KC, Leong W-I, Carlson ME, Oskouian B, Kumar A, Fyrst H, Zhang M, Proia RL, Hoffman EP, Saba JD.** Sphingosine-1-phosphate enhances satellite cell activation in dystrophic muscles through a S1PR2/STAT3 signaling pathway. *PLoS One* 7: e37218, 2012. doi:10.1371/journal.pone.0037218.
42. **Lytton J, Westlin M, Burk SE, Shull GE, MacLennan DH.** Functional comparisons between isoforms of the sarcoplasmic or endoplasmic reticulum family of calcium pumps. *J Biol Chem* 267: 14483–14489, 1992.
43. **Mammucari C, Milan G, Romanello V, Masiero E, Rudolf R, Del Piccolo P, Burden SJ, Di Lisi R, Sandri C, Zhao J, Goldberg AL, Schiaffino S, Sandri M.** FoxO3 controls autophagy in skeletal muscle in vivo. *Cell Metab* 6: 458–471, 2007. doi:10.1016/j.cmet.2007.11.001.
44. **Marsh DR, Criswell DS, Carson JA, Booth FW.** Myogenic regulatory factors during regeneration of skeletal muscle in young, adult, and old rats. *J Appl Physiol (1985)* 83: 1270–1275, 1997.
45. **Marzetti E, Calvani R, Cesari M, Buford TW, Lorenzi M, Behnke BJ, Leeuwenburgh C.** Mitochondrial dysfunction and sarcopenia of aging: from signaling pathways to clinical trials. *Int J Biochem Cell Biol* 45: 2288–2301, 2013. doi:10.1016/j.biocel.2013.06.024.
46. **Mendelson K, Evans T, Hla T.** Sphingosine 1-phosphate signalling. *Development* 141: 5–9, 2014. doi:10.1242/dev.094805.
47. **Nagata Y, Partridge TA, Matsuda R, Zammit PS.** Entry of muscle satellite cells into the cell cycle requires sphingolipid signaling. *J Cell Biol* 174: 245–253, 2006. doi:10.1083/jcb.200605028.
48. **Narici MV, Maffulli N.** Sarcopenia: characteristics, mechanisms and functional significance. *Br Med Bull* 95: 139–159, 2010. doi:10.1093/bmb/ldq008.
49. **Pellegrino MA, Desaphy JF, Brocca L, Pierno S, Camerino DC, Bottinelli R.** Redox homeostasis, oxidative stress and disuse muscle atrophy. *J Physiol* 589: 2147–2160, 2011. doi:10.1113/jphysiol.2010.203232.
50. **Plant DR, Lynch GS.** Excitation-contraction coupling and sarcoplasmic reticulum function in mechanically skinned fibres from fast skeletal muscles of aged mice. *J Physiol* 543: 169–176, 2002. doi:10.1113/jphysiol.2002.022418.
51. **Powers SK, Kavazis AN, McClung JM.** Oxidative stress and disuse muscle atrophy. *J Appl Physiol (1985)* 102: 2389–2397, 2007. doi:10.1152/japplphysiol.01202.2006.
52. **Purves-Smith FM, Solbak NM, Rowan SL, Hepple RT.** Severe atrophy of slow myofibers in aging muscle is concealed by myosin heavy chain co-expression. *Exp Gerontol* 47: 913–918, 2012. doi:10.1016/j.exger.2012.07.013.
53. **Rice KM, Blough ER.** Sarcopenia-related apoptosis is regulated differently in fast- and slow-twitch muscles of the aging F344/N × BN rat model. *Mech Ageing Dev* 127: 670–679, 2006. doi:10.1016/j.mad.2006.03.005.
54. **Rossetto O, Gorza L, Schiavo G, Schiavo N, Scheller RH, Montecucco C.** VAMP/synaptobrevin isoforms 1 and 2 are widely and differentially expressed in nonneuronal tissues. *J Cell Biol* 132: 167–179, 1996. doi:10.1083/jcb.132.1.167.
55. **Sakuma K, Kinoshita M, Ito Y, Aizawa M, Aoi W, Yamaguchi A.** p62/SQSTM1 but not LC3 is accumulated in sarcopenic muscle of mice. *J Cachexia Sarcopenia Muscle* 7: 204–212, 2016. doi:10.1002/jcsm.12045.
56. **Sandri M, Barberi L, Bijlsma AY, Blaauw B, Dyar KA, Milan G, Mammucari C, Meskers CG, Pallafacchina G, Paoli A, Pion D, Roceri M, Romanello V, Serrano AL, Toniolo L, Larsson L, Maier AB, Muñoz-Cánoves P, Musarò A, Pende M, Reggiani C, Rizzuto R, Schiaffino S.** Signalling pathways regulating muscle mass in ageing skeletal muscle: the role of the IGF1-Akt-mTOR-FoxO pathway. *Biogerontology* 14: 303–323, 2013. doi:10.1007/s10522-013-9432-9.
57. **Schiavo G, Shone CC, Bennett MK, Scheller RH, Montecucco C.** Botulinum neurotoxin type C cleaves a single Lys-Ala bond within the carboxyl-terminal region of syntaxins. *J Biol Chem* 270: 10566–10570, 1995. doi:10.1074/jbc.270.18.10566.
58. **Shavlakadze T, McGeachie J, Grounds MD.** Delayed but excellent myogenic stem cell response of regenerating geriatric skeletal muscles in mice. *Biogerontology* 11: 363–376, 2010. doi:10.1007/s10522-009-9260-0.
59. **Sheard PW, Anderson RD.** Age-related loss of muscle fibres is highly variable amongst mouse skeletal muscles. *Biogerontology* 13: 157–167, 2012. doi:10.1007/s10522-011-9365-0.
60. **Takuwa Y, Okamoto Y, Yoshioka K, Takuwa N.** Sphingosine-1-phosphate signaling in physiology and diseases. *Biofactors* 38: 329–337, 2012. doi:10.1002/biof.1030.
61. **Takuwa N, Ohkura S, Takashima S, Ohtani K, Okamoto Y, Tanaka T, Hirano K, Usui S, Wang F, Du W, Yoshioka K, Banno Y, Sasaki M, Ichi I, Okamura M, Sugimoto N, Mizugishi K, Nakanuma Y, Ishii I, Takamura M, Kaneko S, Kojo S, Satouchi K, Mitumori K, Chun J, Takuwa Y.** S1P$_3$-mediated cardiac fibrosis in sphingosine kinase 1 transgenic mice involves reactive oxygen species. *Cardiovasc Res* 85: 484–493, 2010. doi:10.1093/cvr/cvp312.
62. **Valdez G, Tapia JC, Kang H, Clemenson GD Jr, Gage FH, Lichtman JW, Sanes JR.** Attenuation of age-related changes in mouse neuromuscular synapses by caloric restriction and exercise. *Proc Natl Acad Sci USA* 107: 14863–14868, 2010. doi:10.1073/pnas.1002220107.
63. **Voytik SL, Przyborski M, Badylak SF, Konieczny SF.** Differential expression of muscle regulatory factor genes in normal and denervated adult rat hindlimb muscles. *Dev Dyn* 198: 214–224, 1993. doi:10.1002/aja.1001980307.

64. **White Z, White RB, McMahon C, Grounds MD, Shavlakadze T.** High mTORC1 signaling is maintained, while protein degradation pathways are perturbed in old murine skeletal muscles in the fasted state. *Int J Biochem Cell Biol* 78: 10–21, 2016. doi:10.1016/j.biocel.2016.06.012.
65. **Wohlgemuth SE, Seo AY, Marzetti E, Lees HA, Leeuwenburgh C.** Skeletal muscle autophagy and apoptosis during aging: effects of calorie restriction and life-long exercise. *Exp Gerontol* 45: 138–148, 2010. doi:10.1016/j.exger.2009.11.002.
66. **Wood LK, Kayupov E, Gumucio JP, Mendias CL, Claflin DR, Brooks SV.** Intrinsic stiffness of extracellular matrix increases with age in skeletal muscles of mice. *J Appl Physiol (1985)* 117: 363–369, 2014. doi:10.1152/japplphysiol.00256.2014.
67. **Zanin M, Germinario E, Dalla Libera L, Sandonà D, Sabbadini RA, Betto R, Danieli-Betto D.** Trophic action of sphingosine 1-phosphate in denervated rat soleus muscle. *Am J Physiol Cell Physiol* 294: C36–C46, 2008. doi:10.1152/ajpcell.00164.2007.
68. **Zhao B, Ye X, Yu J, Li L, Li W, Li S, Yu J, Lin JD, Wang CY, Chinnaiyan AM, Lai ZC, Guan KL.** TEAD mediates YAP-dependent gene induction and growth control. *Genes Dev* 22: 1962–1971, 2008. doi:10.1101/gad.1664408.

5.2 Congresses attended

10-12 DECEMBER 2014, SFET 2014, Paris, France

BOTULINUM NEUROTOXINS B, F, G, D AND TETANUS NEUROTOXIN ENTRY INTO NERVE TERMINAL

Giulia Zanetti, Marco Pirazzini, Domenico Azarnia Tehran, Thomas Binz, Eric Johnson, Ornella Rossetto, and Cesare Montecucco

13-15 MAY 2015, CNR RETREAT 2015, Pisa, Italy

BOTULINUM NEUROTOXINS B, F, G, D AND TETANUS NEUROTOXIN ENTRY INTO NERVE TERMINAL

Giulia Zanetti, Marco Pirazzini, Domenico Azarnia Tehran, Thomas Binz, Ornella Rossetto, and Cesare Montecucco

16-19 SEPTEMBER 2015, ABCD 2015, Bologna, Italy

BOTULINUM NEUROTOXINS B, F, G, D AND TETANUS NEUROTOXIN ENTRY INTO NERVE TERMINAL

Giulia Zanetti, Marco Pirazzini, Domenico Azarnia Tehran, Thomas Binz, Ornella Rossetto, Cesare Montecucco

13-16 SEPTEMBER 2016, CNR RETREAT 2016, Padova, Italy

ON THE NEUROTOXICITY OF TWO ITALIAN VIPER VENOMS

Giulia Zanetti, Marco Pirazzini, Cesare Montecucco, Carlo Locatelli, Davide Lonati and Ornella Rossetto

21-23 SEPTEMBER 2016, Antidotes and Depth 2016, Pavia, Italy

ON THE NEUROTOXICITY OF TWO ITALIAN VIPER VENOMS

Giulia Zanetti, Marco Pirazzini, Cesare Montecucco, Carlo Locatelli, Davide Lonati and Ornella Rossetto

18-21 JANUARY 2017, TOXINS 2017: Basic Science and Clinical Aspects of Botulinum and Other Neurotoxins, Madrid, Spain

IN VITRO AND IN VIVO EVALUATION OF SYNTAXIN-SPECIFIC BoNT/C

Giulia Zanetti, Marco Pirazzini, Ornella Rossetto, Aram Megighian, Tina Henke, Andreas Rummel, Thomas Binz, Cesare Montecucco

Selected for oral presentation

15-16 SEPTEMBER 2017, Young scientist meeting SIPMeT: Società Italiana di Patologia e Medicina Traslazionale, Milano, Italy

BOTULINUM NEUROTOXIN C MUTANTS REVEAL DIFFERENT EFFECTS OF SYNTAXIN OR SNAP-25 PROTEOLYSIS ON NEUROMUSCULAR TRANSMISSION

Giulia Zanetti, Stefan Sikorra, Andreas Rummel, Nadja Krez, Elisa Duregotti, Samuele Negro, Tina Henke, Ornella Rossetto, Thomas Binz and Marco Pirazzini

20-23 SEPTEMBER 2017, ABCD 2017,Bologna, Italy

BOTULINUM NEUROTOXIN C MUTANTS REVEAL DIFFERENT EFFECTS OF SYNTAXIN OR SNAP-25 PROTEOLYSIS ON NEUROMUSCULAR TRANSMISSION

Giulia Zanetti, Stefan Sikorra, Andreas Rummel, Nadja Krez, Elisa Duregotti, Samuele Negro, Tina Henke, Ornella Rossetto, Thomas Binz and Marco Pirazzini

References

1. Kandel Erik R. SJH, Jessel Thomas M.(2000) Principles of Neural Sciences. Fourth edition, McGraw-Hill.

2. Duregotti E, Zanetti G, Scorzeto M, et al. Snake and Spider Toxins Induce a Rapid Recovery of Function of Botulinum Neurotoxin Paralysed Neuromuscular Junction. Toxins (Basel). 2015;7(12):5322-5336.

3. Rossetto O, Pirazzini M, Montecucco C. Botulinum neurotoxins: genetic, structural and mechanistic insights. Nat Rev Microbiol. 2014;12(8):535-549.

4. Sudhof TC, Rizo J. Synaptic vesicle exocytosis. Cold Spring Harb Perspect Biol. 2011;3(12).

5. Harlow ML, Szule JA, Xu J, Jung JH, Marshall RM, McMahan UJ. Alignment of synaptic vesicle macromolecules with the macromolecules in active zone material that direct vesicle docking. PLoS One. 2013;8(7):e69410.

6. Zhao R, Masayasu H, Holmgren A. Ebselen: a substrate for human thioredoxin reductase strongly stimulating its hydroperoxide reductase activity and a superfast thioredoxin oxidant. Proc Natl Acad Sci U S A. 2002;99(13):8579-8584.

7. Sudhof TC. The presynaptic active zone. Neuron. 2012;75(1):11-25.

8. Sudhof TC. Neurotransmitter release: the last millisecond in the life of a synaptic vesicle. Neuron. 2013;80(3):675-690.

9. Morciano M, Beckhaus T, Karas M, Zimmermann H, Volknandt W. The proteome of the presynaptic active zone: from docked synaptic vesicles to adhesion molecules and maxi-channels. J Neurochem. 2009;108(3):662-675.

10. Megighian A, Zordan M, Pantano S, et al. Evidence for a radial SNARE super-complex mediating neurotransmitter release at the Drosophila neuromuscular junction. J Cell Sci. 2013;126(Pt 14):3134-3140.

11. Pantano S, Montecucco C. The blockade of the neurotransmitter release apparatus by botulinum neurotoxins. Cell Mol Life Sci. 2014;71(5):793-811.

12. Rickman C, Hu K, Carroll J, Davletov B. Self-assembly of SNARE fusion proteins into star-shaped oligomers. Biochem J. 2005;388(Pt 1):75-79.

13. Sudhof TC. A molecular machine for neurotransmitter release: synaptotagmin and beyond. Nat Med. 2013;19(10):1227-1231.

14. Jahn R, Fasshauer D. Molecular machines governing exocytosis of synaptic vesicles. Nature. 2012;490(7419):201-207.

15. Saheki Y, De Camilli P. Synaptic vesicle endocytosis. Cold Spring Harb Perspect Biol. 2012;4(9):a005645.

16. Montecucco C, Rasotto MB. On botulinum neurotoxin variability. MBio. 2015;6(1).

17. Hill KK, Smith TJ. Genetic diversity within Clostridium botulinum serotypes, botulinum neurotoxin gene clusters and toxin subtypes. Curr Top Microbiol Immunol. 2013;364:1-20.

18. Smith TJ, Hill KK, Raphael BH. Historical and current perspectives on Clostridium botulinum diversity. Res Microbiol. 2015;166(4):290-302.

19. Moriishi K, Koura M, Abe N, et al. Mosaic structures of neurotoxins produced from Clostridium botulinum types C and D organisms. Biochim Biophys Acta. 1996;1307(2):123-126.

20. Moriishi K, Koura M, Fujii N, et al. Molecular cloning of the gene encoding the mosaic neurotoxin, composed of parts of botulinum neurotoxin types C1 and D, and PCR detection of this gene from Clostridium botulinum type C organisms. Appl Environ Microbiol. 1996;62(2):662-667.

21. Setlow P JESatsIMD, LR Beuchat (Eds.), Food Micro- biology. Fundamentals and Frontiers. 3rd ed. ASM Press, Washington, DC, pp. 35–67.

22. Hatheway CL JECts-baILC, A Balows, M Sussman (Eds.), Topley & Wilson's Microbiology and Infections. 9th ed. Vol. 2. Systematic Bacteriology. Arnold, London, pp. 731–782.

23. Smith, LDS and Sugiyama H (1988) Botulism: the organism it, the disease, 2nd ed., Charles C Thomas S, IL.

24. Johnson EA, Montecucco C. Botulism. Handb Clin Neurol. 2008;91:333-368.

25. Pirazzini M, Rossetto O, Eleopra R, Montecucco C. Botulinum Neurotoxins: Biology, Pharmacology, and Toxicology. Pharmacol Rev. 2017;69(2):200-235.

26. Koepke R, Sobel J, Arnon SS. Global occurrence of infant botulism, 1976-2006. Pediatrics. 2008;122(1):e73-82.

27. Chertow DS, Tan ET, Maslanka SE, et al. Botulism in 4 adults following cosmetic injections with an unlicensed, highly concentrated botulinum preparation. Jama. 2006;296(20):2476-2479.

28. Arnon SS, Schechter R, Inglesby TV, et al. Botulinum toxin as a biological weapon: medical and public health management. Jama. 2001;285(8):1059-1070.

29. Rawlings ND, Barrett AJ. Homologues of insulinase, a new superfamily of metalloendopeptidases. Biochem J. 1991;275 (Pt 2):389-391.

30. Schiavo G, Rossetto O, Santucci A, DasGupta BR, Montecucco C. Botulinum neurotoxins are zinc proteins. J Biol Chem. 1992;267(33):23479-23483.

31. Gu S, Rumpel S, Zhou J, et al. Botulinum neurotoxin is shielded by NTNHA in an interlocked complex. Science. 2012;335(6071):977-981.

32. Eswaramoorthy S, Sun J, Li H, Singh BR, Swaminathan S. Molecular Assembly of Clostridium botulinum progenitor M complex of type E. Sci Rep. 2015;5:17795.

33. Miyata K, Yoneyama T, Suzuki T, et al. Expression and stability of the nontoxic component of the botulinum toxin complex. Biochem Biophys Res Commun. 2009;384(1):126-130.

34. Ohishi I, Sugii S, Sakaguchi G. Oral toxicities of Clostridium botulinum toxins in response to molecular size. Infect Immun. 1977;16(1):107-109.

35. Ohishi I, Sakaguchi G. Oral toxicities of Clostridium botulinum type C and D toxins of different molecular sizes. Infect Immun. 1980;28(2):303-309.

36. Couesnon A, Molgo J, Connan C, Popoff MR. Preferential entry of botulinum neurotoxin A Hc domain through intestinal crypt cells and targeting to cholinergic neurons of the mouse intestine. PLoS Pathog. 2012;8(3):e1002583.

37. Amatsu S, Sugawara Y, Matsumura T, Kitadokoro K, Fujinaga Y. Crystal structure of Clostridium botulinum whole hemagglutinin reveals a huge triskelion-shaped molecular complex. J Biol Chem. 2013;288(49):35617-35625.

38. Fujinaga Y, Sugawara Y, Matsumura T. Uptake of botulinum neurotoxin in the intestine. Curr Top Microbiol Immunol. 2013;364:45-59.

39. Lee K, Gu S, Jin L, et al. Structure of a bimodular botulinum neurotoxin complex provides insights into its oral toxicity. PLoS Pathog. 2013;9(10):e1003690.

40. Rummel A. The long journey of botulinum neurotoxins into the synapse. Toxicon. 2015;107(Pt A):9-24.

41. Lee K, Lam KH, Kruel AM, et al. Inhibiting oral intoxication of botulinum neurotoxin A complex by carbohydrate receptor mimics. Toxicon. 2015;107(Pt A):43-49.

42. Lam KH, Jin R. Architecture of the botulinum neurotoxin complex: a molecular machine for protection and delivery. Curr Opin Struct Biol. 2015;31:89-95.

43. Simpson L. The life history of a botulinum toxin molecule. Toxicon. 2013;68:40-59.

44. Lamanna C. The most poisonous poison. Science. 1959;130(3378):763-772.

45. Johnson EA, Montecucco C. Botulism. Handb Clin Neurol. 2008;91:333-368.

46. Binz T, Rummel A. Cell entry strategy of clostridial neurotoxins. J Neurochem. 2009;109(6):1584-1595.

47. Lacy DB, Tepp W, Cohen AC, DasGupta BR, Stevens RC. Crystal structure of botulinum neurotoxin type A and implications for toxicity. Nat Struct Biol. 1998;5(10):898-902.

48. Rummel A. Double receptor anchorage of botulinum neurotoxins accounts for their exquisite neurospecificity. Curr Top Microbiol Immunol. 2013;364:61-90.

49. Swaminathan S. Molecular structures and functional relationships in clostridial neurotoxins. Febs j. 2011;278(23):4467-4485.

50. Simpson LL. Identification of the major steps in botulinum toxin action. Annu Rev Pharmacol Toxicol. 2004;44:167-193.

51. Rossetto O, Montecucco C. Presynaptic neurotoxins with enzymatic activities. Handb Exp Pharmacol. 2008(184):129-170.

52. Pirazzini M, Bordin F, Rossetto O, Shone CC, Binz T, Montecucco C. The thioredoxin reductase-thioredoxin system is involved in the entry of tetanus and botulinum neurotoxins in the cytosol of nerve terminals. FEBS Lett. 2013;587(2):150-155.

53. Mazzocchio R, Caleo M. More than at the neuromuscular synapse: actions of botulinum neurotoxin A in the central nervous system. Neuroscientist. 2015;21(1):44-61.
54. Restani L, Antonucci F, Gianfranceschi L, Rossi C, Rossetto O, Caleo M. Evidence for anterograde transport and transcytosis of botulinum neurotoxin A (BoNT/A). J Neurosci. 2011;31(44):15650-15659.
55. Restani L, Giribaldi F, Manich M, et al. Botulinum neurotoxins A and E undergo retrograde axonal transport in primary motor neurons. PLoS Pathog. 2012;8(12):e1003087.
56. Dolly JO, Black J, Williams RS, Melling J. Acceptors for botulinum neurotoxin reside on motor nerve terminals and mediate its internalization. Nature. 1984;307(5950):457-460.
57. Montecucco C. How do tetanus and botulinum toxins bind to neuronal membranes? Trends in biochemical sciences. 1986;11(8):314-317.
58. Matteoli M, Verderio C, Rossetto O, et al. Synaptic vesicle endocytosis mediates the entry of tetanus neurotoxin into hippocampal neurons. Proc Natl Acad Sci U S A. 1996;93(23):13310-13315.
59. Van Heyningen WE. Tentative identification of the tetanus toxin recptor in nervous tissue. J Gen Microbiol. 1959;20(2):310-320.
60. Simpson LL, Rapport MM. The binding of botulinum toxin to membrane lipids: sphingolipids, steroids and fatty acids. J Neurochem. 1971;18(9):1751-1759.
61. Ledeen RW, Diebler MF, Wu G, Lu ZH, Varoqui H. Ganglioside composition of subcellular fractions, including pre- and postsynaptic membranes, from Torpedo electric organ. Neurochem Res. 1993;18(11):1151-1155.
62. Sonnino S, Mauri L, Chigorno V, Prinetti A. Gangliosides as components of lipid membrane domains. Glycobiology. 2007;17(1):1r-13r.
63. Swaminathan S, Eswaramoorthy S. Structural analysis of the catalytic and binding sites of Clostridium botulinum neurotoxin B. Nat Struct Biol. 2000;7(8):693-699.
64. Rummel A, Mahrhold S, Bigalke H, Binz T. The HCC-domain of botulinum neurotoxins A and B exhibits a singular ganglioside binding site displaying serotype specific carbohydrate interaction. Mol Microbiol. 2004;51(3):631-643.
65. Berntsson RP, Peng L, Dong M, Stenmark P. Structure of dual receptor binding to botulinum neurotoxin B. Nat Commun. 2013;4:2058.
66. Karalewitz AP, Fu Z, Baldwin MR, Kim JJ, Barbieri JT. Botulinum neurotoxin serotype C associates with dual ganglioside receptors to facilitate cell entry. J Biol Chem. 2012;287(48):40806-40816.
67. Strotmeier J, Lee K, Volker AK, et al. Botulinum neurotoxin serotype D attacks neurons via two carbohydrate-binding sites in a ganglioside-dependent manner. Biochem J. 2010;431(2):207-216.
68. Zhang Y, Buchko GW, Qin L, Robinson H, Varnum SM. Crystal structure of the receptor binding domain of the botulinum C-D mosaic neurotoxin reveals potential roles of lysines 1118 and 1136 in membrane interactions. Biochem Biophys Res Commun. 2011;404(1):407-412.

69. Nishiki T, Kamata Y, Nemoto Y, et al. Identification of protein receptor for Clostridium botulinum type B neurotoxin in rat brain synaptosomes. J Biol Chem. 1994;269(14):10498-10503.

70. Dong M, Richards DA, Goodnough MC, Tepp WH, Johnson EA, Chapman ER. Synaptotagmins I and II mediate entry of botulinum neurotoxin B into cells. J Cell Biol. 2003;162(7):1293-1303.

71. Rummel A, Karnath T, Henke T, Bigalke H, Binz T. Synaptotagmins I and II act as nerve cell receptors for botulinum neurotoxin G. J Biol Chem. 2004;279(29):30865-30870.

72. Jin R, Rummel A, Binz T, Brunger AT. Botulinum neurotoxin B recognizes its protein receptor with high affinity and specificity. Nature. 2006;444(7122):1092-1095.

73. Dong M, Tepp WH, Liu H, Johnson EA, Chapman ER. Mechanism of botulinum neurotoxin B and G entry into hippocampal neurons. J Cell Biol. 2007;179(7):1511-1522.

74. Peng L, Berntsson RP, Tepp WH, et al. Botulinum neurotoxin D-C uses synaptotagmin I and II as receptors, and human synaptotagmin II is not an effective receptor for type B, D-C and G toxins. J Cell Sci. 2012;125(Pt 13):3233-3242.

75. Willjes G, Mahrhold S, Strotmeier J, Eichner T, Rummel A, Binz T. Botulinum neurotoxin G binds synaptotagmin-II in a mode similar to that of serotype B: tyrosine 1186 and lysine 1191 cause its lower affinity. Biochemistry. 2013;52(22):3930-3938.

76. Dong M, Liu H, Tepp WH, Johnson EA, Janz R, Chapman ER. Glycosylated SV2A and SV2B mediate the entry of botulinum neurotoxin E into neurons. Mol Biol Cell. 2008;19(12):5226-5237.

77. Dong M, Yeh F, Tepp WH, et al. SV2 is the protein receptor for botulinum neurotoxin A. Science. 2006;312(5773):592-596.

78. Rummel A, Hafner K, Mahrhold S, et al. Botulinum neurotoxins C, E and F bind gangliosides via a conserved binding site prior to stimulation-dependent uptake with botulinum neurotoxin F utilising the three isoforms of SV2 as second receptor. J Neurochem. 2009;110(6):1942-1954.

79. Chang WP, Sudhof TC. SV2 renders primed synaptic vesicles competent for Ca2+ -induced exocytosis. J Neurosci. 2009;29(4):883-897.

80. Augustine GJ, Burns ME, DeBello WM, et al. Proteins involved in synaptic vesicle trafficking. J Physiol. 1999;520 Pt 1:33-41.

81. Zhang Y, Varnum SM. The receptor binding domain of botulinum neurotoxin serotype C binds phosphoinositides. Biochimie. 2012;94(3):920-923.

82. Fogolari F, Tosatto SC, Muraro L, Montecucco C. Electric dipole reorientation in the interaction of botulinum neurotoxins with neuronal membranes. FEBS Lett. 2009;583(14):2321-2325.

83. Muraro L, Tosatto S, Motterlini L, Rossetto O, Montecucco C. The N-terminal half of the receptor domain of botulinum neurotoxin A binds to microdomains of the plasma membrane. Biochem Biophys Res Commun. 2009;380(1):76-80.

84. Montal M. Botulinum neurotoxin: a marvel of protein design. Annu Rev Biochem. 2010;79:591-617.
85. Rizzoli SO. Synaptic vesicle recycling: steps and principles. Embo j. 2014;33(8):788-822.
86. Colasante C, Rossetto O, Morbiato L, Pirazzini M, Molgo J, Montecucco C. Botulinum neurotoxin type A is internalized and translocated from small synaptic vesicles at the neuromuscular junction. Mol Neurobiol. 2013;48(1):120-127.
87. Harper CB, Martin S, Nguyen TH, et al. Dynamin inhibition blocks botulinum neurotoxin type A endocytosis in neurons and delays botulism. J Biol Chem. 2011;286(41):35966-35976.
88. Takamori S, Holt M, Stenius K, et al. Molecular anatomy of a trafficking organelle. Cell. 2006;127(4):831-846.
89. Wohlfarth K, Goschel H, Frevert J, Dengler R, Bigalke H. Botulinum A toxins: units versus units. Naunyn Schmiedebergs Arch Pharmacol. 1997;355(3):335-340.
90. Miesenbock G, De Angelis DA, Rothman JE. Visualizing secretion and synaptic transmission with pH-sensitive green fluorescent proteins. Nature. 1998;394(6689):192-195.
91. Sankaranarayanan S, Ryan TA. Real-time measurements of vesicle-SNARE recycling in synapses of the central nervous system. Nat Cell Biol. 2000;2(4):197-204.
92. Ahnert-Hilger G, Holtje M, Pahner I, Winter S, Brunk I. Regulation of vesicular neurotransmitter transporters. Rev Physiol Biochem Pharmacol. 2003;150:140-160.
93. Pirazzini M, Azarnia Tehran D, Leka O, Zanetti G, Rossetto O, Montecucco C. On the translocation of botulinum and tetanus neurotoxins across the membrane of acidic intracellular compartments. Biochim Biophys Acta. 2016;1858(3):467-474.
94. Fischer A, Montal M. Single molecule detection of intermediates during botulinum neurotoxin translocation across membranes. Proc Natl Acad Sci U S A. 2007;104(25):10447-10452.
95. Koriazova LK, Montal M. Translocation of botulinum neurotoxin light chain protease through the heavy chain channel. Nat Struct Biol. 2003;10(1):13-18.
96. Fischer A, Montal M. Molecular dissection of botulinum neurotoxin reveals interdomain chaperone function. Toxicon. 2013;75:101-107.
97. Galloux M, Vitrac H, Montagner C, et al. Membrane Interaction of botulinum neurotoxin A translocation (T) domain. The belt region is a regulatory loop for membrane interaction. J Biol Chem. 2008;283(41):27668-27676.
98. Fischer A. Synchronized chaperone function of botulinum neurotoxin domains mediates light chain translocation into neurons. Curr Top Microbiol Immunol. 2013;364:115-137.
99. Sun S, Suresh S, Liu H, et al. Receptor binding enables botulinum neurotoxin B to sense low pH for translocation channel assembly. Cell Host Microbe. 2011;10(3):237-247.

100. Eswaramoorthy S, Kumaran D, Keller J, Swaminathan S. Role of metals in the biological activity of Clostridium botulinum neurotoxins. Biochemistry. 2004;43(8):2209-2216.

101. Fu FN, Busath DD, Singh BR. Spectroscopic analysis of low pH and lipid-induced structural changes in type A botulinum neurotoxin relevant to membrane channel formation and translocation. Biophys Chem. 2002;99(1):17-29.

102. Puhar A, Johnson EA, Rossetto O, Montecucco C. Comparison of the pH-induced conformational change of different clostridial neurotoxins. Biochem Biophys Res Commun. 2004;319(1):66-71.

103. Montecucco C, Schiavo G, Dasgupta BR. Effect of pH on the interaction of botulinum neurotoxins A, B and E with liposomes. Biochem J. 1989;259(1):47-53.

104. Montecucco C, Schiavo G, Brunner J, Duflot E, Boquet P, Roa M. Tetanus toxin is labeled with photoactivatable phospholipids at low pH. Biochemistry. 1986;25(4):919-924.

105. Zhang S, Finkelstein A, Collier RJ. Evidence that translocation of anthrax toxin's lethal factor is initiated by entry of its N terminus into the protective antigen channel. Proc Natl Acad Sci U S A. 2004;101(48):16756-16761.

106. Neumeyer T, Tonello F, Dal Molin F, Schiffler B, Orlik F, Benz R. Anthrax lethal factor (LF) mediated block of the anthrax protective antigen (PA) ion channel: effect of ionic strength and voltage. Biochemistry. 2006;45(9):3060-3068.

107. Basilio D, Jennings-Antipov LD, Jakes KS, Finkelstein A. Trapping a translocating protein within the anthrax toxin channel: implications for the secondary structure of permeating proteins. J Gen Physiol. 2011;137(4):343-356.

108. Simpson LL, Coffield JA, Bakry N. Inhibition of vacuolar adenosine triphosphatase antagonizes the effects of clostridial neurotoxins but not phospholipase A2 neurotoxins. J Pharmacol Exp Ther. 1994;269(1):256-262.

109. Simpson LL. Ammonium chloride and methylamine hydrochloride antagonize clostridial neurotoxins. J Pharmacol Exp Ther. 1983;225(3):546-552.

110. Keller JE, Cai F, Neale EA. Uptake of botulinum neurotoxin into cultured neurons. Biochemistry. 2004;43(2):526-532.

111. Schiavo G, Papini E, Genna G, Montecucco C. An intact interchain disulfide bond is required for the neurotoxicity of tetanus toxin. Infect Immun. 1990;58(12):4136-4141.

112. de Paiva A, Poulain B, Lawrence GW, Shone CC, Tauc L, Dolly JO. A role for the interchain disulfide or its participating thiols in the internalization of botulinum neurotoxin A revealed by a toxin derivative that binds to ecto-acceptors and inhibits transmitter release intracellularly. J Biol Chem. 1993;268(28):20838-20844.

113. Simpson LL, Maksymowych AB, Park JB, Bora RS. The role of the interchain disulfide bond in governing the pharmacological actions of botulinum toxin. J Pharmacol Exp Ther. 2004;308(3):857-864.
114. Fischer A, Montal M. Crucial role of the disulfide bridge between botulinum neurotoxin light and heavy chains in protease translocation across membranes. J Biol Chem. 2007;282(40):29604-29611. Epub 22007 Jul 29631.
115. Pirazzini M, Rossetto O, Bolognese P, Shone CC, Montecucco C. Double anchorage to the membrane and intact inter-chain disulfide bond are required for the low pH induced entry of tetanus and botulinum neurotoxins into neurons. Cell Microbiol. 2011;13(11):1731-1743. doi: 1710.1111/j.1462-5822.2011.01654.x. Epub 02011 Aug 01625.
116. Schiavo G, Papini E, Genna G, Montecucco C. An intact interchain disulfide bond is required for the neurotoxicity of tetanus toxin. Infect Immun. 1990;58(12):4136-4141.
117. Lopez-Mirabal HR, Winther JR. Redox characteristics of the eukaryotic cytosol. Biochim Biophys Acta. 2008;1783(4):629-640.
118. Arner ES, Holmgren A. Physiological functions of thioredoxin and thioredoxin reductase. Eur J Biochem. 2000;267(20):6102-6109.
119. Hanschmann EM, Godoy JR, Berndt C, Hudemann C, Lillig CH. Thioredoxins, glutaredoxins, and peroxiredoxins--molecular mechanisms and health significance: from cofactors to antioxidants to redox signaling. Antioxid Redox Signal. 2013;19(13):1539-1605.
120. Holmgren A, Lu J. Thioredoxin and thioredoxin reductase: current research with special reference to human disease. Biochem Biophys Res Commun. 2010;396(1):120-124.
121. Powis G, Kirkpatrick DL. Thioredoxin signaling as a target for cancer therapy. Curr Opin Pharmacol. 2007;7(4):392-397.
122. Kistner A, Habermann E. Reductive cleavage of tetanus toxin and botulinum neurotoxin A by the thioredoxin system from brain. Evidence for two redox isomers of tetanus toxin. Naunyn Schmiedebergs Arch Pharmacol. 1992;345(2):227-234.
123. Prast-Nielsen S, Cebula M, Pader I, Arner ES. Noble metal targeting of thioredoxin reductase--covalent complexes with thioredoxin and thioredoxin-related protein of 14 kDa triggered by cisplatin. Free Radic Biol Med. 2010;49(11):1765-1778. Epub 2010 Sep 1717.
124. Montecucco C, Schiavo G. Mechanism of action of tetanus and botulinum neurotoxins. Mol Microbiol. 1994;13(1):1-8.
125. Rossetto O, Schiavo G, Montecucco C, et al. SNARE motif and neurotoxins. Nature. 1994;372(6505):415-416.
126. Pellizzari R, Rossetto O, Lozzi L, et al. Structural determinants of the specificity for synaptic vesicle-associated membrane protein/synaptobrevin of tetanus and botulinum type B and G neurotoxins. J Biol Chem. 1996;271(34):20353-20358.
127. Breidenbach MA, Brunger AT. Substrate recognition strategy for botulinum neurotoxin serotype A. Nature. 2004;432(7019):925-929.

128. Brunger AT, Rummel A. Receptor and substrate interactions of clostridial neurotoxins. Toxicon. 2009;54(5):550-560.

129. Agarwal R, Schmidt JJ, Stafford RG, Swaminathan S. Mode of VAMP substrate recognition and inhibition of Clostridium botulinum neurotoxin F. Nat Struct Mol Biol. 2009;16(7):789-794.

130. Jin R, Sikorra S, Stegmann CM, Pich A, Binz T, Brunger AT. Structural and biochemical studies of botulinum neurotoxin serotype C1 light chain protease: implications for dual substrate specificity. Biochemistry. 2007;46(37):10685-10693.

131. Rossetto O, Morbiato L, Caccin P, Rigoni M, Montecucco C. Presynaptic enzymatic neurotoxins. J Neurochem. 2006;97(6):1534-1545.

132. Schiavo G, Rossetto O, Benfenati F, Poulain B, Montecucco C. Tetanus and botulinum neurotoxins are zinc proteases specific for components of the neuroexocytosis apparatus. Ann N Y Acad Sci. 1994;710:65-75.

133. Foran P, Lawrence GW, Shone CC, Foster KA, Dolly JO. Botulinum neurotoxin C1 cleaves both syntaxin and SNAP-25 in intact and permeabilized chromaffin cells: correlation with its blockade of catecholamine release. Biochemistry. 1996;35(8):2630-2636.

134. Huang X, Wheeler MB, Kang YH, et al. Truncated SNAP-25 (1-197), like botulinum neurotoxin A, can inhibit insulin secretion from HIT-T15 insulinoma cells. Mol Endocrinol. 1998;12(7):1060-1070.

135. Montecucco C, Schiavo G, Pantano S. SNARE complexes and neuroexocytosis: how many, how close? Trends Biochem Sci. 2005;30(7):367-372.

136. Sutton RB, Fasshauer D, Jahn R, Brunger AT. Crystal structure of a SNARE complex involved in synaptic exocytosis at 2.4 A resolution. Nature. 1998;395(6700):347-353.

137. Schiavo G, Matteoli M, Montecucco C. Neurotoxins affecting neuroexocytosis. Physiol Rev. 2000;80(2):717-766.

138. Binz T. Clostridial neurotoxin light chains: devices for SNARE cleavage mediated blockade of neurotransmission. Curr Top Microbiol Immunol. 2013;364:139-157.

139. Gill DM. Bacterial toxins: a table of lethal amounts. Microbiol Rev. 1982;46(1):86-94.

140. Neale EA, Bowers LM, Jia M, Bateman KE, Williamson LC. Botulinum neurotoxin A blocks synaptic vesicle exocytosis but not endocytosis at the nerve terminal. J Cell Biol. 1999;147(6):1249-1260.

141. Montecucco C, Molgo J. Botulinal neurotoxins: revival of an old killer. Curr Opin Pharmacol. 2005;5(3):274-279.

142. Sobel J. Botulism. Clin Infect Dis. 2005;41(8):1167-1173.

143. Duchen LW. An electron microscopic study of the changes induced by botulinum toxin in the motor end-plates of slow and fast skeletal muscle fibres of the mouse. J Neurol Sci. 1971;14(1):47-60.

144. Naumann M, Jankovic J. Safety of botulinum toxin type A: a systematic review and meta-analysis. Curr Med Res Opin. 2004;20(7):981-990.

145. Naumann M, Albanese A, Heinen F, Molenaers G, Relja M. Safety and efficacy of botulinum toxin type A following long-term use. Eur J Neurol. 2006;13 Suppl 4:35-40.
146. Ramirez-Castaneda J, Jankovic J. Long-term efficacy, safety, and side effect profile of botulinum toxin in dystonia: a 20-year follow-up. Toxicon. 2014;90:344-348.
147. Eleopra R, Tugnoli V, Quatrale R, et al. Botulinum neurotoxin serotypes A and C do not affect motor units survival in humans: an electrophysiological study by motor units counting. Clin Neurophysiol. 2002;113(8):1258-1264.
148. Eleopra R, Tugnoli V, Rossetto O, Montecucco C, De Grandis D. Botulinum neurotoxin serotype C: a novel effective botulinum toxin therapy in human. Neurosci Lett. 1997;224(2):91-94.
149. Pellett S, Tepp WH, Whitemarsh RC, Bradshaw M, Johnson EA. In vivo onset and duration of action varies for botulinum neurotoxin A subtypes 1-5. Toxicon. 2015;107(Pt A):37-42.
150. Shoemaker CB, Oyler GA. Persistence of Botulinum neurotoxin inactivation of nerve function. Curr Top Microbiol Immunol. 2013;364:179-196.
151. Patarnello T, Bargelloni L, Rossetto O, Schiavo G, Montecucco C. Neurotransmission and secretion. Nature. 1993;364(6438):581-582.
152. Eleopra R, Montecucco C, Devigili G, et al. Botulinum neurotoxin serotype D is poorly effective in humans: an in vivo electrophysiological study. Clin Neurophysiol. 2013;124(5):999-1004.
153. Peng L, Adler M, Demogines A, et al. Widespread sequence variations in VAMP1 across vertebrates suggest a potential selective pressure from botulinum neurotoxins. PLoS Pathog. 2014;10(7):e1004177.
154. Foran PG, Mohammed N, Lisk GO, et al. Evaluation of the therapeutic usefulness of botulinum neurotoxin B, C1, E, and F compared with the long lasting type A. Basis for distinct durations of inhibition of exocytosis in central neurons. J Biol Chem. 2003;278(2):1363-1371.
155. Eleopra R, Tugnoli V, Quatrale R, Rossetto O, Montecucco C. Different types of botulinum toxin in humans. Mov Disord. 2004;19 Suppl 8:S53-59.
156. Keller JE. Recovery from botulinum neurotoxin poisoning in vivo. Neuroscience. 2006;139(2):629-637.
157. Morbiato L, Carli L, Johnson EA, Montecucco C, Molgo J, Rossetto O. Neuromuscular paralysis and recovery in mice injected with botulinum neurotoxins A and C. Eur J Neurosci. 2007;25(9):2697-2704.
158. Cherington M. Clinical spectrum of botulism. Muscle Nerve. 1998;21(6):701-710.
159. Persell DJ, Arangie P, Young C, et al. Preparing for bioterrorism: category A agents. Nurse Pract. 2001;26(12):12-15, 19-24, 27; quiz 28-19.
160. Rossow H, Kinnunen PM, Nikkari S. [Botulinum toxin as a biological weapon]. Duodecim. 2012;128(16):1678-1684.
161. Possession, use, and transfer of select agents and toxins; biennial review. Final rule. Fed Regist. 2012;77(194):61083-61115.

162. Scott AB, Rosenbaum A, Collins CC. Pharmacologic weakening of extraocular muscles. Invest Ophthalmol. 1973;12(12):924-927.

163. Scott AB. Botulinum toxin injection into extraocular muscles as an alternative to strabismus surgery. Ophthalmology. 1980;87(10):1044-1049.

164. Scott AB, Suzuki D. Systemic toxicity of botulinum toxin by intramuscular injection in the monkey. Mov Disord. 1988;3(4):333-335.

165. Lim EC, Seet RC. Use of botulinum toxin in the neurology clinic. Nat Rev Neurol. 2010;6(11):624-636.

166. Hallett M, Albanese A, Dressler D, et al. Evidence-based review and assessment of botulinum neurotoxin for the treatment of movement disorders. Toxicon. 2013;67:94-114.

167. Naumann M, Dressler D, Hallett M, et al. Evidence-based review and assessment of botulinum neurotoxin for the treatment of secretory disorders. Toxicon. 2013;67:141-152.

168. Rossetto O, Seveso M, Caccin P, Schiavo G, Montecucco C. Tetanus and botulinum neurotoxins: turning bad guys into good by research. Toxicon. 2001;39(1):27-41.

169. Dressler D. Clinical applications of botulinum toxin. Curr Opin Microbiol. 2012;15(3):325-336.

170. Carruthers J, Burgess C, Day D, et al. Consensus Recommendations for Combined Aesthetic Interventions in the Face Using Botulinum Toxin, Fillers, and Energy-Based Devices. Dermatol Surg. 2016;42(5):586-597.

171. Johnson EA. Clostridial toxins as therapeutic agents: benefits of nature's most toxic proteins. Annu Rev Microbiol. 1999;53:551-575.

172. Dolimbek BZ, Aoki KR, Steward LE, Jankovic J, Atassi MZ. Mapping of the regions on the heavy chain of botulinum neurotoxin A (BoNT/A) recognized by antibodies of cervical dystonia patients with immunoresistance to BoNT/A. Mol Immunol. 2007;44(5):1029-1041.

173. Atassi MZ, Jankovic J, Steward LE, Aoki KR, Dolimbek BZ. Molecular immune recognition of botulinum neurotoxin B. The light chain regions that bind human blocking antibodies from toxin-treated cervical dystonia patients. Antigenic structure of the entire BoNT/B molecule. Immunobiology. 2012;217(1):17-27.

174. Peck MW, Smith TJ, Anniballi F, et al. Historical Perspectives and Guidelines for Botulinum Neurotoxin Subtype Nomenclature. Toxins (Basel). 2017;9(1).

175. Smith TJ, Lou J, Geren IN, et al. Sequence variation within botulinum neurotoxin serotypes impacts antibody binding and neutralization. Infect Immun. 2005;73(9):5450-5457.

176. Mazuet C, Ezan E, Volland H, Popoff MR, Becher F. Toxin detection in patients' sera by mass spectrometry during two outbreaks of type A Botulism in France. J Clin Microbiol. 2012;50(12):4091-4094.

177. Webb RP, Smith TJ, Wright P, Brown J, Smith LA. Production of catalytically inactive BoNT/A1 holoprotein and comparison with BoNT/A1 subunit vaccines against toxin subtypes A1, A2, and A3. Vaccine. 2009;27(33):4490-4497.

178. Pirazzini M, Azarnia Tehran D, Zanetti G, et al. The thioredoxin reductase--Thioredoxin redox system cleaves the interchain disulphide bond of botulinum neurotoxins on the cytosolic surface of synaptic vesicles. Toxicon. 2015;107(Pt A):32-36.

179. Agarwal R, Binz T, Swaminathan S. Structural analysis of botulinum neurotoxin serotype F light chain: implications on substrate binding and inhibitor design. Biochemistry. 2005;44(35):11758-11765.

180. Silvaggi NR, Boldt GE, Hixon MS, et al. Structures of Clostridium botulinum Neurotoxin Serotype A Light Chain complexed with small-molecule inhibitors highlight active-site flexibility. Chem Biol. 2007;14(5):533-542.

181. Thanongsaksrikul J, Chaicumpa W. Botulinum neurotoxins and botulism: a novel therapeutic approach. Toxins (Basel). 2011;3(5):469-488.

182. Eswaramoorthy S, Kumaran D, Swaminathan S. Crystallographic evidence for doxorubicin binding to the receptor-binding site in Clostridium botulinum neurotoxin B. Acta Crystallogr D Biol Crystallogr. 2001;57(Pt 11):1743-1746.

183. Li B, Peet NP, Butler MM, Burnett JC, Moir DT, Bowlin TL. Small molecule inhibitors as countermeasures for botulinum neurotoxin intoxication. Molecules. 2010;16(1):202-220.

184. Eleopra R, Tugnoli V, Quatrale R, Rossetto O, Montecucco C, Dressler D. Clinical use of non-A botulinum toxins: botulinum toxin type C and botulinum toxin type F. Neurotox Res. 2006;9(2-3):127-131.

185. Tugnoli V, Eleopra R, Montecucco C, De Grandis D. The therapeutic use of botulinum toxin. Expert Opin Investig Drugs. 1997;6(10):1383-1394.

186. Gillespie EJ, Ho CL, Balaji K, et al. Selective inhibitor of endosomal trafficking pathways exploited by multiple toxins and viruses. Proc Natl Acad Sci U S A. 2013;110(50):E4904-4912.

187. Wang D, Zhang Z, Dong M, Sun S, Chapman ER, Jackson MB. Syntaxin requirement for Ca2+-triggered exocytosis in neurons and endocrine cells demonstrated with an engineered neurotoxin. Biochemistry. 2011;50(14):2711-2713.

188. Eklund MW and Dowell VR (1987) Avian Botulism CC, Thomas S, IL.

189. DS. SL, Hiroshi S. Botulism: the organism, its toxins, the disease. 2nd ed. 1988.

190. Espelund M, Klaveness D. Botulism outbreaks in natural environments - an update. Front Microbiol. 2014;5:287.

191. Anniballi F, Auricchio B, Fiore A, et al. Botulism in Italy, 1986 to 2015. Euro Surveill. 2017;22(24).

192. Peck MW. Clostridium botulinum and the safety of minimally heated, chilled foods: an emerging issue? J Appl Microbiol. 2006;101(3):556-570.

193. Fagan RP, McLaughlin JB, Middaugh JP. Persistence of botulinum toxin in patients' serum: Alaska, 1959-2007. J Infect Dis. 2009;199(7):1029-1031.

194. Sheth AN, Wiersma P, Atrubin D, et al. International outbreak of severe botulism with prolonged toxemia caused by commercial carrot juice. Clin Infect Dis. 2008;47(10):1245-1251.

195. Barash JR, Arnon SS. A novel strain of Clostridium botulinum that produces type B and type H botulinum toxins. J Infect Dis. 2014;209(2):183-191.

196. Barash JR, Arnon SS. Dual toxin-producing strain of Clostridium botulinum type Bf isolated from a California patient with infant botulism. J Clin Microbiol. 2004;42(4):1713-1715.

197. Dover N, Barash JR, Hill KK, et al. Clostridium botulinum strain Af84 contains three neurotoxin gene clusters: bont/A2, bont/F4 and bont/F5. PLoS One. 2013;8(4):e61205.

198. Maslanka SE, Luquez C, Dykes JK, et al. A Novel Botulinum Neurotoxin, Previously Reported as Serotype H, Has a Hybrid-Like Structure With Regions of Similarity to the Structures of Serotypes A and F and Is Neutralized With Serotype A Antitoxin. J Infect Dis. 2016;213(3):379-385.

199. Carli L, Montecucco C, Rossetto O. Assay of diffusion of different botulinum neurotoxin type a formulations injected in the mouse leg. Muscle Nerve. 2009;40(3):374-380.

200. Jankovic J, Schwartz K. Response and immunoresistance to botulinum toxin injections. Neurology. 1995;45(9):1743-1746.

201. Bentivoglio AR, Del Grande A, Petracca M, Ialongo T, Ricciardi L. Clinical differences between botulinum neurotoxin type A and B. Toxicon. 2015;107(Pt A):77-84.

202. Wu YJ, Tejero R, Arancillo M, et al. Syntaxin 1B is important for mouse postnatal survival and proper synaptic function at the mouse neuromuscular junctions. J Neurophysiol. 2015;114(4):2404-2417.

203. Kofuji T, Fujiwara T, Sanada M, Mishima T, Akagawa K. HPC-1/syntaxin 1A and syntaxin 1B play distinct roles in neuronal survival. J Neurochem. 2014;130(4):514-525.

204. Santamato A, Micello MF, Ranieri M, et al. Employment of higher doses of botulinum toxin type A to reduce spasticity after stroke. J Neurol Sci. 2015;350(1-2):1-6.

205. Dressler D, Saberi FA, Kollewe K, Schrader C. Safety aspects of incobotulinumtoxinA high-dose therapy. J Neural Transm (Vienna). 2015;122(2):327-333.

206. Pirazzini M, Henke T, Rossetto O, et al. Neutralisation of specific surface carboxylates speeds up translocation of botulinum neurotoxin type B enzymatic domain. FEBS Lett. 2013;587(23):3831-3836.

Acknowledgments

I thank my family for the support they never missed me, friends and roommates for the good moments spent together. Finally I thank all the members of my laboratory, especially Professor Cesare Montecucco and Marco Pirazzini who have followed me in these years, allowing me to conclude this course in the best ways.